

UNIVERSITAT POLITÈCNICA DE VALÈNCIA
DEPARTAMENTO DE MAQUINAS Y MOTORES
TERMICOS



ANALYTICAL AND EXPERIMENTAL INVESTIGATION OF
MULTI-COMPONENT SURROGATE DIESEL FUELS

Doctoral Thesis

Presented by: Patrick Szymkowicz

Supervised by: Prof. Jesús Benajes

Valencia, Spain
September 2017

DOCTORAL THESIS

ANALYTICAL AND EXPERIMENTAL INVESTIGATION OF MULTI-COMPONENT SURROGATE DIESEL FUELS

Presented by: Patrick Szymkowicz

Supervised by: Prof. Jesús Benajes

EXAMINING BOARD:

President: Dr. José M. Desantes

Secretary: Dr. Juan J. Hernández

Examiner: Dr. Timothy J. Jacobs

REVIEWING BOARD:

Dr. Carlo Beatrice

Dr. Timothy J. Jacobs

Dr. Magín Lapuerta

Valencia, Spain
September 2017

Resumen

El combustible diésel está compuesto por cientos de hidrocarburos cuya presencia y proporción varía dependiendo del origen del crudo, del proceso de refinado, de los requerimientos legislativos, y de muchos otros factores. Para evitar las dificultades que produce esta variabilidad y complejidad en su composición, en los estudios sistemáticos, los investigadores suelen trabajar con combustibles de sustitución, mucho más sencillos, pero que reproducen las propiedades químicas y físicas del gasóleo. Los primeros combustibles de sustitución estuvieron formados por un solo componente, como el n-heptano y el n-dodecano. Recientemente se han desarrollado combustibles de sustitución multi-componentes, que se aplican tanto a estudios experimentales como de modelado. La aplicación sistemática de combustibles de sustitución controlados con precisión es una vía prometedora para mejorar la comprensión de la combustión Diesel, su eficiencia, y sus emisiones y proporciona herramientas para la investigación de sistemas de combustión nuevos y alternativos.

En esta tesis se han empleado métodos experimentales y de cálculo para desarrollar, estudiar y validar una librería de combustibles de sustitución multi-componentes. El primer combustible de sustitución se diseñó para reproducir con precisión las propiedades físicas y químicas de un gasóleo con número de cetano 50 y un índice de hollín umbral (TSI) de 31. El siguiente paso fue crear una biblioteca de combustibles de sustitución con 18 combustibles que pueden modificar independientemente dos propiedades clave del combustible: índice de cetano y TSI. En la biblioteca de combustibles el número de cetano osciló entre 35 y 60 con tres niveles de TSI iguales a 17, 31 y 48 (bajo, medio y alto rango). Los ensayos según la normativa ASTM demostraron una buena coincidencia con las propiedades del gasóleo como densidad, viscosidad, poder calorífico y curvas de destilación.

Para comprobar la validez de la librería, se realizó un estudio experimental comparativo sobre el proceso de combustión, las emisiones gaseosas, hollín y partículas de un gasóleo y de su combustible de sustitución ajustado. El estudio se realizó con un motor monocilíndrico Diesel completamente instrumentado y operando con estrategias de combustión en premezcla parcial (PPCI) y de baja temperatura (LTC), además de la combustión Diesel convencional (CDC). Los parámetros de la combustión como el retraso al encendido y la liberación de calor tanto de baja como de alta temperatura se

aproximaron muy bien. Las emisiones de gases, hollín y partículas también fueron similares al variar el nivel de EGR y la fase de la combustión.

La tesis demuestra que se pueden encontrar combustibles de sustitución perfectamente representativos de un gasóleo corriente, en base a mezclas apropiadas de n-hexadecano, 2,2,4,4,6,8,8-heptamethylnonano, decahidronaftaleno y 1-metilnaftaleno. Asimismo, se concluye que variando la proporción de estos cuatro componentes se puede controlar independientemente el número de cetano y el índice de hollín umbral, a la vez que se mantienen las propiedades físico-químicas y de combustión del gasóleo. La librería de combustibles de sustitución definida en esta tesis es una herramienta a disposición de los investigadores para profundizar en el conocimiento de la combustión diésel y avanzar en el diseño de sistemas futuros de combustión con mejor rendimiento y menores emisiones.

Resum

El combustible Diesel està compost per centenars d'hidrocarburs, la presència i proporció dels quals varia depenent de l'origen del cru, del procés de refinat, dels requeriments legislatius, i de molts altres factors. Per a evitar les dificultats que produeix aquesta variabilitat i complexitat en la seua composició, en els estudis sistemàtics, els investigadors solen treballar amb combustibles de substitució, molt més senzills, però que reproduïxen les propietats químiques i físiques del gasoil. Els primers combustibles de substitució van estar formats per un sol component, com el n-heptà i el n-dodecà. Recentment s'han desenvolupat combustibles de substitució multi-components, que s'apliquen tant a estudis experimentals com de modelatge. L'aplicació sistemàtica de combustibles de substitució controlats amb precisió és una via prometedora per a millorar la comprensió de la combustió Dièsel, la seua eficiència, i les seues emissions i proporciona eines per a la recerca de sistemes de combustió nous i alternatius.

En aquesta tesi s'han emprat mètodes experimentals i de càlcul per a desenvolupar, estudiar i validar una llibreria de combustibles de substitució multi-components. El primer combustible de substitució es va dissenyar per a reproduir amb precisió les propietats físiques i químiques d'un gasoil amb índex de cetà 50 i un índex de sutge límit (TSI) de 31. El següent pas va ser crear una biblioteca de combustibles de substitució amb 18 combustibles que poden modificar independentment dues propietats clau del combustible: índex de cetà i TSI. En la biblioteca de combustibles l'índex de cetà va oscil·lar entre 35 i 60 amb tres nivells de TSI iguals a 17, 31 i 48 (baix, mitjà i alt rang). Els assajos segons la normativa ASTM van demostrar una bona coincidència amb les propietats del gasoil com a densitat, viscositat, poder calorífic i corbes de destil·lació.

Per a comprovar la validesa de la llibreria, es va realitzar un estudi experimental comparatiu sobre el procés de combustió, les emissions gasoses, sutge i partícules d'un gasoil i del seu combustible de substitució ajustat. L'estudi es va realitzar amb un motor monocilíndric Dièsel completament instrumentat i operant amb estratègies de combustió en premescla parcial (PPCI) i de baixa temperatura (LTC), a més de la combustió Dièsel convencional (CDC). Els paràmetres de la combustió com el retard a l'encès i l'alliberament de calor tant de baixa com d'alta temperatura es van aproximar molt bé. Les emissions de gasos, sutge i

partícules també van ser similars en variar el nivell d'EGR i la fase de la combustió.

La tesi demostra que es poden trobar combustibles de substitució perfectament representatius d'un gasoil corrent, sobre la base de mescles apropiades de n-hexadecà, 2,2,4,4,6,8,8-heptamethylnonà, decahidronaftalé i 1-metilnaftaleno. Així mateix, es conclou que variant la proporció d'aquests quatre components es pot controlar independentment l'índex de cetà i l'índex de sutge límit, alhora que es mantenen les propietats físic-químiques i de combustió del gasoil. La llibreria de combustibles de substitució definida en aquesta tesi és una eina a la disposició dels investigadors per a aprofundir en el coneixement de la combustió Diesel i avançar en el disseny de sistemes futurs de combustió amb millor rendiment i menors emissions.

Abstract

Diesel fuel is composed of a complex mixture of hundreds of hydrocarbons that vary globally depending on crude oil sources, refining processes, legislative requirements and other factors. In order to simplify the study of this fuel, researchers create surrogate fuels with a much simpler composition, in an attempt to mimic and control the physical and chemical properties of Diesel fuel. The first surrogates were single-component fuels such as n-heptane and n-dodecane. Recent advancements have provided researchers the ability to develop multi-component surrogate fuels and apply them to both analytical and experimental studies. The systematic application of precisely controlled surrogate fuels promises to further enhance our understanding of Diesel combustion, efficiency, emissions and particulates and provide tools for investigating new and alternative engine combustion systems.

This thesis employed analytical and experimental methods to develop, validate and study a library of multi-component surrogate Diesel fuels. The first step was to design a surrogate fuel to precisely match the physical and chemical properties of a full-range petroleum Diesel fuel with 50 cetane number and a typical threshold soot index value of 31. The next step was to create a Surrogate Fuel Library with 18 fuels that independently varied two key fuel properties: cetane number and threshold soot index. Within the fuel library cetane number ranged from 35 to 60 at three threshold soot index levels of 17, 31 and 48 (low, mid-range and high). Extensive ASTM fuel property tests showed that good agreement with important physical and chemical properties of petroleum Diesel fuel such as density, viscosity, heating value and distillation curve.

An experimental investigation was conducted to evaluate the combustion, emissions, soot and exhaust particles from the petroleum Diesel fuel and the matching surrogate fuel. A fully-instrumented single-cylinder Diesel engine was operated with combustion strategies including Premixed Charge Compression Ignition (PCCI), Low-Temperature Combustion (LTC) and Conventional Diesel Combustion (CDC). For combustion, the ignition delay, low-temperature (first stage) and high temperature (second stage) heat-release matched very well. Gaseous emissions, soot and exhaust particles maintained good agreement as exhaust gas recirculation and combustion phasing were varied.

This thesis demonstrated that fully representative Diesel surrogate fuels could be tailored with the proper blending of the following hydrocarbon components: n-hexadecane, 2,2,4,4,6,8,8-heptamethylnonane, decahydronaphthalene and 1-methylnaphthalene. It was also established that the volumetric blending fractions of these four components could be varied to independently control the fuel cetane number and threshold soot index while retaining the combustion, physical and chemical properties of full-range petroleum Diesel fuel. The Surrogate Fuel Library provided by this thesis supplies Diesel engine researchers and designers the ability to analytically and experimentally vary fuel cetane number and threshold soot index. This new capability to independently vary two key fuel properties provides a means to further enhance the understanding of Diesel combustion and design future combustion systems that improve efficiency and emissions.

To my wife, my family and the God who made us.

*In memory of those who shaped my life
my father, my father-in-law Dedo and my grandparents*

"Be still, and know that I am God"

Psalm 46:10

*"For God so loved the world that he gave his one and only Son,
that whoever believes in him shall not perish but have eternal life."*

John 3:16

"I can do all things through Christ who strengthens me."

Philippians 4:13

Acknowledgements

First, and most importantly, I wish to thank my God. He created me, guides me with His Word, and redeemed me with His sacrifice. I could not draw a single breath or take a simple step without Him.

Each of us has a unique story to tell. My journey as a student at the UPV-CMT began shortly after my 50th birthday. I was a group manager at General Motors Research having a discussion with my Executive Director Dr. Gary Smyth. Gary asked the question "What's next with your career?" I responded "I'd like to finish my PhD." A bit surprised by my answer, Gary smiled and gave his full support. He opened doors within GM and gave me the opportunity to pursue my PhD. I would like to sincerely thank my GM leadership team Dr. Gary Smyth, Michael Harpster, David Brooks and Michael Potter for their tremendous support and encouragement. In addition, I would like to thank General Motors for providing the financial, experimental and analytical resources necessary to execute this research.

With a strong desire to attend the UPV-CMT, I contacted Professor Raul Payri. Raul was excited about the prospect and instrumental in steering me through enrollment process. I became a student at the UPV-CMT with Professor Benajes as my thesis supervisor. I will be forever thankful to Professors Francisco Payri, Jose Maria Desantes and Jesus Benajes for the incredible opportunity to attend the UPV-CMT. In addition, I am grateful to Professor Benajes for supervising and guiding my research and overseeing the writing of this thesis.

My research consisted of a sizeable experimental effort which included the build of a new single-cylinder research engine, the commissioning of a new engine test cell, and months of engine testing. I am very grateful to my friend and colleague Gerry Malta whose never-ending support in the lab went above and beyond the call. Thanks Gerry, I still have all my fingers. I am also very thankful to my friend and colleague Venkatesh Gopalakrishnan for his technical guidance. Venkatesh devoted substantial time honing my research, challenging me with difficult questions and reviewing my thesis. His contributions greatly improved my research. Thanks Venkatesh, I especially value our sushi lunches with a side of surrogate Diesel fuel. I would also like to thank my friends and colleagues Dick Peterson, Vicent Domenech-Llopis, Mike Potter and Alok Warey for providing valuable feedback on my research and reviewing thesis chapters. Lastly, I wish to thank Vicent for helping me understand the UPV processes, navigate the UPV Intranet, upload documents, translate Spanish to English and lots of encouragement.

Contents

Abstract

Acknowledgements

Contents i

List of Figures v

List of Tables xvii

Nomenclaturexxi

1. Introduction 1

1.1. General Context 3

1.2. Objective 4

1.3. Methodology 6

1.4. Thesis Outline 6

1.5. References 7

2. Diesel Fuel Properties 11

2.1. Introduction 13

2.2. Diesel Fuel 14

2.2.1 Diesel Fuel Chemistry 15

2.2.2 Diesel Fuel Properties 24

2.2.3	Diesel Fuel Specifications	31
2.3.	Summary	36
2.4.	References	37
3.	Computational Methods	41
3.1.	Introduction	43
3.2.	Temperature-Dependent Properties	43
3.3.	Master Kinetic Mechanism	44
3.4.	Gas-Phase Reactor Simulation	46
3.5.	Surrogate Blend Modeling	49
3.6.	Summary	58
3.7.	References	59
4.	Experimental Methods	63
4.1.	Introduction	65
4.2.	Test Facility	65
4.3.	Single-Cylinder Research Engine	66
4.4.	Fuel	68
4.5.	Measurements and Controls	68
4.6.	Test Conditions and Procedures	81
4.7.	Summary	84
4.8.	References	84
5.	Surrogate Fuel Development	87
5.1.	Introduction	89
5.2.	Surrogate Fuel Formulation	89
5.2.1	Objectives	90
5.2.2	Target Diesel Fuel	92
5.2.3	Model Fuel Library	93

5.2.4	Surrogate Components and Formulation	95
5.2.5	Surrogate Fuel Library	102
5.2.6	Summary.....	107
5.3.	Predicted and Measured Property Comparisons	107
5.3.1	Cetane Number.....	108
5.3.2	Threshold Soot Index.....	109
5.3.3	Density and Molar H/C.....	110
5.3.4	Lower Heating Value	111
5.3.5	Kinematic Viscosity.....	112
5.3.6	T ₁₀ and T ₉₀ Distillation Temperatures.....	113
5.3.7	Summary.....	115
5.4.	Surrogate and Petroleum Fuel Comparison.....	116
5.4.1	Combustion Properties	116
5.4.2	Physical Properties.....	117
5.4.3	Chemical Properties.....	124
5.4.4	Purity and Contamination	128
5.4.5	Summary.....	130
5.5.	Discussion.....	131
5.6.	Summary	136
5.7.	References	137
6.	Conventional Diesel Combustion	141
6.1.	Introduction.....	143
6.2.	Engine Operating Conditions.....	145
6.3.	Combustion Analysis.....	146
6.4.	Gaseous Emissions.....	162
6.5.	Smoke and Particle Emissions	168
6.6.	Discussion.....	176

6.7.	Summary	183
6.8.	References	184
7.	PCCI and LTC Combustion	189
7.1.	Introduction	191
7.2.	Engine Operating Conditions	193
7.3.	Combustion Analysis	195
7.4.	Gaseous Emissions	214
7.5.	Smoke and Particle Emissions	219
7.6.	Summary	226
7.7.	References	227
8.	Conclusions and Future Research	229
8.1.	Introduction	231
8.2.	Summary	231
8.3.	Conclusions	244
8.4.	Future Research	245
9.	Bibliography	247
10.	Appendix	265
10.1.	Surrogate Fuel Library	267
10.2.	Target and Surrogate Fuel Properties	271
10.3.	Surrogate Fuel Property Validation	276

List of Figures

Figure 2-1: Distillation column showing the separation of crude oil into distillates [2.3].....	15
Figure 2-2: Schematic diagrams for n-octane and iso-octane showing the differences between linear and branched structures.....	16
Figure 2-3: Stick diagrams (top) and ball-and-stick diagrams (beneath) for n-Heptane and n-Hexadecane.....	17
Figure 2-4: Two-ring and branched one-ring cyclo-alkanes.....	18
Figure 2-5: Examples of aromatic structures: benzene, branched aromatics toluene and n-propylbenzene, cyclo-aromatic tetralin and polycyclic aromatic 1-methylnaphthalene.....	19
Figure 2-6: Typical carbon number distribution from No. 2-D Diesel fuel, adapted from [2.1].....	20
Figure 2-7: Detailed characterization quantifying the molecular distribution of seven hydrocarbon classes per carbon atom number [2.13].	21
Figure 2-8: Detailed analysis showing carbon number, hydrocarbon class and molecular structure for three commercial Diesel fuels. Significant variation exists between the Diesel fuels [2.14].	23
Figure 3-1: Heat of vaporization for several hydrocarbon compounds computed from DIPPR correlations.....	44
Figure 3-2: Example of closed-homogeneous reactor temperature simulation for n-heptane and decahydronaphthalene.....	48
Figure 3-3: Ignition delay summary for n-heptane and decahydronaphthalene showing the impact of equivalence ratio and temperature.....	48
Figure 3-4: Surrogate Blend Optimizer (SBO) work diagram, adapted from [3.30].	51

Figure 3-5: Select, preprocess and load the Chemkin chemistry set.	52
Figure 3-6: Select the fuel species to include in the surrogate fuel.	53
Figure 3-7: Input the target values. For the SBO optimizer mode, the fuel property targets were input along with their respective weighting factors. For the SBO property calculator mode, the fuel species composition was input and the fuel property values were left blank. This figure shows a four-component surrogate using the property calculator mode.	54
Figure 3-8: Select solver settings (used defaults).....	55
Figure 3-9: Run the SBO program to calculate surrogate fuel properties. Results were compared with target fuel properties for the given composition.	56
Figure 3-10: Surrogate fuel formulation and predicted properties were exported to a spreadsheet.....	57
Figure 4-1: Schematic diagram of the engine test facility.	65
Figure 4-2: Typical single-cylinder engine configured with an FEV base module.....	66
Figure 4-3: Combustion metrics Peak Cylinder Pressure and Peak Bulk Gas Temperature.	71
Figure 4-4: Heat release for conventional Diesel combustion.	72
Figure 4-5: Combustion metrics: CA50% Mass Burned and 10-90% Mass Burned Duration.	73
Figure 4-6: Fuel injection events and periods based on the high pressure fuel line signal, fuel injector current signal and heat release from a common rail injector with a single-injection strategy.	74
Figure 4-7: Combustion DMS500 MKII Fast Particle Analyzer [4.13].....	77
Figure 4-8: Total, accumulation and nucleation mode spectrums [4.13]. ..	78
Figure 4-9: DMS500 sampling and dilution system [4.13].	79

Figure 4-10: DMS Column [4.13].	79
Figure 5-1: Methodology used to develop surrogate fuel blends.	90
Figure 5-2: Cetane number measurements of full-range petroleum and biodiesel fuels.	92
Figure 5-3: Ignition delay for n-alkane and aromatic compounds. Closed-homogeneous reactor initial pressure = 40 bar and equivalence ratio = 1.0.	97
Figure 5-4: Predicted and IQT measured cetane number for blends of n-hexadecane and heptamethylnonane.	98
Figure 5-5: Low temperature and high temperature ignition delay for a seven-component surrogate, four-component surrogate and n-heptane. Closed-homogeneous reactor initial pressure = 40 bar and equivalence ratio = 1.0.	99
Figure 5-6: Predicted and measured cetane numbers for five surrogate fuels.	108
Figure 5-7: Predicted and measured TSI for five surrogate fuels.	109
Figure 5-8: Predicted and measured density for five surrogate fuels.	110
Figure 5-9: Predicted and measured molar H/C for five surrogate fuels.	110
Figure 5-10: Predicted and measured lower heating value for five surrogate fuels.	111
Figure 5-11: Predicted and measured kinematic viscosity for five surrogate fuels.	112
Figure 5-12: Predicted and measured T_{10} distillation temperature.	114
Figure 5-13: Predicted and measured T_{90} distillation temperature.	114
Figure 5-14: Liquid density temperature dependencies for petroleum Diesel, CN50_TSI31 and the individual surrogate components.	119

Figure 5-15: Dynamic viscosity temperature dependencies for petroleum Diesel fuel, CN50_TSI31 and the individual surrogate components.....	120
Figure 5-16: Surface tension temperature dependencies for petroleum Diesel fuel, CN50_TSI31 and the individual fuel components.....	122
Figure 5-17: Distillation curves for the petroleum Diesel and CN50_TSI31	124
Figure 5-18: Comparison of hydrocarbon classes for a nominal Diesel fuel, scaled and replotted from [5.29], and CN50_TSI31 surrogate fuel (%v/v).	125
Figure 5-19: The effect of varying surrogate fuel formulation on density.	131
Figure 5-20: The effect of varying surrogate fuel formulation on kinematic viscosity.....	132
Figure 5-21: The effect of varying surrogate fuel formulation on lower heating value.....	133
Figure 5-22: The effect of varying surrogate fuel formulation on the fuel energy per unit volume.	133
Figure 5-23: The effect of varying surrogate fuel formulation on the T_{10} distillation temperature.....	134
Figure 5-24: The effect of varying surrogate fuel formulation on the T_{50} distillation temperature.....	135
Figure 5-25: The effect of varying surrogate fuel formulation on the T_{90} distillation temperature.....	135
Figure 6-1: Conventional Diesel Combustion strategy conceptually displayed on a chart of local fuel-equivalence ratio versus local combustion temperature. Figure adapted from [6.13].....	144
Figure 6-2: Heat release characteristics for conventional Diesel combustion. Adapted from [6.8]. (Also appears in Chapter 4 as Figure 4-4.)	144

Figure 6-3: Cylinder pressure for 1500x9 with 0% EGR and with 30% EGR. Injection SOE adjusted to maintain CA50=9 degrees aTDC for all tests.....	147
Figure 6-4: Heat release rates for 1500x9 with 0% EGR and with 30% EGR. Injection SOE adjusted to maintain CA50=9 degrees aTDC for all tests.....	148
Figure 6-5: Cylinder pressure for CA50 sweeps at 1500x9 with 15% EGR.	149
Figure 6-6: Heat release rates for CA50 sweeps at 1500x9 with 15% EGR.	150
Figure 6-7: The required injection SOE to achieve CA50=9 degrees aTDC as EGR level was increased from 0% to 30% at the 1500x9 operating condition.	152
Figure 6-8: The required injection SOE to achieve CA50=6, 9, 12 and 15 degrees aTDC at the 1500x9 operating condition with 15% EGR.	152
Figure 6-9: Effects of EGR on ignition delay at 1500x9 with the injection SOE adjusted to maintain CA50=9 degrees aTDC.	154
Figure 6-10: Effects of combustion phasing on ignition delay at 1500x9 with 15% EGR.	154
Figure 6-11: Effects of EGR on mixing advance time at 1500x9 with the injection SOE adjusted to maintain CA50=9 degrees aTDC.	156
Figure 6-12: Effects of combustion phasing on mixing advance time at 1500x9 with 15% EGR.	156
Figure 6-13: Effects of EGR on peak heat release rate at 1500x9 with the injection SOE adjusted to maintain CA50=9 degrees aTDC.	158
Figure 6-14: Effects of combustion phasing on peak heat release rate at 1500x9 with 15% EGR.	158
Figure 6-15: Effects of EGR on peak bulk gas temperature at 1500x9 with the injection SOE adjusted to maintain CA50=9 degrees aTDC.	159

Figure 6-16: Effects of combustion phasing on peak bulk gas temperature at 1500x9 with 15% EGR.....	159
Figure 6-17: Effects of EGR on 10-90% burn duration at 1500x9 with the injection SOE adjusted to maintain CA50=9 degrees aTDC.....	161
Figure 6-18: Effects of combustion phasing on the 10-90% burn duration at 1500x9 with 15% EGR.....	161
Figure 6-19: Effects of EGR on CO emissions at 1500x9 with the injection SOE adjusted to maintain CA50=9 degrees aTDC.....	164
Figure 6-20: Effects of combustion phasing on CO emissions at 1500x9 with 15% EGR.....	164
Figure 6-21: Effects of EGR on total hydrocarbon emissions at 1500x9 with the injection SOE adjusted to maintain CA50=9 degrees aTDC.....	166
Figure 6-22: Effects of combustion phasing on total hydrocarbon emissions at 1500x9 with 15% EGR.....	166
Figure 6-23: Effects of EGR on NOx emissions at 1500x9 with the injection SOE adjusted to maintain CA50=9 degrees aTDC.....	167
Figure 6-24: Effects of combustion phasing on NOx emissions at 1500x9 with 15% EGR.....	167
Figure 6-25: Effects of EGR on smoke at 1500x9 with the injection SOE adjusted to maintain CA50=9 degrees aTDC.....	169
Figure 6-26: Effects of combustion phasing on smoke at 1500x9 with 15%, 25%, and 30% EGR.....	169
Figure 6-27: Particle size distribution for Diesel and CN50_TSI31 fuels at 1500x9 with 20% EGR and CA50=9 degrees aTDC.....	170
Figure 6-28: Effects of EGR on exhaust particle size distributions for the petroleum Diesel fuel at 1500x9 with CA50=9 degrees aTDC.....	171

Figure 6-29: Effects of EGR on exhaust particle number concentration at 1500x9 with the injection SOE adjusted to maintain CA50=9 degrees aTDC.	173
Figure 6-30: Effects of combustion phasing on particle number concentration at 1500x9 with 15% EGR.....	173
Figure 6-31: Effects of EGR on exhaust particle count mean diameter at 1500x9 with the injection SOE adjusted to maintain CA50=9 degrees aTDC.	174
Figure 6-32: Effects of combustion phasing on exhaust particle count mean diameter at 1500x9 with 15% EGR.	174
Figure 6-33: Closed-homogenous reactor simulation showing the formation of acetylene during the ignition delay period from a four-component surrogate fuel. All fuel components are completely decomposed prior to ignition. Temperature = 1000 °C, Pressure = 50 bar, and Equivalence Ratio=1.0.....	179
Figure 6-34: Closed-homogenous reactor simulation showing the formation of acetylene during the ignition delay period from a seven-component surrogate fuel. All fuel components are completely decomposed prior to ignition. Temperature = 1000 °C, Pressure = 50 bar, and Equivalence Ratio=1.0.....	180
Figure 6-35: Acetylene formed during the ignition delay period for a seven-component and a four-component surrogate both with 50 cetane number and 31 TSI. Temperature = 1000 °C, Pressure = 50 bar, and Equivalence Ratio=1.0.....	181
Figure 6-36: Benzene formed during the ignition delay period for a seven-component and a four-component surrogate both with 50 cetane number and 31 TSI. Temperature = 1000 °C, Pressure = 50 bar, and Equivalence Ratio=1.0.....	181
Figure 7-1: PCCI and Low Temperature Combustion strategies conceptually displayed on a chart of local fuel-equivalence ratio versus local combustion temperature. Figure adapted from Figure 7-1.....	192

Figure 7-2: Heat release characteristics for PCCI combustion.....	192
Figure 7-3: Cylinder pressure for 1500x3 with 0% EGR and with 60% EGR. Injection SOE adjusted to maintain CA50=9 degrees aTDC for all tests.	196
Figure 7-4: Heat release rates for 1500x3 with 0% EGR and with 60% EGR. Injection SOE adjusted to maintain CA50=9 degrees aTDC for all tests.	197
Figure 7-5: Cylinder pressure for CA50 sweeps at 1500x3 with 40% EGR.	198
Figure 7-6: Heat release rates for CA50 sweeps at 1500x3 with 40% EGR.	199
Figure 7-7: Heat release rates at 1500x3 with 0% EGR and 60% EGR. Injection SOE adjusted to maintain CA50=9 degrees aTDC. Y-axis and x-axis scaled to focus on low temperature heat release.....	200
Figure 7-8: Heat release rate plot showing the method to determine the start, end and duration of the low temperature heat release.	201
Figure 7-9: EGR effects on total amount of heat released over the LTHR period and the duration of the LTHR at 1500x3 with the injection SOE adjusted to maintain CA50=9 degrees aTDC.....	202
Figure 7-10: The required injection SOE to achieve CA50=9 degrees aTDC as EGR level was increased from 0% to 60% at the 1500x3 operating condition.	204
Figure 7-11: The required injection SOE to achieve CA50=6, 9, 12 and 15 degrees aTDC at the 1500x3 operating condition with 40% EGR.	204
Figure 7-12: EGR effects on ignition delay at 1500x3 with the injection SOE adjusted to maintain CA50=9 degrees aTDC.....	206
Figure 7-13: Combustion phasing effects on ignition delay at 1500x3 with 40% EGR.....	206
Figure 7-14: Effects of EGR on mixing advance time at 1500x3 with the injection SOE adjusted to maintain CA50=9 degrees aTDC.....	208

Figure 7-15: Effects of combustion phasing on mixing advance time at 1500x3 with 40% EGR.	208
Figure 7-16: EGR effects on peak heat-release rate at 1500x3 with the injection SOE adjusted to maintain CA50=9 degrees aTDC.	210
Figure 7-17: Combustion phasing effects on peak heat-release rate at 1500x3 with 40% EGR.	210
Figure 7-18: EGR effects on peak bulk gas temperature at 1500x3 with the injection SOE adjusted to maintain CA50=9 degrees aTDC.	211
Figure 7-19: Combustion phasing effects on peak bulk gas temperature at 1500x3 with 40% EGR.	211
Figure 7-20: EGR effects on 10-90% burn duration at 1500x3 with the injection SOE adjusted to maintain CA50=9 degrees aTDC.	213
Figure 7-21: Combustion phasing effects on 10-90% burn duration at 1500x3 with 40% EGR.	213
Figure 7-22: Effects of EGR on CO emissions at 1500x3 with the injection SOE adjusted to maintain CA50=9 degrees aTDC.	215
Figure 7-23: Effects of combustion phasing on CO emissions at 1500x3 with 40% EGR.	215
Figure 7-24: Effects of EGR on HC emissions at 1500x3 with the injection SOE adjusted to maintain CA50=9 degrees aTDC.	217
Figure 7-25: Effects of combustion phasing on HC emissions at 1500x3 with 40% EGR.	217
Figure 7-26: Effects of EGR on NOx emissions at 1500x3 with the injection SOE adjusted to maintain CA50=9 degrees aTDC.	218
Figure 7-27: Effects of combustion phasing on NOx emissions at 1500x3 with 40% EGR.	218

Figure 7-28: EGR effects on particle size spectral density for Diesel fuel at 1500x3 with the injection SOE adjusted to maintain CA50=9 degrees aTDC.	220
Figure 7-29: Combustion phasing effects on particle size spectral density for Diesel fuel at 1500x3 with 60% EGR.	221
Figure 7-30: EGR effects on accumulation and nucleation mode particle number concentrations for Diesel and CN50_TSI31 at 1500x3 with the injection SOE adjusted to maintain CA50=9 degrees aTDC.	222
Figure 7-31: Combustion phasing effects on particle number concentration for Diesel and CN50_TSI31 fuels at 1500x3 with 60% EGR.	223
Figure 7-32: EGR effects on particle count median diameter (CMD) for Diesel and CN50_TSI31 fuels at 1500x3 with the injection SOE adjusted to maintain CA50=9 degrees aTDC.	224
Figure 7-33: Combustion phasing effects on particle count median diameter (CMD) for Diesel and CN50_TSI31 fuels at 1500x3 with 60% EGR.	225
Figure 8-1: Surrogate fuel development methodology.	232
Figure 8-2: Predicted and measured cetane numbers. Error bands reflect the reproducibility specified within the ASTM procedure.	235
Figure 8-3: Heat release rates for CA50 sweeps at 1500x9 with 15% EGR.	238
Figure 8-4: Smoke-NOx tradeoff for the target Diesel and CN50_TSI31 fuels.	238
Figure 8-5: Effects of EGR on exhaust particle number concentration at 1500x9 with the injection SOE adjusted to maintain CA50=9 degrees aTDC.	239
Figure 8-6: Effects of EGR on exhaust particle count mean diameter at 1500x9 with the injection SOE adjusted to maintain CA50=9 degrees aTDC.	239

Figure 8-7: Heat release rates from the target Diesel and CN50_TSI31 fuels at 1500x3 with 0% and 60% EGR with the injection SOE adjusted to maintain CA50=9 degrees aTDC.	241
Figure 8-8: Gaseous emission results from an EGR sweep at 1500x3 with the injection SOE adjusted to maintain CA50=9 degrees aTDC.	241
Figure 8-9: EGR effects on accumulation and nucleation mode particle number concentrations for Diesel and CN50_TSI31 at 1500x3 with the injection SOE adjusted to maintain CA50=9 degrees aTDC.	242
Figure 8-10: EGR effects on particle count median diameter (CMD) for Diesel and CN50_TSI31 fuels at 1500x3 with the injection SOE adjusted to maintain CA50=9 degrees aTDC.	242

List of Tables

Table 2-1: Properties of market Diesel fuels	28
Table 2-2: List of representative Diesel fuel hydrocarbon compounds including chemical formula, cetane number, TSI and boiling point [2.1] [2.26].	30
Table 2-3: ASTM D975 Diesel fuel specifications [2.27]	32
Table 2-4: EN590 Diesel fuel specifications [2.28].....	33
Table 2-5: Comparison of ASTM D975 No. 2-D and EN590 fuel specifications.	35
Table 3-1: Progress in the development of surrogate fuel components with detailed kinetic mechanisms. Table taken from reference [3.14].	45
Table 3-2: Parameter inputs for closed-homogeneous reactor simulation.	47
Table 3-3: User input target values for surrogate fuel development.....	50
Table 3-4: Summary of computational methods applied to create surrogate fuel formulations and predicted fuel properties.	58
Table 4-1: Single-cylinder engine characteristics and geometries.	67
Table 4-2: Some properties of the petroleum Diesel fuel tested in this study.	68
Table 4-3: High-speed data signals.....	69
Table 4-4: Engine test conditions.....	83
Table 5-1: Target Diesel fuel properties.	93
Table 5-2: Complete list of the surrogate fuel components available for the formulation of surrogate fuels.	94
Table 5-3: Potential components for Diesel surrogate fuels.	96

Table 5-4: Surrogate Fuel Components.....	100
Table 5-5: Surrogate fuel components and blend formulation for the surrogate fuel developed to match the properties of the target Diesel fuel.	101
Table 5-6: Properties of the target Diesel fuel compared with predicted properties of the surrogate Diesel fuel.....	101
Table 5-7: Surrogate Fuel Library covering a broad range of cetane number and TSI.....	102
Table 5-8: Formulations and predicted properties for surrogate fuels as cetane number varies from 35 to 60 with TSI held at 31.	104
Table 5-9: Formulations and predicted properties for surrogate fuels at TSI values of 17, 31 and 48 with cetane number held at 50.....	106
Table 5-10: Maximum observed difference between predicted and measured fuel properties for five surrogate fuels.....	115
Table 5-11: Combustion properties for petroleum Diesel and CN50_TSI31 surrogate fuel. Fuels properties matched within measurement reproducibility.	117
Table 5-12: Repeatability and reproducibility metrics for ASTM test methods.....	118
Table 5-13: Physical properties for Diesel and CN50_TSI31 surrogate fuels.	118
Table 5-14: ASTM D86 distillation temperatures for Diesel and CN50_TSI31 fuels.....	123
Table 5-15: Alkane, alkene and aromatic hydrocarbons for petroleum Diesel and CN50_TSI31 surrogate fuels.	126
Table 5-16: Carbon, hydrogen, nitrogen and sulfur content in the Petroleum and surrogate fuels.	127

Table 5-17: Properties of aromatic compounds [5.13] [5.14].	127
Table 5-18: Contamination analysis for petroleum Diesel and CN50_TSI31 fuels.	128
Table 5-19: Elemental analysis for fuel-born metals by Inductively Coupled Plasma Atomic Emission Spectrometry (ICP-AES).	129
Table 5-20: Comparison of target Diesel and CN50_TSI31 with ASTM D975 No. 2-D and EN590 fuel specifications.	130
Table 6-1: Engine operating conditions to evaluate the petroleum and surrogate fuels with conventional Diesel combustion.	145
Table 6-2: Properties and components of a seven-component and four-component surrogate fuels with 50 cetane number and 31 TSI.	178
Table 7-1: Engine operating conditions to evaluate the petroleum and surrogate fuels with PCCI and LTC combustion strategies.	194
Table 8-1: The Surrogate Fuel Library.	233
Table 8-2. Surrogate fuel components and blend formulation for the surrogate fuel CN50_TSI31 which was developed to match the properties of the target Diesel fuel.	234
Table 8-3: Maximum observed differences between predicted and measured fuel properties.	235
Table 10-1: Surrogate Fuel Library matrix.	267
Table 10-2: Volume, mass and molar blending fractions and predicted properties for the low sooting tendency surrogate fuels (TSI=17).	268
Table 10-3: Volume, mass and molar blending fractions and predicted properties for the mid sooting tendency surrogate fuels (TSI=31).	269
Table 10-4: Volume, mass and molar blending fractions and predicted properties for the high sooting tendency surrogate fuels (TSI=48).	270

Table 10-5: Five surrogates from the library (highlighted in green) that were blended and comprehensively analyzed with ASTM test procedures.	271
Table 10-6: Fuel combustion properties for the target Diesel fuel and the (5) surrogate fuels.....	272
Table 10-7: Fuel physical properties for the target Diesel fuel and the (5) surrogate fuels.....	272
Table 10-8: Fuel hydrocarbon classes for the target Diesel fuel and the (5) surrogate fuels.....	273
Table 10-9: Fuel distillation temperatures for the target Diesel fuel and the (5) surrogate fuels.....	273
Table 10-10: Fuel chemical (elemental) properties for the target Diesel fuel and the (5) surrogate fuels.	274
Table 10-11: Target Diesel and CN50_TSI31 contamination results.....	275
Table 10-12: Comparison of predicted and measured fuel properties for surrogate fuels with increasing cetane number (40, 50, 60) and a constant TSI=31.....	276
Table 10-13: Comparison of predicted and measured fuel properties for surrogate fuels with increasing TSI (17, 31, 48) and a constant cetane number=50.	277

Nomenclature

Symbol/Acronym	Definition
a2ch3	1-Methylnaphthalene
ASTM	American Society for Testing and Materials
aTDC	After crankshaft top-dead-center
°C	Degrees Celsius
CA50	Crank-angle of 50% mass fraction burned
CAD	Engine crank-angle degree
cc	Cubic centimeter
CMD	Count Median Diameter
CN	Cetane Number
CO	Carbon monoxide
CO ₂	Carbon dioxide
DCN	Derived Cetane Number
decalin	Decahydronaphthalene
DIPPR	Design Institute for Physical Properties
Dp	Diameter of particle
EGR	Exhaust Gas Recirculation
EI-CO	Emission Index CO
EI-THC	Emission Index Total HC
EI-NO _x	Emission Index NO _x
EOE	End of Energizing time of fuel injection
EOI	End of Injection of fuel
FSN	Filter Smoke Number
H/C	Hydrogen-to-carbon ratio
HC	Hydrocarbons
hmn	2,2,4,4,6,8,8-Heptamethylnonane
HTHR	High Temperature Heat Release

IMEP	Indicated Mean Effective Pressure
IQT	Ignition Quality Tester
LTC	Low Temperature Combustion
LTHR	Low Temperature Heat Release
MFC	Model Fuels Consortium
MFC II	Model Fuels Consortium II
MFLSS	Model Fuel Library Subscription Service
molR	Mole ratio
N	Number of particles
N ₂	Nitrogen
nc16h34	n-Hexadecane
NO	Nitric Oxide
NO ₂	Nitrogen Dioxide
NO _x	Nitrous Oxides NO and NO ₂
NR	Not Regulated
NTC	Negative Temperature Coefficient
O ₂	Oxygen
OH	Hydroxyl radical
PCCI	Premixed Charge Compression Ignition
Phi	Equivalence Ratio
SBO	Surrogate Blend Optimizer
SOE	Start of Energizing time of fuel injection
SOI	Start of Injection of fuel
TSI	Threshold Soot Index

1. Introduction

Contents

1.	Introduction	1
1.1.	General Context	3
1.2.	Objectives.....	4
1.3.	Methodology.....	6
1.4.	Thesis Outline.....	6
1.5.	References	7

1.1. General Context

The internal combustion Diesel engine is a highly-versatile power plant for industrial applications and personal mobility. Diesel engines enjoy advantages in efficiency, specific torque, durability, scalability and fuel adaptability [1.1] [1.2] [1.3]. As a result of its importance to society, researchers continue to gain understanding and explore novel combustion systems while engine development engineers work to introduce new Diesel combustion technologies into production [1.4] [1.5] [1.6] [1.7] [1.8]. The continuous improvement of Diesel engine performance, fuel economy, and emissions is required to achieve the complex needs of society [1.9] [1.10].

The application of single-component surrogate fuels, such as n-heptane for combustion kinetics and n-dodecane for physical properties, are well-understood, highly utilized and greatly valued. Through combustion simulation or experimental work, single-component surrogates have played a significant role to expand the fundamental understanding of Diesel combustion. As engineering tools, single-component surrogates have guided the development of conventional and novel Diesel combustion systems [1.11] [1.12] [1.13] [1.14]. To further advance the understanding of Diesel combustion, fully-representative multi-component surrogate fuels are required. This innovation would allow engineers to independently control key fuel properties such as cetane number and the threshold soot index. Recent advances have largely increased the number of pure hydrocarbon fuel components that may be used to formulate Diesel surrogate fuels [1.15] [1.16]. However, as researchers strive to match the combustion and physical properties of Diesel fuel, the complexity of multi-component surrogate fuels has greatly increased. Surrogates assembled with numerous components exceedingly raise the expense of analytical and experimental implementation. For successful industrialization, the tradeoffs between surrogate complexities and predictive combustion simulation accuracy must be understood, rationalized and optimized for the intended application.

This investigation creates fully-representative multi-component surrogate Diesel fuels that are appropriate for both exploratory combustion research and direct application to the engine combustion system design process. The effort must balance complexity and accuracy with usefulness and the ability to industrialize the findings. It is evident that Diesel engine manufacturers

will transition from single-component surrogates to fully-representative multi-component Diesel surrogate fuels as a means to investigate and improve Diesel combustion, efficiency and emissions.

Forces driving this thesis include the understanding that fuel supplies and standards vary regionally and that future Diesel fuels may be considerably different from current fuels. Today, Diesel engine manufacturers encounter a broad range of fuel properties that may influence engine design and the introduction of new technologies. For example, in the United States ASTM D975-16a established a minimum cetane number requirement of 40 whereas in Europe EN 590:2009 required a minimum cetane number of 51. As a result of such variations in fuel properties, Diesel engine combustion system researchers and design engineers require the ability to independently adjust the global fuel properties mimicked by surrogate fuels. New Diesel surrogates are required that vary properties such as cetane number to assess ignition quality and threshold soot index to examine soot and exhaust particle emissions. While doing so other essential Diesel fuel properties such as density, viscosity, heating value and distillation temperatures must be reasonably controlled. It is believed that the systematic application of multi-component surrogate fuels with independent control of fuel cetane number and threshold soot index will enhance the fundamental understanding of combustion, efficiency and emissions. At the same time, improved surrogates may provide a means for future improvements in Diesel spray modeling, combustion simulation, and predictive CO, HC, soot and exhaust particle emissions.

1.2. Objective

The objective of this research is to design and prove fully representative multi-component surrogate Diesel fuels that, along with their chemical kinetic mechanisms, can be brought to routine use in applied research, industrial applications, and most importantly, the designer's toolkit. More representative surrogates should contribute to improvements in predictive combustion simulation. This thesis is intended to provide insight, methods, data and tools for immediate application by researchers and engine developers. For it is in the widespread improvement of engine combustion, efficiency and emissions that the substantial efforts from numerous engine combustion researchers will have the greatest impact on our world.

This thesis integrates a broad range of topics including Diesel combustion, gaseous emissions, exhaust particles, fuel properties, chemical kinetic mechanisms, multi-component fuel modeling and zero-dimensional closed-homogeneous reactor simulation. Each of these research topics are intensely complex. To provide a meaningful contribution, the thesis objective was narrowed and focused to the development of a multi-component surrogate fuel library and the experimental evaluation of a newly developed surrogate fuel.

To achieve the objective this thesis progresses through the following collection of connected activities:

- Establish a development process, including the selection of optimal surrogate fuel components, which can be utilized to create surrogate fuels for intended applications.
- Develop a library of surrogate fuels that closely mimics the physical and chemical properties of petroleum Diesel fuel. This Surrogate Fuel Library will contain 18 surrogate fuels with cetane number ranging from 35 to 60 (in increments of 5) and threshold soot index values of 17, 31 and 48 representative of low, mid-level, and high sooting fuels, respectively.
- Provide surrogate fuel formulations and predict surrogate fuel properties such as cetane number, threshold soot index, density, viscosity, heating value and distillation temperatures.
- Evaluate the surrogate fuel property predictions by comparing predicted and measured fuel properties for a subset of surrogate fuels.
- Demonstrate a good match of the combustion, physical and chemical properties of a multi-component surrogate fuel to the properties of the targeted full-range petroleum Diesel fuel.
- Experimentally evaluate a petroleum Diesel fuel and its matching surrogate fuel with single-cylinder engine tests over a range of engine operating conditions and combustion modes.

1.3. Methodology

This investigation employed analytical tools to develop optimal multi-component surrogate fuels. Detailed ASTM fuel property testing was conducted on a subset of the surrogate fuels. A full-range petroleum Diesel fuel and its matching surrogate were experimentally evaluated in a single-cylinder Diesel engine over a range of engine operating conditions and combustion strategies. The results were reviewed to confirm that the new surrogate fuels are fully-representative of petroleum Diesel fuel.

1.4. Thesis Outline

This thesis is organized into 8 chapters and an Appendix. The content of the chapters and appendix are as follows:

Chapter 1 provides the context and objectives of this thesis.

Chapter 2 is devoted to an elementary review of petroleum Diesel fuel properties.

Chapter 3 describes the computational methods used to conduct this research such as surrogate fuel modeling and gas-phase reactor simulation.

Chapter 4 provides a description of the experimental methods including the single-cylinder Diesel engine, instrumentation, emissions and particle measurements and the engine operating conditions developed for this thesis.

Chapter 5 presents the development of the Surrogate Fuel Library, surrogate fuel property predictions and a detailed comparison of the petroleum Diesel fuel with the surrogate fuel designed to match it.

Chapter 6 gives the results of Diesel engine tests with the petroleum Diesel and its matching surrogate fuel. Tests were conducted at a moderate engine speed and load using a conventional Diesel combustion strategy which included premixed and diffusion combustion regimes. Engine combustion, emissions, soot and exhaust particles are characterized for both fuels.

Chapter 7 provides additional experimental results comparing the Diesel and surrogate fuels under advanced combustion strategies. The fuels were evaluated at a light load operating condition that employed Premixed Charge Compression Ignition (PCCI) and Low Temperature Combustion (LTC) strategies. The low temperature and high temperature heat release were investigated along with emissions and exhaust particles.

Chapter 8 provides the conclusions of this thesis together with proposals for continued research on this topic.

The Appendix contains the formulations and predicted properties for the 18 fuels contained in the Surrogate Fuel Library, complete results of ASTM fuel property evaluations and supplemental data from the Diesel engine testing.

1.5. References

- [1.1] Krieger, R., Siewert, R., Pinson, J., Gallopoulos, N., Hilden, D., Monroe, D., Rask, R., Solomon, A. and Zima, P., "Diesel Engines: One Option to Power Future Personal Transportation Vehicles", *SAE Technical Paper Series*, 1997, doi:10.4271/972683.
- [1.2] Payri, F., Luján, J., Guardiola, C. and Pla, B., "A Challenging Future for the IC Engine: New Technologies and the Control Role", *Oil & Gas Science and Technology - Revue D'IFP Energies Nouvelles* 70(1):15-30, 2014, doi:10.2516/ogst/2014002.
- [1.3] Payri, F., Lopez, J., Pla, B. and Graciano Bustamante, D., "Assessing the Limits of Downsizing in Diesel Engines", *SAE Technical Paper Series*, 2014, doi:10.4271/2014-32-0128.
- [1.4] Jacobs, T., Knafl, A., Bohac, S., Assanis, D. and Szymkowicz, P., "The Development of Throttled and Unthrottled PCI Combustion in a Light-Duty Diesel Engine", *SAE Technical Paper Series*, 2006, doi:10.4271/2006-01-0202.
- [1.5] Di Blasio, G., Beatrice, C. and Molina, S., "Effect of Port Injected Ethanol on Combustion Characteristics in a Dual-Fuel Light Duty

- Diesel Engine", *SAE Technical Paper Series*, 2013, doi:10.4271/2013-01-1692.
- [1.6] Beatrice, C., Avolio, G., Del Giacomo, N. and Guido, C., "Compression Ratio Influence on the Performance of an Advanced Single-Cylinder Diesel Engine Operating in Conventional and Low Temperature Combustion Mode", *SAE Technical Paper Series*, 2008, doi:10.4271/2008-01-1678.
- [1.7] Kokjohn, S., Hanson, R., Splitter, D. and Reitz, R., "Fuel Reactivity Controlled Compression Ignition (RCCI): A Pathway to Controlled High-Efficiency Clean Combustion", *International Journal of Engine Research* 12(3):209-226, 2011, doi:10.1177/1468087411401548.
- [1.8] Benajes, J., García, A., Monsalve-Serrano, J. and Boronat, V., "Achieving Clean and Efficient Engine Operation up to Full Load by Combining Optimized RCCI and Dual-Duel Diesel-Gasoline Combustion Strategies", *Energy Conversion and Management* 136:142-151, 2017, doi:10.1016/j.enconman.2017.01.010.
- [1.9] Chu, S. and Majumdar, A., "Opportunities and Challenges for a Sustainable Energy Future", *Nature* 488(7411):294-303, 2012, doi:10.1038/nature11475.
- [1.10] Sáez-Martínez, F., Lefebvre, G., Hernández, J. and Clark, J., "Drivers of Sustainable Cleaner Production and Sustainable Energy Options", *Journal of Cleaner Production* 138:1-7, 2016, doi:10.1016/j.jclepro.2016.08.094.
- [1.11] Curran, H., Gaffuri, P., Pitz, W. and Westbrook, C., "A Comprehensive Modeling Study of n-Heptane Oxidation", *Combustion and Flame* 114(1-2):149-177, 1998, doi:10.1016/s0010-2180(97)00282-4.
- [1.12] Patel, A., Kong, S. and Reitz, R., "Development and Validation of a Reduced Reaction Mechanism for HCCI Engine Simulations", *SAE Technical Paper Series*, 2004, doi:10.4271/2004-01-0558.
- [1.13] Banerjee, S., Tangko, R., Sheen, D., Wang, H. and Bowman, C., "An Experimental and Kinetic Modeling Study of n-Dodecane Pyrolysis

- and Oxidation", *Combustion and Flame* 163:12-30, 2016, doi:10.1016/j.combustflame.2015.08.005.
- [1.14] Bolla, M., Chishty, M., Hawkes, E. and Kook, S., "Modeling Combustion under Engine Combustion Network Spray A Conditions with Multiple Injections using the Transported Probability Density Function Method", *International Journal of Engine Research* 18(1-2):6-14, 2017, doi:10.1177/1468087416689174.
- [1.15] Westbrook, C., Pitz, W., Herbinet, O., Curran, H. and Silke, E., "A Comprehensive Detailed Chemical Kinetic Reaction Mechanism for Combustion of n-Alkane Hydrocarbons from n-Octane to n-Hexadecane", *Combustion and Flame* 156(1):181-199, 2009, doi:10.1016/j.combustflame.2008.07.014.
- [1.16] Pitz, W. and Mueller, C., "Recent Progress in the Development of Diesel Surrogate Fuels", *Progress in Energy and Combustion Science* 37(3):330-350, 2011, doi:10.1016/j.pecs.2010.06.004.

2. Diesel Fuel Properties

Contents

2.	Diesel Fuel Properties	11
2.1.	Introduction.....	13
2.2.	Diesel Fuel	14
2.3.	Summary	36
2.4	References	37

2.1. Introduction

Rudolf Diesel's original invention was a compression-ignition engine designed to run on coal dust. The design was patented but proved to be unsuccessful. Years later, Rudolf Diesel determined that his engine was better suited for liquid fuels. Kerosene refining resulted in liquid hydrocarbon by-products that were suitable for his compression-ignition combustion system. Engine modifications were made and success was achieved with the liquid fuel. For decades his invention has been continuously advanced and currently powers the world economy through electric energy generation, shipping, transport industries (rail and truck), heavy- and light-duty construction vehicles and personal mobility such as buses and passenger vehicles. Nowadays, the combustion process, the engine and the liquid fuel all bear his name "Diesel".

Diesel fuel is composed of hundreds of hydrocarbon species that are not well-characterized. As a result of this complex and undefined composition, researchers create surrogates for Diesel fuel. A surrogate fuel is a simple analog created from a small set of well-defined hydrocarbon species. The surrogate fuel is designed to mimic the properties of a full-range petroleum Diesel fuel. Surrogate fuels have many applications including Diesel spray characterization, chemical kinetic modeling, combustion, and emissions investigations. The first surrogates consisted of one or two hydrocarbon components that successfully mimicked Diesel fuel properties such as cetane number and lower heating value. However, these simple surrogates could not match other important properties such as the fuel distillation temperatures. Recent work has increased the number of well-characterized hydrocarbons that are representative of Diesel fuel and potentially useful as surrogate fuel components. These efforts have enabled the development of multi-component surrogate fuels that can closely replicate the properties of Diesel fuel.

To provide a basis for the development of surrogate Diesel fuels, this chapter reviews Diesel fuel chemistry, fuel properties, and Diesel fuel specifications for the United States and Europe.

2.2. Diesel Fuel

Diesel fuel is a complex liquid that is used to fuel Diesel engines. The most common form is a fractional distillate of petroleum crude oil and in the context of this thesis is referred to as petroleum Diesel. There are a tremendous amount of ongoing research into advanced, alternative and renewable sources for Diesel fuel such as biodiesel, biomass to liquid (BTL), algae, natural gas to liquid (GTL), coal liquefaction and others. The focus of this thesis, however, is on developing surrogates for petroleum Diesel fuel.

Petroleum Diesel is a mixture of thousands of hydrocarbon compounds. Crude oil refining separates the hydrocarbons by means of a distillation process. An example of a refinery distillation column is shown in Figure 2-1. Diesel fuel is obtained from the hydrocarbons with boiling points in the approximate range of 150 °C to 400 °C (450 °F to 650 °F). In this distillation temperature range, the hydrocarbon molecules generally contain between 8 and 22 carbon atoms. The fuel is further refined to remove impurities such as sulfur and to improve fuel properties and chemistry. Upon distillation, Diesel fuel is primarily composed of hydrocarbon classes which include normal-alkanes, iso-alkanes, cyclo-alkanes and aromatics. The aromatic hydrocarbons are classified by the number benzene rings in the molecule. Mono-aromatics have a single benzene ring and polycyclic aromatic hydrocarbons (PAH) contain two or more benzene rings. More information on Diesel fuels and refining are available from Chevron [2.1], DieselNet [2.2], and 5 Oaks Petroleum [2.3].

Crude oil properties vary widely and is processed by refineries throughout the world. As a result, the properties of petroleum Diesel also vary. Local, national and regional specifications are in place to standardize and improve fuel quality. Examples include the World-Wide Fuels Charter [2.4], the United States EPA Diesel Fuel Standards [2.5], the California Diesel Fuel Program [2.6], and the European Committee for Standardization (CEN) EN 590 and EN 14214 [2.7]. The global efforts to create specifications and improve fuel quality enable technological advancements that can lead to increased engine efficiency and reduced environmental impact of emissions. The marked reduction of fuel-borne sulfur is an example of combined fuel and vehicle improvements to reduce pollutants [2.8].



Figure 2-1: Distillation column showing the separation of crude oil into distillates [2.3].

2.2.1 Diesel Fuel Chemistry

This section introduces the hydrocarbon molecules and classifications of the Diesel fuel chemistry. The information was obtained from references [2.1], [2.9], [2.10], [2.11], and [2.12]. A basic understanding of Diesel fuel chemistry is required. The development of surrogate fuels with desired properties is accomplished by selecting the appropriate hydrocarbon species with the necessary physical and chemical properties. In essence, fuel chemistry establishes the fuel properties.

Alkanes (Paraffins)

A general classification of hydrocarbon molecules that contain only single bonds between the hydrogen and carbon atoms are called alkanes. They are often referred to as saturated hydrocarbons. Alkanes are separated into subclasses based on their molecular structure. These subclasses include normal-alkanes that have a linear structure, iso-alkanes that have a branched structure, and cyclo-alkanes that have a cyclic or ring structure. Understanding the alkane molecular structure is important because the

structure has a significant impact on the physical and chemical properties of the hydrocarbon specie.

Isomers

Isomers are compounds with the same molecular formula but have different molecular structures. A common example of isomers are the octane molecules n-octane and iso-octane. Both molecules have the same chemical formula, C_8H_{18} , but the structures are different, as shown in Figure 2-2. The larger the molecule the more possibilities exist for isomers of that molecule. For example, there are 9 isomers for C_7H_{16} (heptane) while there are 75 isomers for $C_{10}H_{22}$ (decane). With regard to Diesel fuels, the isomers n-hexadecane and 2,2,4,4,6,8,8-heptamethylnonane have important applications to surrogate fuels. These large alkanes have the chemical formula $C_{16}H_{34}$. However, the structural differences significantly affect certain fuel properties, such as cetane number. As a result of structural differences, isomers of the same chemical formula are uniquely different compounds that can have significantly different physical and chemical properties.

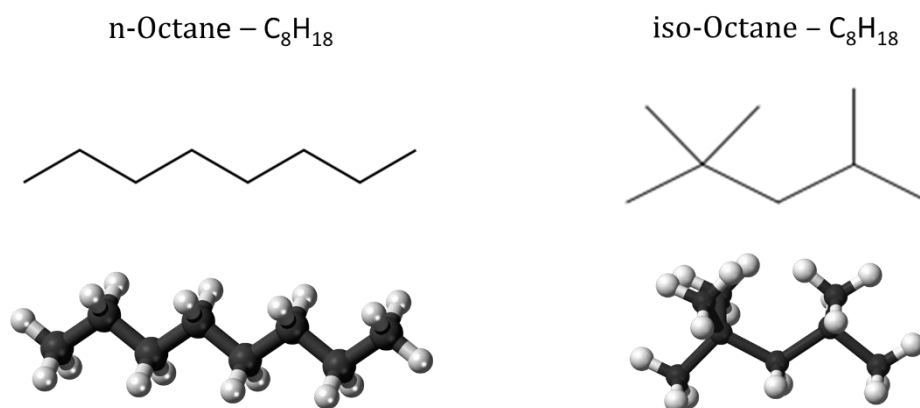


Figure 2-2: Schematic diagrams for n-octane and iso-octane showing the differences between linear and branched structures.

Normal-Alkanes (Normal-Paraffins)

Hydrocarbon molecules where the atoms are linked to have a linear chain-like molecule structure are known as normal-alkanes (n-alkanes). Carbon

atoms along the backbone are bonded to two hydrogen atoms while each end of the molecule is bonded to a methyl group (CH_3). Normal-alkanes have the general molecular formula $\text{C}_n\text{H}_{2n+2}$ where n is the carbon number of the molecule. For example, n-heptane has the molecular formula of C_7H_{16} and n-hexadecane has the formula of $\text{C}_{16}\text{H}_{34}$. Examples of the n-alkane molecular structure are given below in Figure 2-3.

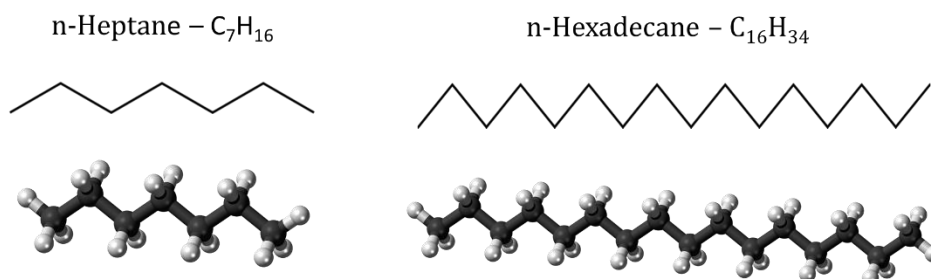


Figure 2-3: Stick diagrams (top) and ball-and-stick diagrams (beneath) for n-Heptane and n-Hexadecane.

Iso-Alkanes (Iso-Paraffins)

Iso-alkanes have a backbone with a chain-like structure, similar to n-alkanes, but also have carbon atoms branching off from the backbone. Each branch ends with a methyl group. Like n-alkanes, iso-alkanes have the general formula $\text{C}_n\text{H}_{2n+2}$. Molecules with the same chemical formula can have different branched structures. As a result, each branched structure is a unique compound with its own physical and chemical properties. The terms iso-alkane and iso-paraffin are often used interchangeably.

Cyclo-Alkanes (Cyclo-Paraffins)

Hydrocarbon compounds where the carbon atoms are arranged in a ring structure with single carbon-carbon bonds are known as cyclo-alkanes. Two or more rings may be linked with some carbon atoms shared by neighboring rings. Cyclo-alkanes may have additional chains branched from a carbon atom contained within the ring structure. These branches end with a methyl group. The occurrence of branched and multiple-ring structures influence the physical properties of the molecule. Referring to Figure 2-4, decalin is a

two-ring cyclo-alkane and butylcyclohexane is a branched, one-ring cyclo-alkane.

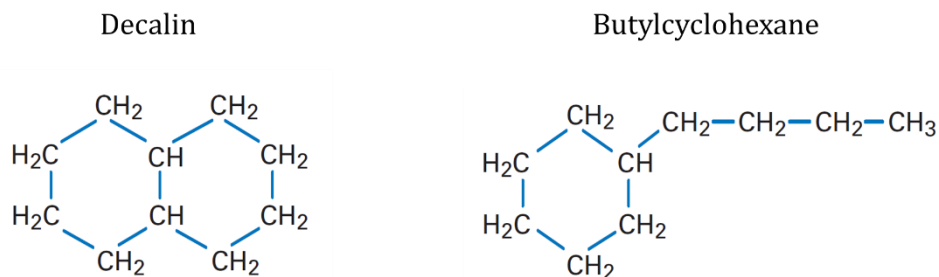


Figure 2-4: Two-ring and branched one-ring cyclo-alkanes.

Alkenes (Olefins)

The alkene hydrocarbon classification is similar to the alkane classification. However, alkene molecules contain at least one carbon-to-carbon double bond. Therefore, alkenes are considered unsaturated hydrocarbons. Similar to alkanes, alkenes are classified as normal-alkenes, iso-alkenes and cyclo-alkenes based on the molecular structures. Alkenes rarely occur in crude oil. They are present in Diesel fuel in small amounts due to refinery processes. As a result, alkenes have not been widely used as components for Diesel surrogate fuels.

Aromatics

Aromatics have an important effect on Diesel fuel properties, combustion, soot formation and PAH emissions. The building block of an aromatic compound is the benzene molecule. Benzene is a hydrocarbon molecule with six carbon atoms that form a regular, planar hexagon ring structure. Each carbon atom along the ring is bonded to a single hydrogen hence, benzene has the molecular formula C_6H_6 . The carbon-to-carbon bonds within the benzene ring have unique attributes. They are often depicted as alternating double and single bonds. More appropriately, the double bonds are actually delocalized and hence more flexible than standard double bonds. Generally, single and double bonds have different lengths. However, due to delocalization every carbon-to-carbon bond in the benzene molecule has the same length. The actual bond length is somewhere between the

single and double bond lengths. The ring structure and the presence of delocalized electrons makes benzene an exceptionally stable molecule. Additional bonds to the benzene ring employ the delocalized electrons and results in a loss of molecular stability.

Hydrocarbon compounds that contain at least one benzene ring are classified as aromatics. Aromatics can have branched chains attached to a carbon atom in the benzene ring. They can also combine to form multi-ring structures. Several examples of aromatics with branched and multi-ring structures are shown in Figure 2-5. Toluene and n-propylbenzene are branched aromatics. Tetralin is an aromatic compound with one benzene ring bonded to one cyclo-alkane ring. Aromatics may also contain more than one benzene ring with some carbon atoms fused to neighboring rings (e.g., 1-methylnaphthalene). Structure plays a significant role in the properties of aromatic hydrocarbons. For example, an increase in the number of benzene rings generally increases density, boiling point and smoke point. Aromatics containing a single benzene ring are classified as mono-aromatics. Polycyclic aromatics contain two or more benzene rings and are also known as polycyclic aromatic hydrocarbons (PAH).

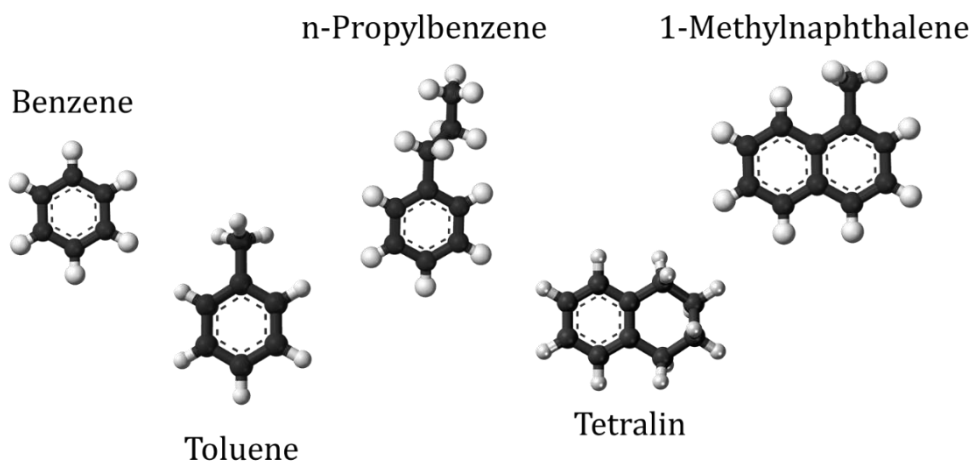


Figure 2-5: Examples of aromatic structures: benzene, branched aromatics toluene and n-propylbenzene, cyclo-aromatic tetralin and polycyclic aromatic 1-methylnaphthalene.

Carbon Atom Number Distribution

The distillation process separates hydrocarbons molecules based on their boiling points. As mentioned earlier, the distillation temperature range for Diesel fuel is from 150 °C to 400 °C. This relatively wide temperature range results in a broad distribution of hydrocarbon molecules (species) whose carbon atom numbers vary from 8 to 24. Figure 2-6 shows the carbon atom number distribution for a typical North American No. 2-D Diesel fuel, adapted from [2.1]. This example shows a fairly normal distribution with approximately 50% of the fuel mass residing in the carbon number range 14-18. The carbon number distributions can vary based on the source of the crude oil and the refining process. The mass percent depicted by each vertical bar contains numerous types of alkane and aromatic hydrocarbon species with varying branched and ring structures. Diesel fuel physical and chemical properties are established by the hydrocarbon species contained within the vertical bars shown in Figure 2-6.

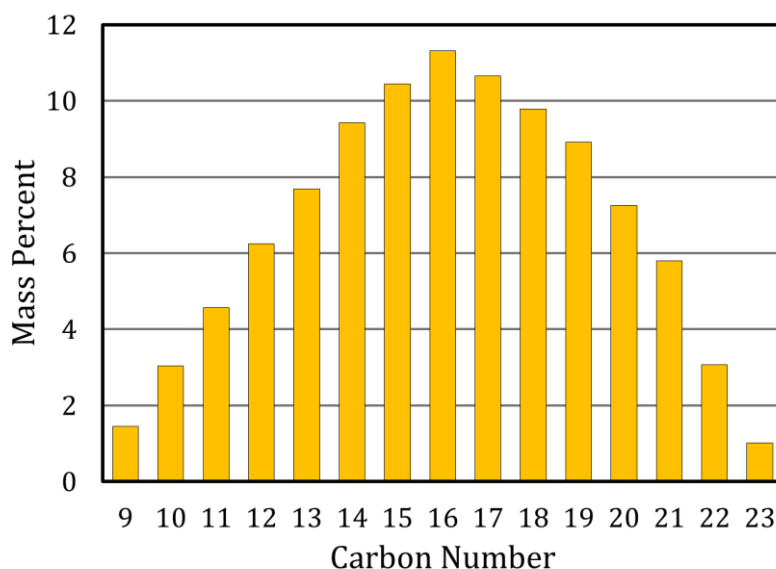


Figure 2-6: Typical carbon number distribution from No. 2-D Diesel fuel, adapted from [2.1].

Hydrocarbon Species in Diesel Fuel

With the understanding that the distribution of hydrocarbon species influences Diesel fuel properties, researchers have employed sophisticated experimental techniques to identify and quantify hydrocarbon classes, molecular structures and individual species in Diesel fuel. Knowledge of the hydrocarbon species can provide insight and potentially explain what controls the physical and chemical fuel properties of Diesel fuel.

Vendeuvre et al., performed detailed characterizations of middle distillate fuels [2.13]. The experimental techniques included ASTM fuel property test methods, gas chromatography (GC), liquid chromatography (LC) and mass spectrometry (MS), and a comprehensive two-dimensional gas chromatography (GC×GC). Figure 2-7 provides an example of the experimental characterization of the fuel. The weight percent for seven hydrocarbon classes were quantified at each carbon atom number. For example, the data showed that triaromatic hydrocarbons were present in the 14-18 carbon number range. (Triaromatic hydrocarbons contain three benzene rings.) Understanding the fuel composition supports the refinery efforts to control the amounts of given hydrocarbon classes, improve fuel quality, and adhere to Diesel fuel specifications.

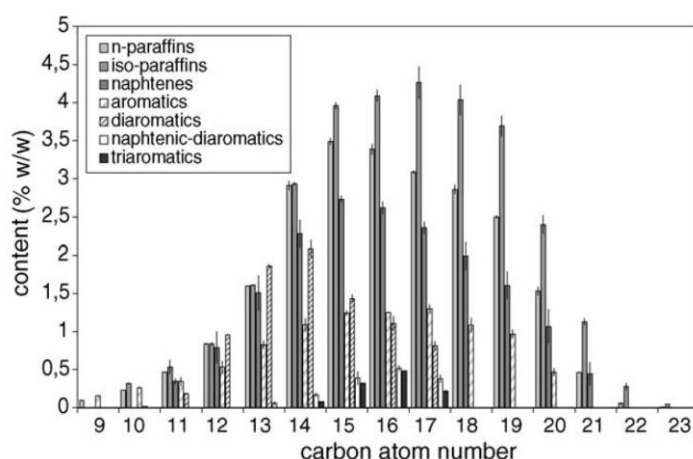


Figure 2-7: Detailed characterization quantifying the molecular distribution of seven hydrocarbon classes per carbon atom number [2.13].

Researchers have gained further insight by applying sophisticated fuel characterization techniques to study the hydrocarbon compositions of market fuels. For example, Farrell, et al., conducted a detailed analysis of three different market fuels [2.14]. The analysis provided the weight percent for several hydrocarbon classes including: n-alkanes, iso-alkanes, cyclo-alkanes and aromatics. For cyclo-alkanes and aromatics, the analysis provided data for one-ring, two-ring, and three-ring compounds. The results in Figure 2-8 show significant differences between the fuels. Fuels A and C had broader carbon atom number distributions than Fuel B. Additionally, the weight percent of Fuel B was dominated by cyclo-alkanes and contained significantly less aromatics. In contrast, the aromatic content of Fuel C was significantly greater than Fuel A and Fuel B. It is clear from this example that significant variations exist in Diesel fuel chemistry. Variations in Diesel fuel chemistry drive the variations observed in Diesel fuel properties.

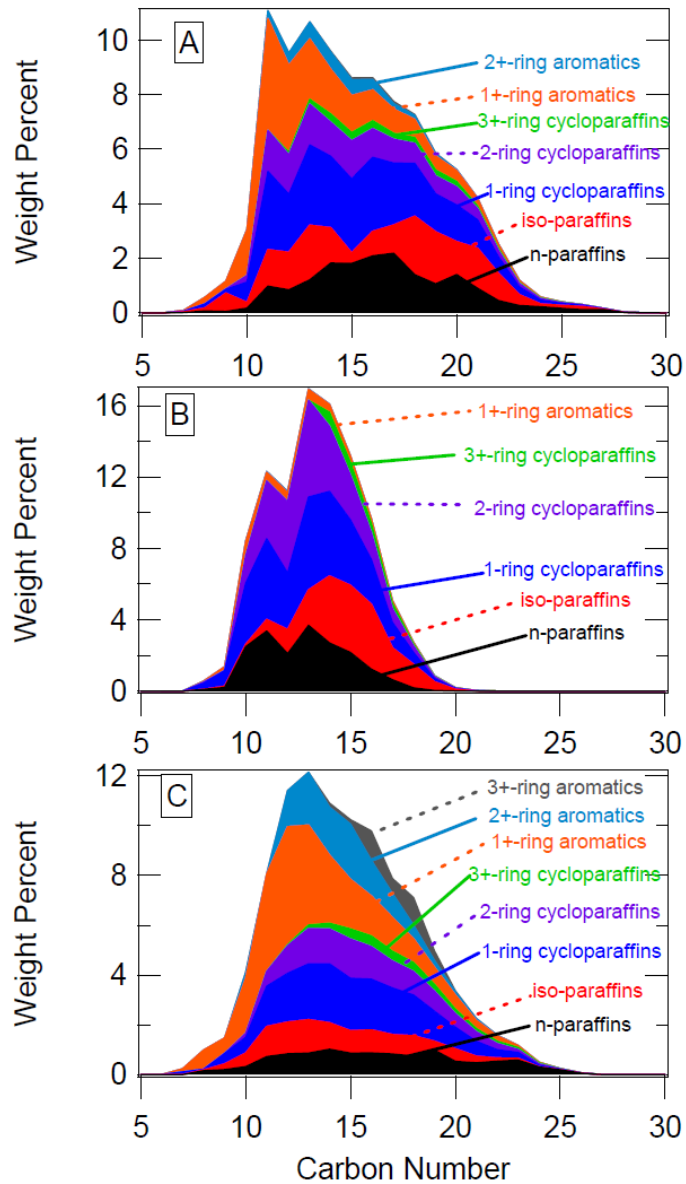


Figure 2-8: Detailed analysis showing carbon number, hydrocarbon class and molecular structure for three commercial Diesel fuels. Significant variation exists between the Diesel fuels [2.14].

2.2.2 Diesel Fuel Properties

This section provides a brief introduction of the fuel properties that are relevant for Diesel combustion and the development of surrogate fuels. References for the information in this section include [2.1], [2.9], [2.10], [2.11], [2.12], and the cited ASTM test procedures.

Cetane Number (CN)

Diesel fuel cetane number is a metric that experimentally quantifies the auto ignition quality of a fuel. Diesel fuels with short ignition delays will have high cetane numbers while fuels with longer ignition delays will have lower cetane numbers. Fuels with high cetane number are generally considered to be higher quality fuels.

Fuel cetane number is an important metric for Diesel engines as it impacts the start of combustion from which greatly influences engine starting, efficiency, performance, emissions and combustion noise. Cetane number can be measured using two different test procedures. ASTM D613 involves testing the fuel in a single-cylinder engine and comparing the measured ignition delay with calibrated reference fuels [2.15]. ASTM D6890 provides an alternative method that measures the ignition delay from injecting the fuel into a high temperature, high pressure constant-volume chamber [2.16]. Again, cetane number is determined by correlating measurements to a set of reference fuels. There are three primary reference fuels for cetane testing: n-hexadecane with CN=100, heptamethylnonane with CN=15 and 1-methylnaphthalene with CN=0. The primary reference fuels are blended to yield reference fuels with varying cetane number allowing improved correlation equations.

Smoke Point

Smoke Point is the maximum smokeless height that can be achieved by a diffusion flame from fuel burned in a wick-fed lamp. ASTM D1322 is the method used to determine the fuel smoke point [2.17]. The test procedure specifies the wick and lamp design and reports the flame height in millimeters. Smoke point is a simple bulk fuel property that relates to a fuel's tendency to produce soot during combustion. Smoke point is an important fuel property for jet fuels and is becoming a useful metric for Diesel fuel.

Fuels with low smoke points are considered to have a higher tendency to produce soot while higher smoke point fuels are considered to have a lower tendency to produce soot.

Threshold Soot Index (TSI)

Threshold Soot Index is another measure of the fuel tendency to create soot in a diffusion flame. The metric is an improvement over the smoke point because it accounts for the fuel molecular weight and differences in smoke point test devices. The metric is defined such that fuels with low sooting tendency will have low TSI values while fuels with high sooting tendency will have high TSI values. For example, n-heptane is a low sooting fuel with a TSI of 3 whereas toluene is a high sooting fuel with a TSI of 40.

TSI is calculated with the method defined by Calcote and Manos [2.18] using the following equation:

$$TSI = a \left(\frac{\text{Fuel Molecular Weight}}{\text{Smoke Point Height}} \right) + b$$

Constants a and b are defined by the test equipment. Smoke point height measurements are from ASTM D1322. In this thesis, the molecular weight of Diesel fuel was assumed to be 200 g/mol. The molecular weight of the surrogate was calculated using a mole-weighted average of the fuel component molecular weights [2.18].

Lower Heating Value

The Lower Heating Value (LHV) is the amount of thermal energy released when a unit mass of fuel is burned at constant pressure (also known as the net heat of combustion). Test procedure ASTM D240N determines the lower heating value by burning fuel in an oxygen bomb calorimeter under prescribed conditions. Temperature measurements before, during and after are used to compute the lower heating value. At the end of the procedure all of the combustion products are in the gaseous state and water is in the vapor state. Therefore, the energy required to vaporize the water is not included in the heat release [2.19]. The lower heating value is required to calculate engine efficiency and other performance metrics.

Density

Fuel density is the mass per unit volume at a specific temperature and is measured by ASTM [2.20]. Density is a temperature-dependent property and as such, fuel density decreases as temperature increases. Density is an important physical property that is used in combination with other properties to characterize Diesel fuel. For example, fuel density together with the lower heating value determine how much fuel energy is injected into the engine with each injection event. Density is driven by the hydrocarbon composition of the fuel. For example, aromatic hydrocarbons have higher density than alkanes. Therefore, Diesel fuels with high density may contain higher amounts of aromatics.

Kinematic and Dynamic Viscosity

Liquid viscosity is a measure of a fluid's resistance to deformation by shear stress. Diesel fuel kinematic viscosity (ν) is measured using the ASTM D445 test procedure. The dynamic viscosity (μ) is calculated by multiplying the kinematic viscosity (ν) by the fuel density (ρ) [2.21]. Viscosity is an important physical property for Diesel fuel. It impacts the work required to pump the fuel through filters and lines. It can also impact the operation of high-pressure fuel pumps and injectors especially when the fuel also serves as a lubricant. Viscosity is a temperature-dependent property. As temperature increases the viscosity of Diesel fuel decreases. During fuel injection, Diesel fuel viscosity, and its temperature-dependency, influences the fuel spray breakup into droplets.

Distillation Curve

ASTM D86 defines a test method to quantify the boiling range characteristics of petroleum products, also known as the distillation curve. During the procedure, a 100-ml fuel sample is distilled at ambient pressure using a prescribed distillation apparatus and protocol. The test results generate a distillation curve by correlating the volume percent evaporated, or volume percent recovered, with the corresponding temperature [2.22]. The distillation curve defines the fuel boiling range, provides insight into the fuel composition and the potential behavior of the fuel under given conditions. In direct-injection Diesel engine, fuel volatility can impact the fuel vapor distribution in the combustion chamber and influence the combustion

process in several ways. The low temperature volatility affects fuel vapor under cold conditions which influences engine starting and warm-up. The high temperature volatility reflects to some extent the amount of higher molecular weight hydrocarbons present in the fuel which can influence the formation of soot and other emissions.

Hydrocarbon and Aromatic Composition

ASTM D1319 provides a simple volume percent characterization of Diesel fuel into three hydrocarbon classifications: alkanes, alkenes and aromatics [2.23]. The test procedure does not characterize the n-alkane, iso-alkane or cyclo-alkane content of the fuel. To further characterize the aromatic hydrocarbons, the ASTM D5186 test procedure separates the aromatic hydrocarbons into three classifications: total aromatics, mono-cyclic aromatics (one benzene ring) and poly-cyclic aromatics (more than one benzene ring) [2.24]. The aromatics are measured on a percent mass basis. Understanding the aromatic content provides important insight into other fuel properties. For example, aromatic compounds generally have higher density and higher smoke points than alkanes.

Flash Point

The Pensky-Martens closed-cup flash point test defined in the ASTM D93 test procedure provides one measure of flash point for petroleum Diesel. The method quantifies the tendency of the fuel to form a flammable mixture with air under controlled laboratory conditions in the 40 to 370°C temperature range. It is important to note that the flash point reported by ASTM D93 is for one specific test apparatus and cannot be correlated with flash point measurements from a different apparatus [2.25]. Pensky-Martens flash point measurements are useful for comparing fuels. However, it is only one of many properties that are required to assess the overall flammability hazard of Diesel and other fuels. With respect to surrogate fuels, and this thesis, the flash point determined the safe handling procedures for the single-component and multi-component surrogate fuels.

Properties of Market Diesel Fuels

To explore differences in Diesel fuel properties, five market Diesel fuels were collected and analyzed. The results are presented in Table 2-1. Although not an exhaustive list of fuels, the results show considerable differences in the fuel properties for the five Diesel fuels. For example, the cetane number ranged from 44.2 for the Tar Sands Diesel to 55.8 for the Swedish Class-I fuel. Moreover, many of the Swedish Class-I fuel properties were considerably different from the other fuels. The viscosity and distillation temperatures were lower for the Swedish Class-I fuel. In addition, the alkane content was very high and the aromatic content was very low. Substantial differences in fuel properties present challenges for surrogate Diesel fuels. For example, a surrogate fuel designed to mimic the properties of the Tar Sands Diesel may not be adequate to represent the Swedish Class-I fuel. As result, surrogate fuels may need to be individually tailored to represent specific fuels. Another approach is to develop a library of surrogate fuels with properties that are tailored to cover a broad range of market fuels. Such an approach would provide a consistent set of surrogate fuels for research topics and Diesel combustion system development.

Table 2-1: Properties of market Diesel fuels.

Fuel Property	ULSD High-Cetane	ULSD Mid-Cetane	Swedish Class-I	Euro Cert	Tar Sands Diesel
Cetane Number	50.9	45.0	55.8	50.4	44.2
Net Heat of Combustion (MJ/kg)	42.86	43.04	43.50	43.19	43.08
Density at 15 °C (kg/m ³)	849.0	838.8	808.9	836.3	838.9
Kinematic Viscosity at 40 °C (cSt)	3.060	2.266	1.821	2.631	2.257
Distillation Temperature - T ₁₀ at 10 %v/v (°C)	227	204	197	187	200
Distillation Temperature - T ₅₀ at 50 %v/v (°C)	237	240	224	276	247
Distillation Temperature - T ₉₀ at 90 %v/v (°C)	312	312	269	326	303
Alkanes (volume %)	76.0	72.3	92.4	81.9	80.7
Alkenes (volume %)	7.5	6.8	4.1	5.0	3.0
Aromatics (volume %)	16.5	20.9	3.5	13.1	16.3
Total Aromatics (mass %)	16.4	20.3	3.2	13	16.9
Mono-Cyclic Aromatics (mass %)	16.2	19.2	2.9	9.3	16.5
Poly-Cyclic Aromatics (mass %)	0.2	1.0	0.3	3.7	0.4

Properties of Hydrocarbon Classes and Species

The previous sections provided an introduction of Diesel fuel chemistry, fuel properties and property data for several market Diesel fuels. The next step towards successfully formulating surrogate fuels is to gain an understanding of the properties of individual hydrocarbon species that are representative of Diesel fuel hydrocarbons. Table 2-2 provides the chemical formula, cetane number, TSI, density and boiling point for 35 hydrocarbon species separated into four classifications. Although property data was not available for all fuels, a study of the properties provided valuable insight and trends within hydrocarbon classifications. The observations are summarized below:

n-Alkanes

- Cetane number increased with carbon number (54-110)
- TSI was very low and essentially constant (~6)
- Density increased with carbon number (0.683-0.789 g/ml)
- Boiling point increased with carbon number (99-344 °C)

iso-Alkanes

- Cetane number varied by compound (14-67)
- TSI varied by compound (limited data)
- Density increased with carbon number (limited data)
- Boiling point increased with carbon number (limited data)

cyclo-Alkanes

- Cetane number varied by compound (18-70)
- TSI varied by compound (limited data)
- Density varied by compound (limited data)
- Boiling point increased with carbon number (81-282 °C)

Aromatics

- Cetane number was generally low and varied by compound
- TSI varied was generally high and varied by compound (31-100)
- Density varied by compound (0.862-1.041 g/ml)
- Boiling point increased with carbon number (81-282 °C)

Table 2-2: List of representative Diesel fuel hydrocarbon compounds including chemical formula, cetane number, TSI and boiling point [2.1] [2.26].

Class	Representative Compound	Formula	Cetane Number	TSI	Density (g/ml)	Boiling Point (°C)
n-Alkanes	Heptane	C ₇ H ₁₆	54	3	0.683	99
	Decane	C ₁₀ H ₂₂	77	5	0.730	174
	Dodecane	C ₁₂ H ₂₆	84	6	0.750	216
	Pentadecane	C ₁₅ H ₃₂	96	6	0.769	269
	Hexadecane	C ₁₆ H ₃₄	100	6	0.773	287
	Eicosane	C ₂₀ H ₄₂	110	6	0.789	344
iso-Alkanes	Iso-Hexane	C ₆ H ₁₄	34	3	0.653	61
	Iso-Octane	C ₈ H ₁₈	14	7	0.692	99
	3-Ethyldecane	C ₁₂ H ₂₆	48			209
	4,5-Diethyloctane	C ₁₂ H ₂₆	20			193
	Heptamethylnonane	C ₁₆ H ₃₄	15	21	0.793	240
	8-Propylpentadecane	C ₁₈ H ₃₈	48			
	7,8-Diethyltetradecane	C ₁₈ H ₃₈	67			
	9,10-Dimethyloctane	C ₂₀ H ₄₂	59			
cyclo-Alkanes	Cyclohexane	C ₆ H ₁₂	18	4	0.779	81
	Methylcyclohexane	C ₇ H ₁₄	22	5	0.770	101
	Decahydronaphthalene	C ₁₀ H ₁₈	44	20	0.896	186
	n-Butylcyclohexane	C ₁₀ H ₂₀			0.818	181
	n-Pentocyclopentane	C ₁₀ H ₂₀				181
	3-Cyclohexylhexane	C ₁₂ H ₂₄	36			216
	n-Nonylcyclohexane	C ₁₅ H ₃₀				282
	n-Decylcyclopentane	C ₁₅ H ₃₀				279
	2-Methyl-3-cyclohexylnonane	C ₁₅ H ₃₀	70			
	2-Cyclohexyltetradecane	C ₂₀ H ₄₂	57			
Aromatics	Benzene	C ₆ H ₆	11	31	0.874	80
	Toluene	C ₇ H ₈	3	40	0.865	111
	Styrene	C ₈ H ₈	7	67	0.909	145
	Ethylbenzene	C ₈ H ₁₀	7	54	0.867	136
	m-Xylene	C ₈ H ₁₀	3	51	0.864	139
	n-Propylbenzene	C ₉ H ₁₂	7	53	0.862	159
	Trimethylbenzene	C ₉ H ₁₂	9	51	0.876	170
	Naphthalene	C ₁₀ H ₈	23	100	1.025	218
	1-Methylnaphthalene	C ₁₁ H ₁₀	0	100	1.001	245
	Biphenyl	C ₁₂ H ₁₀	21		1.041	256
	n-Tetradecylbenzene	C ₂₀ H ₃₄	72			

2.2.3 Diesel Fuel Specifications

As mentioned above, Diesel fuel properties vary across geographical regions and seasons. Crude oil sources and refinery processes can also effect Diesel fuel properties. Local, national and regional agencies have adopted specifications to control selected Diesel fuel properties to specified values or ranges. Diesel fuels are classified into several grades and the specifications can vary between the grades. Examples of Diesel fuel specifications include ASTM D975 for North America [2.27] and EN590 for the European Union [2.28]. Table 2-3 shows the ASTM D975 specifications for several grades of Diesel fuel while Table 2-4 provides the EN590 specifications. This thesis focused on Grade No. 2-D for ASTM D975.

In the context of this thesis, a fully-representative surrogate Diesel fuel must replicate the properties of a full-range petroleum Diesel fuel. The surrogate Diesel fuel properties should be compared with regulated fuel specifications to recognize and account for any discrepancies. The intent is to understand where and why surrogate fuel properties are not aligned with the specifications.

A comparison of ASTM D975 and EN590 reveals differences in regulated properties and test methods. Several Diesel fuel properties are not regulated, such as Lower Heating Value and TSI. Regulated properties that can influence Diesel fuel spray, combustion, and emissions are summarized in Table 2-5.

Table 2-3: ASTM D975 Diesel fuel specifications [2.27]


D975 – 16a
TABLE 1 Detailed Requirements for Diesel Fuel Oils^{A, B}

Property	ASTM Test Method ^C	Grade						
		No. 1-D S15	No. 1-D S500 ^D	No. 1-D S5000 ^E	No. 2-D S15 ^F	No. 2-D S500 ^{D, F}	No. 2-D S5000 ^{E, F}	No. 4-D ^E
Flash Point, °C, min.	D93	38	38	38	52 ^F	52 ^F	52 ^F	55
Water and Sediment, percent volume, max	D2709 D1796 D86	0.05	0.05	0.05	0.05	0.05	0.05	...
Distillation Temperature, °C 90 %, percent volume recovered								0.50
min		282 ^F	282 ^F	282 ^F	...
max		288	288	288	338	338	338	...
Kinematic Viscosity, mm ² /S at 40 °C	D445							
min		1.3	1.3	1.3	1.9 ^F	1.9 ^F	1.9 ^F	5.5
max		2.4	2.4	2.4	4.1	4.1	4.1	24.0
Ash percent mass, max	D482	0.01	0.01	0.01	0.01	0.01	0.01	0.10
Sulfur, ppm (µg/g) ^G max	D5453	15	15
percent mass, max	D2622 ^H	...	0.05	0.50	...	0.05	0.50	2.00
Copper strip corrosion rating, max (3 h at a minimum control temperature of 50 °C)	D130	No. 3	No. 3	No. 3	No. 3	No. 3	No. 3	...
Cetane number, min ^I	D613	40 ^J	40 ^J	40 ^J	40 ^J	40 ^J	40 ^J	30 ^J
One of the following properties must be met:								
(1) Cetane index, min.	D976–80 ^H	40	40	...	40	40
(2) Aromaticity, percent volume, max	D1319 ^H	35	35	...	35	35
Operability Requirements								
Cloud point, °C, max	D2500	K	K	K	K	K	K	...
or								
LTF/CFPP, °C, max	D4539/D6371							
Ramsbottom carbon residue on 10 % distillation residue, percent mass, max	D524	0.15	0.15	0.15	0.35	0.35	0.35	...
Lubricity, HFRR @ 60 °C, micron, max	D6079/D7688	520	520	520	520	520	520	...
Conductivity, pS/m or Conductivity Units (C.U.), min	D2624/D4308	25 ^L	25 ^L	25 ^L	25 ^L	25 ^L	25 ^L	...

^A To meet special operating conditions, modifications of individual limiting requirements may be agreed upon between purchaser, seller, and manufacturer.

^B See Sections 6 and 7 for further statements on diesel fuel requirements.

^C The test methods indicated are the approved referee methods. Other acceptable methods are indicated in 5.1.

^D Under United States regulations, if Grades No. 1–D S500 or No. 2–D S500 are sold for tax exempt purposes then, at or beyond terminal storage tanks, they are required by 26 CFR Part 48 to contain the dye Solvent Red 164 at a concentration spectrally equivalent to 3.9 lb of the solid dye standard Solvent Red 26 per thousand barrels of diesel fuel or kerosine, or the tax must be collected.

^E Under United States regulations, Grades No. 1–D S5000, No. 2–D S5000, and No. 4–D are required by 40 CFR Part 80 to contain a sufficient amount of the dye Solvent Red 164 so its presence is visually apparent. At or beyond terminal storage tanks, they are required by 26 CFR Part 48 to contain the dye Solvent Red 164 at a concentration spectrally equivalent to 3.9 lb of the solid dye standard Solvent Red 26 per thousand barrels of diesel fuel or kerosine.

^F When a cloud point less than –12 °C is specified, as can occur during cold months, it is permitted and normal blending practice to combine Grades No. 1 and No. 2 to meet the low temperature requirements. In that case, the minimum flash point shall be 38 °C, the minimum viscosity at 40 °C shall be 1.7 mm²/s, and the minimum 90 % recovered temperature shall be waived.

^G Other sulfur limits can apply in selected areas in the United States and in other countries.

^H These test methods are specified in 40 CFR Part 80 for S500 grades.

^I Where cetane number by Test Method D613 is not available, Test Method D4737 can be used as an approximation. Although biodiesel blends are excluded from the scope of Test Method D4737, the results of Test Method D4737 for up to B5 blends can be used as an approximation.

^J Low ambient temperatures as well as engine operation at high altitudes may require the use of fuels with higher cetane ratings.

^K It is unrealistic to specify low temperature properties that will ensure satisfactory operation at all ambient conditions. In general, cloud point (or wax appearance point) Low Temperature Flow Test, and Cold Filter Plugging Point Test may be used as an estimate of operating temperature limits for Grades No. 1–D S15; No. 2–D S15; No. 1–D S500; No. 2–D S500; and No. 1–D S5000 and No. 2–D S5000 diesel fuel oils. However, satisfactory operation below the cloud point (or wax appearance point) may be achieved depending on equipment design, operating conditions, and the use of flow-improver additives as described in X5.1.2. Appropriate low temperature operability properties should be agreed upon between the fuel supplier and purchaser for the intended use and expected ambient temperatures. Test Methods D4539 and D6371 may be especially useful to estimate vehicle low temperature operability limits when flow improvers are used. Due to fuel delivery system, engine design, and test method differences, low temperature operability tests may not provide the same degree of protection in various vehicle operating classes. Tenth percentile minimum air temperatures for U.S. locations are provided in Appendix X5 as a means of estimating expected regional temperatures. The tenth percentile minimum air temperatures can be used to estimate expected regional target temperatures for use with Test Methods D2500, D4539, and D6371. Refer to X5.1.3 for further general guidance on test application.

^L The electrical conductivity of the diesel fuel is measured at the time and temperature of the fuel at delivery. The 25 pS/m minimum conductivity requirement applies at all instances of high velocity transfer (7 m/s) but sometimes lower velocities, see 8.1 for detailed requirements into mobile transport (for example, tanker trucks, rail cars, and barges).

Table 2-4: EN590 Diesel fuel specifications [2.28].

Property	Unit	Limits		Test method ^a (See 2. Normative references)	
		minimum	maximum		
Cetane number ^b		51,0	–	EN ISO 5165 EN 15195	
Cetane index		46,0	–	EN ISO 4264	
Density at 15 °C ^c	kg/m³	820,0	845,0	EN ISO 3675 EN ISO 12185	
Polycyclic aromatic hydrocarbons ^d	% (m/m)	–	11	EN 12916	
Sulfur content ^e	mg/kg	–	50,0 until 2008-12-31	EN ISO 20846 EN ISO 20847 EN ISO 20884	
			10,0	EN ISO 20846 EN ISO 20884	
Flash point	°C	Above 55	–	EN ISO 2719	
Carbon residue ^f (on 10 % distillation residue)	% (m/m)	–	0,30	EN ISO 10370	
Ash content	% (m/m)	–	0,01	EN ISO 6245	
Water content	mg/kg	–	200	EN ISO 12937	
Total contamination	mg/kg	–	24	EN 12662 ^g	
Copper strip corrosion (3 h at 50 °C)	rating	class 1		EN ISO 2160	
Fatty acid methyl ester (FAME) content ^h	% (V/V)	-	7,0	EN 14078	
Oxidation stability	g/m ³	–	25	EN ISO 12205	
	h	20	-	EN 15751 ⁱ	
Lubricity, corrected wear scar diameter (wsd 1,4) at 60 °C	µm	–	460	EN ISO 12156-1	
Viscosity at 40 °C	mm ² /s	2,00	4,50	EN ISO 3104	
Distillation ^{k, l}				EN ISO 3405	
% (V/V) recovered at 250 °C	% (V/V)	85	< 65		
% (V/V) recovered at 350 °C	% (V/V)				
95 % (V/V) recovered at	°C		360		

NOTE Requirements in bold refer to the European Fuels Directive 98/70/EC [1], including Amendment 2003/17/EC [2]

^a See also 5.6.1
^b See also 5.6.4
^c See also 5.6.2
^d For the purposes of this European Standard, polycyclic aromatic hydrocarbons are defined as the total aromatic hydrocarbon content less the mono-aromatic hydrocarbon content, both as determined by EN 12916.
^e See also 5.6.3
^f See also 5.4.2 and Annex A
^g Further investigation into the total contamination test method to improve the precision, particularly in the presence of FAME, is being carried out by CEN
^h FAME shall meet the requirements of EN 14214
ⁱ For diesel fuel containing FAME above 2 % (V/V) this is an additional requirement. This is an interim requirement, under revision by CEN, when more technical data on oxidation stability and field performance of diesel fuels will be available.
^k For the calculation of the cetane index the 10 %, 50 % and 90 % (V/V) recovery points are also needed.
^l The limits for distillation at 250 °C and 350 °C are included for diesel fuel in line with EU Common Customs tariff.

ASTM D975 calls for the cetane number to exceed 40 while EN590 calls for cetane number to exceed 51. The substantial differences between the specifications can result in large variations in cetane numbers across regions. For example, a worldwide survey of winter Diesel fuel reports mean cetane numbers ranging from 44 to 63 [2.29]. Thus, engine and vehicle manufactures must account for potentially large disparities in fuel cetane number across countries and regions. To support engine development, surrogate fuels need to be formulated to cover a broad range of cetane number.

Specifications for aromatic content vary between the standards. ASTM D975 regulates the total aromatics by volume percent whereas as EN590 regulates the polycyclic aromatics by mass percent. Diesel fuel density is regulated by EN590 but is not regulated by ASTM D975. The regulated ranges for kinematic viscosity regulations are comparable. Differences also exist between the regulated fuel distillation temperatures. ASTM D975 and EN590 regulate the top end of the fuel distillation curves. ASTM D975 regulates the minimum and maximum temperatures for the 90% volume distillation temperature. EN590 regulates the maximum allowable temperature for the 95% volume distillation and several other points on the distillation curve.

One of the requirements set forth in this thesis is to develop surrogate fuels that are fully-representative of petroleum Diesel fuels. Thus, in addition to comparing the surrogate fuel properties with the petroleum Diesel fuel, the surrogate properties should also be compared with fuel regulations. Any discrepancies should be identified and if necessary resolved.

Table 2-5: Comparison of ASTM D975 No. 2-D and EN590 fuel specifications.

Fuel Property	Units	ASTM D975	EN590
Cetane Number		>40	>51
Threshold Soot Index (TSI)		Not Regulated	Not Regulated
Total Aromatics (mono and polycyclic)	%v/v	<35	Not Regulated
Polycyclic Aromatics (PAH)	%m/m	Not Regulated	<11
Density at 15 °C	g/ml	Not Regulated	0.820-0.845
Lower Heating Value		Not Regulated	Not Regulated
Viscosity at 40 °C		1.9-4.1	2.0-4.5
Distillation Temperature at 90 %v/v	°C	Min @ 282 Max @ 338	Not Regulated
Distillation Temperature at 95 %v/v	°C	Not Regulated	Max @ 360

2.3. Summary

Diesel fuel chemistry is remarkably complex and highly variable. Hundreds of different hydrocarbons species are contained in Diesel fuel. It is important to understand the composition of Diesel fuel as it affects the physical and chemical properties of the fuel. Understanding Diesel fuel composition is also necessary for the development of surrogate fuels where a surrogate containing very few hydrocarbon species is attempting to mimic the properties of a real fuel that contains hundreds of species. The hydrocarbon species contained in Diesel fuel are often separated into classifications based on molecular structure. These classifications include normal-alkanes, iso-alkanes, cyclo-alkanes and aromatics. The aromatics can be classified by the number of benzene rings in the molecule.

When formulating a surrogate fuel it is important to quantify the properties of the target petroleum Diesel fuel. Key Diesel fuel properties include cetane number, threshold soot index, lower heating value, density, kinematic viscosity, distillation temperatures and aromatic content. With the properties of the target Diesel fuel established, it may be useful to identify the properties that must closely match the target fuel. For example, matching the cetane number may be more important than matching the distillation curve.

2.4. References

- [2.1] Chevron, "Diesel Fuels Technical Review", *Chevron Products Company*,
<http://www.chevron.com/products/prodserv/fuels/bulletin/diesel>, 2007.
- [2.2] DieselNet, "Diesel Fuels", *DieselNet Internet Resources*,
<https://www.dieselnet.com/links/fuel.html>, 2017.
- [2.3] 5 Oaks Commodities, "Petroleum Products", *5 Oaks Commodities*,
<http://www.5oakscommodities.com/petroleum-products.html>, 2017.
- [2.4] ACEA, "Worldwide Fuel Charter 2013", *European Automobile Manufacturers' Association*,
<http://www.acea.be/publications/article/worldwide-fuel-charter>, 2017.
- [2.5] US EPA, "Diesel Fuel Standards", *US EPA*,
<https://www.epa.gov/diesel-fuel-standards>, 2017.
- [2.6] California Environmental Protection Agency – Air Resources Board, "California Diesel Fuel Program", *California Environmental Protection Agency*,
<https://www.arb.ca.gov/fuels/diesel/diesel.htm>, 2017.
- [2.7] European Committee for Standardization (CEN), "Fuel", *European Committee for Standardization*,
<https://www.cen.eu/work/areas/energy/fuel/Pages/default.aspx>, 2017.
- [2.8] Marsh, G., Hill, N. and Sully, J., "Consultation on the Need to Reduce the Sulphur Content of Petrol and Diesel Fuels Below 50 PPM: A Policy Makers Summary", *AEA Technology Environment*, 2000.
- [2.9] DieselNet, "What is Diesel Fuel", *DieselNet Internet Resources*,
https://www.dieselnet.com/tech/fuel_diesel.php, 2017.

- [2.10] Wade, L., "Organic chemistry", Prentice Hall, Upper Saddle River, N.J., 2003.
- [2.11] Totten, G., Westbrook, S. and Shah, R., "Fuels and lubricants handbook", 1st ed., ASTM International, West Conshohocken, Pa, 2003.
- [2.12] Heywood, J., "Internal combustion engine fundamentals", 1st ed., McGraw-Hill, New York, 1988.
- [2.13] Vendeuvre, C., Ruiz-Guerrero, R., Bertoncini, F., Duval, L., Thiébaud, D. and Hennion, M., "Characterisation of Middle-Distillates by Comprehensive Two-Dimensional Gas Chromatography (GC×GC): A Powerful Alternative for Performing Various Standard Analysis of Middle-Distillates", *Journal Of Chromatography A* 1086(1-2):21-28, 2005, doi:10.1016/j.chroma.2005.05.106.
- [2.14] Farrell, J., Cernansky, N., Dryer, F., Law, C., Friend, D., Hergart, C., McDavid, R., Patel, A., Mueller, C. and Pitsch, H., "Development of an Experimental Database and Kinetic Models for Surrogate Diesel Fuels", *SAE Technical Paper Series*, 2007, doi:10.4271/2007-01-0201.
- [2.15] ASTM International, "Test Method for Cetane Number of Diesel Fuel Oil", *ASTM International*, ASTM D 613-13, May 2017, doi:10.1520/d0613-13.
- [2.16] ASTM International, "Test Method for Determination of Ignition Delay and Derived Cetane Number (DCN) of Diesel Fuel Oils by Combustion in a Constant Volume Chamber", *ASTM International*, ASTM D 6890, May 2017, doi:10.1520/d6890-13b.
- [2.17] ASTM International, "Test Method for Smoke Point of Kerosine and Aviation Turbine Fuel", *ASTM International*, ASTM D 1322-12, May 2017, doi:10.1520/d1322-12.
- [2.18] Calcote, H. and Manos, D., "Effect of Molecular Structure on Incipient Soot Formation", *Combustion And Flame* 49(1-3):289-304, 1983, doi:10.1016/0010-2180(83)90172-4.

- [2.19] ASTM International, "Standard Test Method for Heat of Combustion of Liquid Hydrocarbon Fuels by Bomb Calorimeter", *ASTM International*, ASTM D 240-09, 2009.
- [2.20] ASTM International, "Test Method for Density, Relative Density, and API Gravity of Liquids by Digital Density Meter", *ASTM International*, ASTM D 4052-11, 2011, doi:10.1520/d4052-11.
- [2.21] ASTM International, "Test Method for Kinematic Viscosity of Transparent and Opaque Liquids (and Calculation of Dynamic Viscosity)", *ASTM International*, ASTM D 445-12, 2012, doi:10.1520/d0445-12.
- [2.22] ASTM International, "Test Method for Distillation of Petroleum Products at Atmospheric Pressure", *ASTM International*, ASTM D 86-12, May 2017, doi:10.1520/d0086-12.
- [2.23] ASTM International, "Test Method for Hydrocarbon Types in Liquid Petroleum Products by Fluorescent Indicator Adsorption", *ASTM International*, ASTM D 1319-13, May 2017, doi:10.1520/d1319-13.
- [2.24] ASTM International, "Standard Test Method for Determination of the Aromatic Content and Polynuclear Aromatic Content of Diesel Fuels and Aviation Turbine Fuels By Supercritical Fluid Chromatography", *ASTM International*, ASTM D 5186, May 2017.
- [2.25] ASTM International, "Test Methods for Flash Point by Pensky-Martens Closed Cup Tester", *ASTM International*, ASTM D 93-13, May 2017, doi:10.1520/d0093-13.
- [2.26] ANSYS, "ANSYS Model Fuel Library", *ANSYS, Inc.*, 2016.
- [2.27] ASTM International, "Specification for Diesel Fuel Oils", *ASTM International*, ASTM D 975-16a, 2016, doi:10.1520/d0975-16a.
- [2.28] European Committee for Standardization (CEN), "Automotive fuels - Diesel - Requirements and test methods", *European Committee for Standardization*, EN 590:2009: E, 2009.

- [2.29] Infineum International, Limited, "Worldwide Winter Diesel Fuel Quality Survey 2014", Infineum International Limited, 2014.

3. Computational Methods

Contents

3.	Computational Methods.....	41
3.1.	Introduction.....	43
3.2.	Temperature Dependent Properties	43
3.3.	Master Kinetic Mechanism.....	44
3.4.	Gas-Phase Reactor Simulation	46
3.5.	Surrogate Blend Modeling.....	49
3.6.	Summary	58
3.7.	References	59

3.1. Introduction

The computational methods described in this chapter were utilized to develop the Surrogate Fuel Library discussed in Chapter 5. Computational activities were conducted at General Motors Global Research and Development using commercially available subscription services and software.

3.2. Temperature-Dependent Properties

The Diesel spray is a very complex process governed by many factors such as the injector nozzle design, ambient conditions and the physical properties of liquid fuels. Diesel spray models include several temperature-dependent physical properties to calculate phenomena such as breakup, atomization, droplet collision and coalescence, and droplet evaporation. To support spray modeling, surrogate fuels must closely mimic the temperature-dependent physical properties of the target Diesel fuel. These properties include density, specific heat, viscosity, vapor pressure, heat of vaporization, surface tension and thermal conductivity. For multi-component surrogate fuels, the temperature-dependent properties are required for each fuel component.

The Design Institute for Physical Properties (DIPPR) and the American Institute of Chemical Engineers collaborated to create an extensive property database of chemical compounds. The DIPPR database contains 49 constant thermo-physical properties and 15 temperature-dependent properties for 2,278 compounds [3.1]. DIPPR correlations are routinely used by researchers to obtain the properties of pure compounds for applications such as modeling liquid spray penetration, evaporation and combustion [3.2] [3.3] [3.4] [3.5] [3.6] [3.7] [3.8].

This thesis employed DIPPR correlations to calculate the temperature-dependent properties for surrogate fuel components. The liquid properties included density, viscosity, surface tension, vapor pressure, specific heat, heat of vaporization and thermal conductivity. As an example, Figure 3-1 shows the heat of vaporization versus temperature for several hydrocarbon compounds. Significant differences between the compounds are evident. In Chapter 5, computed temperature-dependent properties for pure

hydrocarbon compounds are compared with measured properties from a surrogate fuel and a petroleum Diesel fuel.

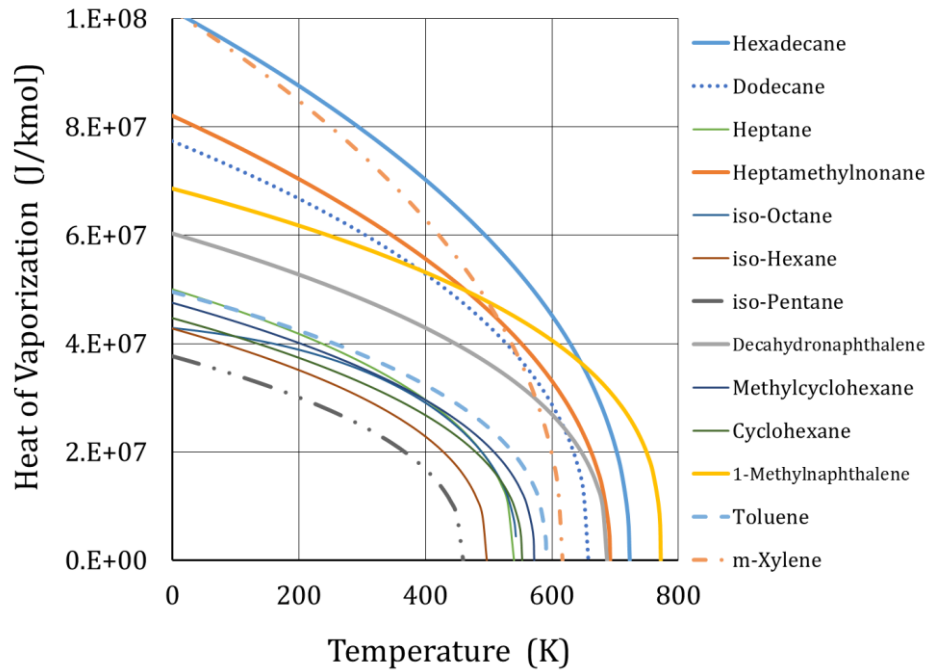


Figure 3-1: Heat of vaporization for several hydrocarbon compounds computed from DIPPR correlations.

3.3. Master Kinetic Mechanism

There has been, and continues to be, substantial progress in the development of detailed kinetic mechanisms for surrogate fuel components [3.9]. For example, researchers have made great progress in developing state-of-the-art detailed and reduced mechanisms for n-heptane [3.10], [3.11], [3.12]. Indeed, n-heptane is probably the most widely used surrogate fuel for Diesel combustion simulation. Expanding the list of n-alkane mechanisms, Westbrook et al, developed detailed kinetic mechanisms for n-alkane compounds from n-octane to n-hexadecane [3.13]. Combining detailed mechanisms from numerous sources, Naik et al, generated a master mechanism consisting of 3,809 species and 15,678 reactions, see Table 3-1 [3.14]. In all, the rapid pace of advancement in the development of kinetic mechanisms for surrogate fuel components has been very impressive.

Table 3-1: Progress in the development of surrogate fuel components with detailed kinetic mechanisms. Table taken from reference [3.14].

No.	Component	Mechanism source	Component class	Gasoline surrogate	Diesel Surrogate
1	<i>n</i> -Butane	Curran et al. [12]	n-alkane	X	
2	<i>n</i> -Pentane	Curran et al. [12]	n-alkane	X	
3	<i>n</i> -Hexane	Curran et al. [12]	n-alkane	X	
4	<i>n</i> -Heptane	Curran et al. [12]	n-alkane	X	X
5	<i>n</i> -Octane	Westbrook et al. [6]	n-alkane		X
6	<i>n</i> -Decane	Westbrook et al. [6]	n-alkane		X
7	<i>n</i> -Dodecane	Westbrook et al. [6]	n-alkane		X
8	<i>n</i> -Tetradecane	Westbrook et al. [6]	n-alkane		X
9	<i>n</i> -Hexadecane	Westbrook et al. [6]	n-alkane		X
10	<i>iso</i> -Pentane	Curran et al. [1]	Iso-alkane	X	
11	<i>iso</i> -Hexane	Curran et al. [1]	Iso-alkane	X	
12	<i>Iso</i> -Octane	Curran et al. [1]	Iso-alkane	X	X
13	Heptamethyl nonane	Westbrook et al. [13]	Iso-alkane		X
14	1-pentene	Naik et al. [14]	Olefin	X	
15	2-pentene	Naik et al. [14]	Olefin	X	
16	1-hexene	Naik et al. [14]	Olefin	X	X
17	2-hexene	Mehl et al. [7]	Olefin	X	X
18	3-hexene	Mehl et al. [7]	Olefin	X	X
19	MCH	Pitz et al. [9]	Cyclo-paraffin	X	X
20	Toluene	Naik et al. [2]	1-ring aromatics	X	X
21	<i>n</i> -Propylbenzene	Naik et al. [14]	1-ring aromatics	X	X
22	<i>o</i> -Xylene	ENSIC [15]	1-ring aromatics	X	X
23	<i>m</i> -Xylene	ENSIC [15]	1-ring aromatics	X	X
24	<i>p</i> -Xylene	ENSIC [15]	1-ring aromatics	X	X
25	1-Methyl naphthalene	Naik et al. [14]	2-ring aromatics		X
26	Ethanol	Marinov et al. [16]	Oxygenates	X	
A	NO _x	Multiple sources [17-19]		X	X
B	PAH	Multiple sources [20-22]		X	X

Recognizing industry's need for accurate surrogate fuel models, detailed chemical kinetic mechanisms and advanced combustion simulation tools, Reaction Design teamed with energy companies, automotive and engine manufacturers, and leading academic consultants to form the Model Fuels Consortium (MFC) [3.15] [3.16] [3.17]. The Model Fuels Consortium operated from 2006 through 2008 and made significant contributions that increased the pool of surrogate fuel species and validated kinetic mechanisms. In 2009 the MFC II was launched and operated through 2012. As the consortium came to a close, Reaction Design initiated the Model Fuel Library Subscription Service (MFLSS) to continue the development of mechanisms and improvements in the combustion simulation toolchain [3.18].

Over a decades work by the MFC and MFLSS resulted in perhaps the world's most comprehensive, validated chemical kinetic mechanism database for surrogate fuel components [3.19]. The 2016 Model Fuel Library contains detailed, validated master kinetic mechanisms for over 65 fuel components [3.20] [3.21]. The library may be employed to develop surrogates for gasoline, Diesel, jet fuel, biofuels and fuel blends.

This thesis employed the 2015 Model Fuel Library and the accompanying Diesel Fuel Master Kinetic Mechanism. The kinetic mechanism was used for closed-homogenous gas-phase reactor simulations and for surrogate fuel modeling. The Diesel Fuel Master Mechanism consisted of 55 fuel components, 5,155 chemical species and 31,084 chemical reactions [3.22].

3.4. Gas-Phase Reactor Simulation

The ignition process and certain combustion species were examined for several surrogate fuel components and multi-component surrogates. This was accomplished with 0-dimensional, transient, closed-homogeneous gas-phase reactor simulations using Chemkin-Pro [3.23] [3.24]. The closed-homogeneous reactor model assumed the volume was constant and the mass was evenly distributed throughout the reactor. The reactor was configured without heat loss i.e., the reactor wall temperatures equaled the gas temperature. The oxidizer was air (nitrogen and oxygen) without EGR or other species. A 400-point matrix of reactor initial temperature, pressure and equivalence ratio conditions was created. The matrix initial conditions were representative of in-cylinder engine conditions near the time of fuel injection for moderate engine speeds and loads. Simulations were conducted for each condition using several pure hydrocarbon species and multi-components surrogates. Table 3-2 provides the essential inputs and reactor conditions used in this research.

The reactor simulations were primarily used to investigate the ignition and the Negative Temperature Coefficient (NTC) behavior of pure hydrocarbon compounds. As an example, Figure 3-2 shows simulation results for n-heptane (a single-component Diesel surrogate fuel) and decahydronaphthalene (a compound used in multi-component surrogate fuels). The figure shows n-heptane had much shorter low-temperature and high-temperature ignition delays. In Figure 3-3, the ignition delay behavior for n-heptane and decahydronaphthalene are shown as temperature and

equivalence ratio were varied. The simulation efforts demonstrated that fuel species had different responses to changes in temperature and equivalence ratio. Understanding the ignition behavior of pure hydrocarbon species helped guide the selection of surrogate components. Evaluations of multi-component surrogates confirmed the ignition behavior as surrogates were designed with different cetane numbers.

Table 3-2: Parameter inputs for closed-homogeneous reactor simulation.

Parameter	Input Value(s)
Chemistry Set	2015 MFL Diesel Master Mechanism 5,155 Species, 31,084 Reactions
Reactor Type	Closed-Homogeneous
Reactor Problem Type	Constrain Volume and Solve Energy Equation
Reactor End Time	0.003 seconds
Reactor Initial Temperature	800 – 1400 K (10 conditions)
Reactor Initial Equivalence Ratio	0.5 – 4.0 (10 conditions)
Reactor Initial Pressure	40, 50, 60, 70 bar
Reactor Heat Loss	0.00 calories/second
Reactor Surface Temperature	Same as Gas Temperature
Reactant Species	Varied
Oxidizer Mixture	Air (no EGR or other species)
Complete Combustion Products	N ₂ , CO ₂ , H ₂ O
Solver Settings	Default
Ignition Delay	OH Species Maximum Fraction
Heat Release	Integrate Gas Phase Reactions

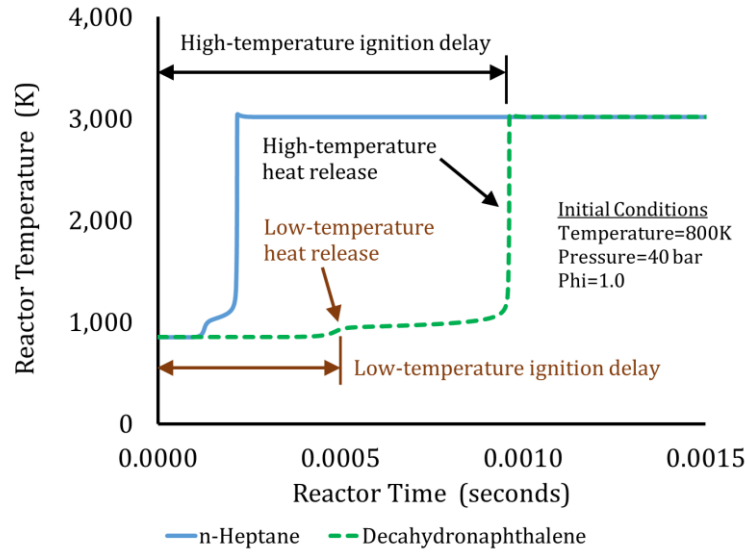


Figure 3-2: Example of closed-homogeneous reactor temperature simulation for n-heptane and decahydronaphthalene.

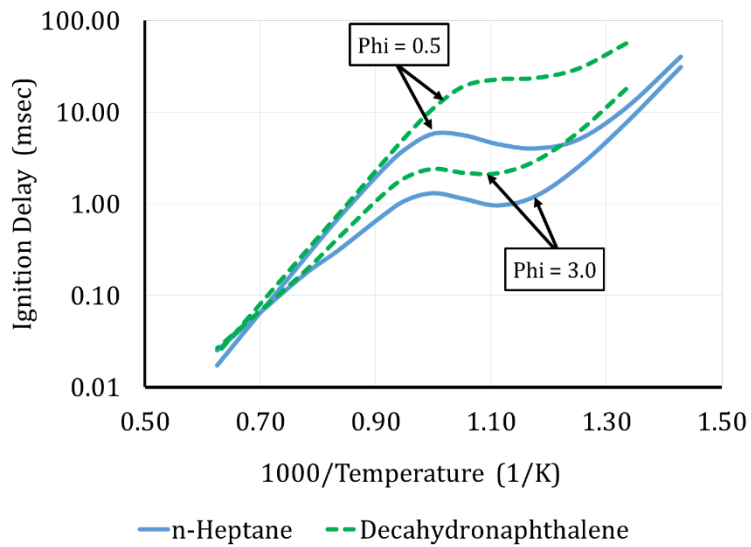


Figure 3-3: Ignition delay summary for n-heptane and decahydronaphthalene showing the impact of equivalence ratio and temperature.

3.5. Surrogate Blend Modeling

A goal of this thesis was to create a library of surrogate fuels for both industrial application (combustion system design) and for continued exploratory research. Developing the fuel formulations for the library posed a challenge. Global properties such as cetane number, threshold soot index, density, and distillation temperatures needed to be precisely modeled for multi-component surrogates. The impact of hydrocarbon component selections and blending proportions on fuel properties needed to be understood to develop optimal surrogates with the minimum number of components.

A review of the literature revealed several methods to formulate surrogate fuels. Most methods were aimed at creating a single surrogate fuel for a specific application. For example, Payri et al, used a two-component surrogate to better represent Diesel fuel [3.25]. This was accomplished by adding a branched-benzene compound, m-xylene, to n-dodecane. Detailed kinetic mechanisms for both components were readily available and assembled into a mechanism for the surrogate. Hernandez et al. developed a two-component surrogate using n-heptane and toluene to study HCCI combustion [3.26]. The components were selected based on the literature and available kinetic mechanisms. The mixture ratio was determined by comparing experimental and modeled ignition delays. Dooley et al. utilized a systematic methodology based on chemical group theory to compose a three-component jet fuel surrogate consisting of n-decane, iso-octane and toluene [3.27]. The surrogate mixture was able to reproduce the cetane number, hydrogen-to-carbon ratio and threshold soot index for the target jet fuel. Liang et al. employed the Surrogate Blend Optimizer (SBO) to achieve a multi-component blend that closely mimicked the cetane number, hydrogen-to-carbon ratio, lower heating value and 50% volume distillation temperature of a target Diesel fuel [3.28]. The four-component surrogate consisted of n-tetradecane, n-decane, heptamethylnonane, and 1-methylnaphthalene. Mueller et al. created an eight-component surrogate to closely match the chemical and physical properties of a target Diesel fuel [3.29]. Their method employed a multi-property regression model to systematically match key fuel properties including molecular structures, cetane number, and distillation curve characteristics. Naik et al. also used the Surrogate Blend Optimizer to create surrogate fuels for gasoline and

Diesel fuels [3.14]. The gasoline surrogate consisted of eight components. Two Diesel surrogates were developed. A four-component surrogate and a more complex seven-component surrogate. The four-component and seven-component surrogates were targeted at the same petroleum Diesel fuel. Naik et al. showed the Surrogate Blend Optimizer was capable of optimizing surrogate blends to achieve the target fuel properties. Based on the successful results achieved by Liang and Naik, the Surrogate Blend Optimizer was selected to develop the surrogate fuels for this thesis. In this research the Surrogate Blend Optimizer was employed to model surrogate fuel properties, understand the impact of various compounds on the surrogate properties, and create the blend mixtures needed to generate a library of surrogate fuel formulations.

Surrogate Blend Optimizer

The Model Fuel Library, Chemkin-Pro, Reaction Workbench and the Surrogate Blend Optimizer (SBO) were products of ANSYS, Inc. A Chemkin mechanism (also called Chemistry Set) that contained fuel species information such as physical, chemical and thermodynamic properties was required to run the SBO. The surrogate fuel composition was determined by a genetic optimization procedure that minimized the differences between user specified fuel properties and their computed values [3.30]. Upon iteration and convergence, the SBO delivered the surrogate composition that best matched the properties of the target fuel provided. The volume or mole fraction of each fuel specie was reported. Table 3-3 shows the fuel properties that the user could exercise as input target values for the surrogate fuel blend optimizer.

Table 3-3: User input target values for surrogate fuel development.

Cetane Number	
Research Octane Number	
Motor Octane Number	
Molar Hydrogen-to-Carbon Ratio	
Threshold Soot Index	
Liquid Density	g/cm ³
Kinematic Viscosity	cSt
Lower Heating Value	MJ/kg
Distillation Curve from 10 to 90 %v/v	Degrees C, K, F or R

The Surrogate Blend Optimizer could function in two modes. In the optimizer mode, the SBO operated with the work flow process given in Figure 3-4 [3.30]. To generate a surrogate composition, the user selected the fuel species and then input fuel property values desired for the surrogate fuel. Weighting factors could also be applied to prioritize the role of the property in determining the surrogate blend composition. The SBO executed its routines and provided the best overall surrogate composition that matched the input target fuel properties.

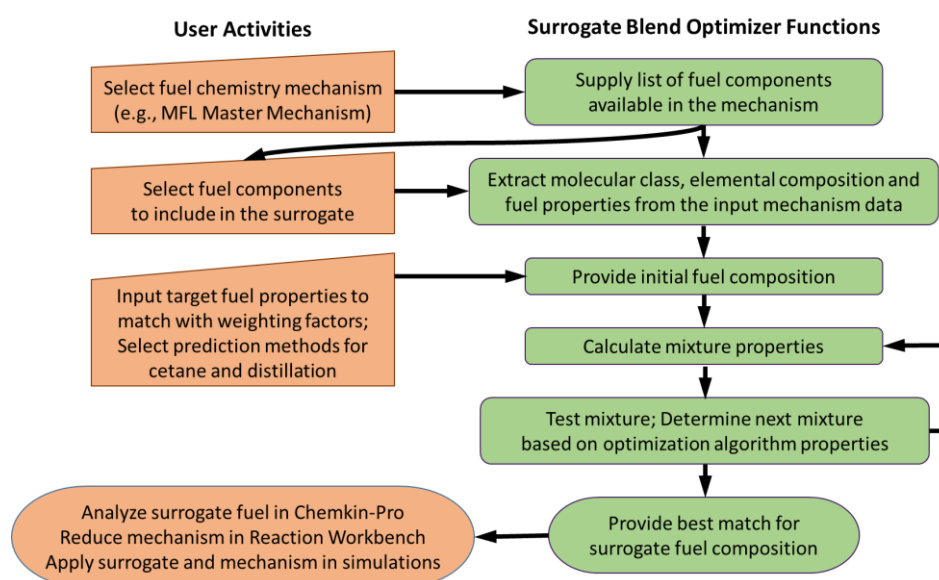


Figure 3-4: Surrogate Blend Optimizer (SBO) work diagram, adapted from [3.30].

The SBO could also operate in a fuel property calculator mode. In this mode, the surrogate fuel composition (species and volume or mole fractions) was already known and provided as inputs. Given the surrogate composition, the Surrogate Blend Optimizer would calculate the fuel properties shown in Table 3-3.

The property calculator mode was heavily used during the development of the Surrogate Fuel Library discussed in Chapter 5. The process is described in detail below and shown in Figure 3-5 through Figure 3-10.

Calculator Mode Step 1. A Chemkin chemistry set, complete with property tags for the fuel species, was selected, preprocessed and loaded (Figure 3-5). This thesis employed Diesel fuel chemistry sets from the 2015 Model Fuel Library.

Calculator Mode Step 2. The surrogate fuel species were selected from the list of available species (Figure 3-6).

Calculator Mode Step 3. The volume fractions for each selected fuel component were entered (Figure 3-7). Units and calculation methods for cetane number and distillation temperatures were selected. The Linear Blending Option was chosen for cetane number prediction and the Staged Equilibrium Option was selected as the preferred method to simulate the ASTM D86 distillation curve. The solver settings were kept at their default values (Figure 3-8).

Calculator Mode Step 4. The SBO program was run, converged and the results were displayed on the computer screen (Figure 3-9). The predicted properties were reviewed and compared to the desired values for the surrogate. If the desired properties were achieved the SBO results were exported to a file (Figure 3-10). If the desired properties were not obtained the user would return to Step 3 and iterate by adjusting the fuel component volume fractions.

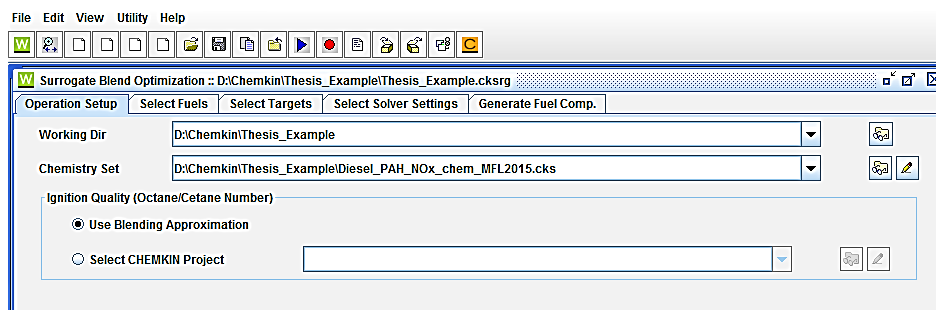


Figure 3-5: Select, preprocess and load the Chemkin chemistry set.

File Edit View Utility Help

W Surrogate Blend Optimization - D:\Chemkin\Thesis_Example\Thesis_Example.cksrsg

Operation Setup Select Fuels Select Targets Select Solver Settings Generate Fuel Comp.

Select the fuel species used in the surrogate.

Fuel Class	Species Name	Common Name	Cetane Number	Rating
Alcohol	<input type="checkbox"/> c2h5oh	Ethanol	12	rating: A
Alcohol	<input type="checkbox"/> ch3oh	Methanol	3	rating: A
Alcohol	<input type="checkbox"/> nc4h9oh	n-Butanol	17	rating: A
Alkenes	<input type="checkbox"/> c5h10-1	1-Pentene	24.4	rating: A
Alkenes	<input type="checkbox"/> c5h10-2	2-Pentene	17	rating: B
Alkenes	<input type="checkbox"/> c6h12-1	1-Hexene	27	rating: A
Alkenes	<input type="checkbox"/> c6h12-2	2-Hexene	20	rating: B
Alkenes	<input type="checkbox"/> c6h12-3	3-Hexene	16	rating: B
Aromatics	<input checked="" type="checkbox"/> a2ch3	1-Methylnaphthalene	0	rating: B
Aromatics	<input type="checkbox"/> c6h5c2h5	Ethylbenzene	7.4	rating: B
Aromatics	<input type="checkbox"/> c6h5c3h7	n-Propylbenzene	7.6	rating: B
Aromatics	<input type="checkbox"/> c6h5ch3	Toluene	2.6	rating: B
Aromatics	<input type="checkbox"/> c6h6	Benzene	10.7	rating: B
Aromatics	<input type="checkbox"/> m-xylene	m-Xylene	2.6	rating: B
Aromatics	<input type="checkbox"/> naph	Naphthalene	22.6	rating: B
Aromatics	<input type="checkbox"/> o-xylene	o-Xylene	8.3	rating: B
Aromatics	<input type="checkbox"/> p-xylene	p-Xylene	2.6	rating: B
Aromatics	<input type="checkbox"/> styr	Styrene	7.4	no rating
Aromatics	<input type="checkbox"/> tmb124	1,2,4-Trimethylbenzene (TMB)	8.9	rating: B
Cyclic-ether	<input type="checkbox"/> c4h8o1-4	Tetrahydrofuran (THF)	18	rating: B
Cyclic-ether	<input type="checkbox"/> etfe	Ethyltetrahydrofurfuryl ether (ETFE)	82	rating: B
Cyclo-alkenes	<input type="checkbox"/> cy13pd	Cyclopentadiene	0	no rating
Cycloalkanes	<input type="checkbox"/> chx	Cyclohexane	18.5	rating: B
Cycloalkanes	<input checked="" type="checkbox"/> decalin	Decalin	44	rating: B
Cycloalkanes	<input type="checkbox"/> mch	Methylcyclohexane	22.5	rating: A
Ether	<input type="checkbox"/> ch3och3	Dimethyl ether (DME)	55	rating: A
Ether	<input type="checkbox"/> mtbe	Methyl tert-butyl ether (MTBE)	24	rating: A
Hydrogen	<input type="checkbox"/> h2	Hydrogen	0	rating: A
Sulfur compounds	<input type="checkbox"/> h2s	Hydrogen sulfide		rating: B

4 fuels have been selected.

Previous Next

Fuel Specie	Chemkin Name
n-hexadecane	nc16h34
heptamethylnonane	hmn
decahydronaphthalene	decalin
1-methylnaphthalene	a2ch3

Figure 3-6: Select the fuel species to include in the surrogate fuel.

Surrogate Blend Optimization : D:\Chemkin\Thesis_Example\Thesis_Example.cksrcg

Operation Setup | Select Fuels | Select Targets | Select Solver Settings | Generate Fuel Comp.

Fuel Classes	Target	Weighting Factor
Unit: Volume Fraction		
Aromatics	0.12	10.0
a2ch3	0.12	10.0
Cycloalkanes	0.18	10.0
decalin	0.18	10.0
iso-Alkanes	0.33	10.0
hmn	0.33	10.0
n-Alkanes	0.37	10.0
nc16h34	0.37	10.0

Ignition Quality

Linear Nonlinear

Cetane Number 1.0

Research Octane Number 1.0

Motored Octane Number 1.0

Carbon Ratio

Molar H/C Ratio 1.0

Threshold Sooting Index

T.S.I. 1.0

Liquid Density

Unit: g/cm3

Liquid Density 1.0

Liquid Kinematic Viscosity

Unit: cSt

Temperature [K] 298.14

Kinematic Viscosity 1.0

Lower Heating Value

Unit: MJ/Kg

L.H.V. 1.0

Distillation curve

Combining rule: Mass Fraction

Method: Staged Equilibrium

Unit: C

Previous Next

Input Species Volume Fraction

Select Units & Calculation Methods

Figure 3-7: Input the target values. For the SBO optimizer mode, the fuel property targets were input along with their respective weighting factors. For the SBO property calculator mode, the fuel species composition was input and the fuel property values were left blank. This figure shows a four-component surrogate using the property calculator mode.

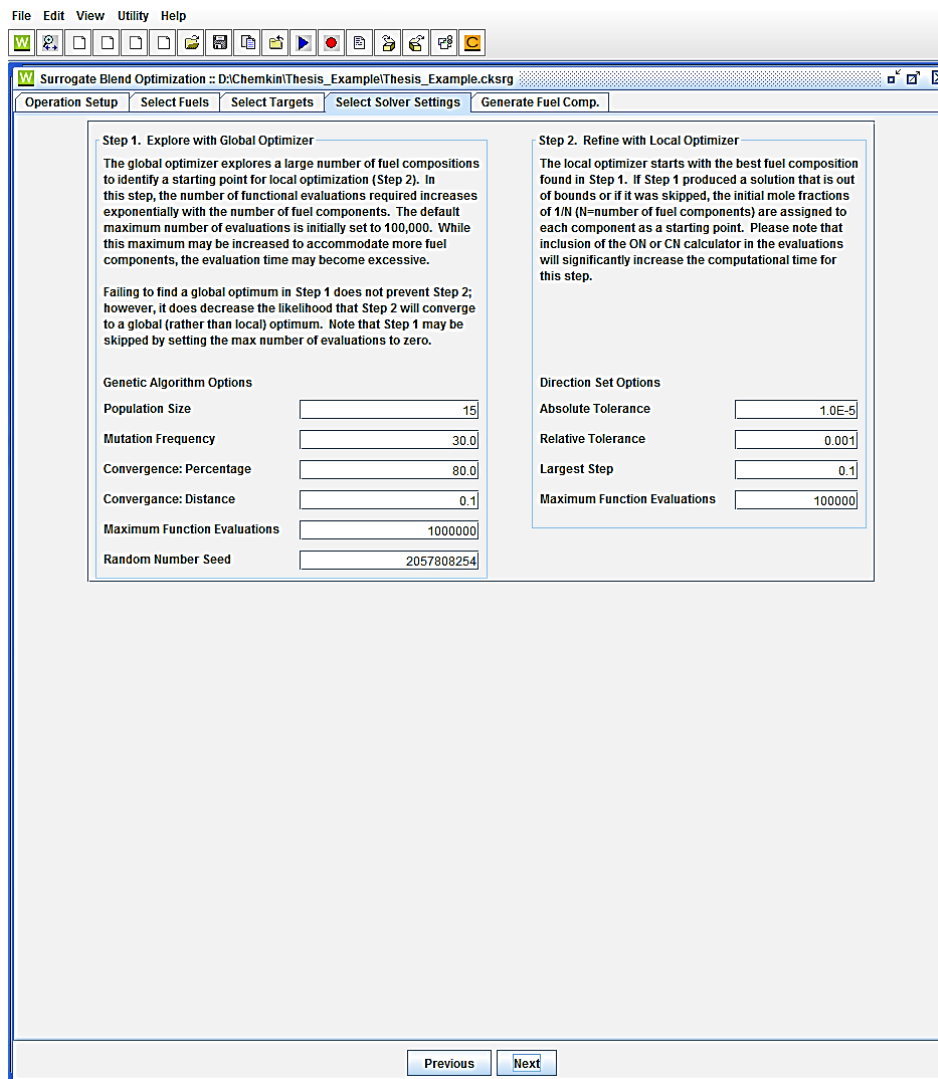


Figure 3-8: Select solver settings (used defaults).

The screenshot displays the Surrogate Blend Optimization (SBO) software interface. The main window shows a table of fuel properties and an information dialog box indicating 'Optimization converged'.

[Species]	[Volume fraction]	[Name]	[Units]	[Target]	[Result]	[Weighting Factor]	[Calculation Method]
a2ch3	0.1200	Aromatics	Volume fraction	0.12	0.1200	10.0	
decalin	0.1800	a2ch3	Volume fraction	0.12	0.1200	10.0	
hmn	0.3300	Cycloalkanes	Volume fraction	0.18	0.1800	10.0	
nct6h34	0.3700	decalin	Volume fraction	0.18	0.1800	10.0	
		iso-Alkanes	Volume fraction	0.33	0.3300	10.0	
		hmn	Volume fraction	0.33	0.3300	10.0	
		n-Alkanes	Volume fraction	0.37	0.3700	10.0	
		nct6h34	Volume fraction	0.37	0.3700	10.0	
		Cetane Number			49.87	1.0	(Linear evaluation)
		Research Octane Number			44.22	1.0	(Linear evaluation)
		Motored Octane Number			41.52	1.0	(Linear evaluation)
		Molar H/C Ratio			1.8721	1.0	
		T.S.I.			31.5240	1.0	
		Liquid Density	g/cm3		0.8207	1.0	
		Kinematic Viscosity	cSt		3.6367	1.0	
		L.H.V.	MJ/kg		43.81	1.0	
		T10	C		229.2	1.0	Staged Equilibrium
		T20	C		234.0	1.0	Staged Equilibrium
		T30	C		238.9	1.0	Staged Equilibrium
		T40	C		244.3	1.0	Staged Equilibrium
		T50	C		250.1	1.0	Staged Equilibrium
		T60	C		256.9	1.0	Staged Equilibrium
		T70	C		263.4	1.0	Staged Equilibrium
		T80	C		270.2	1.0	Staged Equilibrium
		T90	C		277.7	1.0	Staged Equilibrium
		[Genetic Algorithm Parameter]	[Value]				
		Maximum Function Evaluations			1000000		
		Convergence Distance			0.1		
		Percentage Distance			80.0		
		Sample Size			15		
		Mutation Frequency			30.0		
		Random Seed			2057808254		
		[Direction Set Parameter]	[Value]				
		Maximum Function Evaluations			100000		
		Largest Step			0.1		
		Absolute Tolerance			1.0e-5		
		Relative Tolerance			0.001		

An information dialog box is displayed in the foreground, containing the text: "Optimization converged." and an "OK" button.

Buttons at the bottom of the main window include: Run, Export, Distillation, Start Mechanism Reduction, and Previous.

Figure 3-9: Run the SBO program to calculate surrogate fuel properties. Results were compared with target fuel properties for the given composition.

	A	B	C	D	E	F
	[Name]	[Units]	[Target]	[Result]	[Weighting Factor]	[Calculation Method]
2	Aromatics	Volume fraction	0.12	0.12	10	
3	a2ch3	Volume fraction	0.12	0.12	10	
4	Cycloalkanes	Volume fraction	0.18	0.18	10	
5	decalin	Volume fraction	0.18	0.18	10	
6	iso-Alkanes	Volume fraction	0.33	0.33	10	
7	hmn	Volume fraction	0.33	0.33	10	
8	n-Alkanes	Volume fraction	0.37	0.37	10	
9	nc16h34	Volume fraction	0.37	0.37	10	
10	Cetane Number			49.87	1	(Linear evaluation)
11	Research Octane Number			44.22	1	(Linear evaluation)
12	Motored Octane Number			41.52	1	(Linear evaluation)
13	Molar H/C Ratio			1.8721	1	
14	T.S.I.			31.524	1	
15	Liquid Density	g/cm3		0.8207	1	
16	Kinematic Viscosity	cSt		3.6367	1	
17	L.H.V.	MJ/kg		43.81	1	
18	T10	C		229.2	1	Staged Equilibrium
19	T20	C		234	1	Staged Equilibrium
20	T30	C		238.9	1	Staged Equilibrium
21	T40	C		244.3	1	Staged Equilibrium
22	T50	C		250.1	1	Staged Equilibrium
23	T60	C		256.9	1	Staged Equilibrium
24	T70	C		263.4	1	Staged Equilibrium
25	T80	C		270.2	1	Staged Equilibrium
26	T90	C		277.7	1	Staged Equilibrium
27	mass fraction (or mass)					
28	a2ch3	0.1449				
29	decalin	0.1945				
30	hmn	0.3156				
31	nc16h34	0.3450				

Figure 3-10: Surrogate fuel formulation and predicted properties were exported to a spreadsheet.

3.6. Summary

Recent advancements have greatly improved the computational toolchain used to formulate surrogate fuel blends and to predict surrogate fuel properties. The pool of surrogate fuel species with detailed kinetic mechanisms has grown considerably. Simulation tools have been specifically developed to create surrogate fuel with optimized compositions that satisfy specific fuel property requirements. This thesis employed the latest computational methods to determine surrogate fuel formulations that achieved specific fuel property targets. The computational methods described in this chapter and summarized in Table 3-4 were applied to develop the Surrogate Fuel Library discussed in Chapter 5.

Table 3-4: Summary of computational methods applied to create surrogate fuel formulations and predicted fuel properties.

Description	Method
Temperature-Dependent Properties of Pure Fuel Species	DIPPR Correlations
Master Chemical Kinetic Mechanism	2015 Model Fuel Library
0-Dimensional Gas-Phase Reactor Simulations	Closed-Homogeneous Reactor using Chemkin-Pro
Surrogate Fuel Formulation and Property Prediction	Surrogate Blend Optimizer using Reaction Workbench

3.7. References

- [3.1] Design Institute for Physical Properties, "AIChE DIPPR Project 801 - Full Version", *KNovel Corporation*, (2005; 2008-2012; 2015; 2016)", [Http://App.Knovel.Com/Hotlink/Toc/Id:Kpdipprpf7/Dippr-Project-801-Full/Dippr-Project-801-Full](http://App.Knovel.Com/Hotlink/Toc/Id:Kpdipprpf7/Dippr-Project-801-Full/Dippr-Project-801-Full), 2016.
- [3.2] Siebers, D., "Scaling Liquid-Phase Fuel Penetration in Diesel Sprays Based on Mixing-Limited Vaporization", *SAE Technical Paper Series* 1999-01-0528, 1999.
- [3.3] Dong-Ryul, R. and Farrel, P., "Air Flow Characteristics Surrounding Evaporating Transient Diesel Sprays", *SAE Technical Paper Series* 2002-01-0499, 2002.
- [3.4] Farrell, J., Cernansky, N., Dryer, F., Law, C., Friend, D., Hergart, C., McDavid, R., Patel, A., Mueller, C. and Pitsch, H., "Development of an Experimental Database and Kinetic Models for Surrogate Diesel Fuels", *SAE Technical Paper Series* 2007-01-0201, 2007.
- [3.5] Fisher, B. and Mueller, C., "Effects of Injection Pressure, Injection-Rate Shape, and Heat Release on Liquid Length", *SAE International Journal of Engines* 5(2):415-429, 2012, doi:10.4271/2012-01-0463.
- [3.6] Kim, D., Martz, J. and Violi, A., "A surrogate for emulating the physical and chemical properties of conventional jet fuel", *Combustion and Flame* 161(6):1489-1498, 2014, doi:10.1016/j.combustflame.2013.12.015.
- [3.7] Abianeh, O., Oehlschlaeger, M. and Sung, C., "A surrogate mixture and kinetic mechanism for emulating the evaporation and autoignition characteristics of gasoline fuel", *Combustion and Flame* 162(10):3773-3784, 2015, doi:10.1016/j.combustflame.2015.07.015.
- [3.8] Fisher, B. and Mueller, C., "Liquid penetration length of heptamethylnonane and trimethylpentane under unsteady in-

- cylinder conditions", *Fuel* 89(10):2673-2696, 2010, doi:10.1016/j.fuel.2010.04.024.
- [3.9] Pitz, W. and Mueller, C., "Recent Progress in the Development of Diesel Surrogate Fuels", *Progress in Energy and Combustion Science* 37(3):330-350, 2011, doi:10.1016/j.peccs.2010.06.004.
- [3.10] Lindstedt, R. and Maurice, L., "Detailed Kinetic Modelling of n-Heptane Combustion", *Combustion Science and Technology* 107(4-6):317-353, 1995, doi:10.1080/00102209508907810.
- [3.11] Curran, H., Gaffuri, P., Pitz, W. and Westbrook, C., "A Comprehensive Modeling Study of n-Heptane Oxidation", *Combustion and Flame* 114(1-2):149-177, 1998, doi:10.1016/s0010-2180(97)00282-4.
- [3.12] Tao, F., Reitz, R. and Foster, D., "Revisit of Diesel Reference Fuel (n-Heptane) Mechanism Applied to Multidimensional Diesel Ignition and Combustion Simulations", Seventeenth International Multidimensional Engine Modeling User's Group Meeting, 2007.
- [3.13] Westbrook, C., Pitz, W., Herbinet, O., Curran, H. and Silke, E., "A comprehensive detailed chemical kinetic reaction mechanism for combustion of n-alkane hydrocarbons from n-octane to n-hexadecane", *Combustion and Flame* 156(1):181-199, 2009, doi:10.1016/j.combustflame.2008.07.014.
- [3.14] Naik, C., Puduppakkam, K., Wang, C., Kottalam, J., Liang, L., Hodgson, D. and Meeks, E., "Applying Detailed Kinetics to Realistic Engine Simulation: the Surrogate Blend Optimizer and Mechanism Reduction Strategies", *SAE International Journal of Engines* 3(1):241-259, 2010, doi:10.4271/2010-01-0541.
- [3.15] Meeks, E., "Consortium Advances Combustion Simulation for Engine Design", *Automotive Industries*, Issue: Feb 2009, 2009. http://www.automotive-industry.com/Adv/Previous/show_issue.php?id=2449#sthash.FazeWLfS.dpbs, 2017.

- [3.16] Sutton, M., "GM Joins Advanced Fuel-Modeling and Simulation Group", *Wards Auto*, September 20, 2007. <http://wardsauto.com/news-analysis/gm-joins-advanced-fuel-modeling-and-simulation-group>, 2017.
- [3.17] Flores, V., "Reaction Design's Automotive Fuels Consortium Revs Up with Five New Members," *Reaction Design*, April 16, 2007. <http://www.modelfuelsconsortium.com/news/39/95/Reaction-Design-s-Automotive-Fuels-Consortium-Revs-Up-with-Five-New-Members/>, 2017.
- [3.18] Green Car Congress, "Reaction Design introduces model fuel library resulting from work of Model Fuels Consortium", *Green Car Congress*, November 14, 2010. <http://www.greencarcongress.com/2012/11/reaction-design-introduces-model-fuel-library-resulting-from-work-of-model-fuels-consortium.html>, 2017.
- [3.19] Flores, V., "Reaction Design Introduces Industry's Most Well Validated Model Fuel Library", *Reaction Design*, November 7, 2012. <http://www.reactiondesign.com/news/2/95/Reaction-Design-Introduces-Industry-s-Most-Well-Validated-Model-Fuel-Library/>, 2017.
- [3.20] ANSYS, "ANSYS Model Fuel Library", *ANSYS, Inc.*, 2016.
- [3.21] ANSYS, "The Model Fuels Library: Accurate Combustion Chemistry for the Real World", *ANSYS, Inc.*, 2016. <http://www.ansys.com/-/media/Ansys/corporate/resourcelibrary/brochure/ansys-model-fuel-library-brochure.pdf>, 2017.
- [3.22] ANSYS, "ANSYS Model Fuel Library", *ANSYS, Inc.*, 2015.
- [3.23] ANSYS, "ANSYS Chemkin-Pro Theory Manual", *ANSYS, Inc.*, 2017.
- [3.24] ANSYS, "ANSYS Chemkin-Pro Input Manual", *ANSYS, Inc.*, 2017.

- [3.25] Payri, R., Viera, J., Pei, Y. and Som, S., "Experimental and numerical study of lift-off length and ignition delay of a two-component diesel surrogate", *Fuel* 158:957-967, 2015, doi:10.1016/j.fuel.2014.11.072.
- [3.26] Hernandez, J., Sanz-Argent, J., Benajes, J. and Molina, S., "Selection of a diesel fuel surrogate for the prediction of auto-ignition under HCCI engine conditions", *Fuel* 87(6):655-665, 2008, doi:10.1016/j.fuel.2007.05.019.
- [3.27] Dooley, S., Won, S., Chaos, M., Heyne, J., Ju, Y., Dryer, F., Kumar, K., Sung, C., Wang, H., Oehlschlaeger, M., Santoro, R. and Litzinger, T., "A jet fuel surrogate formulated by real fuel properties", *Combustion and Flame* 157(12):2333-2339, 2010, doi:10.1016/j.combustflame.2010.07.001.
- [3.28] Liang, L., Naik, C., Puduppakkam, K., Wang, C., Modak, A., Meeks, E., Ge, H., Reitz, R. and Rutland, C., "Efficient Simulation of Diesel Engine Combustion Using Realistic Chemical Kinetics in CFD", *SAE Technical Paper Series*, 2010, doi:10.4271/2010-01-0178.
- [3.29] Mueller, C., Cannella, W., Bruno, T., Bunting, B., Dettman, H., Franz, J., Huber, M., Natarajan, M., Pitz, W., Ratcliff, M. and Wright, K., "Methodology for Formulating Diesel Surrogate Fuels with Accurate Compositional, Ignition-Quality, and Volatility Characteristics", *Energy & Fuels* 26(6):3284-3303, 2012, doi:10.1021/ef300303e.
- [3.30] ANSYS, "ANSYS Chemkin Reaction Workbench Manual", ANSYS, Inc., 2017.

4. Experimental Methods

Contents

4.	Experimental Methods	63
4.1.	Introduction.....	65
4.2.	Test Facility.....	65
4.3.	Single-Cylinder Research Engine.....	66
4.4.	Fuel.....	68
4.5.	Measurements and Controls	68
4.6.	Test Conditions and Procedures.....	81
4.7.	Summary	84
4.8.	References	84

4.1. Introduction

All experimental work was conducted at the General Motors Global Research and Development facility located in Warren, Michigan, USA. Testing was conducted in a state-of-the-art engine dynamometer test cell. The test setup and results are reported in this thesis. Where appropriate, calculations are referenced to consistent methods found in the literature.

4.2. Test Facility

A schematic diagram of the engine-dynamometer test facility is shown in Figure 4-1. The facility was designed for steady-state single-cylinder engine testing and instrumented to provide engine combustion, performance, emissions, soot and exhaust particle data. The engine, fuels, and primary features of the test facility are provided in the following sections.

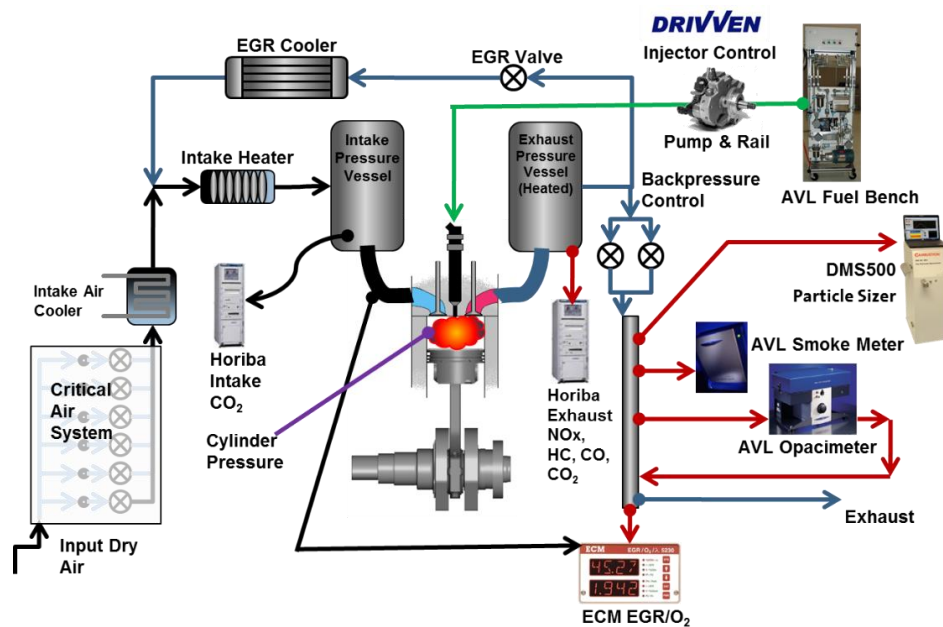


Figure 4-1: Schematic diagram of the engine test facility.

4.3. Single-Cylinder Research Engine

The experiments were carried out using a fully instrumented single-cylinder Diesel engine with contemporary technology. The engine crankcase was an FEV Systemmotor E12-56 base module with a balance mechanism for the crankshaft, connecting rod and piston assembly. A cylinder head was fitted to the FEV base module. This required numerous modifications to the cylinder head and a custom-designed intermediate piece to serve as the engine block that mated the head assembly to the crankcase. The compression ratio was set at 16:1 by shimming the intermediate piece. Figure 4-2 shows a typical single-cylinder engine configured with the FEV base module. The primary engine characteristics are given in Table 4-1. The piston pin offset sign convention was negative (-) when the pin offset was toward the minor thrust side of the cylinder, i.e., the expansion side of crankshaft rotation. Swirl ratio was determined using a method consistent with the impulse torque meter approach described by Heywood [4.1].

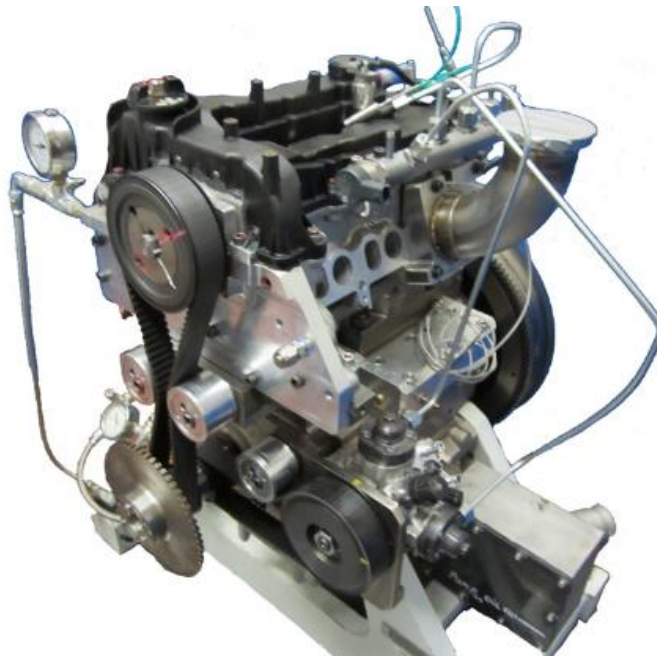


Figure 4-2: Typical single-cylinder engine configured with an FEV base module.

Table 4-1: Single-cylinder engine characteristics and geometries.

Parameter	Units	Value
Compression Ratio		16.0
Bore	mm	79.7
Stroke	mm	80.1
Connecting Rod Length	mm	140.0
Piston Pin Offset	mm	-0.15
Swirl Ratio		2.9
Combustion Chamber		Re-entrant Bowl
Fuel Injector		Denso G3.5s
Number of Nozzle Holes		8
Nozzle Diameter	mm	0.116
Nozzle Flow Number	cc / 30 s	340
Nozzle Included Angle	degrees	155

Intake System

Intake pressure was closed-loop controlled by the test cell system which was capable of providing intake pressures up to 3 bar. The intake air and EGR were passed through heat exchangers for temperature control. The combined air-EGR mixture was then heated with an electric element. A closed-loop control system was used to maintain the intake charge temperature at 50 ± 1 °C for all test points. A large intake pressure vessel with pressure relief was used to dampen intake pulsations. Near the cylinder head, the intake runner was instrumented for temperature, static and high-speed dynamic pressure and probes for the ECM EGR-O₂ measurement system.

Exhaust System

A parallel system of control valves were used for closed-loop control of the exhaust pressure. The exhaust runner was instrumented for temperature, static and high-speed dynamic pressures. A large pressure vessel was used to dampen pressure pulsations. Gaseous emissions were sampled from the pressure vessel. A custom exhaust sampling tube downstream of the control valves was designed for sampling exhaust particles, smoke and soot and for the ECM EGR-O₂ measurement system probes. Care was taken to ensure the

sampling probe locations and device back flows did not confound any the measurement systems. This included time-sequencing the data acquisition process.

The entire exhaust system was insulated and electrically heated to maintain a surface metal temperature greater than 200 °C. Exhaust system heating was employed to avoid hydrocarbon adsorption and condensation and to minimize thermophoresis effects which drive exhaust aerosols and particles to the walls.

4.4. Fuel

A full-range petroleum Diesel fuel and several multi-component surrogate fuels were tested in the single-cylinder engine. Some properties for the petroleum Diesel fuel are given in Table 4-2 while the Appendix contains detailed information for all of the fuels.

Table 4-2: Some properties of the petroleum Diesel fuel tested in this study.

Property	Units	Value
Cetane Number		50.9
Threshold Soot Index	mm	33.57
Density at 15 degrees C	g/ml	0.849
Lower Heating Value	MJ/kg	43.004
Distillation Temperature - 10% v/v	°C	226.8
Distillation Temperature - 90% v/v	°C	311.7

4.5. Measurements and Controls

The prominent measurement systems are described in this section.

Test Cell Data Acquisition and Control System

The AnD Technology ADAPT System was the heart of the test facility [4.2]. All of the measurement systems were interfaced to ADAPT for monitoring, data acquisition, real-time engineering calculations and closed-loop control. The ADAPT system controlled most test cell systems such as the engine dynamometer, oil and coolant system, critical air flow system, heating and cooling systems using General Motors proprietary software and algorithms.

Low speed data channels were continuously scanned at 100 hertz. During data acquisition, the signals were sampled for 90 seconds and averaged. ADAPT was integrated with the AnD Combustion Analysis System (CAS) to provide real-time cylinder-pressure based combustion diagnostics.

Real-Time Combustion Analysis System (CAS)

The AnD Technology CAS is a real-time, high-speed-data acquisition and analysis system designed for engine cylinder-pressure based combustion analysis. Classical combustion diagnostics such as peak cylinder pressure, mean effective pressure, combustion burn duration, and many others, are calculated from cylinder pressure and other high-speed data acquired by the system [4.3].

The calculation of indicated, net and pumping mean effective pressures (IMEP, NMEP, PMEP) were consistent with methods reported in Heywood [4.1] and the UPV-CMT analysis code CALMEC from Lapuerta [4.4] and Payri [4.5]. A modified Rassweiler-Withrow type heat-release analysis provided combustion burn periods from which combustion phasing parameters such as the crank-angle of 50% mass burned fraction were obtained. Further details were given in the CAS Reference Manual [4.6].

Table 4-3 shows the high-speed data that were acquired by the CAS system. Data were sampled for 150 consecutive engine cycles at a crank-angle resolution of 0.2 degrees. This data were combined with the ADAPT low-speed data and post-processed to provide a database in engineering units.

Table 4-3: High-speed data signals.

Signal	Units
Engine Cylinder Pressure	kPa
High Pressure Fuel Line	bar
Fuel Injector Current Signal	A
Intake Runner Pressure	kPa
Exhaust Runner Pressure	kPa

Post-Processing Combustion Analysis

Low-speed and high-speed data were post-processed using a proprietary software package developed by General Motors Research and Development. The package used standardized routines to calculate engine performance parameters such as net thermal efficiency, emissions and heat release parameters. The package provided results consistent with the CALMEC software developed at the UPV-CMT [4.4] [4.5]. In this thesis, the apparent heat-release was calculated as described by Heywood [4.1] and Gatowski et al. [4.7] and for brevity is referred to as heat-release (J) or heat-release rate (J/CAD).

Figure 4-3 shows cylinder pressure measurement as a function of the engine crank-angle position and the bulk gas temperature computed from the cylinder pressure and the ideal gas law [4.7]. For this thesis, crankshaft top-dead-center (TDC) for the compression stroke was defined as 0 degrees. Crank angles after top-dead-center (aTDC) were defined with positive values while negative values represent before top-dead-center. The figure also shows the commonly used combustion metrics: peak cylinder pressure and peak bulk gas temperature.

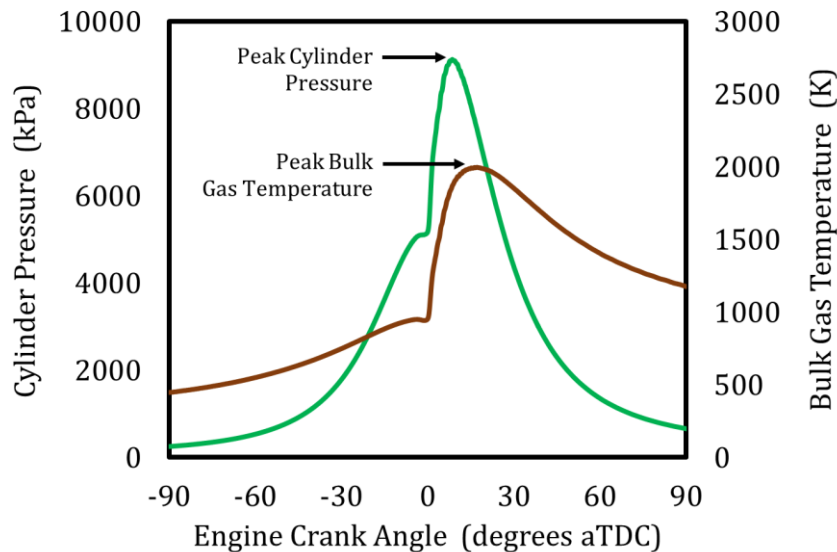


Figure 4-3: Combustion metrics Peak Cylinder Pressure and Peak Bulk Gas Temperature.

The apparent heat-release rate for a moderate engine speed and load is shown for conventional Diesel combustion in Figure 4-4. The combustion process in the figure can be characterized by a low-temperature heat release (LTHR) zone that occurred before top-dead-center and a high-temperature heat release (HTHR) zone that occurred after top-dead-center. The HTHR was initiated by a rapid premixed combustion zone. Upon consumption of the premixed portion, the remaining fuel was burned by diffusion combustion. The peak heat release rate is a combustion metric used in this thesis to characterize the overall heat release process. This was used to quantify combustion discrepancies that may have resulted from fuel property variations. The heat-release regions shown in Figure 4-4 (LTHR, premixed and diffusion combustion) depend on the several factors including the Diesel fuel properties and the engine operating conditions. For example, low-speed and light-load operating conditions may result in predominantly premixed combustion. Operating at high engine speeds and high loads may reduce or eliminate the LTHR, reduce the premixed combustion and result in predominantly diffusion combustion. The oscillations observed during

the diffusion combustion region are an artifact of the cylinder-pressure measurements.

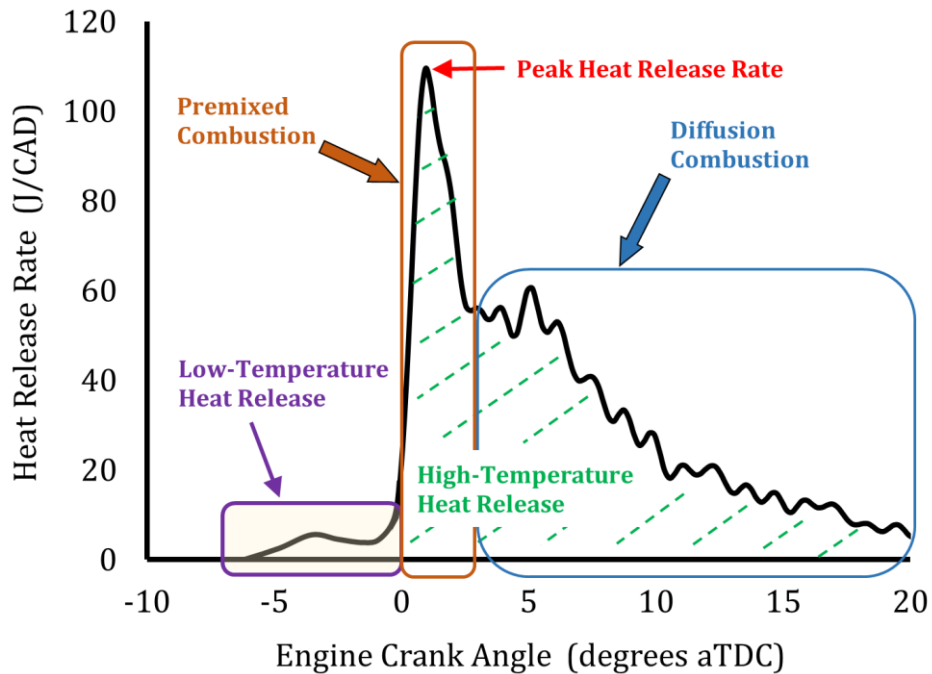


Figure 4-4: Heat release for conventional Diesel combustion.

The heat-release rate was integrated and expressed as a percentage of the mass burned Figure 4-5. The figure depicts the crank-angle of the 50% mass burn (CA50%) which is a combustion metric used to quantify combustion phasing. Combustion duration was measured by the duration between the 10% and 90% mass burn locations, as shown in the figure.

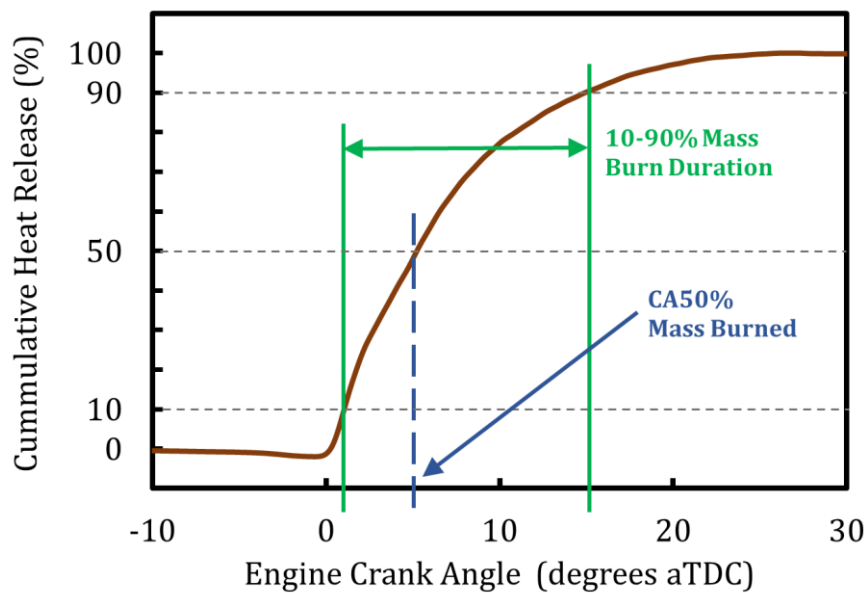


Figure 4-5: Combustion metrics: CA50% Mass Burned and 10-90% Mass Burned Duration.

The fuel injector current signal, high pressure fuel line signal and heat-release rate were analyzed to quantify fuel injection events, ignition (onset of high-temperature heat release), ignition delay, mixing advance time and other events related to injection and combustion, see Figure 4-6. The Start of Energizing and End of Energizing were determined from the fuel injector current signal. The Start of Injection and the End of Injection were determined from the high pressure fuel line signal. Ignition was defined as the crank-angle of 5% mass burned (CA05) which identified the onset of the high-temperature heat release. Ignition delay was computed as the period from the Start of Injection to ignition. The Mixing Advance Time quantified the period between the End of Injection and Ignition.

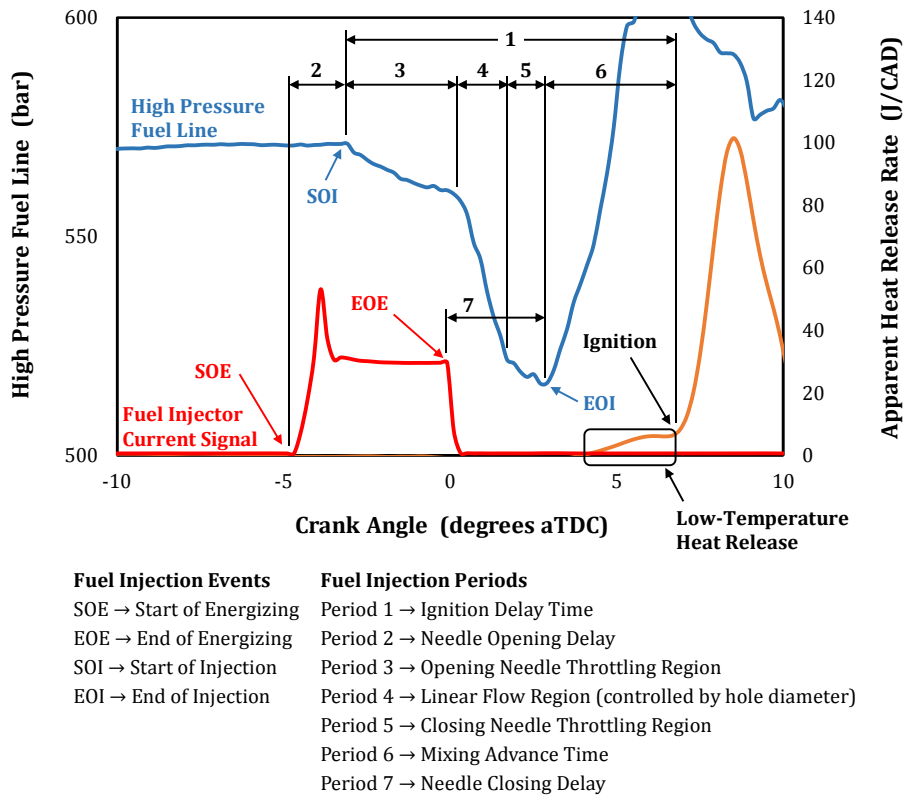


Figure 4-6: Fuel injection events and periods based on the high pressure fuel line signal, fuel injector current signal and heat release from a common rail injector with a single-injection strategy.

Combustion Measurements

For cylinder pressure measurements, the glow plug hole was machined and fitted with a custom designed adapter to flush-mount a Kistler Type 6125C10 combustion pressure sensor. The high pressure fuel line connecting the rail to the injector was fitted with a Kistler Type 4067C3000S dynamic pressure sensor to infer start of injection from the fuel pressure signal as shown in Figure 4-6. Engine crankshaft position was measured by a Kistler Type 2613B crank angle encoder with a resolution of 0.2 crank-angle degrees.

Emission Measurements

Gaseous emissions consisting of exhaust CO₂, CO, HC, NO_x and O₂ and intake CO₂ were measured with a dual sample line Horiba Mexa D7500EGR emission bench. All sample lines were heated and the NO_x and HC analyzers were contained in separately heated ovens. The emission bench was modified for high-pressure intake CO₂ sampling. The bench featured two exhaust sample lines with two complete sets of gas analyzers. Exhaust samples were taken from two locations and the measurements were compared to ensure data accuracy and quality. An additional quality check was made by routinely sampling from cylinders of premixed gases of known concentrations. This technique validates the entire sampling and measurement system. Data from the emission bench were transmitted to the test cell data acquisition system (ADAPT) where dry and wet emission concentrations were monitored and recorded.

Exhaust Gas Recirculation (EGR)

The EGR system employed a control valve to modulate flow and a heat exchanger to control EGR temperature. The EGR was mixed with the intake air upstream of the intake pressure vessel in a manner that thoroughly mixed the air with the EGR. Intake gas was sampled from the pressure vessel to measure the intake CO₂ concentration. Wet mass percent EGR was calculated using the standard General Motors analysis software which provided results consistent with CALMEC [4.4] [4.5].

Exhaust Smoke Measurements

Smoke was measured using the AVL Smoke Meter 415SE with the heated sampling system option. The AVL 415SE applies the traditional filter paper blackening method. Data are reported as Filter Smoke Number (FSN) and soot concentration ($\mu\text{g}/\text{m}^3$) using paper blackening correlations provided by AVL and built into the instrument [4.8]. Three successive samples were averaged for each measurement. Care was taken to maximize measurement accuracy including the heated sampling system, sample probe installation, sampling time optimization and calibration of the sample line volume. For conventional combustion modes where the total particulate mass is dominated by carbon, a commonly used correlation between filter smoke

number and exhaust particulate emission index provides a reasonable approximation for particulate mass [4.9] [4.10]. Such correlations are less useful when a substantial fraction of the particulate mass is from volatile organics or when the filter smoke numbers are very low (<0.2).

Exhaust Opacity Measurements

Opacity was measured with the AVL Opacimeter 439. This device uses a light extinction method to quantify the opacity of the engine exhaust. A small continuous exhaust sample is passed through a heated chamber with an optical measurement system [4.11]. This device provides a continuous measurement of exhaust opacity which is very useful when setting engine operating conditions. Opacity data is also valuable for correlating with smoke measurements to ensure data quality. Care must be taken with the location of the return sample line as it is diluted with air and will impact downstream measurements.

Exhaust Particle Measurements

Exhaust particle number density and size distribution were characterized with the Cambustion DMS500 fast particle analyzer shown in Figure 4-7. The DMS500 uses electrical particle mobility measurements to make particle size and particle number measurements. Figure 4-8 shows DMS500 measurements of the particle size spectral density for the total spectrum (discrete mode), accumulation mode spectrum (solid particles) and nucleation mode (volatile particles).



Main Unit



Heated Sample Line



Vacuum Pump

Figure 4-7: Cambustion DMS500 MKII Fast Particulate Analyzer [4.13].

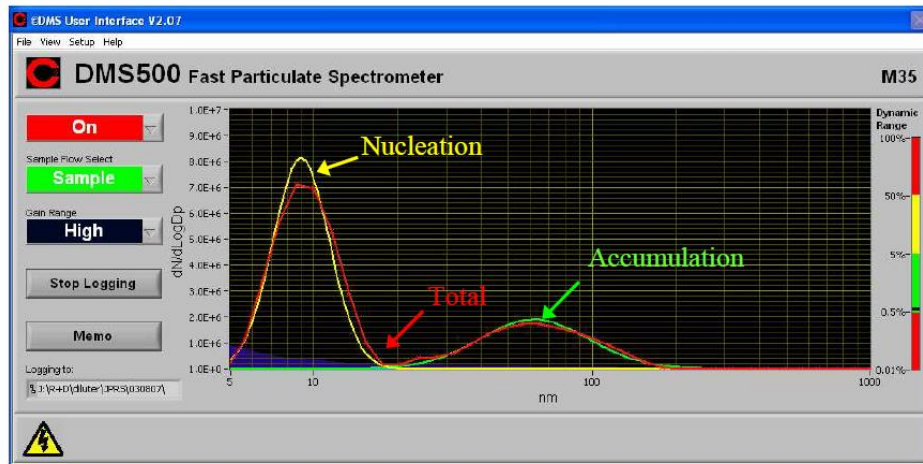


Figure 4-8: Total, accumulation and nucleation mode spectrums [4.13].

The measurement principle is shown in Figure 4-9 and Figure 4-10. The exhaust sample is drawn, diluted and passed through a cyclone to remove large particles from the stream. Then the sample undergoes a second dilution stage, passes through a High Efficiency Particulate Air (HEPA) filter and is sent to the measurement column with electrometer detectors. At the column inlet, the sample is passed through a unipolar corona charger that electrically charges each particle with a charge that's approximately equal to the particle surface area. The charged particles then enter a classification column and travel along the classifier. A high voltage electrode in the center of the classifier repels the charged particles from the column center towards the detectors. Smaller particles are more aerodynamically mobile and land on classifiers near the column entrance. Larger particles are accumulated in detectors axially along the length of the column. When a charged particle contacts a detector the charge is transferred to an amplifier which receives signals from 22 detectors to determine particle flux. Software calibrations calculate the particle size and particle number spectrums. A Diesel-specific particle calibration determines particle mass and total particle number density from the spectrums.

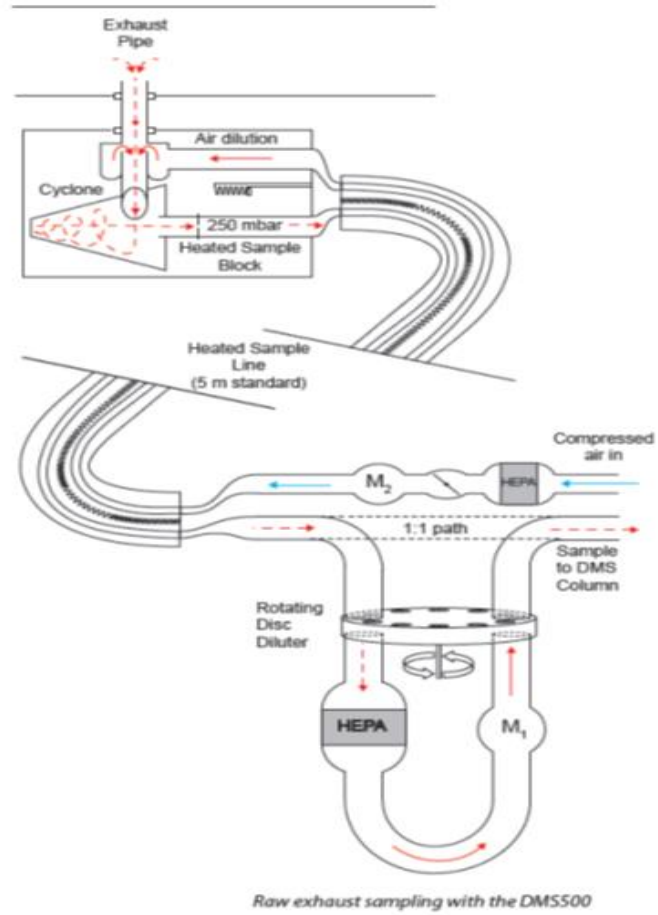


Figure 4-9: DMS500 sampling and dilution system [4.13].

Operating Principle

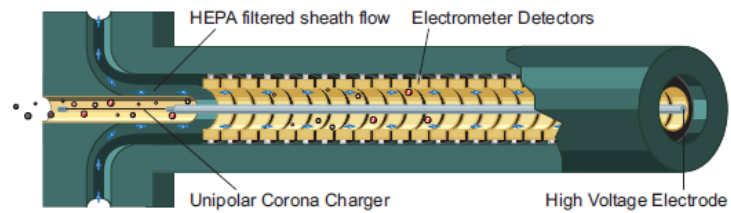


Figure 4-10: DMS Column [4.13].

Post-Processing Exhaust Particle Analysis

Exhaust particle data were post-processed with software provided by Cambustion [4.12] [4.13]. Data summaries included statics that described the particle distribution such as total particle number concentration and particle geometric mean diameter. Particle spectral analysis were performed on the discrete mode, accumulation mode and nucleation mode particles.

Air Flow

A critical air flow supply system provided accurately controlled intake air pressure and precise mass flow measurement. The system, which was custom designed and supplied by Flow Systems Inc., consisted of six precision nozzles of varying size that are calibrated as sonic flow nozzles. Mass flow is calculated using the nozzle calibrations and pressure drop across the nozzles (provided the flow has achieved the sonic condition). The critical air flow system was integrated into the test cell control system which provided accurate closed-loop control of intake pressure and air flow.

Fuel Flow

An AVL P404 Fuel Measurement Cart supplied low pressure fuel to the high-pressure fuel pump. The cart provided fuel conditioning, density and mass flow measurements. Due to the very low flow rates typical of single-cylinder engines at light loads, a special low-flow fuel meter with a high-precision calibration was installed in the cart.

Temperature

All temperatures were measured with K-type thermocouples which were part of the standard test cell configuration. Gas and fluid temperatures (air, EGR, oil, coolant) were measured by positioning the thermocouple end tip in the center of the flow stream. Surface thermocouples were welded throughout the intake and exhaust system to monitor and control surface temperatures.

Pressure

Static pressures were measured with transducers appropriately sized for the required pressure ranges. High-speed pressure measurements were made in the intake and exhaust runners. Dynamic intake pressure was measured with the Kistler Type 4045A5 piezoresistive absolute pressure sensor. The water-cooled Kistler Type 4049A10S piezoresistive absolute pressure was used to measure dynamic exhaust pressure.

Controls

A commercially available system known as DRIVVEN was used to control the fuel injection system [4.14]. This steady-state controller was capable of providing up to 5 fuel injection events per engine cycle. DRIVVEN also controlled the high-pressure fuel pump which could deliver up to 1600 bar fuel pressure. DRIVVEN was interfaced to ADAPT for data transfer and operational control.

4.6. Test Conditions and Procedures

In this thesis, engine test condition nomenclature was defined by engine speed and IMEP. For example, 1500x3 represented the 1500 r/min and 3 bar IMEP test condition while 1500x9 represented the 1500 r/min and 9 bar IMEP.

Test Conditions

The engine and fuels were tested at two operating conditions. A moderate engine speed and load was used to evaluate the fuels under conventional Diesel combustion conditions. The engine speed was maintained at 1500 r/min and the engine load was held constant at 9 bar IMEP. This operating condition was designated as 1500x9. A light-load condition was also tested to investigate advanced combustion strategies known as Premixed Charge Compression Ignition (PCCI) and Low Temperature Combustion (LTC). The light-load condition was operated at 1500 r/min and 3 bar IMEP and labeled 1500x3. The engine test conditions are given in Table 4-4 and described below.

EGR and combustion phasing are calibration parameters that can have the greatest influence on combustion and emissions. Thus, these parameters were systematically varied to comprehend their individual and combined effects. EGR was varied from 0% to a maximum dilution tolerance using six EGR levels to define the response. The dilution tolerance was defined by combustion instability, increased HC or CO emission or smoke exceeding FSN=3. Combustion phasing, as measured by CA50, was varied from advanced to retarded in fixed increments of CA50 = 6, 9, 12 and 15 degrees aTDC. The resulting matrix of EGR and CA50 sweeps consisted of 24 test points.

The intake pressure was set primarily based on the engine speed and load. The pressure differential between the intake and exhaust was fixed for each operating condition. In practice, a turbocharged engine does not function in this manner. However, maintaining a constant pressure differential does provide useful results and is very pragmatic for running the single-cylinder engine tests.

A single injection strategy was run for all tests. This was selected to simplify the combustion process for improved analysis of fuel property effects. Additionally, a single injection strategy allows for improved comparisons with future spray experiments and combustion simulations.

Table 4-4: Engine test conditions.

Operating Condition	Units	1500x9	1500x3
Engine Speed	r/min	1500	1500
Engine IMEP	bar	9	3
Fuel Injection Pressure	bar	650	550
Intake Pressure	kPaA	121	102
Exhaust Pressure	kPaA	128	106
Fuel Injection Strategy		Single	Single
Intake Temperature	°C	50	50
Swirl Ratio		2.9	2.9
EGR Level	%	0, 10, 15, 20, 25, 30	0, 20, 40, 50, 55, 60
CA50	degrees aTDC	6, 9, 12, 15	6, 9, 12, 15

Test Procedure

At each operating condition, data was collected for the 24-point test matrix which swept EGR and CA50. The matrix was repeated for each of the fuels tested in the engine. The following test procedure was used to collect the data for each operating condition and for each fuel:

- 1) Perform instrument calibrations and checks (e.g., emission bench).
- 2) Operate at a high-load condition (1500x16) for 15 minutes to stabilize the engine, intake and exhaust system temperatures as well as combustion system deposits and hydrocarbons adsorbed on the exhaust system walls.
- 3) Collect data at three check point conditions. Checkpoints were run at 1500 r/min with motoring, 3 bar and 16 bar IMEP loads. The test

results were examined to confirm the engine and facility were operating properly.

- 4) Collect data for each of the 24 points in the EGRxCA50 matrix. Includes stabilization periods which varied with operating conditions.
- 5) Collect data at the three check point conditions and review data for consistency.

4.7. Summary

A highly-instrumented engine-dynamometer test cell was fitted with a single-cylinder Diesel engine for engine combustion, performance and emission testing. The facility was used to collect data at engine conditions that employed conventional and advanced combustion strategies. The engine response to parametric variations in EGR and combustion phasing were measured for each operating condition. The entire test sequence was conducted with a full petroleum Diesel fuel then repeated with a multi-component surrogate fuel.

4.8. References

- [4.1] Heywood, J., "Internal combustion engine fundamentals", 1st ed., McGraw-Hill, New York, 1988.
- [4.2] A&D Technology, "ADAPT Test Automation System", *A&D Technology, Inc.*, 2014. <http://www.aanddtech.com/ADAPT.html>, 2014.
- [4.3] A&D Technology, "Phoenix AM/RT Combustion Analysis Systems" *A&D Technology, Inc.*, 2014. <http://www.aanddtech.com/Phoenix.html>, 2017.
- [4.4] Lapuerta, M., Armas, O. and Hernández, J., "Diagnosis of DI Diesel combustion from in-cylinder pressure signal by estimation of mean thermodynamic properties of the gas", *Applied Thermal Engineering* 19(5):513-529, 1999, doi:10.1016/s1359-4311(98)00075-1.

- [4.5] Payri, F., Molina, S., Martín, J. and Armas, O., "Influence of measurement errors and estimated parameters on combustion diagnosis", *Applied Thermal Engineering* 26(2-3):226-236, 2006, doi:10.1016/j.applthermaleng.2005.05.006.
- [4.6] A&D Technology, "CAS 4.0 Reference Manual", *A&D Technology, Inc.*, First Edition, 2009.
- [4.7] Gatowski, J., Balles, E., Chun, K., Nelson, F., Ekchian, J. and Heywood, J., "Heat Release Analysis of Engine Pressure Data", *SAE Technical Paper Series*, 1984, doi:10.4271/841359.
- [4.8] AVL, "Smoke Value Measurement with the Filter-Paper-Method, AT1007E, Rev. 02", *AVL List GmbH*, Graz, Austria, 2nd ed., 2005.
- [4.9] Kirchen, P., Boulouchos, K., Obrecht, P. and Bertola, A., "Exhaust-Stream and In-Cylinder Measurements and Analysis of the Soot Emissions from a Common Rail Diesel Engine using Two Fuels", *ASME 2009 Internal Combustion Engine Division Fall Technical Conference*, ASME Internal Combustion Engine Division, Lucerne, Switzerland, 2009.
- [4.10] Northrop, W., Bohac, S., Chin, J. and Assanis, D., "Comparison of Filter Smoke Number and Elemental Carbon Mass From Partially Premixed Low Temperature Combustion in a Direct-Injection Diesel Engine", *Journal Of Engineering For Gas Turbines And Power* 133(10):102804, 2011, doi:10.1115/1.4002918.
- [4.11] AVL, "AVL Product Description, Emission Test Instruments - AVL 439 Opacimeter", *AVL List GmbH*, Graz, Austria, 2008.
- [4.12] Cambustion, "DMS500 Fast Particle Analyzer", *Cambustion Limited*, Cambridge, UK, 2014, <http://www.cambustion.com/products/dms500>, 2017.
- [4.13] Cambustion, "DMS500 User Manual Version 3.1", *Cambustion Limited*, Cambridge, UK, 2010, <http://www.cambustion.com>, 2017.

- [4.14] National Instruments, "Powertrain Controls - National Instruments", *National Instruments*, 2015.
<http://www.ni.com/powertrain-controls/>, formerly
<http://www.drivven.com>, 2016.

5. Surrogate Fuel Development

Contents

5.	Surrogate Fuel Development.....	87
5.1.	Introduction.....	89
5.2.	Surrogate Fuel Formulation.....	89
5.3.	Predicted and Measured Property Comparisons.....	107
5.4.	Surrogate and Petroleum Fuel Comparison.....	116
5.5.	Discussion.....	131
5.6.	Summary and Conclusions.....	136
5.7.	References	137

5.1. Introduction

In recent times, multi-component surrogate fuels were developed to mimic the properties of various petroleum Diesel fuels [5.1] [5.2] [5.3] [5.4] [5.5] [5.6] [5.7]. While providing great value for combustion simulation and experimental research, the surrogates generally lacked the ability to vary important fuel properties such as ignition quality and sooting tendency. Within this chapter, a Diesel Surrogate Fuel Library was developed to provide researchers with the ability to select surrogate fuels with different values of cetane number and sooting tendency.

The chapter begins with the methodology to blend surrogate fuels that achieved the required values for cetane number, sooting tendency and other fuel properties. Utilizing the methodology, blend formulas were developed for a Surrogate Fuel Library that consisted of 18 fuels. The library included cetane numbers of 35, 40, 45, 50, 55, and 60 with TSI values of 17, 31, and 48 at each cetane number. Key fuel properties were predicted using the ANSYS Surrogate Blend Optimizer. Several surrogate fuels were blended, their properties were measured using ASTM test procedures and then compared to the predicted properties.

5.2. Surrogate Fuel Formulation

A methodology was developed to formulate the surrogate fuel components and blending volumes required to achieve the overall objectives and the required surrogate fuel properties. A schematic of the methodology is presented in Figure 5-1 and described in the sections that follow. The objectives, target Diesel fuel properties and the Model Fuel Library were part of an initial investigation that determined the hydrocarbon species used for the surrogate fuel components. Cetane number and TSI values were assigned to each fuel in the library. Given the surrogate components and desired values for cetane number and TSI, the surrogate blend was optimized adhering to a set of blending rules developed within this thesis. The blend optimization was repeated for each fuel in the library. The surrogate formulation and predicted properties were tabulated and entered into the Surrogate Fuel Library for further analysis.

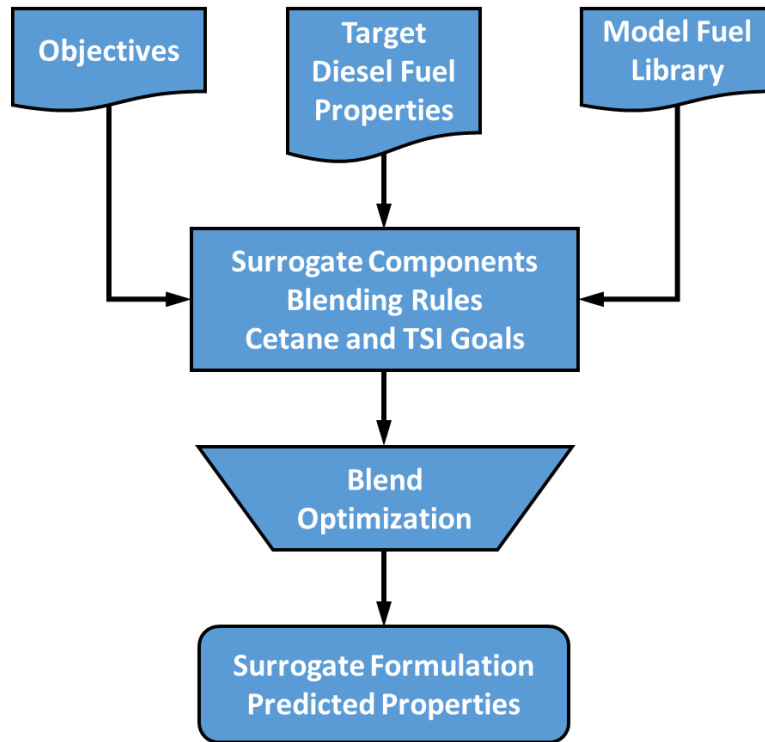


Figure 5-1: Methodology used to develop surrogate fuel blends.

5.2.1 Objectives

One of the desired outcomes of this research was to bring multi-component surrogate fuels closer to routine use by the automotive industry. To this end, several objectives were placed on the multi-component surrogate fuels developed through this investigation.

Global Objectives

- The Surrogate Fuel Library must contain one fully-representative surrogate that closely matches the combustion, physical and chemical properties of a full-range petroleum Diesel fuel (target Diesel fuel).

- The Surrogate Fuel Library must span a broad range of cetane number and threshold soot index while maintaining representative values for density, viscosity, surface tension and heating value.
- The Surrogate Fuel Library must provide the surrogate formulations and key properties such as density, viscosity, heating value and distillation curves for each fuel.
- The number of surrogate fuel components must be kept to a minimum to manage increased complexity, kinetic mechanism size, computational and experimental expenses.

Cetane Number

- Precise control of surrogate fuel cetane number was required. The library must cover the cetane number range of globally available production Diesel fuels. Finally, the library needed to include reasonable surrogates to represent potential next-generation fuels which may extend the cetane number range as low as 35 for naphtha-like fuels [5.8] [5.9] or as high as 60 for synthetic fuels [5.10] [5.11].

Sooting Tendency

- Three levels of sooting tendency were required. Low (TSI=17), mid (TSI=31) and high (TSI=48) sooting tendencies were chosen to reproduce global variations observed in production fuels. In addition, a broad sooting tendency range would support future investigations to expand the understanding of the physical and chemical factors influencing soot and particle emissions.

Surrogate Components

- The components must have validated, detailed kinetic mechanisms.
- The required combustion, physical, chemical and temperature-dependent properties must be available for the surrogate components.
- Must be able to acquire the components with high-purity and large quantities (30-60 liters) to support experimental work.
- Must be able to store, blend and safely handle the components (flash point, toxicity, etc.).

5.2.2 Target Diesel Fuel

In this thesis the term target Diesel fuel was defined as an available market fuel that could be used for engine research and development, vehicle testing and suitable for end use by vehicle owners. The term full-range petroleum Diesel was synonymous with this definition. The literature review in Chapter 2 showed Diesel fuel properties vary widely based on geographical region, season, regulations and other factors. During the selection of a target Diesel fuel, properties from several market fuels were collected and analyzed. The cetane number results for some of these fuels are given in Figure 5-2 in which cetane number ranged from 44 to 56.



Figure 5-2: Cetane number measurements of full-range petroleum and biodiesel fuels.

Upon analysis, the Ultra-Low Sulfur Diesel (ULSD) High Cetane fuel was selected as the target Diesel fuel. This fuel was chosen because it was commonly used for combustion system development and several of its properties were more tightly controlled than common market fuels [5.12]. In addition, the cetane number and TSI for this fuel were near the middle of the ranges observed for commercially-available Diesel fuels. Some of the key properties for the target Diesel fuel are given in Table 5-1 while more detailed properties are given later in this chapter and in the Appendix.

Table 5-1: Target Diesel fuel properties.

Fuel Property	Units	ASTM Method	Target Diesel Fuel
Cetane Number		D6890	50.9
Smoke Point		D1322	19
Threshold Soot Index			31
Lower Heating Value	MJ/kg	D240N	43.004
Density at 15 °C	g/ml	D4052	0.8489
Kinematic Viscosity at 40 °C	cSt	D445	3.063
Molar H/C	M/M	J1829	1.851
Distillation Temperature T ₁₀	°C	D86	227
Distillation Temperature T ₅₀	°C	D86	281
Distillation Temperature T ₉₀	°C	D86	312
Saturated Hydrocarbons	%v/v	D1319	76.0
Olefinic Hydrocarbons	%v/v	D1319	7.5
Aromatic Hydrocarbons	%v/v	D1319	16.5

5.2.3 Model Fuel Library

The ANSYS Model Fuel Library (MFL) was selected to provide the most comprehensively available list of surrogate fuel components with corresponding property information and detailed kinetic mechanisms. This library included over a dozen different fuel classes and 55 pure fuel components. Table 5-2 shows the distribution of fuel components among the fuel classes, specie or compound name and chemical formula for all of the components available in the Model Fuel Library [5.13].

Table 5-2: Complete list of the surrogate fuel components available for the formulation of surrogate fuels.

Normal-Alkanes	
Compound	Formula
Methane	CH ₄
Ethane	C ₂ H ₆
Propane	C ₃ H ₈
n-Butane	C ₄ H ₁₀
n-Pentane	C ₅ H ₁₂
n-Hexane	C ₆ H ₁₄
n-Heptane	C ₇ H ₁₆
n-Octane	C ₈ H ₁₈
n-Nonane	C ₉ H ₂₀
n-Decane	C ₁₀ H ₂₂
n-Undecane	C ₁₁ H ₂₄
n-Dodecane	C ₁₂ H ₂₆
n-Tridecane	C ₁₃ H ₂₈
n-Tetradecane	C ₁₄ H ₃₀
n-Pentadecane	C ₁₅ H ₃₂
n-Hexadecane	C ₁₆ H ₃₄
n-Octadecane	C ₁₈ H ₃₈
n-Eicosane	C ₂₀ H ₄₂

Cyclo-Alkanes	
Compound	Formula
Cyclohexane	C ₆ H ₁₂
Methylcyclohexane	C ₇ H ₁₄
Decahydronaphthalene	C ₁₀ H ₁₈

iso-Alkanes	
Compound	Formula
iso-Butane	C ₄ H ₁₀
iso-Pentane	C ₅ H ₁₂
neo-Pentane	C ₅ H ₁₂
iso-Hexane	C ₆ H ₁₄
iso-Octane	C ₈ H ₁₈
Heptamethylnonane	C ₆ H ₁₄

Aromatics	
Compound	Formula
Benzene	C ₆ H ₆
Toluene	C ₇ H ₈
Styrene	C ₈ H ₈
Ethylbenzene	C ₈ H ₁₀
m-Xylene	C ₈ H ₁₀
o-Xylene	C ₈ H ₁₀
p-Xylene	C ₈ H ₁₀
n-Propylbenzene	C ₉ H ₁₂
Trimethylbenzene	C ₉ H ₁₂
Naphthalene	C ₁₀ H ₈
1-Methylnaphthalene	C ₁₁ H ₁₀

Alkenes	
Compound	Formula
Cyclopentadiene	C ₅ H ₆
1-Pentene	C ₅ H ₁₀
2-Pentene	C ₅ H ₁₀
2-Methyl-2-Butene	C ₅ H ₁₀
1-Hexene	C ₆ H ₁₂
2-Hexene	C ₆ H ₁₂
3-Hexene	C ₆ H ₁₂

Hydrogen Compounds	
Compound	Formula
Hydrogen	H ₂
Hydrogen Sulfide	H ₂ S

Alcohols	
Compound	Formula
Methanol	CH ₃ OH
Ethanol	C ₂ H ₆ O
n-Butanol	C ₄ H ₁₀ O

Ethers	
Dimethyl Ether	
Methyl Tert-Butyl Ether	
Tetrahydrofuran	
Ethyltetrahydrofurfuryether	

5.2.4 Surrogate Components and Formulation

The complete list of surrogate components in the MFL was studied. Fuel properties such as cetane number, TSI, density, viscosity, heating value and boiling point were tabulated and reviewed. The first task was to reduce the list of 55 components to manageable number. This task focused on retaining fuel components with properties that were representative of Diesel fuel and eliminating species with non-representative properties. The following guidelines were applied to remove fuel species from consideration:

- Remove hydrocarbon classes that were not typically present in Diesel fuel in substantial volume (<10% v/v). For example, alcohols, ethers, hydrogen, hydrogen sulfide.
- Remove species that had boiling points that were beyond the distillation temperature range of the target Diesel fuel. For example, most alkenes had low boiling points.
- Remove species that were problematic for blending and conducting experimental investigations. For example, eicosane and naphthalene were solid at room temperature.
- Use a single species to represent a group of species with similar properties. For example, m-xylene was used to represent several aromatics including benzene, ethylbenzene, o-xylene, p-xylene and n-propylbenzene.

This process of analysis and species removal shortened the list of surrogate components from 55 to the 13 potential components given in Table 5-3. The compounds were grouped into their respective hydrocarbon classes. Some key properties are given in the table.

Table 5-3: Potential components for Diesel surrogate fuels.

	Cetane Number	TSI	Density (g/ml)	LHV (MJ/kg)	Boiling Point (°C)
Target Diesel Fuel →	50	31	0.849	43.00	T ₉₀ = 312

n-Alkanes

n-Hexadecane	100	6	0.773	45.23	287
n-Dodecane	83.8	6	0.750	44.23	216
n-Decane	76.7	4.5	0.730	44.56	174
n-Heptane	54.4	2.7	0.683	44.56	98

iso-Alkanes

Heptamethylnonane	15	21	0.793	44.38	240
iso-Octane	14	6.8	0.692	44.65	99

cyclo-Alkanes

Decahydronaphthalene	44	20	0.896	43.02	187
Methylcyclohexane	22.5	5	0.770	43.72	101
Cyclohexane	18.5	3.5	0.779	43.98	81

Aromatics

1-Methylnaphthalene	0	100	1.001	40.27	245
1,2,4-Trimethylbenzene	8.9	51	0.876	41.64	169
m-Xylene	2.6	51	0.864	40.81	139
Toluene	2.6	40	0.865	40.72	111

Given the component list in Table 5-3, the next step was to develop a surrogate fuel to match the properties of the target Diesel fuel shown in Table 5-1. Preliminary simulations demonstrated that the Surrogate Blend Optimizer was limited to optimizing surrogates with a maximum of 8 components. Therefore, other means would be required to select a subset of the 13 components given in Table 5-3. A detailed investigation was conducted to identify the surrogate components that could best achieve the objectives set forth in Section 5.2.1 and create a surrogate that closely matched properties of the target Diesel fuel. For brevity, the highlights of this investigation are summarized below:

- The Surrogate Blend Optimizer was used to generate numerous multi-component surrogate fuels. The number of components ranged from 2 through 8. Sensitivity studies were conducted to identify components that had small influences on achieving the desired properties. The influences could be small due to the component properties or a small component volume fraction determined by the optimizer (<5% v/v).
- Closed-homogeneous reactor simulations were conducted to examine the Negative Temperature Coefficient (NTC) region for the surrogate components. Comparisons were made between components in the same hydrocarbon class. For example, Figure 5-3 shows the n-alkanes were found to have significantly different NTC behavior. There were also substantial differences between the hydrocarbon classes. For example, the aromatics had significantly longer ignition delay and did not exhibit NTC behavior.

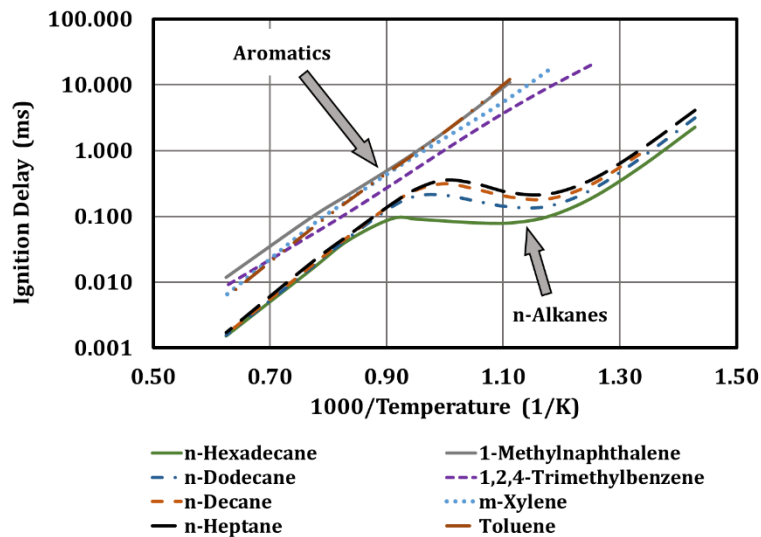


Figure 5-3: Ignition delay for n-alkane and aromatic compounds. Closed-homogeneous reactor initial pressure = 40 bar and equivalence ratio = 1.0.

- Several surrogates were blended and tested for cetane number using an Ignition Quality Tester (IQT) following ASTM D6890. The impact of several component blend concentrations on cetane number were evaluated. For example, it was determined that the concentrations of n-hexadecane and heptamethylnonane could be manipulated to precisely control cetane number with minimal impact on the other fuel properties (density, heating value, viscosity). Predicted and measured cetane numbers for blends of n-hexadecane and heptamethylnonane are provided in Figure 5-4. Good agreement was obtained. Additional IQT testing was conducted to confirm the Surrogate Blend Optimizer cetane number predictions for various multi-component surrogate blends. In general, there was good agreement between predicted and measured cetane number - although some modest discrepancies were observed.

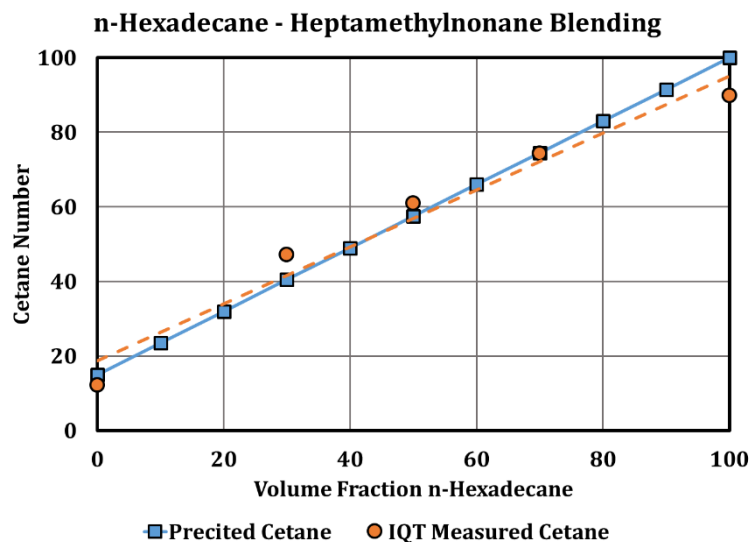


Figure 5-4: Predicted and IQT measured cetane number for blends of n-hexadecane and heptamethylnonane.

- The original list of 13 components was further reduced and divided into 2 sets. The first set contained the best seven components and the second set the best four components. Using the Surrogate Blend Optimizer, surrogate formulations were created for each set. The optimizer was set to match the target Diesel fuel properties shown

in Table 5-1. The predicted fuel properties for the optimized seven-component surrogate and the optimized four-component surrogate were similar and closely matched the target Diesel fuel properties. A set of closed-homogeneous reactor simulations were run using both surrogates along with n-heptane. Ignition delays for low temperature and high temperature chemistry are shown in Figure 5-5. The ignition delays for the seven-component and four-component surrogates had very close agreement. Results were similar at other reactor conditions. Close agreement was also found with reactor species such as acetylene, ethane and benzene.

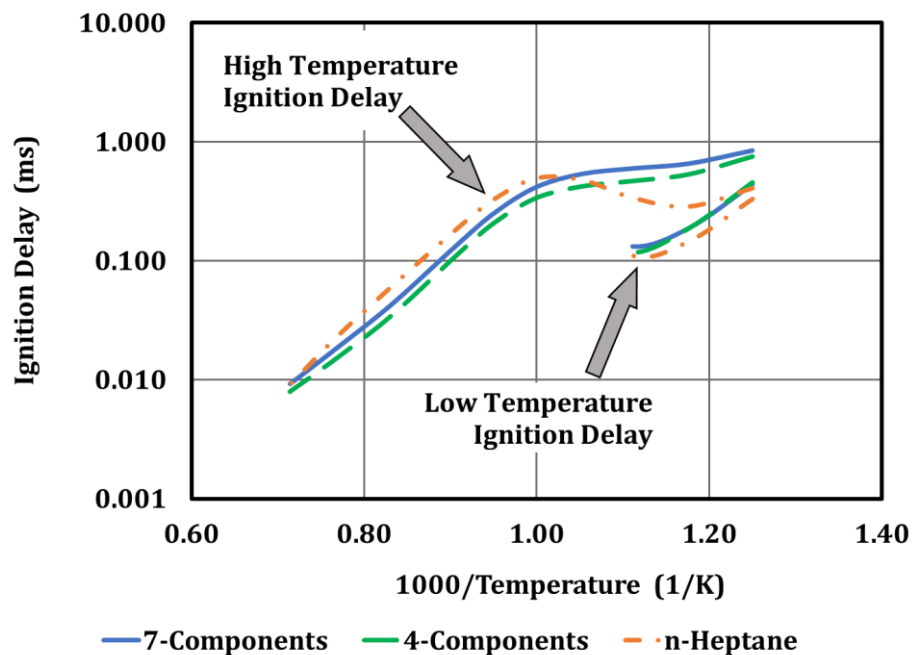


Figure 5-5: Low temperature and high temperature ignition delay for a seven-component surrogate, four-component surrogate and n-heptane. Closed-homogeneous reactor initial pressure = 40 bar and equivalence ratio = 1.0.

From the above investigation it was concluded that the four-component surrogate best achieved the objectives given in Section 5.2.1. Thus, the surrogate fuels developed in this thesis would use the following

components: n-hexadecane to represent the n-alkane class, heptamethylnonane to represent the iso-alkane class, decahydronaphthalene to represent the cyclo-alkane class and aromatics would be represented by 1-methylnaphthalene. General information and properties for the selected surrogate components are provided in Table 5-4 [5.13] [5.14].

Table 5-4: Surrogate Fuel Components.

Parameter	Normal-Hexadecane	Heptamethyl-nonane	Decahydro-naphthalene	1-Methyl-naphthalene
Hydrocarbon Class	n-Alkane	iso-Alkane	Cycloalkane	Aromatic
Chemical Formula	C ₁₆ H ₃₄	C ₁₆ H ₃₄	C ₁₀ H ₁₈	C ₁₁ H ₁₀
Molecular Weight (g/mol)	226.45	226.45	138.25	142.2
CAS Number	544-76-3	4390-04-9	91-17-8	90-12-0
Purity (%)	99	87	99	97
Cetane Number	100	15	44	0
Threshold Soot Index	6	21	20	100
Density at 25° C (g/ml)	0.773	0.793	0.896	1.001
Lower Heating Value (MJ/kg)	45.23	44.38	43.02	40.27
Boiling Point (°C)	287	240	187	242
Kinematic Viscosity (cSt)	3.975	4.293	2.254	2.861

The formulation of the four-component surrogate developed to match the target Diesel fuel is given in Table 5-5. The predicted surrogate fuel properties are given with the target Diesel fuel properties in Table 5-6. The

results showed the predicted surrogate fuel properties closely matched the target Diesel fuel. A more detailed comparison and analysis of the surrogate and target fuels is provided in Section 5.4.

Table 5-5: Surrogate fuel components and blend formulation for the surrogate fuel developed to match the properties of the target Diesel fuel.

Hydrocarbon Class	Surrogate Fuel Specie	Volume Fraction
n-Alkanes	n-Hexadecane	0.37
iso-Alkanes	Heptamethylnonane	0.33
cyclo-Alkanes	Decahydronaphthalene	0.18
Aromatics	1-Methylnaphthalene	0.12

Table 5-6: Properties of the target Diesel fuel compared with predicted properties of the surrogate Diesel fuel.

Fuel Property	Units	Target Diesel Fuel	Surrogate Diesel Fuel
Cetane Number		50.9	49.87
Smoke Point		19	18.8
Threshold Soot Index		31	31.5
Lower Heating Value	MJ/kg	43.004	43.81
Density at 15 °C	g/ml	0.8489	0.821
Kinematic Viscosity at 40 °C	cSt	3.063	2.41
Molar H/C	M/M	1.851	1.872
Distillation Temperature T ₁₀	°C	227	229
Distillation Temperature T ₅₀	°C	281	250
Distillation Temperature T ₉₀	°C	312	278
Saturated Hydrocarbons	%v/v	76.0	88.0
Olefinic Hydrocarbons	%v/v	7.5	0
Aromatic Hydrocarbons	%v/v	16.5	12.0

5.2.5 Surrogate Fuel Library

Following the development of a surrogate fuel formulation that matched the properties of the target Diesel fuel, the next step was to develop a library of surrogate fuels that independently varied cetane number and TSI. As stated in Section 5.2.1, the desired cetane number range spanned from 35 to 60. According to ASTM D6890, the cetane number measurement reproducibility is 2.618. Thus, it was decided that the library of fuels would vary cetane number in increments of 5 which provided cetane number values of 35, 40, 45, 50, 55 and 60. With 3 levels of TSI for each cetane number the library would contain 18 fuels. A naming convention was created to identify the surrogates within the library. The convention used the prefix CN followed the cetane number, an underscore, then the prefix TSI followed by the threshold soot index value. For example, surrogate CN50_TSI31 was a fuel with 50 cetane number and 31 TSI. The library is provided in Table 5-7. Note that CN50_TSI31 was the surrogate designed to match the target Diesel fuel.

Table 5-7: Surrogate Fuel Library covering a broad range of cetane number and TSI.

	Low Soot Fuels TSI=17	Mid Soot Fuels TSI = 31	High Soot Fuels TSI = 48
CN=35	CN35_TSI17	CN35_TSI31	CN35_TSI48
CN=40	CN40_TSI17	CN40_TSI31	CN40_TSI48
CN=45	CN45_TSI17	CN45_TSI31	CN45_TSI48
CN=50	CN50_TSI17	CN50_TSI31 <i>Target Diesel Fuel</i>	CN50_TSI48
CN=55	CN55_TSI17	CN55_TSI31	CN55_TSI48
CN=60	CN60_TSI17	CN60_TSI31	CN60_TSI48

Work to this point determined the properties of the target Diesel fuel, the formulation of surrogate CN50_TSI31 with predicted properties that closely matched the target Diesel fuel, the number of fuels in the library, the desired cetane number and TSI for each fuel, and the four hydrocarbon components

used to create the surrogate fuels. The next step towards completing the library was to develop the formulations i.e., the component blend fractions, for the remaining 17 fuels.

Referring to Table 5-4, there was a substantial difference in cetane number between n-hexadecane (CN=100) and heptamethylnonane (CN=15) while the remaining properties of these two components had similar values. This suggested that the relative fractions of these two species could be tuned to vary cetane number. If the sum of the n-hexadecane and heptamethylnonane fractions were held constant then the impact of varying these two components on the remaining fuel properties would be relatively small. For surrogate CN50_TSI31, the volume fractions of n-hexadecane and heptamethylnonane totaled 0.7. This notion established a blending rule. Namely, the volume fractions of n-hexadecane and heptamethylnonane would be tuned to control cetane number while the sum of the volume fractions for these two components must equal 0.7 to hold the remaining fuel properties at reasonably constant values.

To evaluate this blending rule, the Surrogate Blend Optimizer was used in the Calculator Mode described in Chapter 3.5. The calculator mode was preferred to adhere to the blending rule while holding the volume fraction of decahydronaphthalene to 0.18 and 1-methylnaphthalene to 0.12. Beginning with the formulation for CN50_TSI31, the volume fractions of n-hexadecane and heptamethylnonane were tuned using the process described in Chapter 3.5 to achieve surrogate fuels with cetane numbers of 35, 40, 45, 55 and 60. Overall, excellent results were obtained. In two cases the blend fractions of decahydronaphthalene and 1-methylnaphthalene were modestly adjusted to hold TSI=31. The results of this exercise are summarized in Table 5-8 for fuels with TSI=31. The volume, mole and mass fractions for the surrogate components are given followed by the predicted fuel properties. Volume fractions are for the liquid phase and provided for blending the surrogate fuels. The results in Table 5-8 show relatively small differences in TSI, density, lower heating value, molar H/C and kinematic viscosity were observed for the six surrogates. As expected, the distillation temperatures modestly increased as the volume fraction of n-hexadecane was raised.

Table 5-8: Formulations and predicted properties for surrogate fuels as cetane number varies from 35 to 60 with TSI held at 31.

Fuel Property	Units	CN35_TSI31	CN40_TSI31	CN45_TSI31	CN50_TSI31	CN55_TSI31	CN60_TSI31
n-Hexadecane	v/v	0.19	0.26	0.31	0.37	0.43	0.48
Heptamethylnonane	v/v	0.51	0.44	0.39	0.33	0.27	0.22
Decahydronaphthalene	v/v	0.20	0.18	0.19	0.18	0.18	0.18
1-Methylnaphthalene	v/v	0.10	0.12	0.11	0.12	0.12	0.12
n-Hexadecane	m/m	0.177	0.242	0.289	0.345	0.401	0.449
Heptamethylnonane	m/m	0.487	0.420	0.373	0.316	0.259	0.211
Decahydronaphthalene	m/m	0.216	0.194	0.205	0.195	0.195	0.195
1-Methylnaphthalene	m/m	0.121	0.145	0.133	0.145	0.145	0.145
n-Hexadecane	M/M	0.146	0.200	0.239	0.285	0.332	0.371
Heptamethylnonane	M/M	0.403	0.347	0.308	0.261	0.214	0.174
Decahydronaphthalene	M/M	0.292	0.263	0.278	0.263	0.264	0.264
1-Methylnaphthalene	M/M	0.159	0.190	0.175	0.191	0.191	0.191
Cetane Number		35.5	40.5	45.2	49.9	55.0	59.2
Threshold Soot Index		31.1	32.8	30.9	31.5	30.8	30.3
Saturated Hydrocarbons	%v/v	90.0	88.0	89.0	88.0	88.0	88.0
Olefinic Hydrocarbons	%v/v	0.0	0.0	0.0	0.0	0.0	0.0
Aromatic Hydrocarbons	%v/v	10.0	12.0	11.0	12.0	12.0	12.0
Density at 25 °C	g/cm ³	0.820	0.822	0.820	0.821	0.820	0.819
Lower Heating Value	MJ/kg	43.740	43.730	43.800	43.810	43.860	43.900
Molar H/C		1.897	1.873	1.884	1.872	1.872	1.871
Kinematic Viscosity at 25 °C	cSt	3.6817	3.6716	3.6497	3.6367	3.6176	3.6017
Distillation Temperature - T ₁₀	°C	224.1	226.8	227.0	229.2	230.9	231.8
Distillation Temperature - T ₂₀	°C	227.1	230.8	231.5	234.0	235.5	236.9
Distillation Temperature - T ₃₀	°C	231.4	234.5	236.0	238.9	241.2	243.1
Distillation Temperature - T ₄₀	°C	235.4	239.3	241.2	244.3	247.0	249.5
Distillation Temperature - T ₅₀	°C	239.9	244.3	246.9	250.1	254.0	256.9
Distillation Temperature - T ₆₀	°C	245.0	249.4	252.7	256.9	260.4	263.9
Distillation Temperature - T ₇₀	°C	250.7	255.4	259.5	263.4	267.2	270.2
Distillation Temperature - T ₈₀	°C	257.0	262.2	266.8	270.2	274.2	276.7
Distillation Temperature - T ₉₀	°C	265.7	271.7	274.8	277.7	279.9	281.8

The next step towards completing the Surrogate Fuel Library was to determine a method that would control the TSI. In a manner similar to the cetane number blending rule, there was a substantial difference in TSI between decahydronaphthalene (TSI=20) and 1-methylnaphthalene (TSI=100) while the remaining fuel properties for these components varied in moderation. This implied that the relative fractions of these two components could be adjusted to vary TSI. A second blending rule was instituted: the volume fractions of decahydronaphthalene and 1-methylnaphthalene would be adjusted to control TSI while the sum of the volume fractions for these two components should be held near to 0.3. It was recognized that some tweaking would be necessary to achieve the target properties.

To create surrogate fuels with the lowest possible sooting tendency, the TSI=17 fuels were formulated without 1-methylnaphthalene. Hence, these surrogates contained 3-components that were all saturated hydrocarbon compounds (no carbon-carbon double bonds or benzene rings). Using the cetane number and TSI blending rules as a guide, the Surrogate Blend Optimizer was utilized to formulate fuel CN50_TSI17. The optimized blend was also determined for the high sooting TSI=48 surrogate CN50_TSI48 which contained a relatively large volume fraction of 1-methylnaphthalene.

The TSI blending rule was evaluated by comparing the predicted properties of three fuels with 50 cetane number, namely CN50_TSI17, CN50_TSI31 and CN50_TSI48. The results are provided in Table 5-9. In general, good results were obtained. Moderate differences in density and distillation temperatures were observed. These results were expected considering the density and boiling point differences between decahydronaphthalene and 1-methylnaphthalene.

Successful results were obtained from the cetane number and TSI blending rules. Thus, the formulations and predicted properties for the remaining fuels in the Surrogate Fuel Library were systematically determined using the Surrogate Blend Optimizer in Calculator Mode guided by the cetane number and TSI blending rules. Complete results for the 18 surrogate fuels are provided in the Appendix.

Table 5-9: Formulations and predicted properties for surrogate fuels at TSI values of 17, 31 and 48 with cetane number held at 50.

Fuel Property	Units	CN50_TSI17	CN50_TSI31	CN50_TSI48
n-Hexadecane	v/v	0.34	0.37	0.42
Heptamethylnonane	v/v	0.33	0.33	0.25
Decahydronaphthalene	v/v	0.33	0.18	0.06
1-Methylnaphthalene	v/v	0.00	0.12	0.27
n-Hexadecane	m/m	0.320	0.345	0.384
Heptamethylnonane	m/m	0.319	0.316	0.234
Decahydronaphthalene	m/m	0.361	0.195	0.063
1-Methylnaphthalene	m/m	0.000	0.145	0.319
n-Hexadecane	M/M	0.261	0.285	0.312
Heptamethylnonane	M/M	0.259	0.261	0.190
Decahydronaphthalene	M/M	0.480	0.263	0.084
1-Methylnaphthalene	M/M	0.000	0.191	0.413
Cetane Number		53.5	49.9	48.4
Threshold Soot Index		16.6	31.5	48.9
Saturated Hydrocarbons	%v/v	100.0	88.0	73.0
Olefinic Hydrocarbons	%v/v	0.0	0.0	0.0
Aromatic Hydrocarbons	%v/v	0.0	12.0	27.0
Density at 25 °C	g/cm ³	0.806	0.821	0.845
Lower Heating Value	MJ/kg	44.160	43.810	43.310
Molar H/C		2.016	1.872	1.693
Kinematic Viscosity at 25 °C	cSt	3.5122	3.6367	3.6507
Distillation Temperature - T ₁₀	°C	216.5	229.2	241.8
Distillation Temperature - T ₂₀	°C	221.2	234.0	244.2
Distillation Temperature - T ₃₀	°C	226.8	238.9	246.8
Distillation Temperature - T ₄₀	°C	234.5	244.3	249.4
Distillation Temperature - T ₅₀	°C	244.3	250.1	252.5
Distillation Temperature - T ₆₀	°C	254.6	256.9	256.8
Distillation Temperature - T ₇₀	°C	264.6	263.4	261.9
Distillation Temperature - T ₈₀	°C	272.2	270.2	268.9
Distillation Temperature - T ₉₀	°C	278.5	277.7	277.6

5.2.6 Summary

A process was developed to create surrogates that achieved several objectives including independent control of cetane number and TSI using the minimum number of surrogate fuel components. The Surrogate Blend Optimizer was used to determine the surrogate fuel formulations and predicted properties. A four-component surrogate fuel that consisted of n-hexadecane, heptamethylnonane, decahydronaphthalene and 1-methylnaphthalene was formulated to match the properties of a target Diesel fuel. Analysis of the formulation coupled with preliminary studies of multi-component blends resulted in a set of blending rules that successfully guided the formulation of the remaining surrogate fuels. As a result of this effort, the fuel formulations and predicted properties were created for the entire Surrogate Fuel Library which contained 18 fuels that covered a broad range of cetane number and sooting tendency. The fuel formulations and property predictions for cetane number, TSI, density, lower heating value, molar hydrogen-to-carbon ratio, kinematic viscosity and the distillation curve from T_{10} to T_{90} were tabulated and provided in the Appendix.

5.3. Predicted and Measured Property Comparisons

This section compares the surrogate fuel properties predicted by the ANSYS Surrogate Blend Optimizer with actual test results. Five surrogates from the library were precision blended and characterized with a comprehensive set of ASTM tests. Surrogate fuels CN40_TSI31, CN50_TSI31 and CN60_TSI31 were used to compare fuel properties as n-hexadecane and heptamethylnonane were varied to change cetane number. In a similar manner, surrogates CN50_TSI17, CN50_TSI31 and CN50_TSI48 were used to compare fuel properties as decahydronaphthalene and 1-methylnaphthalene were varied to change TSI. The Appendix contains tables for all of the ASTM test results along with the predicted surrogate fuel properties.

The following sections summarize the data in chart form and reviews the results. The height of the error bars shown on the measured data match the ASTM reproducibility for the given fuel property. The error bars for TSI were calculated based on the reproducibility of the smoke point test.

5.3.1 Cetane Number

Figure 5-6 shows that the cetane number predictions for the five evaluated surrogates were reasonably well matched by the measured values.

Fuels CN40_TSI31, CN50_TSI31 and CN60_TSI31 followed the expected trend of increasing cetane number and the predicted values were precisely matched by the test results.

Fuels CN50_TSI17, CN50_TSI31 and CN50_TSI48 were reasonably constant at the expected value of 50 cetane number. Fuel CN50_TSI17 had a predicted cetane number of 53.5 compared to a measured value of 50.1. For this instance, the Surrogate Blend Optimizer slightly over-predicted the cetane number. In the case of fuel CN50_TSI48, the Surrogate Blend Optimizer slightly under-predicted the cetane number. For these three surrogates, a trend of decreasing predicted cetane number was observed as TSI increased from 17 to 48. However, this trend was not confirmed by the measured values.

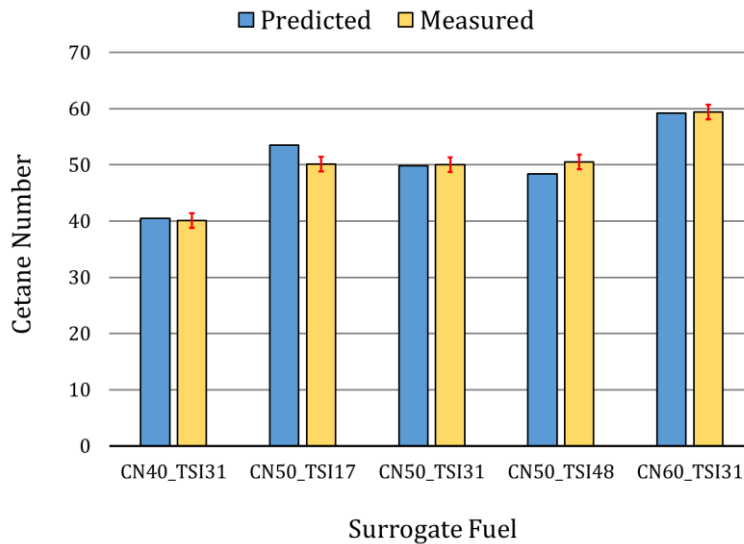


Figure 5-6: Predicted and measured cetane numbers for five surrogate fuels.

5.3.2 Threshold Soot Index

The results for Threshold Soot Index are given in Figure 5-7. Overall, the SBO predictions were closely matched by the measured results.

Fuels CN40_TSI31, CN50_TSI31 and CN60_TSI31 were formulated to have the same sooting tendency. For these fuels, the predicted and measured values repeated with nearly identical results. This was an expected outcome because these fuels had the same volume fractions of decahydronaphthalene and 1-methylnaphthalene (the components driving the sooting tendency). The predicted values were slightly lower than measured values. Fuels CN50_TSI17, CN50_TSI31 and CN50_TSI48 showed the expected trend and good agreement as the sooting tendency was increased.

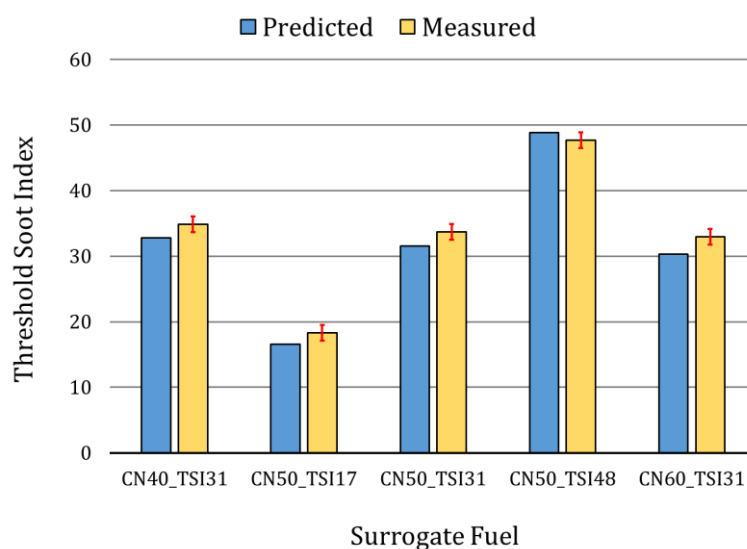


Figure 5-7: Predicted and measured TSI for five surrogate fuels.

5.3.3 Density and Molar H/C

Figure 5-8 and Figure 5-9 illustrate that the SBO predictions for fuel density and molar H/C were precisely matched by the test results. The differences between predicted and measured results were within 0.5%.

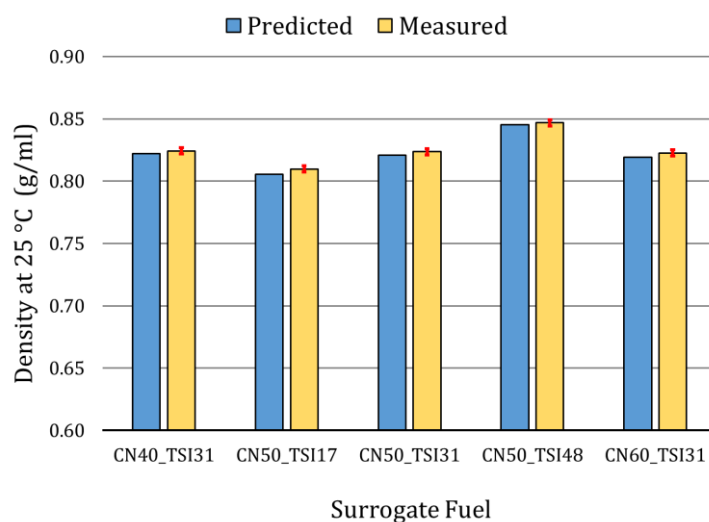


Figure 5-8: Predicted and measured density for five surrogate fuels.

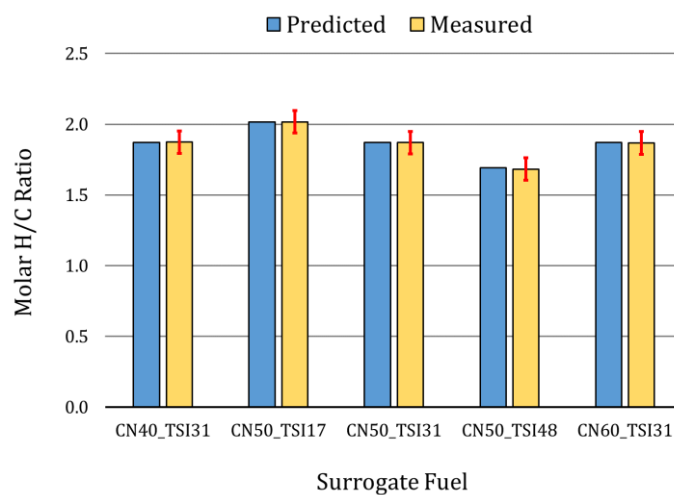


Figure 5-9: Predicted and measured molar H/C for five surrogate fuels.

5.3.4 Lower Heating Value

The results for lower heating value are given in Figure 5-10. For all of the evaluated surrogates, the predicted values were 1-2% greater than the measured results.

The predicted values for fuels CN40_TSI31, CN50_TSI31 and CN60_TSI31 showed a slight increase as cetane number was increased. This was an expected trend because cetane number was increased by raising the n-hexadecane volume fraction and this component had the highest heating value. The measured results did not capture this trend because the differences were within the measurement reproducibility.

The SBO predictions also show a decreasing heating value trend as the TSI was increased from 17 to 48, refer to fuels CN50_TSI17, CN50_TSI31 and CN50_TSI48. This trend was anticipated because TSI was increased by raising the volume fraction of 1-methylnaphthalene which had the lowest heating value of all the surrogate components. The measured results for CN50_TSI17 did not follow the expected trend and had a lower than expected heated value.

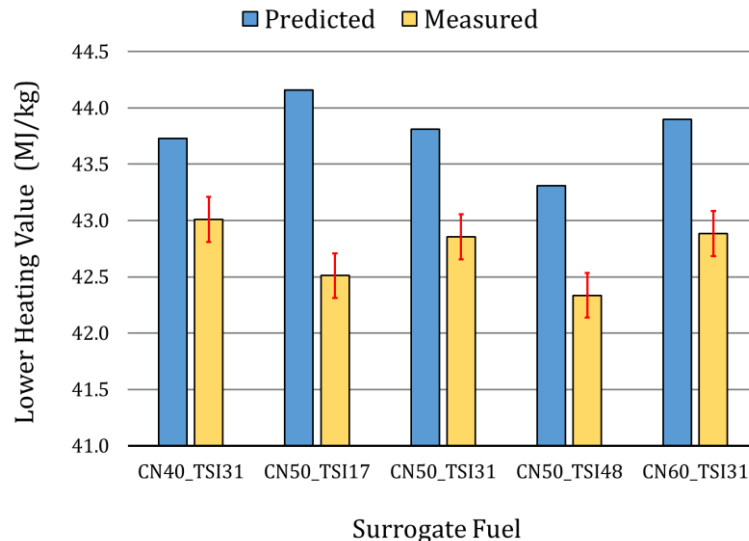


Figure 5-10: Predicted and measured lower heating value for five surrogate fuels.

5.3.5 Kinematic Viscosity

The predicted and measured values for kinematic viscosity are given in Figure 5-11. For all of the surrogates, the predicted values were 10-15% greater than the measured values.

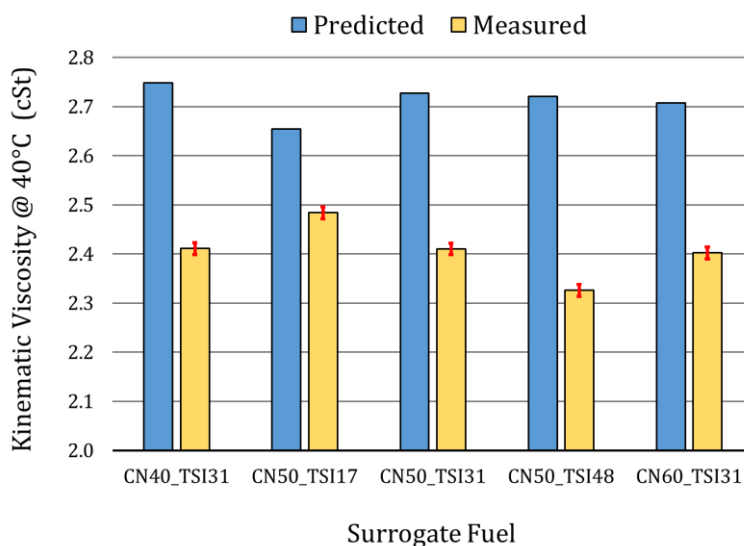


Figure 5-11: Predicted and measured kinematic viscosity for five surrogate fuels.

Some conflicting trends appeared in the results. Recall the blending rules for these surrogates stated that the combined volume fraction of n-hexadecane and heptamethylnonane was held constant at 0.7 and the combined volume fraction of decahydronaphthalene and 1-methylnaphthalene was maintained at 0.3. Referring to Table 5-4, the kinematic viscosity of n-hexadecane was close to heptamethylnonane. Similarly, the kinematic viscosity of decahydronaphthalene and 1-methylnaphthalene were close. Since the sum of these pairs of components were held constant by the blending rule, the kinematic viscosity should be relatively constant for the surrogate fuels. The predicted values confirmed this expectation showing little difference between the surrogates. The measured values show the kinematic viscosity for fuels CN40_TSI31, CN50_TSI31 and CN60_TSI31 are essentially the same. However, an apparent trend is observed with fuels CN50_TSI17, CN50_TSI31 and CN50_TSI48. For these fuels, the measured kinematic viscosity decreased as TSI was increased. This was an unexpected result because the kinematic viscosity of 1-methylnaphthalene was greater

than decahydronaphthalene. The observed trend in the measured values for these three surrogates is the reverse of what would be expected considering the blending volumes and viscosity of the individual components.

5.3.6 T_{10} and T_{90} Distillation Temperatures

The predicted surrogate fuel distillation curves were validated by evaluating the T_{10} and T_{90} distillation temperatures. Of the four surrogate components, decahydronaphthalene had the lowest boiling point. Heptamethylnonane and 1-methylnaphthalene had nearly the same boiling point and n-hexadecane had the highest boiling point (see Table 5-4). Therefore, trends observed in T_{10} should correlate strongly with the volume fraction of decahydronaphthalene and modelsty with n-hexadecane while trends in T_{90} should correlate strongly with the n-hexadecane volume fraction.

The T_{10} distillation temperatures are provided in Figure 5-12. In general, the predicted temperatures for T_{10} were 5-10 °C greater than the measured values.

A modestly increasing T_{10} trend was observed in surrogates CN40_TSI31, CN50_TSI31 and CN60_TSI31. For these fuels the decahydronaphthalene volume fraction was constant. However, the volume fraction of n-hexadecane was increased to raise the cetane number. This resulted in the observed increasing T_{10} trend with cetane number.

A more significant trend was observed with fuels CN50_TSI17, CN50_TSI31 and CN50_TSI48. First, of all the evaluated surrogates, CN50_TSI17 had the highest volume fraction of decahydronaphthalene, which resulted in the lowest observed value for T_{10} . As TSI was increased from 17 to 48, the volume fraction of decahydronaphthalene was decreased from 0.33 to 0.06. This resulted in a 25 °C increase in T_{10} .

Figure 5-13 gives the T_{90} distillation temperatures for the surrogates. For all of the fuels, the predicted values for T_{90} were greater than the measured values. In general, the predicted temperatures for T_{90} were up to 5 °C higher than the measured values.

As expected, as cetane number increased in surrogates CN40_TSI31, CN50_TSI31 and CN60_TSI31 the T_{90} also increased. The total change in T_{90} from 40 to 60 cetane number was about 10 °C.

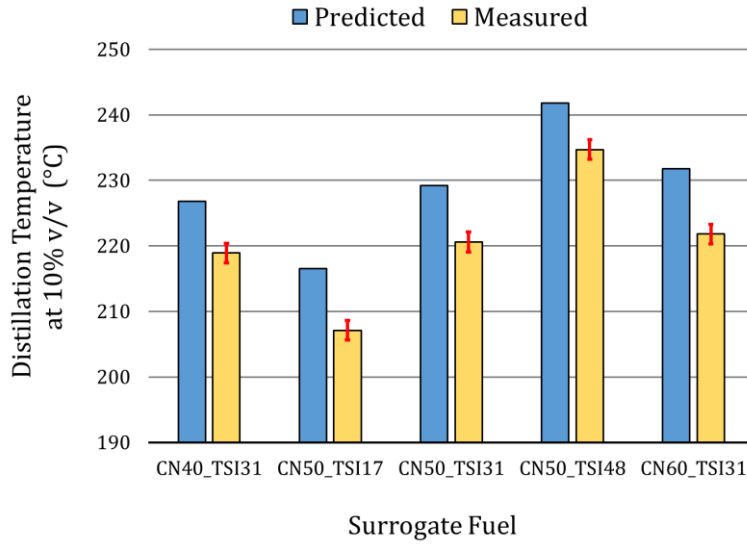


Figure 5-12: Predicted and measured T_{10} distillation temperature.

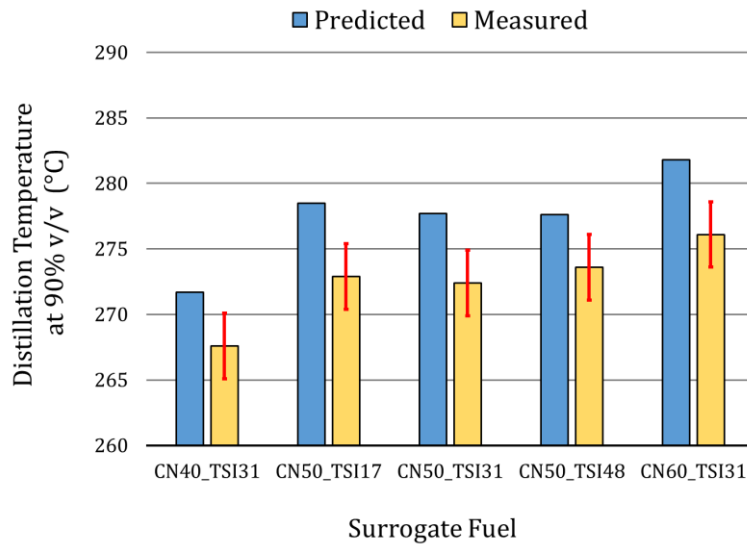


Figure 5-13: Predicted and measured T_{90} distillation temperature.

5.3.7 Summary

This section evaluated the properties predicted by the Surrogate Blend Optimizer. Five surrogate fuels were selected from the Surrogate Fuel Library, precision blended and extensively analyzed with ASTM tests. All of the predicted properties were found to be in good agreement with the measured values. For the five surrogate fuels that were evaluated, the maximum observed differences between the predicted and measured values are listed below in Table 5-10.

Table 5-10: Maximum observed difference between predicted and measured fuel properties for five surrogate fuels.

Fuel Property	Maximum Observed Difference between Predicted and Measured Fuel Properties
Cetane Number	Within measurement error
TSI	Within measurement error
Density	2%
Lower Heating Value	4%
Kinematic Viscosity	15%
Distillation Temperature T ₁₀	10 °C
Distillation Temperature T ₉₀	6 °C

5.4. Surrogate and Petroleum Fuel Comparison

This section presents the results of detailed ASTM testing of surrogate fuel CN50_TSI31 and the target full-range petroleum Diesel fuel. The combustion, physical and chemical properties, as well as purity and contamination, were compared and discussed. The complete results of the ATSM testing of both fuels are provided in the Appendix.

Where applicable, fuel properties were compared to specifications found in ASTM D975-16a “Standard Specification for Diesel Fuel Oils” [5.15] and EN590:2009 “Automotive fuels - Diesel - Requirements and test methods” [5.16].

5.4.1 Combustion Properties

While designing surrogate CN50_TSI31 to mimic the properties of the target petroleum Diesel fuel, highest priority was given to match cetane number and TSI. The next priorities were fuel density, heating value and viscosity. There was less flexibility towards matching the distillation curve. This was a result of the decision to limit the surrogate to 4 components. However, the boiling points of the surrogate components ranged from 187 °C to 287 °C which reasonably spanned the T_{10} - T_{90} temperature range of the target Diesel distillation curve.

Cetane Number

Fuel cetane number was measured following ASTM D6890 (Constant Volume Method). The results are given in Table 5-11. At a nominal 50 cetane number, ASTM D6890 provided a reproducibility of 2.618 cetane number [5.17]. The constant volume method, D6890, was repeated numerous times by different laboratories with excellent reproducibility. The ASTM cetane number measurements suggest the petroleum Diesel and surrogate CN50_TSI31 match cetane number within the error of the test procedures.

Smoke Point and Threshold Soot Index

Smoke point was quantified by ASTM D1322 using the SP10–Automated Smoke Point Tester which provided improved accuracy compared to the standard smoke point lamp [5.18]. ASTM D1322 provided a smoke point repeatability of 2 mm and a reproducibility of 3 mm [5.19]. Table 5-11

shows a smoke point of 19 mm for Diesel and 18.8 for CN50_TSI31. A match within the measurement error.

Threshold Soot Index (TSI) was calculated using the method defined by Calcote and Manos [5.20]. Given the smoke point results from ASTM D1322, it was concluded that the sooting tendency of the two fuels, as quantified by smoke point and TSI, are matched within the margin of measurement error.

Lower Heating Value

The lower heating value was quantified by ASTM D240N which provided a reproducibility of 0.4 MJ/kg [5.21]. Test results show the lower heating value for petroleum Diesel was 43.004 while the surrogate CN50_TSI31 was 42.857 MJ/kg. With a difference of only 0.147 MJ/kg between the two fuels, it was concluded that CN50_TSI31 matched the lower heating value of the petroleum Diesel fuel within the measurement limitations.

Table 5-11: Combustion properties for petroleum Diesel and CN50_TSI31 surrogate fuel. Fuels properties matched within measurement reproducibility.

Combustion Properties	Units	ASTM Method	Petroleum Diesel Fuel	CN50_TSI31 Surrogate
Cetane Number (Constant Volume Chamber)		D6890	50.9	50.1
Smoke Point	mm	D1322	19.0	18.8
Threshold Soot Index			31.0	33.7
Lower Heating Value	MJ/kg	D240N	43.004	42.857

5.4.2 Physical Properties

This section compares the density, viscosity, surface tension and distillation curve properties of the target Diesel fuel and CN50_TSI31. The Repeatability and Reproducibility metrics for several ASTM procedures are given in Table 5-12 [5.22] [5.23] [5.24]. Repeatability was determined by conducting tests at the same facility using the same method, the same material, the same equipment, and the same operator within a short time frame.

Reproducibility was established by conducting the same test method on the same material using different laboratories. The ASTM test results for Diesel and CN50_TSI31 fuels are shown in Table 5-13. The temperature-dependency for density, dynamic viscosity and surface tension are shown in Figure 5-14, Figure 5-15 and Figure 5-16, respectively. In the figures, ASTM measurements for CN50_TSI31 and the Diesel fuel are shown with symbols. Design Institute for Physical Properties (DIPPR) correlations are used to calculate the temperature dependencies for the surrogate fuel components [5.25].

Table 5-12: Repeatability and reproducibility metrics for ASTM test methods.

Physical Properties	Units	ASTM Method	Repeatability	Reproducibility
Density at 15 °C	g/ml	D4052	0.00016	0.0052
Kinematic Viscosity at 40 °C	cSt	D445	0.008	0.023
Surface Tension	N/m	D3825	na	na

Table 5-13: Physical properties for Diesel and CN50_TSI31 surrogate fuels.

Physical Properties	Units	ASTM Method	Petroleum Diesel Fuel	CN50_TSI31 Surrogate
Density at 15 °C	g/ml	D4052	0.849	0.831
Kinematic Viscosity at 40 °C	cSt	D445	3.06	2.41
Surface Tension	N/m	D3825	0.0312	0.0273

Density

ASTM tests reported densities of 0.849 g/ml for Diesel and 0.831 g/ml for CN50_TSI31, see Table 5-13. Typical Diesel fuel has a nominal density of 0.85 g/ml and ranges between 0.88 and 0.82 [5.26]. EN590:2009

established a range of 0.845–0.820 g/ml while ASTM D975-16a did not include a density requirement. Considering the reproducibility of the measurement, both fuels achieved the EN590:2009 density requirement.

The density temperature dependency was characterized by measuring the fuel density at 15, 40, 60, and 90 °C. DIPPR correlations were used to calculate the densities of the surrogate fuel components. In addition, a representative temperature dependency for CN50_TSI31 was calculated using a mole-weighted average of the individual components. The measured and calculated results are shown in Figure 5-14. Temperature had a nearly linear effect on density in the range of 0-650 K. The measured densities for CN50_TSI31 and petroleum Diesel followed the temperature trend observed with the surrogate components. Overall, the results indicated that the density of CN50_TSI31 closely matched the petroleum Diesel fuel.

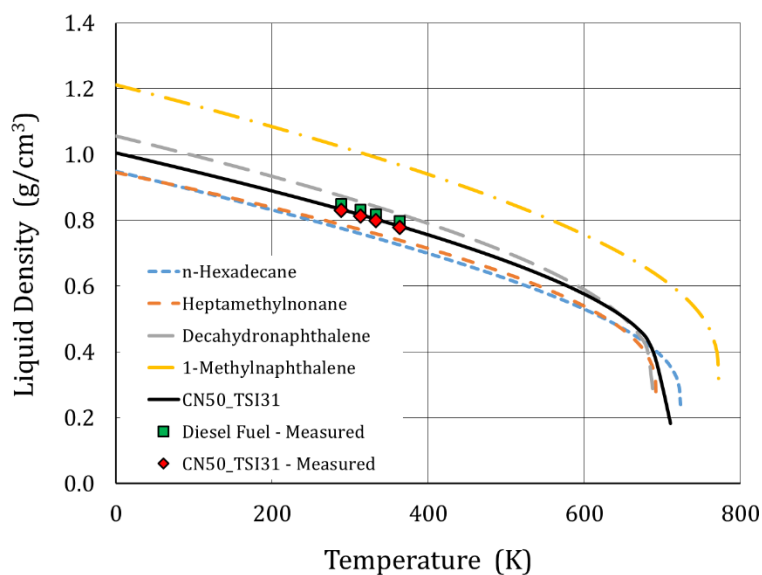


Figure 5-14: Liquid density temperature dependencies for petroleum Diesel, CN50_TSI31 and the individual surrogate components.

Viscosity

ASTM D975-16a required the kinematic viscosity at 40 °C to be in the range of 1.9-4.1cSt while EN590:2009 had a range of 2.0-4.5 cSt. Both fuels met the

requirements for kinematic viscosity with Diesel at 3.06 cSt and CN50_TSI31 at 2.41 cSt.

The viscosity temperature dependency was characterized by measuring the kinematic viscosity at 40, 80, 100 and 120 °C and converting the results to dynamic viscosity [5.23]. DIPPR correlations were used to calculate the dynamic viscosities for the surrogate fuel components. The measured and calculated results are shown in Figure 5-15.

The temperature dependency showed viscosity rapidly decreased as temperature increased. Differences between the fuels and surrogate fuel components were minimal above 400 K (127 °C). Decahydronaphthalene had a lower viscosity than the other surrogate components and was likely the cause for the lower viscosity of CN50_TSI31. As temperature approached typical values for warmed-up engine coolant (90 °C, 363 K), the observed differences in dynamic viscosity were minimal.

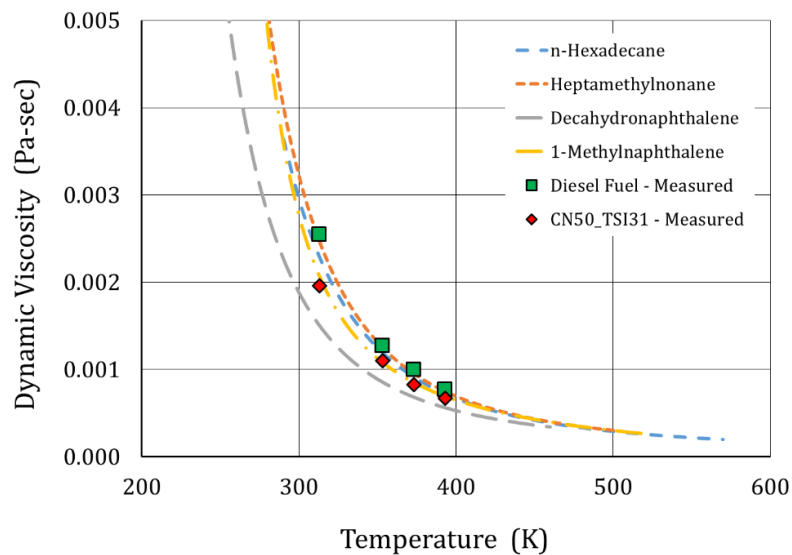


Figure 5-15: Dynamic viscosity temperature dependencies for petroleum Diesel fuel, CN50_TSI31 and the individual surrogate components.

Surface Tension

As of this writing, ASTM D3825 did not provide statements on the precision, repeatability and reproducibility of surface tension measurements. In addition, surface tension requirements were not established in ASTM D975-16a or EN590:2009. Also, surface tension measurements were only available at 25 °C. Due to the high cost of the ASTM D3825 procedure, testing was limited to the target Diesel and surrogate fuel.

In this work, the surface tension of Diesel was measured at 0.0312 N/m while the CN50_TSI31 surrogate was 0.0273 N/m. In other works, Wang, et al. reported a Diesel fuel surface tension of 0.028 N/m which was very close to surrogate CN50_TSI31 [5.27]. Ra, et al. investigated the effects of fuel properties with Diesel and Biodiesel surrogates and reported approximately 0.026 N/m for a Diesel surrogate fuel [5.28]. Ra et al. noted that surface tension changes in the Diesel fuel were found to have a very small impact on the amount of vaporized fuel at the end of injection and the positioning of combustion phasing as measured by CA50. The surface tensions for CN50_TSI31 and the target Diesel fuel were found to be in reasonable agreement with values in the literature. The relatively small surface tension differences between the target Diesel and CN50_TSI31 surrogate are not expected to have a noticeable impact on the fuel injection system or the characteristics of the Diesel spray.

DIPPR correlations were used to calculate the surface tension for the surrogate fuel components. The calculated and measured values are shown in Figure 5-16. The measured values were in good agreement with the calculated surface tensions.

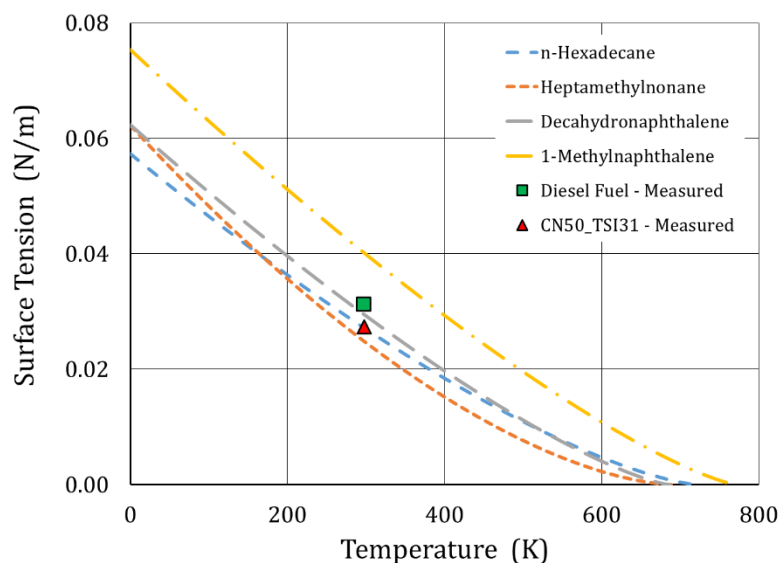


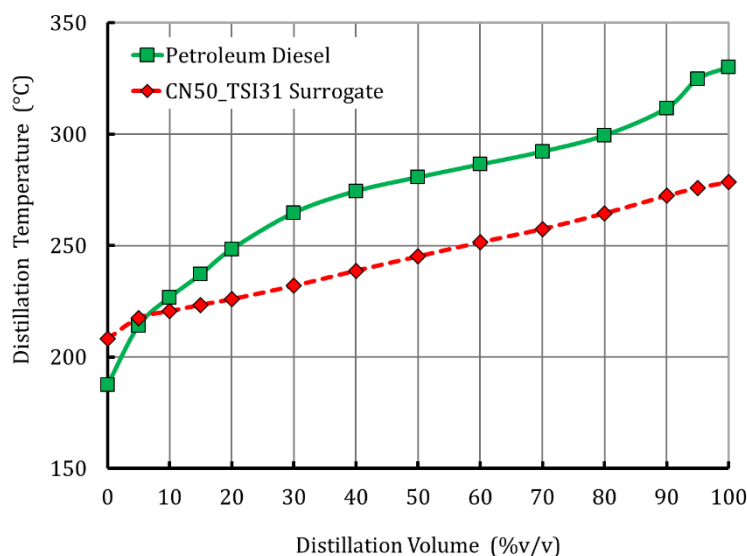
Figure 5-16: Surface tension temperature dependencies for petroleum Diesel fuel, CN50_TSI31 and the individual fuel components.

Distillation Curve

The distillation curve characteristics for the fuels were measured by ASTM D86 and the results are presented in Table 5-14 and Figure 5-17. Test results showed reasonable agreement over the entire distillation temperature range. At T_{10} surrogate CN50_TSI31 had a distillation temperature that was only 6.2 °C less than the target Diesel fuel. In the mid-range from T_{30} to T_{80} the surrogate was 35 °C lower. At the final boiling point, CN50_TSI31 was 51.1 °C lower than the target Diesel fuel. The lower distillation temperatures for CN50_TSI31 resulted from the decision to exclude n-alkanes larger than n-hexadecane. Regarding the fuel specifications, ASTM D975-16a established a T_{90} temperature range of 282-338 °C. The petroleum Diesel fuel was within this range while CN50_TSI31 was 10 °C less than the required minimum temperature for T_{90} .

Table 5-14: ASTM D86 distillation temperatures for Diesel and CN50_TSI31 fuels.

Distillation Temperatures	Petroleum Diesel Fuel (°C)	CN50_TSI31 Surrogate (°C)	Temperature Difference (°C)
Distillation Temperature - Initial Boiling Point	187.4	208.1	-20.7
Distillation Temperature - 5% v/v	214.1	217.5	-3.4
Distillation Temperature - 10% v/v	226.8	220.6	6.2
Distillation Temperature - 15% v/v	237.1	223.4	13.7
Distillation Temperature - 20% v/v	248.4	225.9	22.5
Distillation Temperature - 30% v/v	264.8	231.9	32.9
Distillation Temperature - 40% v/v	274.5	238.7	35.8
Distillation Temperature - 50% v/v	280.7	245.2	35.5
Distillation Temperature - 60% v/v	286.4	251.5	34.9
Distillation Temperature - 70% v/v	292.2	257.4	34.8
Distillation Temperature - 80% v/v	299.5	264.5	35.0
Distillation Temperature - 90% v/v	311.7	272.4	39.3
Distillation Temperature - 95% v/v	324.8	275.9	48.9
Distillation Temperature - Final Boiling Point	330.1	278.6	51.5



4

Figure 5-17: Distillation curves for the petroleum Diesel and CN50_TSI31

5.4.3 Chemical Properties

Figure 5-18 shows the hydrocarbon classes for a nominal Diesel fuel, scaled and replotted from Pitz et al. [5.29], compared to the hydrocarbon classes in the surrogate fuel CN50_TSI31. The hydrocarbon classes from reference [5.29] were used in the figure because data quantifying the volume percent of normal-alkanes, iso-alkanes and cyclo-alkanes were not available for the target petroleum Diesel fuel from this thesis. Figure 5-18 shows that the surrogate fuel CN50_TSI31 contained a higher volume percent of normal-alkanes and a lower volume percent of cyclo-alkanes compared to the nominal Diesel fuel from Pitz et al. [5.29]. The iso-alkanes and aromatics were reasonably well represented by surrogate CN50_TSI31. In this work, n-alkanes were represented by n-hexadecane, iso-alkanes by heptamethylnonane, cyclo-alkanes were represented by decahydronaphthalene and aromatics were represented by 1-methylnaphthalene.

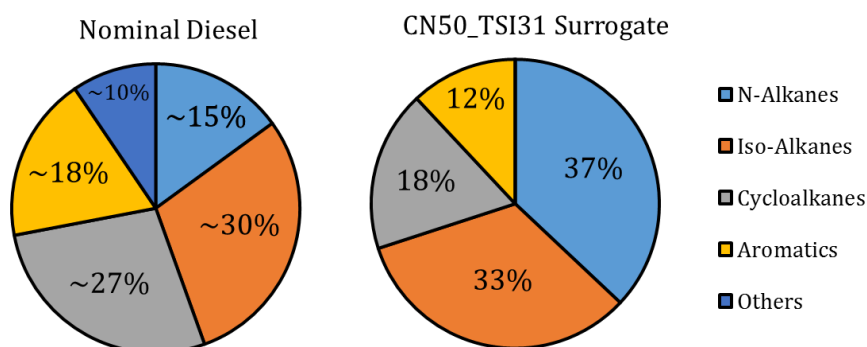


Figure 5-18: Comparison of hydrocarbon classes for a nominal Diesel fuel, scaled and replotted from [5.29], and CN50_TSI31 surrogate fuel (%v/v).

The surrogate and target petroleum Diesel fuels were characterized by two ASTM test methods that provided a simplified view of the hydrocarbon classes. ASTM D1319 used a fluorescent indicator adsorption method to characterize the fuel in terms of three classes: alkanes, alkenes (olefins) and aromatics. ASTM D5186 characterized the aromatics into three subclasses: total, mono-cyclic and poly-cyclic aromatics using supercritical fluid chromatography. The ASTM results are shown in Table 5-15 and discussed below.

On a volume basis, CN50_TSI31 has slightly more alkanes than the petroleum Diesel. The surrogate was precisely blended to contain 88% alkanes while the test results show 82.7% for the surrogate and 76% for the petroleum Diesel.

ASTM D1319 test showed that the petroleum Diesel contained 7.5% alkenes. The surrogate was formulated without alkenes. However, test results showed the surrogate fuel contained 4.9% alkenes. This may have resulted from detection errors. There is also the possibility that some alkenes were present as impurities in the surrogate components. If alkenes were present in the surrogate fuel, the concentrations were small and can be neglected for the purpose of this research.

Table 5-15: Alkane, alkene and aromatic hydrocarbons for petroleum Diesel and CN50_TSI31 surrogate fuels.

Hydrocarbon Classes	Units	ASTM Method	Petroleum Diesel Fuel	CN50_TSI31 Surrogate
Alkane Hydrocarbons	%v/v	D1319	76.0	82.7
Alkene Hydrocarbons	%v/v	D1319	7.5	4.9
Aromatic Hydrocarbons	%v/v	D1319	16.5	12.4
Total Aromatic Hydrocarbons	%m/m	D5186	16.4	16.4
Mono-Cyclic Aromatics	%m/m	D5186	16.2	0.4
Poly-Cyclic Aromatics	%m/m	D5186	0.2	16.0

On a volume basis, CN50_TSI31 contained slightly less aromatics than the Diesel fuel. CN50_TSI31 was precisely blended to contain 12% aromatics which is in very good agreement with the ASTM result. On a mass basis, ASTM tests showed the total aromatics were the same for both fuels. This was an intended result because the petroleum Diesel contained mono-cyclic aromatics which generally had lower densities than poly-cyclic aromatics. CN50_TSI31 was formulated with 1-methylnaphthalene; a poly-cyclic aromatic with a density that is roughly 15% higher than many mono-cyclic aromatics, as shown in Table 5-17.

Elemental Properties

The fuel hydrogen and carbon content matched very well with differences less than 1%, see Table 5-16. The surrogate fuel was found to have trace amounts of nitrogen and sulfur. The source of nitrogen was unknown. After discussions with the fuel supplier it was concluded that 1-methylnaphthalene likely contained trace amounts of the sulfur containing compound 2-(2-methylbenzyl)thiophene (C₁₂H₁₂S). While present, the nitrogen and sulfur concentrations were too low to have a significant on the spray, combustion and emission performance of the surrogate fuel.

Table 5-16: Carbon, hydrogen, nitrogen and sulfur content in the Petroleum and surrogate fuels.

Elemental Properties	Units	ASTM Method	Petroleum Diesel Fuel	CN50_TSI31 Surrogate
Carbon Content	%m/m	D5291	86.38	86.07
Hydrogen Content	%m/m	D5291	13.42	13.51
Nitrogen Content	%m/m	D4629	0.0001	0.0285
Sulfur Content	ppm	D7039	9.4	1405.5
Hydrogen-to-Carbon Molar Ratio	molR	SAE J1829	1.85	1.87
Stoichiometric Air-Fuel Ratio		SAE J1829	14.58	14.60

Although the trace amount of sulfur was not expected to affect combustion and emissions, some consideration was given to replace 1-methylnaphthalene with a different aromatic compound. Key properties of aromatics that have detailed kinetic mechanisms and commonly appear in surrogate fuels are shown in Table 5-17.

Table 5-17: Properties of aromatic compounds [5.13] [5.14].

Aromatic Compound	Cetane Number	TSI	Boiling Point (°C)	Density (g/ml)
1-Methylnaphthalene	0	100	245	1.001
Toluene	2.6	40	111	0.865
m-Xylene	2.6	51	139	0.864
n-Propylbenzene	7.6	53	159	0.862
1,2,4-Trimethylbenzene	8.9	51	169	0.876

A separate surrogate blending and optimization study was conducted replacing 1-methylnaphthalene with the aromatics shown in Table 5-17. Upon analysis it was concluded that a suitable aromatic replacement was not readily available. While these aromatics had cetane numbers that were reasonably close to 1-methylnaphthalene, they all had much lower sooting tendencies, boiling points and densities. Use of these mono-cyclic aromatic compounds in place of 1-methylnaphthalene would have prevented surrogate CN50_TSI31 from closely matching the combustion, physical and chemical properties of the petroleum Diesel fuel.

5.4.4 Purity and Contamination

During the fuel sourcing process, efforts were made to acquire the highest quality petroleum fuel and the purest available surrogate components. However, the potential for contamination remained. Fuels with particle contamination may affect exhaust particle number and size distribution measurements. Therefore, the fuels were tested for the most common contaminants such as particles, ash, sulfates, water and metals. The results shown in Table 5-18 and Table 5-19 show the petroleum Diesel and CN50_TSI31 surrogate fuels were free of these contaminants.

Table 5-18: Contamination analysis for petroleum Diesel and CN50_TSI31 fuels.

Fuel Contamination	Units	ASTM Method	Petroleum Diesel Fuel	CN50_TSI31 Surrogate
Particulate Contamination	mg/l	D6217	1	0.9
Ash Contamination	%m/m	D482	<0.001	<0.001
Sulfated Ash Content	%m/m	D874	<0.001	<0.001
Water & Sediment	%v/v	D2709	< 0.005	< 0.005
Water (H ₂ O) Content	ppm	D6304	35	7
Total Chloride	ppm	D7328	1	0
Existent Inorganic Sulfate	ppm	D7328	0.4	0
Potential Sulfate	ppm	D7328	0.3	0

Table 5-19: Elemental analysis for fuel-born metals by Inductively Coupled Plasma Atomic Emission Spectrometry (ICP-AES).

Elemental Analysis - Metals	Units	ASTM Method	Petroleum Diesel Fuel	CN50_TSI31 Surrogate
Aluminum (Al)	ppm	D5185	<1	<1
Barium (Ba)	ppm	D5185	<1	<1
Boron (B)	ppm	D5185	<1	1
Cadmium (Cd)	ppm	D5185	<1	<1
Calcium (Ca)	ppm	D5185	<1	<1
Chromium (Cr)	ppm	D5185	<1	<1
Copper (Cu)	ppm	D5185	<1	<1
Iron (Fe)	ppm	D5185	<1	<1
Lead (Pb)	ppm	D5185	<1	<1
Magnesium (Mg)	ppm	D5185	<1	<1
Manganese (Mn)	ppm	D5185	<1	<1
Molybdenum (Mo)	ppm	D5185	<1	<1
Nickel (Ni)	ppm	D5185	<1	<1
Phosphorus (P)	ppm	D5185	<1	<1
Potassium (K)	ppm	D5185	<5	<5
Silicon (Si)	ppm	D5185	<1	<1
Silver (Ag)	ppm	D5185	<1	<1
Sodium (Na)	ppm	D5185	<5	<5
Strontium (Sr)	ppm	D5185	<1	<1
Tin (Sn)	ppm	D5185	<1	<1
Titanium (Ti)	ppm	D5185	<1	<1
Vanadium (V)	ppm	D5185	<1	<1
Zinc (Zn)	ppm	D5185	<1	1

5.4.5 Summary

This section conducted a detailed evaluation of measured fuel properties from surrogate CN50_TSI31 and the target Diesel fuel. Excellent agreement was obtained with the combustion, physical and chemical properties. Modest differences were observed with the distillation curves. The surrogate properties were also compared to the ASTM D975-16a and EN590:2009 fuel specifications and achieved good results as summarized in Table 5-20. The results provided additional validation for the development methodology and the surrogate fuels.

Table 5-20: Comparison of target Diesel and CN50_TSI31 with ASTM D975 No. 2-D and EN590 fuel specifications.

Fuel Property	ASTM D975	EN590	Target Diesel	Surrogate CN50_TSI31
Cetane Number	>40	>51	50.9	50.1
TSI	NR	NR	33.5	33.7
Lower Heating Value (MJ/kg)	NR	NR	43.004	42.857
Density at 15 °C (g/ml)	NR	0.820-0.845	0.849	0.831
Viscosity at 40 °C (cSt)	1.9-4.1	2.0-4.5	3.06	2.41
Surface Tension (N/m)	NR	NR	0.0312	0.0273
Distillation Temperature at 90%v/v (°C)	Min @ 282 Max @ 338	NR	311.7	272.4
Distillation Temperature at 95%v/v (°C)	NR	Max @ 360	324.8	275.9
Total Aromatics (%v/v)	<35	NR	16.5	12.4
Polycyclic Aromatics (%m/m)	NR	<11	0.2	16.0

5.5. Discussion

While formulating the surrogate fuels, recall that cetane number was controlled by adjusting the volume fractions of n-hexadecane and heptamethylnonane while TSI was varied by altering decahydronaphthalene and 1-methylnaphthalene. This section discusses effects that manipulating these fuel species had on the global fuel properties of the surrogate fuels. It also compares the predicted properties for the 18 surrogates in the library with measured properties from five Diesel fuels obtained from the global market. Density, kinematic viscosity, heating value and distillation temperature were analyzed. Distillation temperatures were summarized by evaluating the 10, 50 and 90 %v/v temperatures (also called T_{10} , T_{50} and T_{90}).

For the figures in this section, the chart on the left shows the predicted values for the 18 surrogate fuels. The surrogates are grouped by their TSI values and then sorted in order of increasing cetane number. The chart on the right shows measured values from the market Diesel fuels that were collected and analyzed.

Density

Results for density are shown in Figure 5-19. Since n-hexadecane and heptamethylnonane had the same density, manipulating their volume fractions to control cetane number did not impact the density of the surrogate fuels. Adjusting the other surrogate components to control TSI had a modest impact on density. The figure shows density increased by about 5% as the TSI was increased from TSI=17 to 48. The surrogate fuel densities are generally within the range spanned by the market Diesel fuels.

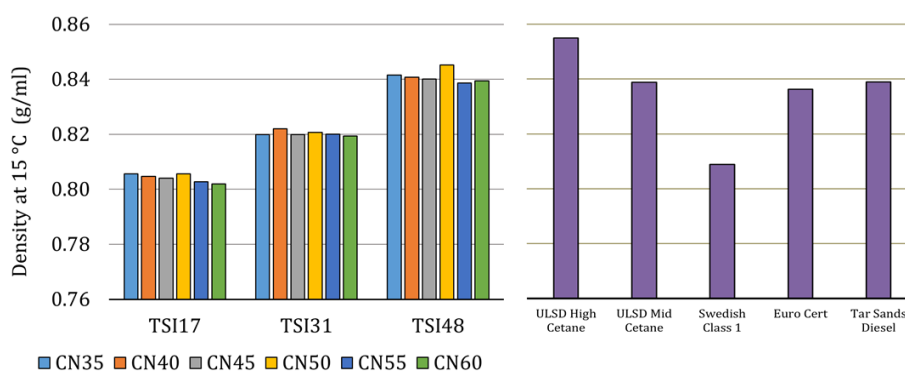


Figure 5-19: The effect of varying surrogate fuel formulation on density.

Kinematic Viscosity

The results for kinematic viscosity are shown in Figure 5-20. Adjusting the volumetric blend ratios to control cetane number and TSI had very little impact on kinematic viscosity. As cetane number varied from 35 to 60 the viscosity decreased by less than 0.1 cSt. Increasing the TSI from 17 to 48 increased viscosity by slightly more than 0.1 cSt. The EN590 specification called for kinematic viscosity to be in the range of 2.0-4.5cSt. All of the surrogate fuels are within the specification. The figure also shows the kinematic viscosity of the surrogate fuels was within the range of the market Diesel fuels. However, the market fuels had much more variability than the surrogates.

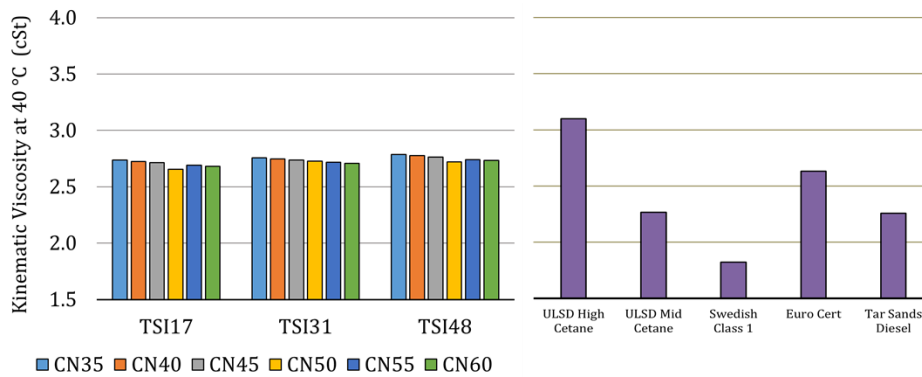


Figure 5-20: The effect of varying surrogate fuel formulation on kinematic viscosity.

Heating Value

Figure 5-21 shows the heating values for the surrogate and market Diesel fuels. The results show that adjustments to the blend fractions to control cetane number and TSI had minor effects on the lower heating value. The largest difference was on the order of 2%. The surrogates had slightly higher heating values than the market fuels.

The energy density was calculated by multiplying the fuel density and heating values. The results given in Figure 5-22 show the energy per unit volume for the surrogates and the market fuels were in very good

agreement. The average for all of the fuels was about 36 J/ml and the range observed for the surrogates and the market fuels were nearly the same.

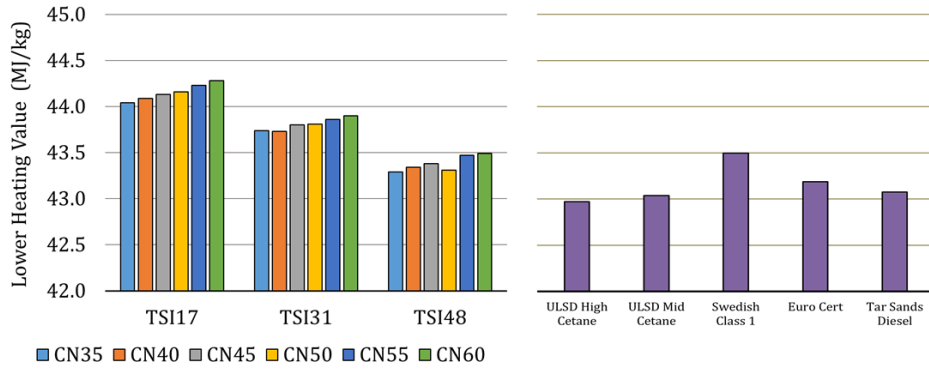


Figure 5-21: The effect of varying surrogate fuel formulation on lower heating value.

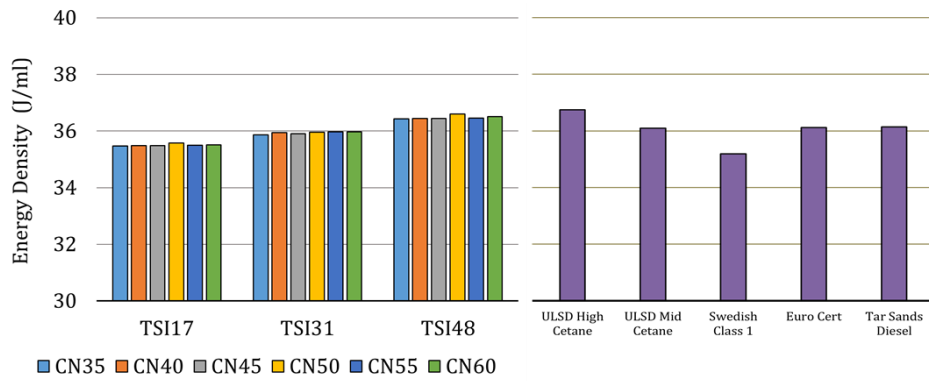


Figure 5-22: The effect of varying surrogate fuel formulation on the fuel energy per unit volume.

Distillation Curve

The effect of varying surrogate fuel formulation on the T_{10} , T_{50} , and T_{90} distillation temperatures is shown in Figure 5-23, Figure 5-24 and Figure 5-25, respectively.

Figure 5-23 shows that changes made with the component volume fractions to control cetane number and TSI had relatively small impact on the initial part of the distillation curve (T_{10}). Consider the set of fuels with TSI=17. As cetane number increased from 35 to 60 the T_{10} increased by about 10 °C. The cetane number effect was nearly the same for the surrogates with TSI=31 and TSI=48. For a given cetane number, the impact of increasing TSI from 17 to 31 was also about 10 °C. Overall, the surrogates tend to have a slightly higher T_{10} than the market fuels.

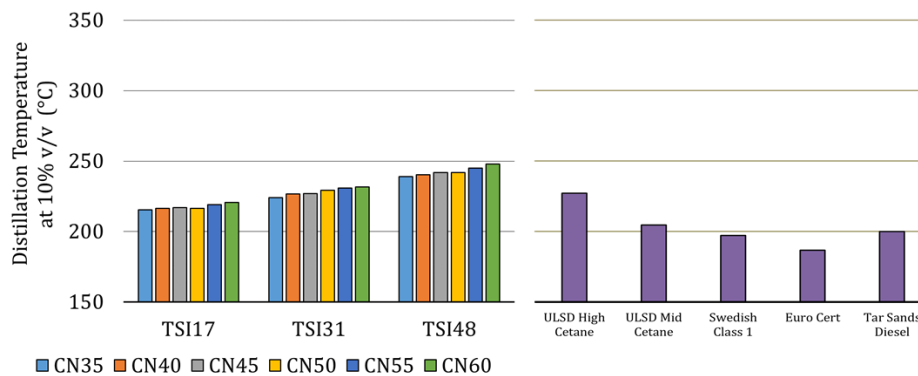


Figure 5-23: The effect of varying surrogate fuel formulation on the T_{10} distillation temperature.

Regarding the middle of the distillation curves, Figure 5-24 shows that T_{50} was slightly influenced by the blend changes to control cetane number but was essentially not affected by blend changes to control TSI. The figure also shows that the range for T_{50} was broader for the market fuels and overlapped the surrogates.

Figure 5-25 shows the T_{90} results for the end of the distillation curve closely follow the trends observed for T_{50} . On average, the surrogate fuels have a slightly lower T_{90} but fall within the range of the market fuels.

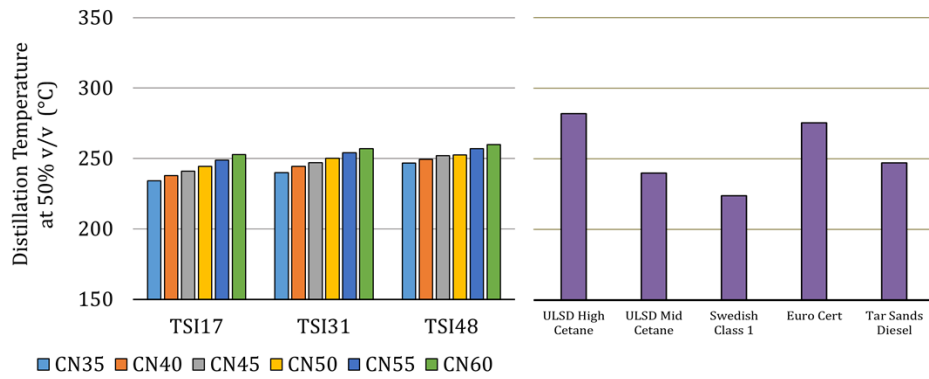


Figure 5-24: The effect of varying surrogate fuel formulation on the T_{50} distillation temperature.

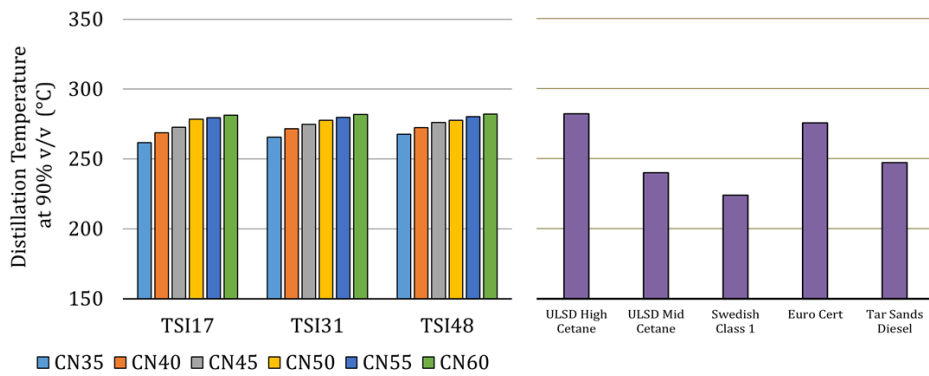


Figure 5-25: The effect of varying surrogate fuel formulation on the T_{90} distillation temperature.

5.6. Summary

A methodology was developed to formulate a surrogate fuel that achieved the stated objectives and closely matched the properties of a full-range petroleum Diesel fuel. The four-component surrogate consisted of n-hexadecane, heptamethylnonane, decahydronaphthalene and 1-methylnaphthalene. The methodology was further applied to develop the formulations and predicted properties for a Surrogate Fuel Library that consisted of 18 fuels with independent control of cetane number and TSI. Five surrogate fuels were chosen from the library, precision blended, analyzed and compared with the predicted properties for these fuels. Good agreement was obtained between the predicted and measured properties which validated the methodology and the property predictions for the Surrogate Fuel Library.

As cetane number and TSI changed throughout the Surrogate Fuel Library, the impact on other fuel properties were generally small and in most instances negligible. The surrogate fuel properties were either within or very close to the Diesel fuel specifications given in ASTM D975a or EN590:2009. A comparison of the 18 surrogate fuels with five market Diesel fuels showed good agreement for density, kinematic viscosity, heating value, energy density (J/ml) and distillation temperatures. Given these results, the surrogate fuels developed in this thesis were concluded to be fully-representative of petroleum Diesel fuels. The surrogates closely matched the combustion, physical and chemical properties of petroleum Diesel fuel while providing independent control of cetane number and TSI.

5.7. References

- [5.1] Ahmedi, A., Ahmed, S. and Kalghatgi, G., "Simulating Combustion in a PCI (Premixed Compression Ignition) Engine using DI-SRM and 3 Components Surrogate Model", *Combustion and Flame* 162(10):3728-3739, 2015, doi:10.1016/j.combustflame.2015.07.011.
- [5.2] Anand, K., Ra, Y., Reitz, R. and Bunting, B., "Surrogate Model Development for Fuels for Advanced Combustion Engines", *Energy & Fuels* 25(4):1474-1484, 2011, doi:10.1021/ef101719a.
- [5.3] Ciajolo, A., D'Anna, A., Barbella, R. and Bertoli, C., "Combustion of Tetradecane and Tetradecane/ α -Methylnaphthalene in a Diesel Engine with Regard to Soot and PAH Formation", *Combustion Science and Technology* 87(1-6):127-137, 1993, doi:10.1080/00102209208947211.
- [5.4] Diez, A., Crookes, R. and Lovas, T., "Experimental studies of autoignition and soot formation of diesel surrogate fuels", *Proceedings of The Institution of Mechanical Engineers, Part D: Journal of Automobile Engineering* 227(5):656-664, 2012, doi:10.1177/0954407012458402.
- [5.5] Hakka, M., Glaude, P., Herbinet, O. and Battin-Leclerc, F., "Experimental Study of the Oxidation of Large Surrogates for Diesel and Biodiesel Fuels", *Combustion and Flame* 156(11):2129-2144, 2009, doi:10.1016/j.combustflame.2009.06.003.
- [5.6] Kalghatgi, G., Hildingsson, L., Harrison, A. and Johansson, B., "Surrogate Fuels for Premixed Combustion in Compression Ignition Engines", *International Journal of Engine Research* 12(5):452-465, 2011, doi:10.1177/1468087411409307.
- [5.7] Luo, J., Yao, M., Liu, H. and Yang, B., "Experimental and Numerical Study on Suitable Diesel Fuel Surrogates in Low Temperature Combustion Conditions", *Fuel* 97:621-629, 2012, doi:10.1016/j.fuel.2012.02.057.

- [5.8] Yang, H., Shuai, S., Wang, Z., Wang, J. and Xu, H., "New Premixed Compression Ignition Concept for Direct Injection IC Engines Fueled with Straight-Run Naphtha", *Energy Conversion and Management* 68:161-168, 2013, doi:10.1016/j.enconman.2013.01.006.
- [5.9] Chang, J., Kalghatgi, G., Amer, A., Adomeit, P., Rohs, H. and Heuser, B., "Vehicle Demonstration of Naphtha Fuel Achieving Both High Efficiency and Drivability with EURO6 Engine-Out NOx Emission", *SAE International Journal of Engines* 6(1):101-119, 2013, doi:10.4271/2013-01-0267.
- [5.10] Abu-Jrai, A., Rodríguez-Fernández, J., Tsolakis, A., Megaritis, A., Theinnoi, K., Cracknell, R. and Clark, R., "Performance, Combustion and Emissions of a Diesel Engine Operated with Reformed EGR. Comparison of Diesel and GTL Fuelling", *Fuel* 88(6):1031-1041, 2009, doi:10.1016/j.fuel.2008.12.001.
- [5.11] Labeckas, G. and Slavinskas, S., "Performance and Emission Characteristics of a Direct Injection Diesel Engine Operating on KDV Synthetic Diesel Fuel", *Energy Conversion and Management* 66:173-188, 2013, doi:10.1016/j.enconman.2012.10.004.
- [5.12] Szymkowicz, P., Personal Communication with Fuels Group, General Motors Global Research and Development, 2017.
- [5.13] ANSYS, "ANSYS Model Fuel Library", *ANSYS, Inc.*, 2016.
- [5.14] ANSYS, "Surrogate Blend Optimizer", *ANSYS, Inc.*, 2016.
- [5.15] ASTM International, "Specification for Diesel Fuel Oils", *ASTM International*, ASTM D 975-16a, 2016, doi:10.1520/d0975-16a.
- [5.16] European Committee for Standardization (CEN), "Automotive fuels - Diesel - Requirements and test methods", *European Committee for Standardization*, EN 590:2009: E, 2009.
- [5.17] ASTM International, "Test Method for Determination of Ignition Delay and Derived Cetane Number (DCN) of Diesel Fuel Oils by

- Combustion in a Constant Volume Chamber”, *ASTM International*, ASTM D 6890, May 2017, doi:10.1520/d6890-13b.
- [5.18] DC Scientific, "SP10–Automated Smoke Point", *DC Scientific - Petroleum Testing Equipment*, 2017.
- [5.19] ASTM International, "Test Method for Smoke Point of Kerosine and Aviation Turbine Fuel", *ASTM International*, ASTM D 1322-12, May 2017, doi:10.1520/d1322-12.
- [5.20] Calcote, H. and Manos, D., "Effect of Molecular Structure on Incipient Soot Formation", *Combustion and Flame* 49(1-3):289-304, 1983, doi:10.1016/0010-2180(83)90172-4.
- [5.21] ASTM International, "Standard Test Method for Heat of Combustion of Liquid Hydrocarbon Fuels by Bomb Calorimeter", *ASTM International*, ASTM D 240-09, 2009.
- [5.22] ASTM International, "Test Method for Density, Relative Density, and API Gravity of Liquids by Digital Density Meter", *ASTM International*, ASTM D 4052-11, 2011, doi:10.1520/d4052-11.
- [5.23] ASTM International, "Test Method for Kinematic Viscosity of Transparent and Opaque Liquids (and Calculation of Dynamic Viscosity)", *ASTM International*, ASTM D 445-12, 2012, doi:10.1520/d0445-12.
- [5.24] ASTM International, "Test Method for Dynamic Surface Tension by the Fast-Bubble Technique", *ASTM International*, ASTM D 3825-09, 2009, doi:10.1520/d3825-09.
- [5.25] Design Institute for Physical Properties, "AIChE DIPPR Project 801 - Full Version", *KNovel Corporation*, (2005; 2008-2012; 2015; 2016)",
<http://App.Knovel.Com/Hotlink/Toc/Id:Kpdipprpf7/Dippr-Project-801-Full/Dippr-Project-801-Full>, 2016.
- [5.26] Chevron, "Diesel Fuels Technical Review", *Chevron Products Company*

<http://www.chevron.com/products/prodserv/fuels/bulletin/diesel>, 2007.

- [5.27] Wang, F., Wu, J. and Liu, Z., "Surface Tensions of Mixtures of Diesel Oil or Gasoline and Dimethoxymethane, Dimethyl Carbonate, or Ethanol", *Energy & Fuels* 20(6):2471-2474, 2006, doi:10.1021/ef060231c.
- [5.28] Ra, Y., Reitz, R., McFarlane, J. and Daw, C., "Effects of Fuel Physical Properties on Diesel Engine Combustion using Diesel and Biodiesel Fuels", *SAE International Journal of Fuels and Lubricants* 1(1):703-718, 2008, doi:10.4271/2008-01-1379.
- [5.29] Pitz, W., Westbrook, C., Herbinet, O. and Silke, E., "Progress in Chemical Kinetic Modeling for Surrogate Fuels", *7th International Conference on Modeling and Diagnostics for Advanced Engine Systems*, COMODIA 2008, Sapporo, Japan: Pages 9-15, 2008.

6. Conventional Diesel Combustion

Contents

6.	Conventional Diesel Combustion	141
6.1.	Introduction.....	143
6.2.	Engine Operating Conditions.....	145
6.3.	Combustion Analysis.....	146
6.4.	Gaseous Emissions.....	162
6.5.	Smoke and Particle Emissions	168
6.6.	Discussion.....	176
6.7.	Summary	183
6.8.	References	184

6.1. Introduction

Results from Chapter 5 demonstrated the combustion, physical and chemical properties of the four-component surrogate fuel CN50_TSI31 closely mimicked the petroleum Diesel fuel. In particular the cetane number and TSI matched within experimental accuracy. The goal of this chapter was to experimentally evaluate and compare the Diesel engine combustion, emissions and exhaust particles from the target petroleum Diesel fuel and the four-component surrogate fuel CN50_TSI31.

Single-cylinder engine tests provided a means for excellent control and reproducibility of the operating conditions compared to multi-cylinder engine tests [6.1]. Both fuels were subjected to numerous, highly complex physical processes that occur within the Diesel spray, evaporation and fuel-air mixture formation [6.2] [6.3] [6.4] [6.5] [6.6] [6.7]. The resulting engine combustion was also exceedingly complex [6.8] [6.9] [6.10]. A schematic representation of conventional Diesel combustion is presented in Figure 6-1 which shows the local equivalence ratio as a function of the local temperature [6.11] [6.12] [6.13]. The schematic suggests that conventional Diesel combustion encounters rich and lean local conditions that promote soot and NO_x formation, respectively. In-cylinder soot formation and oxidation is a remarkably complex process [6.14] [6.15]. Thus, transitioning the engine from low soot to high soot operating conditions would provide an excellent assessment of the surrogate fuel. NO_x formation is also shown to be equivalence ratio and temperature dependent. To reproduce the NO_x emissions from the target Diesel fuel, the surrogate must provide equivalent heat release, local temperatures and local equivalence ratios.

In Figure 6-2, a typical heat release profile is given [6.8]. The figure suggests that conventional combustion may experience regions of low-temperature and high-temperature heat release. For this research, the low-temperature heat-release provided a means to compare the low-temperature reaction kinetics for both fuels. Furthermore, the high-temperature heat release, which consists of premixed and diffusion combustion zones, provided complex combustion environments for the fuels. High-temperature kinetics and mixing-controlled combustion zones steered the emissions and soot formation. Therefore, in addition to mixture preparation, the surrogate fuel needed to closely match the high-temperature heat release profile of the

target Diesel fuel. In these regards, the engine data can be used as a crucial test for the surrogate fuel.

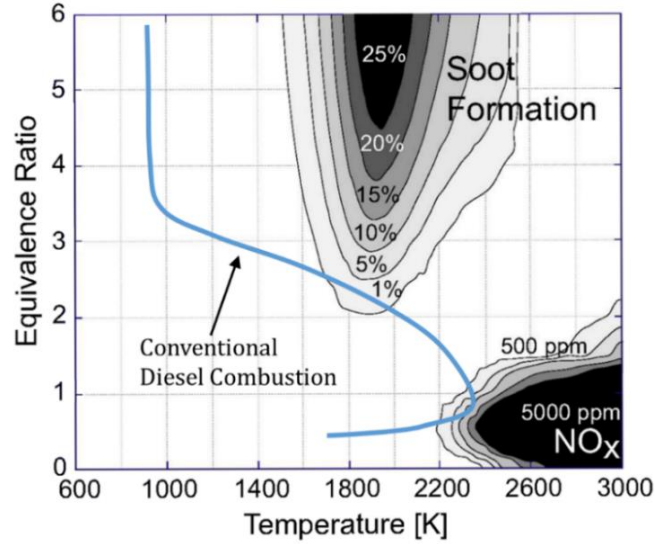


Figure 6-1: Conventional Diesel Combustion strategy conceptually displayed on a chart of local fuel-equivalence ratio versus local combustion temperature. Figure adapted from [6.13].

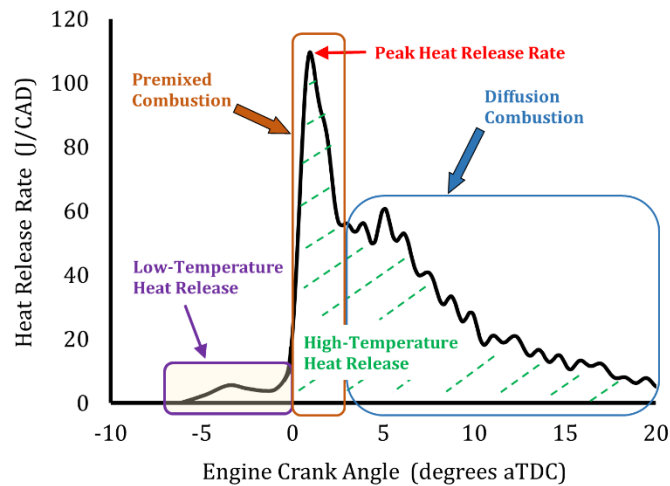


Figure 6-2: Heat release characteristics for conventional Diesel combustion. Adapted from [6.8]. (Also appears in Chapter 4 as Figure 4-4.)

6.2. Engine Operating Conditions

A moderate engine speed and load was used to evaluate the fuels under conventional Diesel combustion conditions. The engine speed was maintained at 1500 r/min and the engine load was held constant at 9 bar IMEP by adjusting the fuel injection quantity at each condition. This test condition was also referred to as 1500x9. Two engine calibration parameters that have significant effects on combustion and emissions are EGR dilution and combustion phasing [6.16] [6.17] [6.18] [6.19]. Therefore, a test matrix was developed for 1500x9 that independently varied EGR and combustion phasing while holding other operating conditions constant. EGR was varied from 0 to a maximum of 30% (defined by excessive smoke). At each EGR level, the combustion phasing, as quantified by the crank-angle of 50% mass burned (CA50) was tested at 6, 9, 12 and 15 degrees aTDC. The CA50 values were set by adjusting the start of the injector energizing time. All tests were run with a single injection strategy, 50 °C intake temperature and the swirl ratio maintained at 2.9. The 1500x9 operating conditions are summarized in Table 6-1. The resulting matrix contained 24 test points for each fuel.

Table 6-1: Engine operating conditions to evaluate the petroleum and surrogate fuels with conventional Diesel combustion.

Operating Condition	Units	1500x9
Engine Speed	r/min	1500
Engine IMEP	bar	9
Fuel Injection Pressure	bar	650
Intake Pressure	kPaA	121
Exhaust Pressure	kPaA	128
Fuel Injection Strategy		Single
Intake Temperature	°C	50
Swirl Ratio		2.9
EGR Level	%	0, 10, 15, 20, 25, 30
CA50	degrees aTDC	6, 9, 12, 15

6.3. Combustion Analysis

At each test condition, the instantaneous cylinder-pressure data signal was digitized for 150 consecutive engine cycles at a crank-angle resolution of 0.2 degrees. Several other high-speed data channels were also digitized such as the fuel pressure at the inlet to the injector. As presented in Chapter 4, the data were analyzed to provide comprehensive combustion diagnostics that describe the combustion event. In this Chapter the following the combustion parameters were employed to characterize the combustion process:

- Cylinder Pressure
- Apparent Heat Release Rate
- Low-Temperature Heat Release (LTHR)
- High-Temperature Heat Release (HTHR)
- Fuel Injector Start of Energizing (SOE)
- Ignition Delay Time
- Mixing Advance Time
- Peak Heat Release Rate
- Peak Bulk Gas Temperature
- 10-90% Burn Duration

The initial analysis began by examining the cylinder pressure measurements and the resulting heat release profiles at 1500x9 with 0% EGR and a maximum of 30% EGR. For both tests the combustion phasing was set at CA50=9 degrees aTDC which was the optimal combustion phasing for efficiency. Cylinder pressure is shown in Figure 6-3 and apparent heat release rate is given in Figure 6-4. The solid colored lines were data from the engine operating with the target Diesel fuel. The overlaid dashed lines were data from the surrogate fuel.

The effects of EGR on cylinder pressure were clearly noticeable. Compared to 0% EGR, the 30% EGR level delayed ignition and increased the cylinder pressure rise rate. Very good agreement was found between the target Diesel and surrogate fuels. For example, with 0% EGR, the target Diesel fuel had a peak pressure of 8,434 kPa while the surrogate peak pressure was 8,471 kPa (a difference of less than 0.5%).

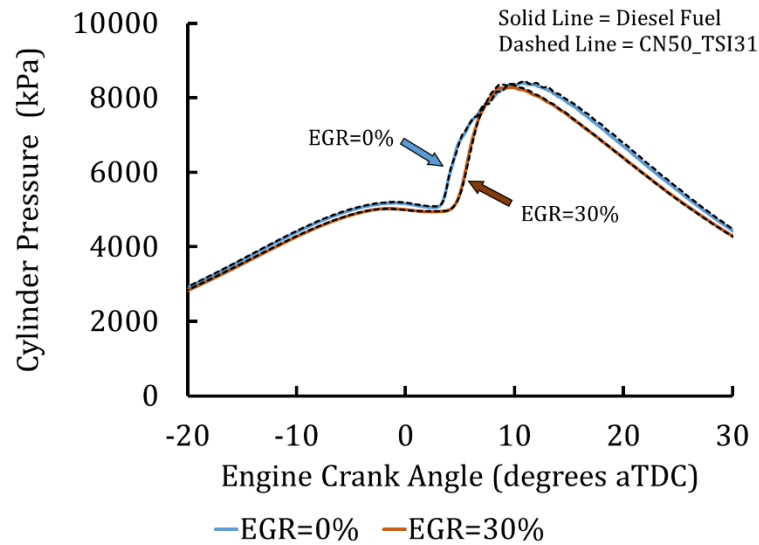


Figure 6-3: Cylinder pressure for 1500x9 with 0% EGR and with 30% EGR. Injection SOE adjusted to maintain CA50=9 degrees aTDC for all tests.

The heat release analysis provided more interesting results. First, the 0% EGR condition showed a relatively small low-temperature heat release followed by the premixed combustion, and finally a prolonged diffusion combustion region. The surrogate fuel heat release rates precisely matched the target Diesel fuel. For example, at 0% EGR the peak heat release rate for the target Diesel fuel was 112.4 J/CAD while the surrogate fuel peak heat release rate was 111.7 J/CAD (about 0.6% difference). Second, it was clear from Figure 6-4 that the heat release rate was significantly affected by the high EGR level. The low-temperature heat release was greatly extended by the EGR. The premixed combustion was much greater and possessed a higher peak heat release rate. With more fuel consumed in the premixed combustion region the diffusion combustion was substantially reduced. Again, the surrogate fuel precisely matched low-temperature, premixed and diffusion combustion zones from the target Diesel fuel. For example, at 30% EGR the target Diesel fuel had a peak heat release rate of 135.6 J/CAD compared to 134.6 J/CAD for the surrogate fuel (about 0.7% difference).

Figure 6-4 shows the nature of the heat release changed from premixed + diffusion (0% EGR) to mostly premixed combustion (30% EGR). And most

importantly, the heat release from the surrogate fuel was essentially indistinguishable from the target Diesel fuel. Later in this chapter it will be shown that the high EGR level significantly increased the ignition delay which provided more time for low-temperature heat release reactions and more time for fuel vaporization and mixing. As a result, more fuel was burned in the premixed combustion region.

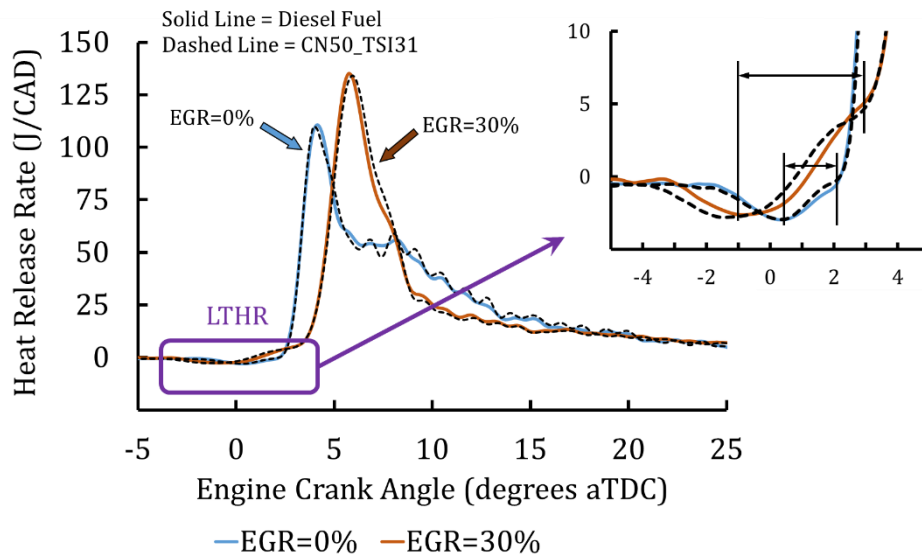


Figure 6-4: Heat release rates for 1500x9 with 0% EGR and with 30% EGR. Injection SOE adjusted to maintain CA50=9 degrees aTDC for all tests.

After gaining some understanding of the EGR effects on combustion at this 1500x9 condition, the next step was to learn the effects of combustion phasing on the cylinder pressure measurements and the heat release rates. Figure 6-5 shows cylinder pressure measurements at the 1500x9 condition with 15% EGR. The impact of combustion phasing was plainly noticed and had a profound effect on the cylinder pressure. As combustion was retarded from CA50=6 to CA50=15 the ignition and peak cylinder pressure moved later into the expansion stroke. The peak cylinder pressure was significantly reduced and a modest increase in the cylinder pressure rise rate was evident. Regarding the fuels, the figure shows that for each condition the cylinder pressure histories for the surrogate and target Diesel fuels were in very close agreement. For the CA50=6 condition, the target Diesel fuel had a peak

pressure of 8,962 kPa compared to 9,079 kPa for the surrogate fuel; a difference of less than 1.4%.

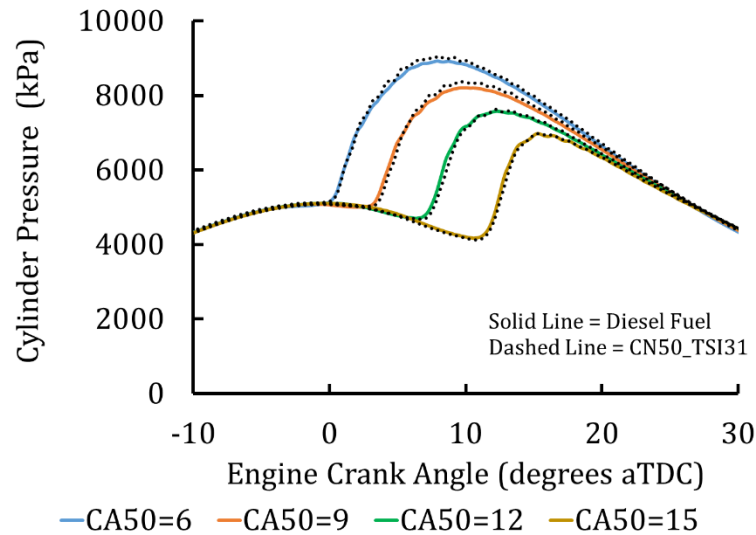


Figure 6-5: Cylinder pressure for CA50 sweeps at 1500x9 with 15% EGR.

The cylinder pressure data were processed to obtain the apparent heat release results shown in Figure 6-6. The data illustrates the profound effect the combustion phasing has on the heat release rates. First, as combustion phasing was retarded, ignition delay was increased and the low-temperature heat release measurably increased. With more time for fuel vaporization and mixing the premixed combustion region increased and subsequently the amount of diffusion combustion decreased. With more fuel consumed in the premixed region, the peak heat release rate increased markedly and moved further into the expansion stroke. For this 1500x9 condition, combustion phasing influenced all of the primary characteristics of conventional Diesel combustion which made this an excellent condition to assess the surrogate fuel. The results in Figure 6-6 demonstrate that the surrogate fuel precisely followed the heat release characteristics of the target Diesel fuel. For example, at CA50=15 degrees aTDC the target Diesel fuel had a peak heat release rate of 168.2 J/CAD which occurred at 12.7 degrees aTDC. The surrogate fuel had a peak heat release rate of 165.5 J/CAD at degrees 12.9 degrees aTDC. Such close agreements were encouraging and crucial findings

that suggested the surrogate fuel was reproducing the spray, evaporation, vapor distribution, mixing, ignition and combustion characteristics of the target Diesel fuel.

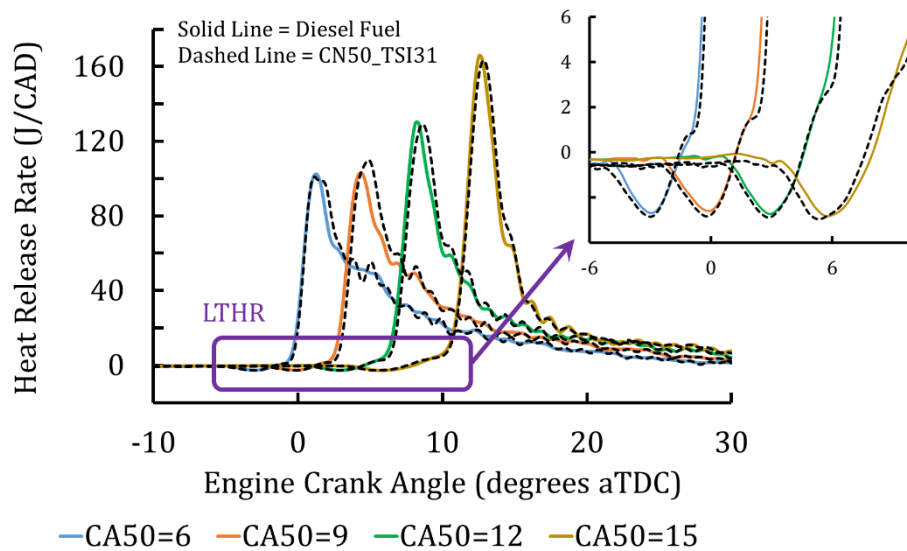


Figure 6-6: Heat release rates for CA50 sweeps at 1500x9 with 15% EGR.

The above analysis investigated the cylinder pressure and heat release rates as the EGR and combustion phasing were varied. The respective impact on the heat release was clearly shown and good agreement between the surrogate and target Diesel fuels was obtained. In the next segment the combustion analysis was expanded by examining the impact of the EGR and combustion phasing sweeps on specific combustion metrics such as ignition delay, peak heat release rate and the 10-90% burn duration.

During the investigation it was determined that the body of engine test data was well described by comparing data from an EGR sweep with constant combustion phasing and also by evaluating data from a combustion phasing sweep at a constant EGR level. This provided independent evaluations of the effects of EGR and combustion phasing with clear figures that compared the response of the target Diesel and surrogate fuels. For brevity, this thesis presented data from an EGR sweep with CA50=9 degrees aTDC. For the combustion phasing sweep, data was shown as CA50 was swept from 6 to 15 degrees aTDC with 15% EGR which was midway between 0% EGR and the

smoke-limited 30% EGR level. The comparisons between the target and surrogate fuels shown within this section were consistent with the data collected at other EGR levels and combustion phasing.

Injection Start of Energizing (SOE)

The SOE data from the EGR and CA50 sweeps are shown in Figure 6-7 and Figure 6-8, respectively. At the start of the EGR sweep, the injection SOE was about -5.5 degrees aTDC. As EGR was increased, the injection SOE required more advance to maintain CA50=9. The data shows that the SOE timing was a modestly sensitive linear function of the EGR level. From 0% to 30% EGR, the SOE required only 2 degrees of additional advance to maintain the combustion phasing at CA50=9 degrees aTDC. A much wider advance of SOE was observed during the CA50 sweep (Figure 6-8). From the most advanced (CA50=6) to the most retarded (CA50=15) combustion phasing the SOE changed by almost 8 degrees. The required SOE response to changes in CA50 was essentially one-to-one.

As mentioned above, the EGR sweep required relatively small changes in SOE to maintain constant combustion phasing while the CA50 sweep resulted in wide changes in the SOE. For both sweeps, the data from the target Diesel and CN50_TSI31 surrogate fuel were effectively identical. For these 1500x9 operating conditions the fuels required the same SOE to control the combustion phasing to the same set points. This was an encouraging result since the CA50 set points spanned a broad range from advanced to retarded phasing. With the SOE timings closely repeated, it was concluded that for each test point the target Diesel and surrogate fuels were injected into the same in-cylinder conditions namely, temperature, pressure, density, mixture motion, and piston position.

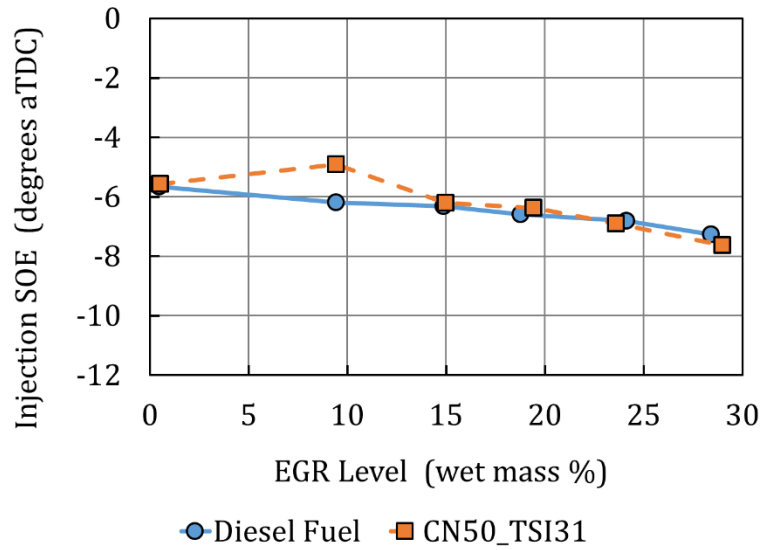


Figure 6-7: The required injection SOE to achieve $CA_{50}=9$ degrees aTDC as EGR level was increased from 0% to 30% at the 1500x9 operating condition.

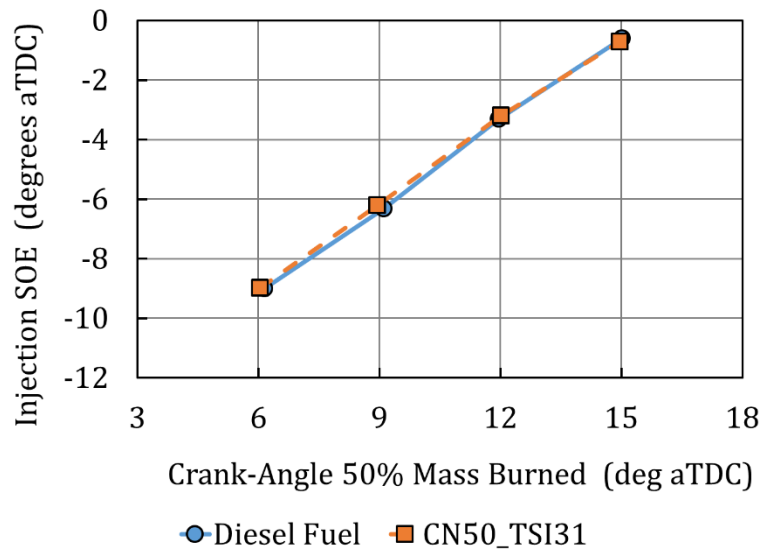


Figure 6-8: The required injection SOE to achieve $CA_{50}=6, 9, 12$ and 15 degrees aTDC at the 1500x9 operating condition with 15% EGR.

Ignition Delay

The ignition delay was determined from the fuel pressure and heat release data as shown in Chapter 4, Figure 4-6. Ignition was defined as the crank angle of 5% mass fraction burned. The results from the EGR sweeps are presented in Figure 6-9 while the CA50 sweep results are provided Figure 6-10. At the 1500x9 condition adding EGR increased the ignition delay. The ignition delay was observed to increase at an increasing rate with EGR. From 0% EGR to 15% EGR the ignition delay increased by 1 crank-angle degree. However, from 15% to 30% EGR the ignition delay increased by 2 degrees. The CA50 sweeps also showed that the ignition delay grew at an increasing rate as combustion was retarded from CA50=6 to 15 degrees aTDC.

Referring back to Figure 6-4, increasing the ignition delay profoundly impacted the low-temperature heat release and the distribution of fuel consumed by the premixed and diffusion combustion regions. Thus, it is critically important for the surrogate fuel to match the ignition delay of the target fuel. Otherwise, the mixture preparation and fuel division between the low-temperature, premixed and diffusion combustion would vary between the fuels.

For the data collected during the EGR and CA50 sweeps, the ignition delay from the surrogate fuel precisely matched the ignition delay from the target Diesel fuel. Even the observed trends where ignition delay increased at increasing rates were accurately duplicated. For the EGR sweeps the maximum difference in ignition delay between the target Diesel fuel and the surrogate fuel was only 0.4 crank-angle degrees which occurred at the 30% EGR condition.

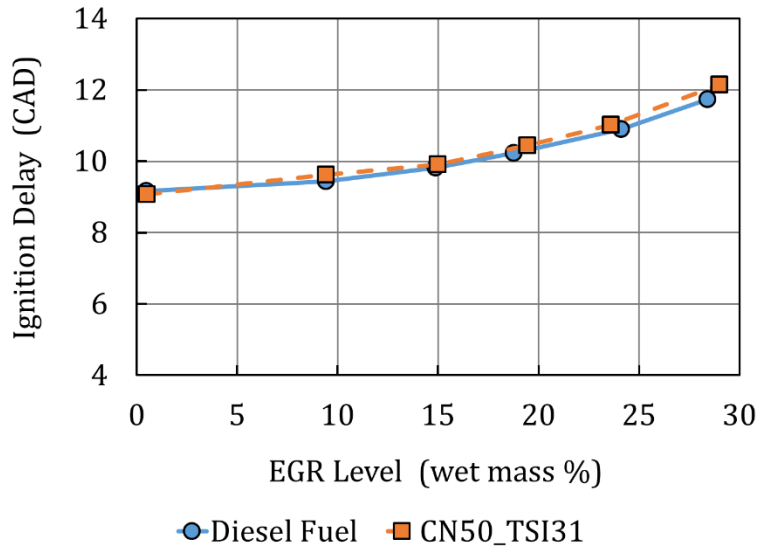


Figure 6-9: Effects of EGR on ignition delay at 1500x9 with the injection SOE adjusted to maintain CA50=9 degrees aTDC.

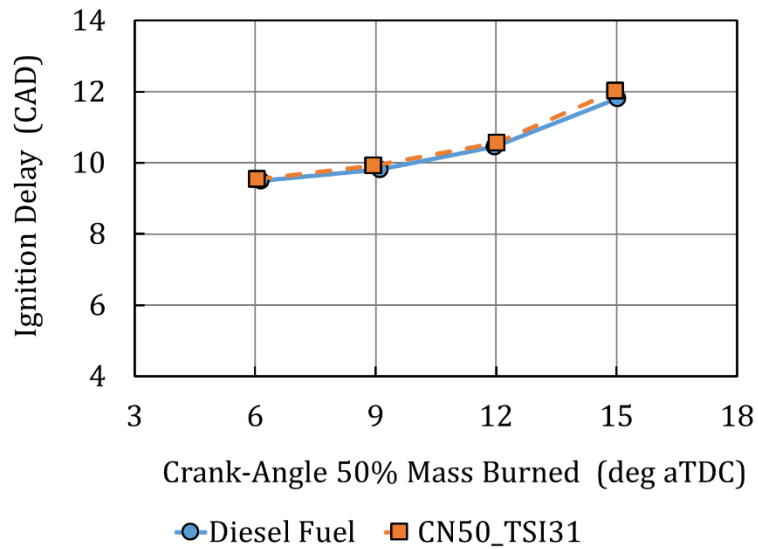


Figure 6-10: Effects of combustion phasing on ignition delay at 1500x9 with 15% EGR.

Mixing Advance Time

The mixing advance time was defined as the period between the end of fuel injection and the ignition or the beginning of the high-temperature heat release. The end of fuel injection was detected from the pressure measured in the high-pressure fuel line approximately 5 mm from the injector inlet. Again, ignition was defined as the crank angle of 5% mass fraction burned. A schematic diagram of the methodology is given in Chapter 4, Figure 4-6.

For both fuels to undergo the same mixture formation process, it was vitally important to provide the same time period for spray formation, vaporization and mixing. This was accomplished by ensuring the mixing advance times for both fuels were in good agreement throughout the EGR and CA50 sweeps.

Figure 6-11 shows the effect of EGR on the mixing advance times. At the 1500x9 condition without EGR the mixing advance time was about 2 crank-angle degrees (0.2 ms). As EGR was increased and injection timing was advanced to maintain combustion phasing the mixing advance time also increased. At 30% EGR the mixing advance time more than doubled to almost 5 degrees (0.5 ms). The impact of combustion phasing on the mixing advance time at the 1500x9 condition with 15% EGR is provided in Figure 6-12. Retarding the combustion phasing increased ignition delay (Figure 6-10) which correspondingly increased the mixing advance time.

The effects of EGR and combustion phasing on ignition delay corresponded to nearly identical changes in the mixing advance time. This finding suggested that the target Diesel and surrogate fuels experienced the same in-cylinder conditions and mixture preparation periods. For this to occur the test-to-test differences in the intake charge temperature, mass, fuel injection pressure and rate of injection, and EGR level must not significantly impact the low-temperature heat release and ignition delay. In addition, fuel property differences, such as the distillation temperatures, must not have had a significant effect on the mixture formation, the initial stages of combustion and subsequently the high-temperature heat release. This was a very encouraging result. Throughout the EGR and CA50 sweeps, the data suggests the injection, mixture preparation and early combustion processes for the surrogate fuel were essentially identical to the target Diesel fuel.

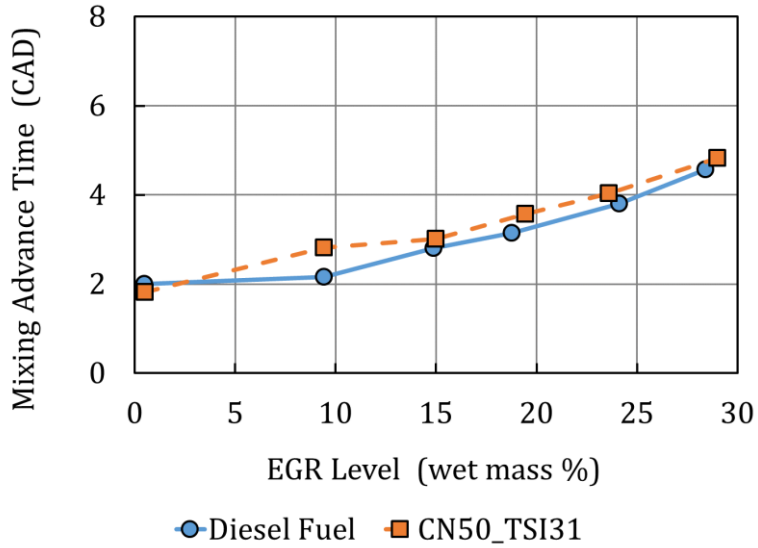


Figure 6-11: Effects of EGR on mixing advance time at 1500x9 with the injection SOE adjusted to maintain CA50=9 degrees aTDC.

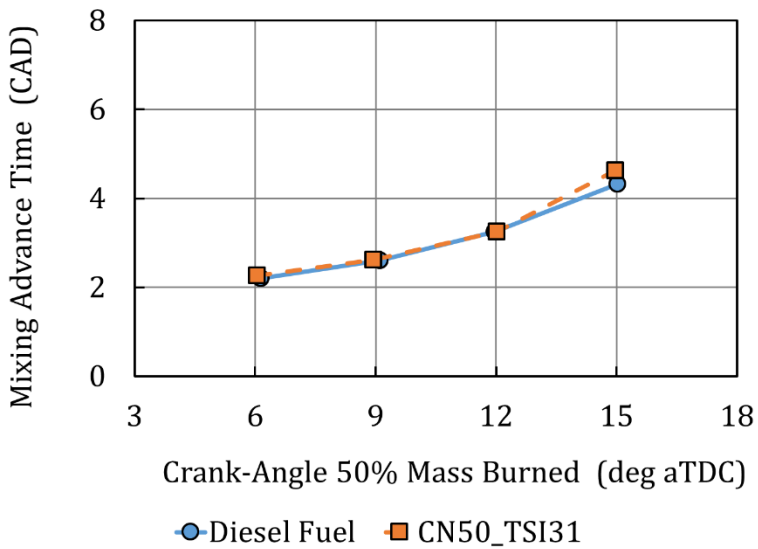


Figure 6-12: Effects of combustion phasing on mixing advance time at 1500x9 with 15% EGR.

Peak Heat Release Rate

Peak heat release rates from the EGR sweep are shown in Figure 6-13. In general, EGR levels less than 15% did not impact the peak heat release rate. Above 15% EGR the peak heat release rate modestly increased with EGR. For example, at 15% EGR the peak heat release rate was about 108 J/CAD and increased to about 135 J/CAD at 30% EGR. Presumably the longer ignition delays caused by the EGR dilution increased the amount of fuel consumed in the premixed combustion region which raised the peak heat release rate. Peak heat release rates from the combustion phasing sweep at 15% EGR are presented in Figure 6-14. The data showed that for these operating conditions, retarded combustion phasing had a much greater impact on peak heat release rate than EGR dilution. At CA50=6, the peak heat release rate was about 103 J/CAD and increased to about 167 J/CAD at CA50=15 degrees aTDC. In general, for both fuels, the EGR and combustion phasing sweeps had the same impact on peak heat release rate. The maximum difference between the two fuels was observed at 15% EGR with CA50=9 degrees aTDC and was found to be only about 7 J/CAD. In most instances the fuels were effectively the same. Overall, the peak heat release rate data suggested that the fuel distribution between the premixed and diffusion combustion regions were the same for both fuels.

Peak Bulk Gas Temperature

Bulk gas temperatures were computed from the cylinder pressure measurements using methods described in Chapter 4. Peak bulk gas temperatures from the EGR sweep are given in Figure 6-15 and the outcomes from the CA50 sweep are shown in Figure 6-16. For 1500x9 with CA50 held constant at 9 degrees aTDC, adding EGR to the intake charge lowered the peak bulk gas temperature. From 0% EGR to 30% the peak bulk gas temperature was reduced from about 2000 K to 1800 K in a linear manner. At the 15% EGR condition, retarding the combustion phasing from CA50=6 to 15 degrees aTDC lowered the peak bulk gas temperature from around 1950 K to 1850 K with a linear trend. Regarding the fuels, the results show very good agreement between the surrogate and target Diesel fuel. The maximum difference of 30 K was observed at 0% EGR with CA50=9 degrees aTDC.

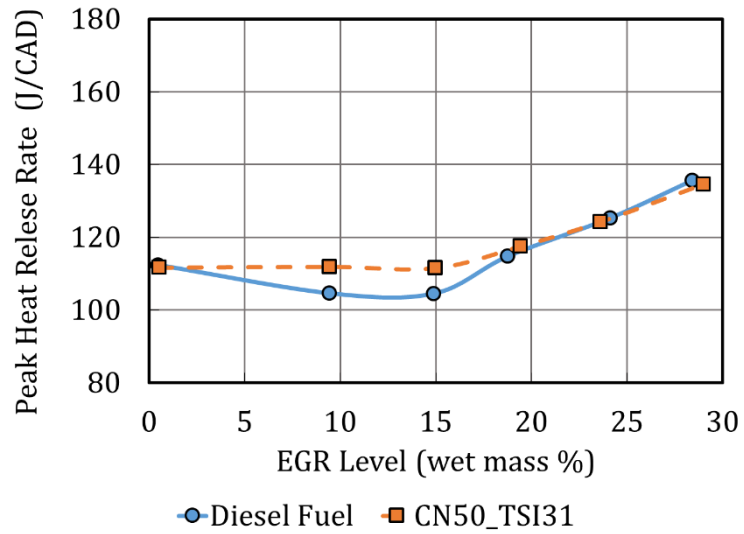


Figure 6-13: Effects of EGR on peak heat release rate at 1500x9 with the injection SOE adjusted to maintain CA50=9 degrees aTDC.

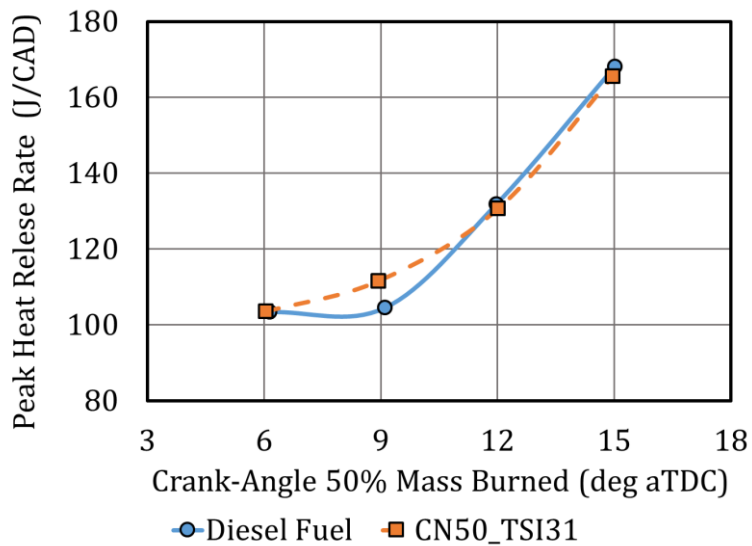


Figure 6-14: Effects of combustion phasing on peak heat release rate at 1500x9 with 15% EGR.

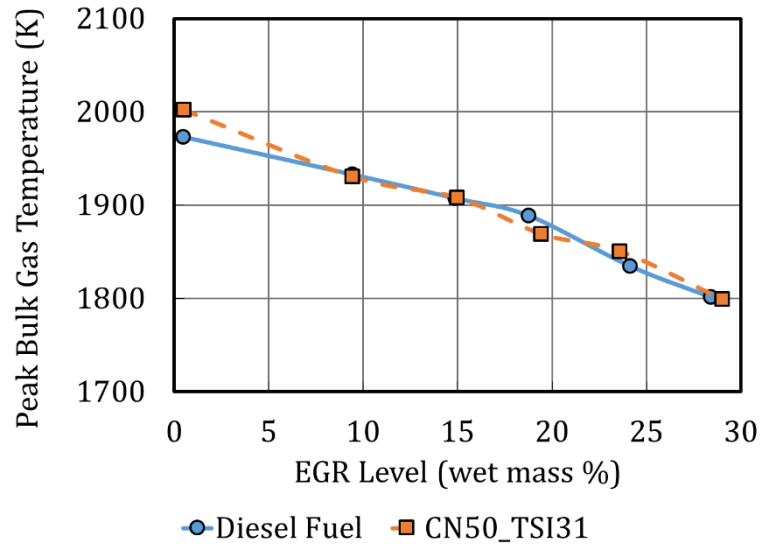


Figure 6-15: Effects of EGR on peak bulk gas temperature at 1500x9 with the injection SOE adjusted to maintain CA50=9 degrees aTDC.

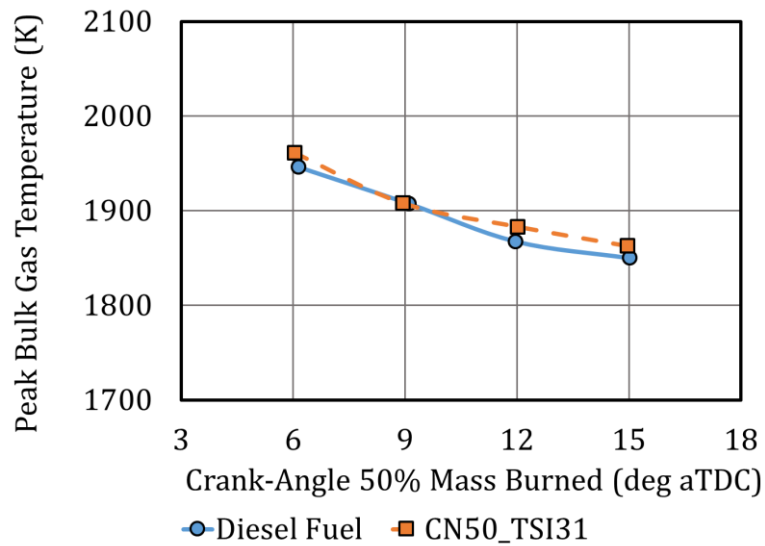


Figure 6-16: Effects of combustion phasing on peak bulk gas temperature at 1500x9 with 15% EGR.

10-90% Burn Duration

The 10-90% burn duration is a combustion metric associated with the period that consumes the majority of the fuel. It is sometimes referred to as the bulk burn period. The interval starts at the 10% burn point to avoid the low-temperature heat release region and ends at the 90% point to avoid the extended asymptote that can occur in the cumulative heat release beyond the 90% burn point (Figure 4-5). As such, the 10-90% burn duration was intended to include the premixed and diffusion combustion regions. As shown in Figure 6-17, the 10-90% burn duration increased linearly with EGR. From 0% to 30% EGR the 10-90% burn duration respectively increased from about 15 degrees to around 21 degrees. Figure 6-18 shows the combustion phasing sweep had a very modest impact on the 10-90% burn duration. From CA50=6 to CA50=15 degrees aTDC the 10-90% burn duration increased by about 1 crank-angle-degree.

At the 1500x9 operating conditions, the 10-90% burn durations from the surrogate and target Diesel fuels had very close agreement. From Figure 6-17, below 20% EGR the difference in the 10-90% burn duration between the fuels was less than 0.5 crank-angle degrees. At 30% EGR, the 10-90% burn duration for the surrogate fuel was 2 crank-angle degrees longer than the target Diesel fuel. It's not clear whether this was a result of the fuel or if differences in repeating the operating conditions impacted the latter stages of combustion duration. For example, at high EGR levels combustion may become more sensitive to modest changes in intake pressure and temperature. For the combustion phasing sweep in Figure 6-18, the agreement in the 10-90% burn duration was exceptional with a maximum difference between the fuels of only 0.3 crank-angle-degrees.

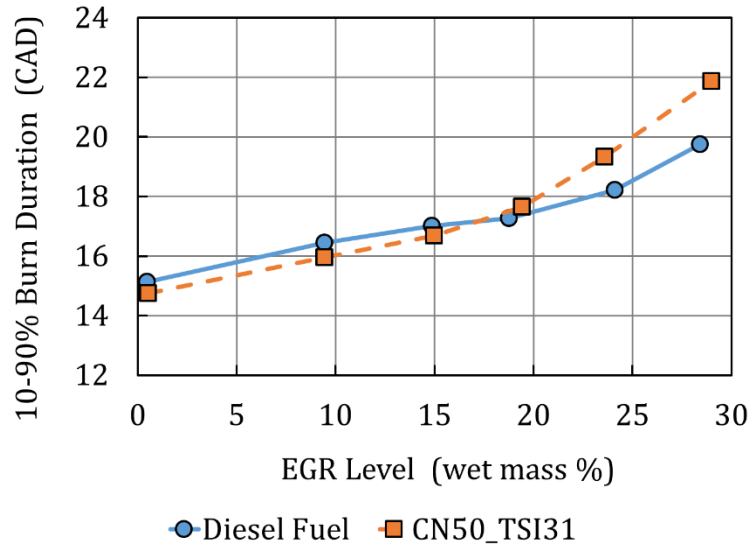


Figure 6-17: Effects of EGR on 10-90% burn duration at 1500x9 with the injection SOE adjusted to maintain CA50=9 degrees aTDC.

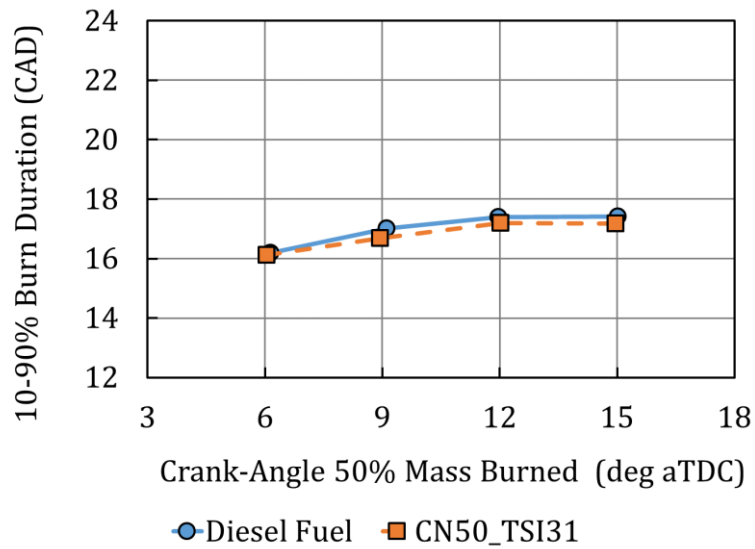


Figure 6-18: Effects of combustion phasing on the 10-90% burn duration at 1500x9 with 15% EGR.

6.4. Gaseous Emissions

Conventional Diesel combustion is heterogeneous in nature as the fuel-air mixture is stratified in the combustion chamber. The gas-phase emissions, specifically CO, HC and NO_x, depend on the local conditions during the combustion cycle and the fuel properties.

CO and HC in the exhaust are predominantly the result of incomplete combustion. CO is a combustion intermediate whereas as HC can be unburned or partially oxidized fuel. The emission of CO and HC from the engine depends on their formation and consumption during combustion and their post-combustion oxidation late in the cycle prior to the opening of the exhaust valve. The entire process is primarily governed by the presence of oxidants, temperature, mixing and residence time. During premixed combustion, over-mixing of the fuel and air can lead to excessively lean mixtures. For diffusion combustion under-mixing can result in over rich mixtures. The addition of EGR into the combustion chamber can exacerbate the over-lean or over-rich conditions by lowering the local oxygen concentration and temperature. Spray interactions with surfaces and combustion quenching in the squish volume are additional sources of CO and HC emissions [6.8] [6.19] [6.20] [6.21].

NO is formed by the oxidation of nitrogen during combustion. Smaller amounts of NO further oxidize to form NO₂ depending on conditions. In general, the NO_x emitted from conventional Diesel combustion contains 70-95% NO with the balance primarily NO₂ [6.22] [6.23] [6.24]. Several reactions occur during combustion that can result in NO_x formation. These reactions are strongly affected by temperature, reacting species, residence time and pressure. For the 1500x9 operating condition it was believed that the thermal mechanism, also known as the extended Zeldovich mechanism, was responsible for the NO_x formation. This mechanism is very temperature sensitive. Referring back to Figure 6-1, NO_x formation is essentially insignificant when local combustion temperatures are less than 1800 K. For conventional combustion with premixed and diffusion zones, work from Alkidas [6.25] and Dec [6.26] suggested that NO_x was formed during diffusion combustion where high temperatures, oxygen and residence time are sufficient to form NO.

Physical properties of fuel influence mixture preparation during the ignition delay period, liquid penetration, fuel vapor distribution and the local fuel-air mixture during combustion. During the engine tests the operating conditions were precisely reproduced for both fuels (fuel mass, injection pressure, air and EGR flow, etc.). Given the close repetition of the test conditions and the good agreement obtained in the combustion results given in the previous section, any differences in gas-phase emissions would be attributed to the effect of the properties of the fuel on emission formation and consumption.

Carbon Monoxide

CO emissions for the EGR sweep are shown in Figure 6-19 and the results from the combustion phasing sweep in Figure 6-20. For both fuels, very close agreement was obtained at all operating conditions. For the EGR sweep, CO was very low from 0-20% EGR. At 30% EGR the CO increased by an order of magnitude. This increase was attributed to insufficient local oxygen levels required to complete the oxidation of CO to CO₂. This was concluded because there was little change in bulk gas temperature and residence time between 25% and 30% EGR. During the combustion phasing sweep, CO slightly increased as CA50 was retarded. As combustion was retarded the premixed fraction and peak heat release rates increased while the bulk gas temperatures were somewhat lower. As multiple changes occurred in the combustion process it is difficult to identify the direct cause of the CO increase. Nevertheless, even with the slight changes in combustion conditions resulting from the CA50 sweep the surrogate fuel continued to closely match the CO emissions from the target Diesel fuel. The only noticeable difference occurred at CA50=15 degrees aTDC where the EI-CO of the target Diesel fuel exceeded the surrogate fuel; 3.4 g/kg-fuel compared to 2.9 g/kg-fuel, respectively.

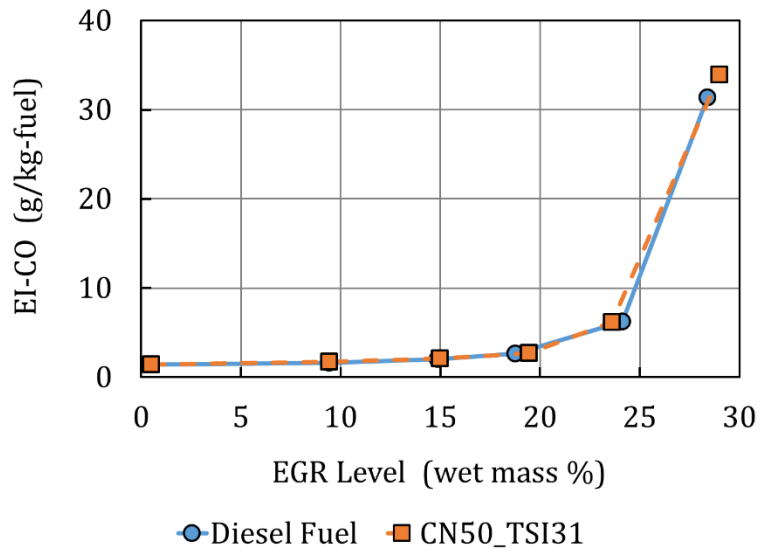


Figure 6-19: Effects of EGR on CO emissions at 1500x9 with the injection SOE adjusted to maintain CA50=9 degrees aTDC.

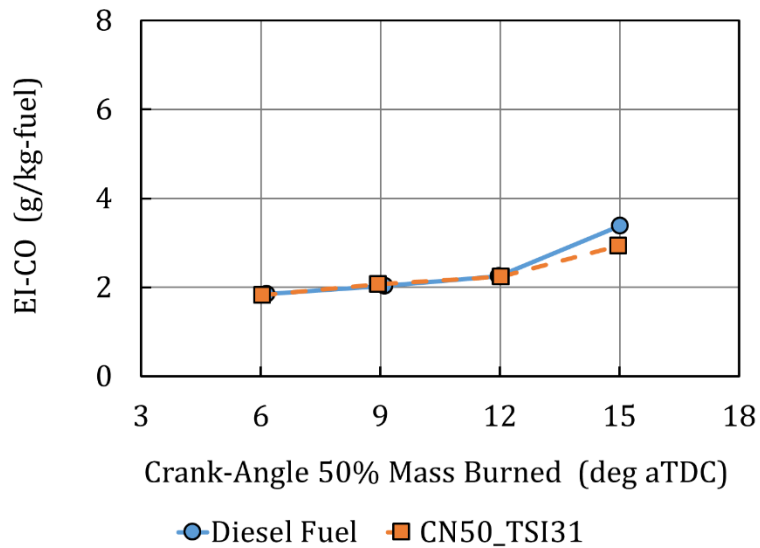


Figure 6-20: Effects of combustion phasing on CO emissions at 1500x9 with 15% EGR.

Hydrocarbons

The exhaust HC emissions for the EGR sweep are given in Figure 6-21 and the results from the combustion phasing sweep are provided in Figure 6-22. The HC emissions were very low and basically did not change with EGR or CA50. For the combined EGR and CA50 sweeps the target Diesel fuel had an average EI-HC=1.02 g/kg-fuel while the surrogate fuel averaged EI-HC=0.85 g/kg-fuel. The results suggest that the local combustion conditions provided sufficient oxygen, temperature, mixing and residence time for nearly complete combustion of the fuel at the 1500x9 operating conditions.

Nitrogen Oxides

Figure 6-23 shows the effects of EGR on NO_x emission while Figure 6-24 gives the influence of combustion phasing. For the EGR sweep, NO_x was reduced by two mechanisms. First, the EGR displaced intake air lowering the local oxygen concentration during combustion. Second, the intake CO₂ had the added effect of increasing the heat capacity of the intake charge which lowered combustion temperatures. For the CA50 sweep, the EGR level was held at 15%. Retarding the combustion resulted in lower temperatures that reduced the NO_x emission.

For both the EGR sweep and the CA50 sweep, the NO_x emissions from the surrogate and target Diesel fuels were nearly identical. The only noticeable difference occurred at 15% EGR and CA50=15 degrees aTDC where the target Diesel fuel had EI-NO_x=12.2 g/kg-fuel and the surrogate fuel had EI-NO_x=14.3 g/kg-fuel. Otherwise, the close agreement in NO_x emissions was an expected result. First, the heating values for the fuels were closely matched thus they would release the same amount of energy during combustion. Second, the operating conditions for testing the fuels were precisely repeated providing the same engine thermal environment, charge mass and constituents. Finally, the combustion results in the previous section showed very close agreement in ignition delay, heat release, peak bulk gas temperatures, peak cylinder pressures and combustion duration. Thus, the conditions that drive NO_x formation, namely temperature, reacting species, residence time and pressure were essentially the same for both fuels.

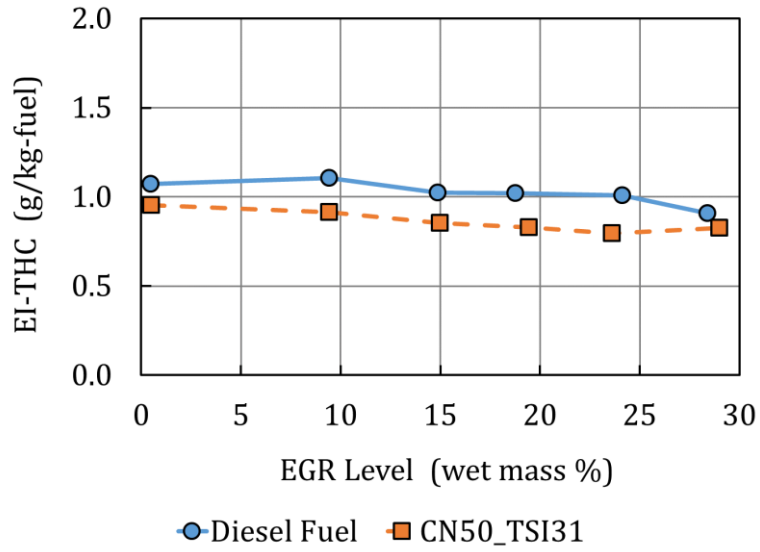


Figure 6-21: Effects of EGR on total hydrocarbon emissions at 1500x9 with the injection SOE adjusted to maintain CA50=9 degrees aTDC.

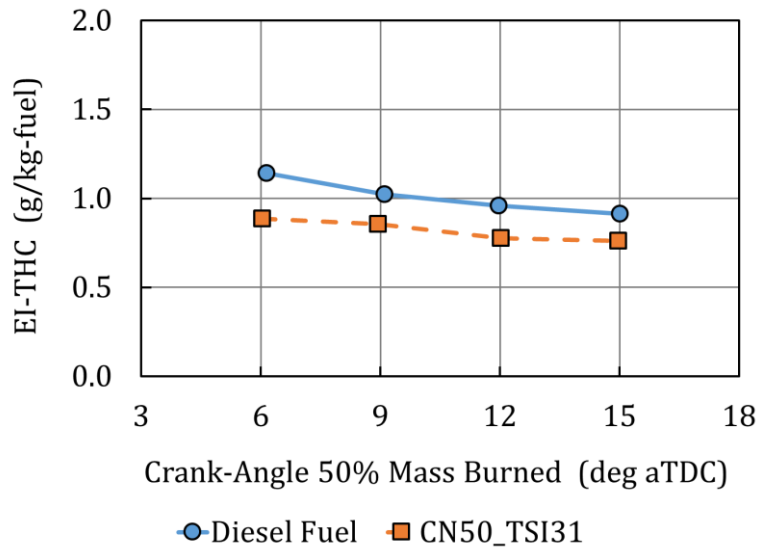


Figure 6-22: Effects of combustion phasing on total hydrocarbon emissions at 1500x9 with 15% EGR.

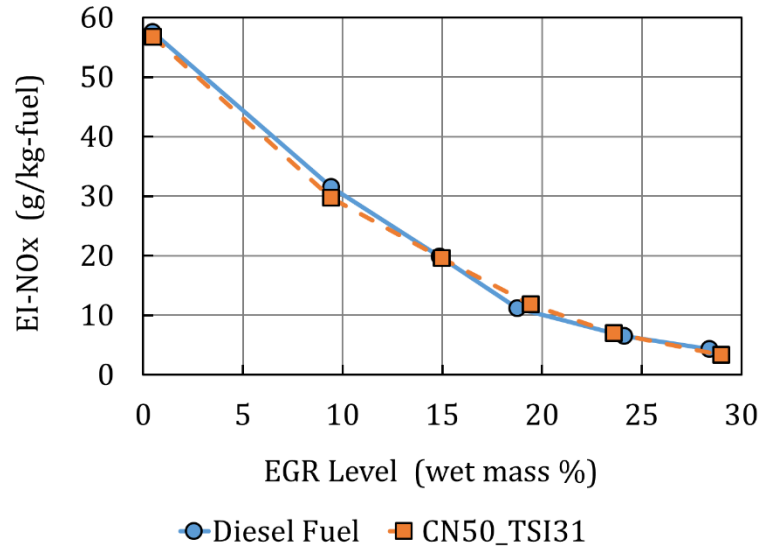


Figure 6-23: Effects of EGR on NOx emissions at 1500x9 with the injection SOE adjusted to maintain CA50=9 degrees aTDC.

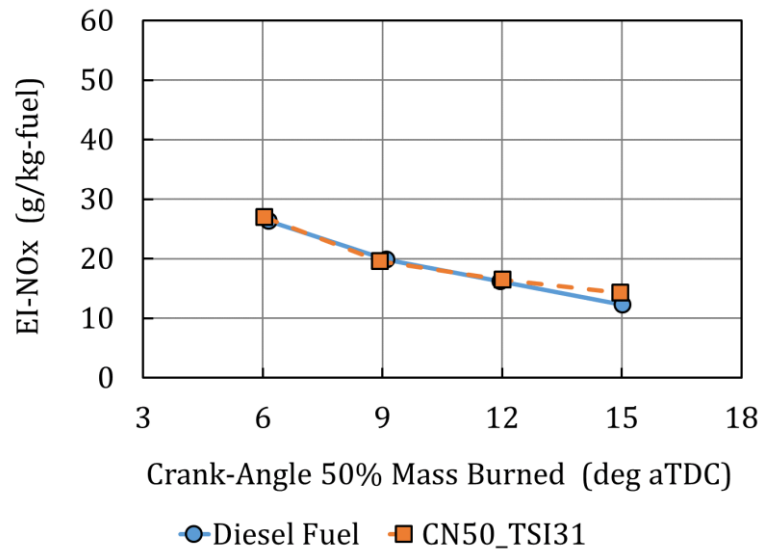


Figure 6-24: Effects of combustion phasing on NOx emissions at 1500x9 with 15% EGR.

6.5. Smoke and Particle Emissions

In Chapter 5, the sooting tendency of the target Diesel fuel was measured by a simple smoke point candle test. With this data, surrogate fuel CN50_TS131 was formulated to precisely match the smoke point of the target Diesel fuel. Diffusion combustion within a candle flame is a complex process. However, combustion within a Diesel engine is exceedingly more complicated. This posed the question: In a contemporary Diesel engine, will a full-range petroleum Diesel fuel and a four-component surrogate fuel with the same smoke point have the same exhaust smoke and particle emissions? Data presented earlier in this chapter showed the engine combustion and gaseous emissions from both fuels had exceptionally good agreement. This section examines the hypothesis that the smoke point, or threshold soot index, may be used to formulate a surrogate fuel that will produce the same exhaust smoke and particles as the full-range petroleum Diesel fuel.

Exhaust Smoke

The results from the EGR sweeps are given in Figure 6-25. It is immediately evident that the surrogate and target Diesel fuels produce the same smoke at these conditions. Very low smoke levels were produced from 0 to 20% EGR. The smoke measurements ranged from 0.07 to 0.33 FSN. Above 20% EGR, smoke increased exponentially with EGR. At all conditions, the surrogate fuel precisely matched the smoke produced by the full-range petroleum Diesel fuel. At 30% EGR, the target Diesel and surrogate fuel smoke numbers were 3.32 and 3.20 FSN, respectively.

Earlier in this chapter, Figure 6-6 demonstrated that combustion phasing may influence the premixed and diffusion combustion regions. Thus, depending on the engine conditions, it is conceivable that combustion phasing may affect smoke emissions. Figure 6-26 shows results from the combustion phasing sweeps. For 15% and 25% EGR, combustion phasing did not affect exhaust smoke. However, at 30% EGR retarding the combustion phasing from CA50=9 to CA50=15 degrees aTDC reduced smoke from 3.32 to 2.03 FSN for the target Diesel fuel. Results were similar for the surrogate fuel. Overall, the smoke emissions from the engine operating on the surrogate and target Diesel fuels had very good agreement. The largest discrepancies occurred with CA50=12 and CA50=15 degrees aTDC at 30% EGR. At these conditions the surrogate fuel smoke was 0.4 and 0.3 FSN higher than the target Diesel fuel, respectively.

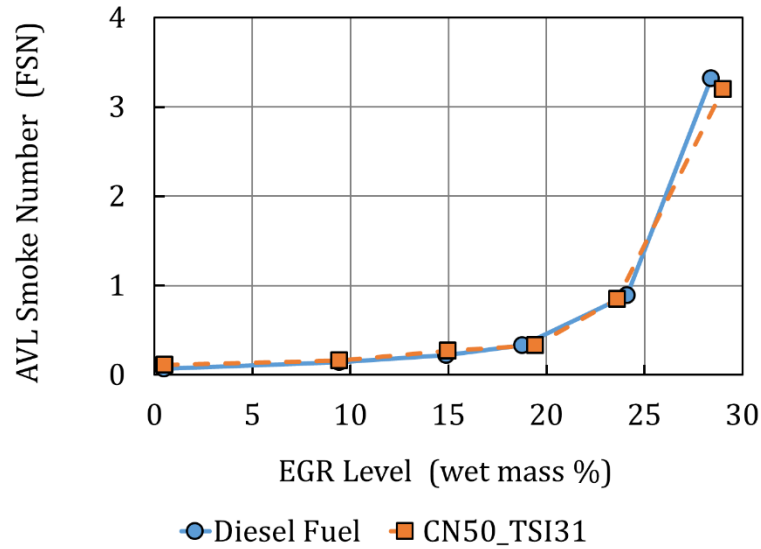


Figure 6-25: Effects of EGR on smoke at 1500x9 with the injection SOE adjusted to maintain CA50=9 degrees aTDC.

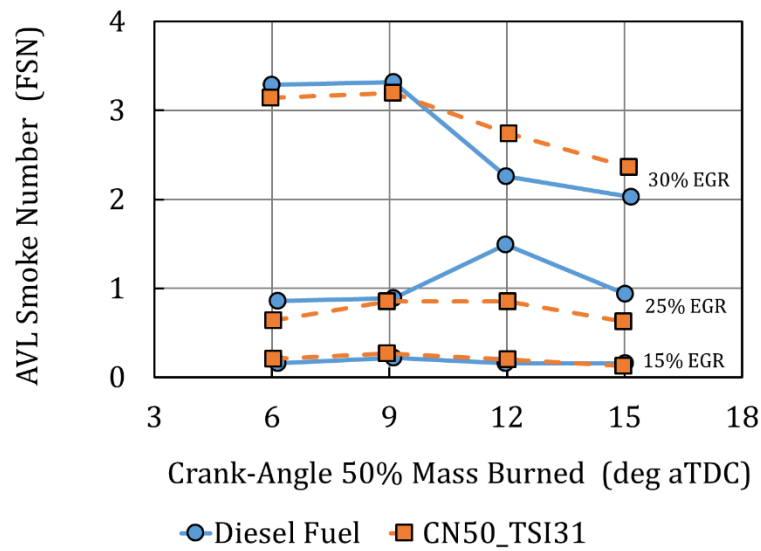


Figure 6-26: Effects of combustion phasing on smoke at 1500x9 with 15%, 25%, and 30% EGR.

Exhaust Particles

The exhaust particles were measured at each operating condition using the Cambustion DMS500 as described in Chapter 4. The particle number (N) and particle diameter (Dp) were determined by the measurements. The particle expression $dN/d\log Dp$ was plotted as a function of the particle diameter (Dp) which provided particle size distributions for analysis [6.14] [6.15]. An example is given in Figure 6-27. The data were acquired at the 1500x9 condition with 20% EGR and the combustion phasing set to CA50=9 degrees aTDC. Nucleation mode particles were considered to be volatile materials which may or may not have solid cores. At the 1500x9 condition the nucleation mode particles were at or near the detectability limit of the test apparatus. The accumulation mode particles were considered to be solid agglomerates of smaller primary carbonaceous particles [6.14] [6.15]. In Figure 6-27, Diesel fuel results are shown with a solid line and the surrogate fuel data are shown with a dashed line. The particles exhibited a bimodal distribution with the nucleation mode particles having diameters ranging from 10-30 nm and the accumulation mode particles having diameters greater than 30 nm. The count median diameter (CMD) for nucleation and accumulation particles was defined as the peak of each mode.

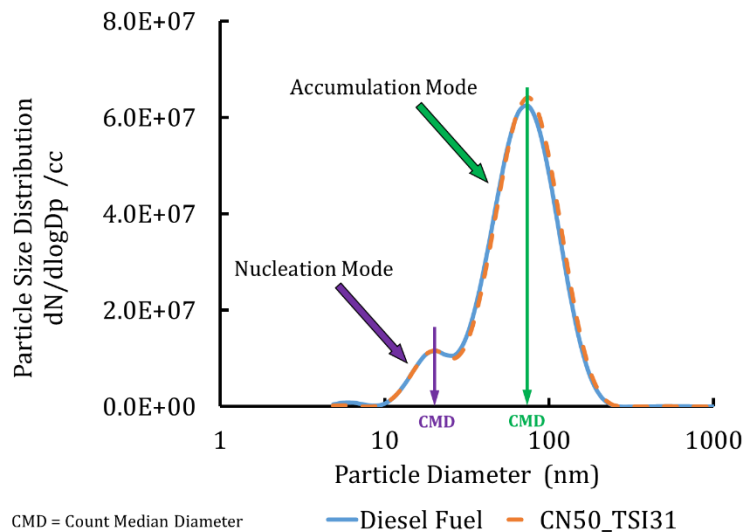


Figure 6-27: Particle size distribution for Diesel and CN50_TSI31 fuels at 1500x9 with 20% EGR and CA50=9 degrees aTDC.

An analysis of the particle size distributions from several engine tests indicated that engine conditions could greatly effect the exhaust particles. For example, Figure 6-28 shows the effect of EGR on the particle size distributions from the target Diesel fuel. In this example, the number of accumulation mode particles vastly increased with EGR. Such large changes in the particle size distributions made it difficult to comprehend the EGR effects on the nucleation and accumulation mode particles. It was also difficult to compare the fuels by overlaying results on these plots. Therefore, two statistics were applied to the nucleation and accumulation modes to describe the particle size distributions. The first statistic was the particle number concentration (N/cc) which was calculated from the integrated particle size distributions for each mode. That is to say, the nucleation and accumulation mode particles were integrated separately. The second statistic was the particle count median diameter (CMD) which was the particle diameter at the peak of each mode, as shown in Figure 6-27. The particle number concentrations and count median diameters provided quantitative statistics that effectively described the effects of EGR and CA50 on the particle size distributions and provided a clear method to compare exhaust particles from the surrogate and target Diesel fuels.

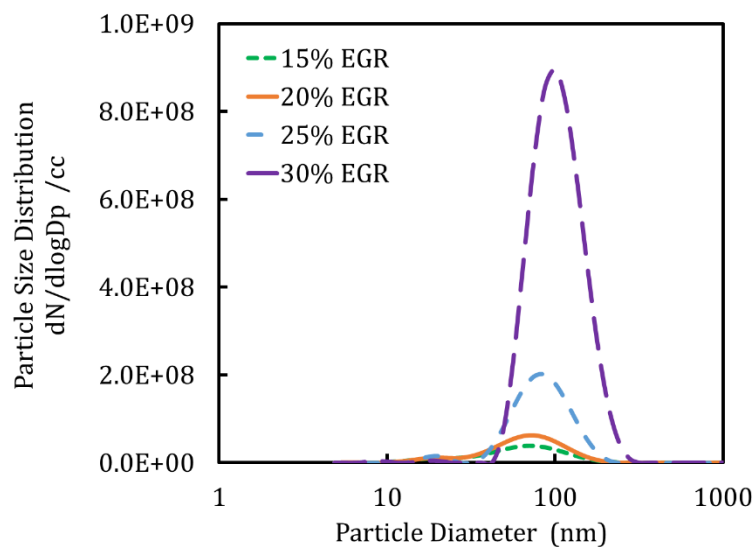


Figure 6-28: Effects of EGR on exhaust particle size distributions for the petroleum Diesel fuel at 1500x9 with CA50=9 degrees aTDC.

The effects of EGR on the particle number concentrations is given in Figure 6-29. The data were acquired at the 1500x9 condition with the combustion phasing set at CA50=9 degrees aTDC. The figure provides the nucleation and accumulation mode results for both fuels. At the 1500x9 conditions, the nucleation mode particles were very low. In several instances the DMS500 was not able to detect any nucleation mode particles. In addition, EGR did not affect the number of nucleation mode particles. Expanding the scale on Figure 6-29 would reveal that EGR had a slight impact on the number of accumulation mode particles as EGR was increased from 0 to 20%. The effect was similar to the smoke results given in Figure 6-25. At 0% EGR the accumulation mode particle number concentration was around $4.0\text{E}+06$ N/cc and increased to around $2.0\text{E}+07$ N/cc with 20% EGR. Above 20% EGR the number of accumulation mode particles increased markedly with EGR. At 30% EGR the number of accumulation mode particles were very high. For Diesel fuel the accumulation mode particle number concentration was $2.2\text{E}+08$ N/cc while the surrogate fuel was $2.9\text{E}+08$ N/cc. Recall from Figure 6-25 that the smoke number exceeded 3 FSN at this condition.

Figure 6-30 shows the results from a combustion phasing sweep at the 1500x9 condition with 15% EGR. Again, the nucleation mode particles were at or near the detection limit and the results were inconclusive. The accumulation mode particle number concentrations averaged $1.3\text{E}+07$ N/cc and were not affected by combustion phasing or the fuels.

The particle count median diameter (CMD) results from the EGR sweeps are presented in Figure 6-31. The nucleation mode CMD was not influenced by EGR and remained constant at about 27 nm. From 0 to 20% EGR the accumulation mode CMD was reasonably constant and averaged about 80 nm. Above 20% EGR the CMD increased linearly with EGR. At 30% EGR the accumulation mode CMD had increased to about 120 nm.

Count median diameter results from the combustion phasing sweep are given in Figure 6-32. At the 1500x9 condition with 15% EGR combustion phasing or fuel type did not influence the nucleation or accumulation particle CMD. The accumulation mode particles had an average CMD of 82 nm while the nucleation mode particles averaged 27 nm.

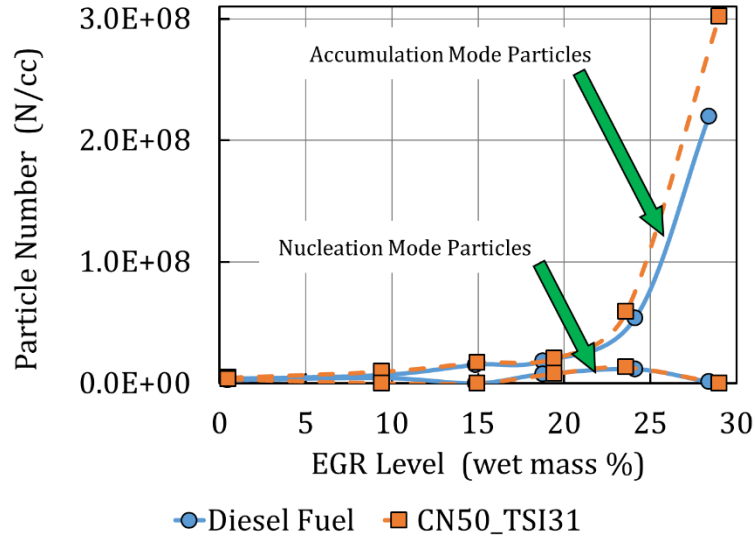


Figure 6-29: Effects of EGR on exhaust particle number concentration at 1500x9 with the injection SOE adjusted to maintain CA50=9 degrees aTDC.

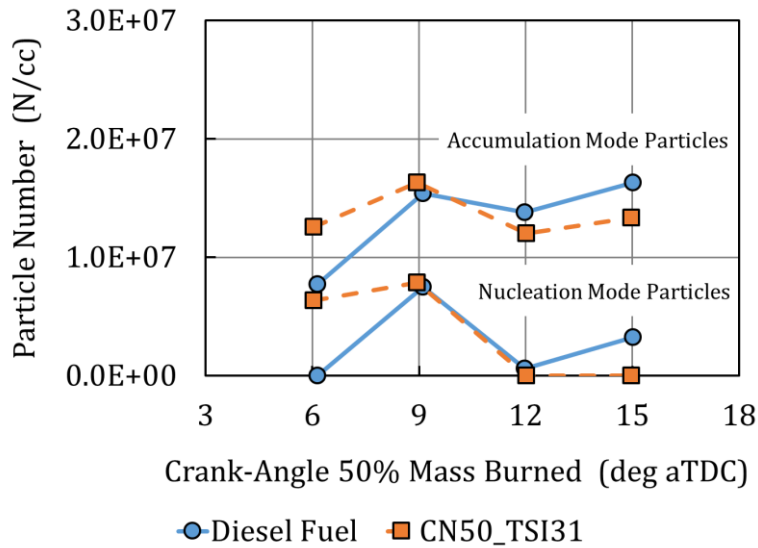


Figure 6-30: Effects of combustion phasing on particle number concentration at 1500x9 with 15% EGR.

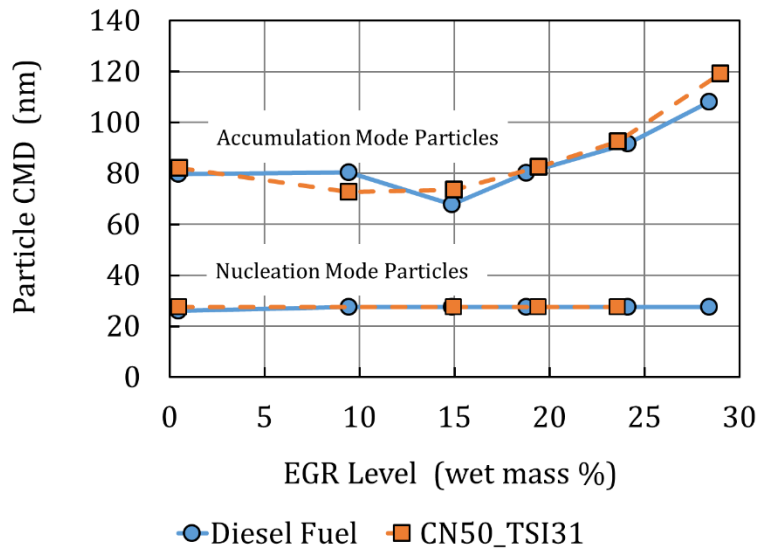


Figure 6-31: Effects of EGR on exhaust particle count mean diameter at 1500x9 with the injection SOE adjusted to maintain CA50=9 degrees aTDC.

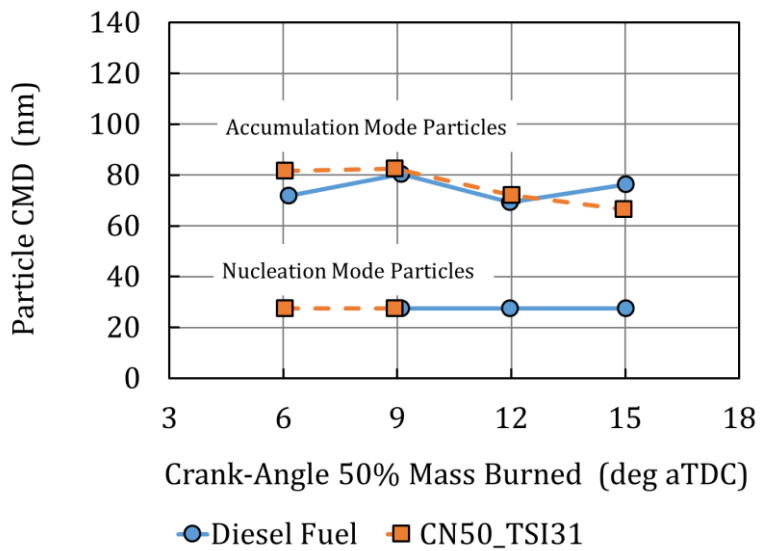


Figure 6-32: Effects of combustion phasing on exhaust particle count mean diameter at 1500x9 with 15% EGR.

The test data shown in Figure 6-29 through Figure 6-32 indicate that the particle number concentration and count median diameter produced by the target Diesel fuel were accurately reproduced when the engine was operated on the surrogate fuel. In Figure 6-29, the largest difference in particle number concentration was observed at the 30% EGR condition where the smoke measurements exceeded 3 FSN. Also, in Figure 6-31 the largest difference in CMD was observed at 30% EGR. While running the engine tests it was noted that operating at conditions with high smoke numbers increased the variability in the particle measurements. At the 25% EGR condition (smoke ~ 0.9 FSN) the target Diesel and surrogate fuels had much better agreement. The Diesel fuel had a particle number concentration of $5.2E+07$ N/cc and the surrogate fuel had a number concentration of $5.9E+07$ N/cc. Also at 25% EGR the agreement was much better for the accumulation mode CMD. The Diesel fuel had an accumulation mode particle CMD of 91.6 nm and the surrogate fuel was 92.5 nm.

The engine test results at the 1500x9 condition showed the exhaust smoke, particle number concentration and particle CMD for the target Diesel fuel and surrogate CN50_TSI31 were in very good agreement. This is a very important finding that suggests the smoke point can be used as a constraint to formulate relatively simple multi-component surrogate fuels that will match the exhaust smoke and particles from very complex full-range petroleum Diesel fuels.

6.6. Discussion

As noted in Chapter 2, the individual hydrocarbon compounds in full-range petroleum Diesel fuel are numerous and very complex. Yet the test results showed that a relatively simple four-component surrogate fuel accurately reproduced the combustion and gaseous emissions results from engine tests with a full-range petroleum Diesel fuel. In fact, the exhaust soot and particle size distributions were also reproduced by the surrogate fuel. These results are intriguing since the target Diesel fuel does not contain any of the four hydrocarbon compounds contained in the surrogate fuel. This section explores a hypothesis that was developed to explain the experimental observations from Chapters 5 and 6.

In previous work, Kee et al. demonstrated that during the ignition delay time fuel is rapidly dehydrogenated and decomposed to form low boiling point unsaturated hydrocarbons such as acetylene (C_2H_2), ethylene (C_2H_4), and propene (C_3H_6) [6.27]. Other researchers have employed shock tubes and other devices to study the dehydrogenation, pyrolysis and oxidation of hydrocarbon fuels [6.28] [6.29] [6.30] [6.31] [6.32] [6.33]. In general, researchers have reported the initial formation of low-boiling point hydrocarbons followed by the formation of benzene rings. The hydrocarbon compounds in the fuel, such as aromatic content, influences the decomposition and subsequent formation of unsaturated, light hydrocarbons.

With this understanding, the following hypothesis was developed to explain why the two fuels composed of completely different hydrocarbon compounds resulted in essentially the same Diesel engine combustion, gaseous emissions, exhaust soot and particle distributions at the 1500x9 engine operating conditions.

Hypothesis: The mechanisms governing combustion and emissions are largely dependent on temperature, pressure, oxygen, and hydrocarbon chemistry. The closely-controlled engine conditions provided the same in-cylinder temperature, pressure, oxygen and carbon dioxide for both fuels. During the low-temperature and high-temperature combustion regions, the surrogate fuel decomposed to form the same effective unsaturated, light hydrocarbon chemistry as the target Diesel fuel. As a result, the engine

combustion, gaseous emissions, exhaust soot and particle emissions were essentially the same for both fuels.

This hypothesis was explored by investigating the low-temperature fuel decomposition and unsaturated, light hydrocarbon formation for two surrogate fuels with the same physical and chemical properties but containing different hydrocarbon compounds.

As discussed in Chapter 5, a seven-component surrogate was formulated with the Surrogate Blend Optimizer to match the target Diesel fuel properties. The four-component surrogate CN50_TSI31 and the seven-component surrogate both have 50 cetane number and 31 TSI. The heating value, density, viscosity, molar H/C and distillation temperatures are in very close agreement. The properties and formulations of the seven-component and four-component surrogate fuels are given in Table 6-2. The seven-component surrogate contains one additional cycloalkane, methylcyclohexane, and two additional aromatics, 1,2,4-trimethylbenzene and n-propylbenzene. The additional aromatics have 1 benzene ring whereas 1-methylnaphthalene has 2 benzene rings. Table 6-2 shows the two surrogate fuels have the same global fuel properties but consist of different hydrocarbon compounds.

The low-temperature fuel decomposition for the surrogates were investigated using closed-homogeneous reactor simulations. The reactor setup was described in Chapter 4. For brevity, results are shown for the following initial reactor conditions: Temperature = 1000 °C, Pressure = 50 bar, and Equivalence Ratio=1.0. Acetylene and benzene formation were selected to show the formation of small, unsaturated hydrocarbons that are thought to be the initial constituents of primary soot particles.

Table 6-2: Properties and components of a seven-component and four-component surrogate fuels with 50 cetane number and 31 TSI.

Fuel Property	Units	Seven-Component Surrogate	Four-Component Surrogate
Cetane Number		50.0	49.87
Threshold Soot Index		30.1	31.5
Lower Heating Value	MJ/kg	43.774	43.81
Density @ 15 °C	g/ml	0.817	0.821
Kinematic Viscosity @ 25 °C	cSt	3.38	3.64
Molar H/C	M/M	1.861	1.872
Distillation Temperature T ₁₀	°C	211	229
Distillation Temperature T ₅₀	°C	249	250
Distillation Temperature T ₉₀	°C	279	278
Fuel Component	Units	Seven-Component Surrogate	Four-Component Surrogate
n-Hexadecane	M/M	0.28	0.285
Heptamethylnonane	M/M	0.21	0.261
Decahydronaphthalene	M/M	0.21	0.263
Methylcyclohexane	M/M	0.03	0.0
1-Methylnaphthalene	M/M	0.12	0.191
1,2,4-Trimethylbenzene	M/M	0.13	0.0
n-Propylbenzene	M/M	0.02	0.0

Figure 6-33 shows the simulation results for the four-component surrogate fuel. At the given reactor conditions, fuel decomposition started at 0.00004 seconds which coincided with acetylene formation. As the fuel components decomposed the acetylene concentration steadily increased. The aromatic component, 1-methylnaphthalene, had the slowest initial decomposition then rapidly decomposed prior to ignition. All of the fuel components were completely decomposed prior to ignition which corresponded with a spike

in the acetylene concentration. The high-temperature combustion was very rapid and consumed all of the acetylene.

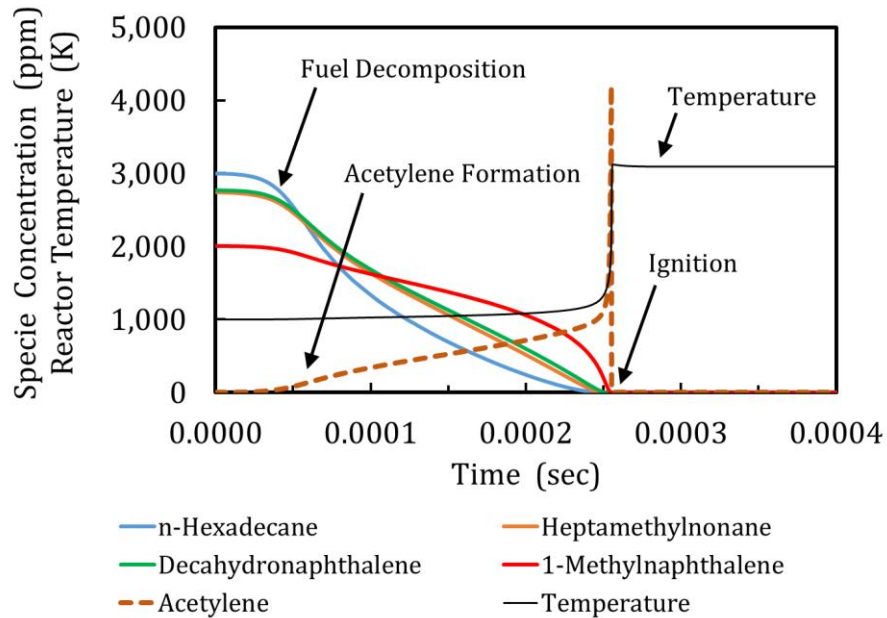


Figure 6-33: Closed-homogenous reactor simulation showing the formation of acetylene during the ignition delay period from a four-component surrogate fuel. All fuel components are completely decomposed prior to ignition. Temperature = 1000 °C, Pressure = 50 bar, and Equivalence Ratio=1.0

The reactor simulation results for the seven-component surrogate are shown in Figure 6-34. Overall, the fuel decomposition and acetylene formation followed the trends for the four-component surrogate. The 1-ring aromatic compounds 1,2,4-trimethylbenzene and n-propylbenzene mimicked the slow-start, fast-finish decomposition characteristics of the 2-ring aromatic 1-methylnaphthalene. All of the fuel components were completely decomposed prior to ignition. The ignition delay for the seven-component surrogate was 0.00006 seconds (0.06 ms) longer than the four-component surrogate (a relatively insignificant difference).

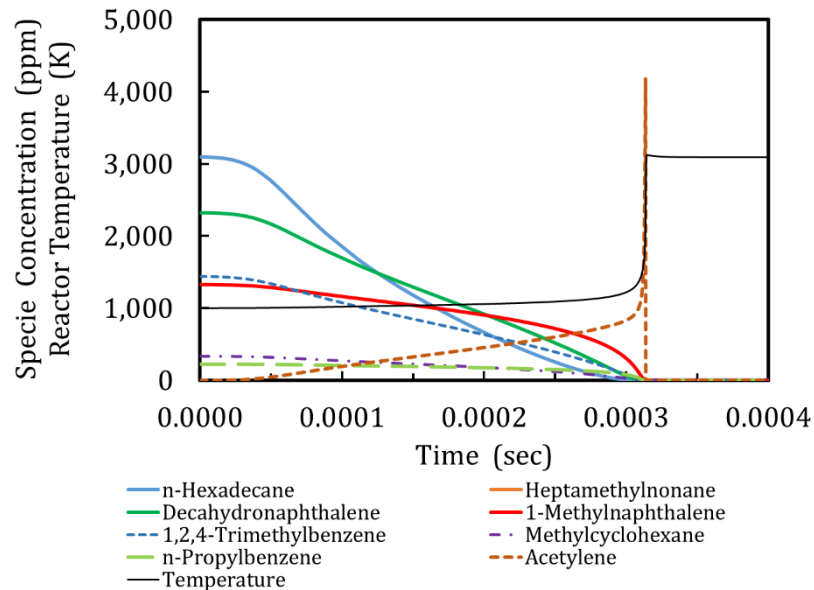


Figure 6-34: Closed-homogenous reactor simulation showing the formation of acetylene during the ignition delay period from a seven-component surrogate fuel. All fuel components are completely decomposed prior to ignition. Temperature = 1000 °C, Pressure = 50 bar, and Equivalence Ratio=1.0.

Figure 6-35 shows the low-temperature acetylene formation for the surrogate fuels. Acetylene production began at the same time for both fuels, presumably from the more reactive fuel components n-hexadecane and decahydronaphthalene. The slightly longer ignition delay of the seven-component surrogate lowered the rate of acetylene production. However, upon decomposition of the fuels and at the onset of ignition, the four-component and seven-component surrogates essentially had the same acetylene concentration of approximately 1000 ppm. During the high temperature combustion, the peak acetylene concentrations from both surrogates were basically the same and reached approximately 4100 ppm.

The simulation results for benzene formation are shown in Figure 6-36. During the ignition delay period, the low-temperature reactions formed benzene which increased exponentially until ignition. Again, the longer ignition delay of the seven-component fuel lowered the rate of benzene

production. However, at the onset of ignition the peak benzene for both surrogates were essentially the same and reached approximately 430 ppm.

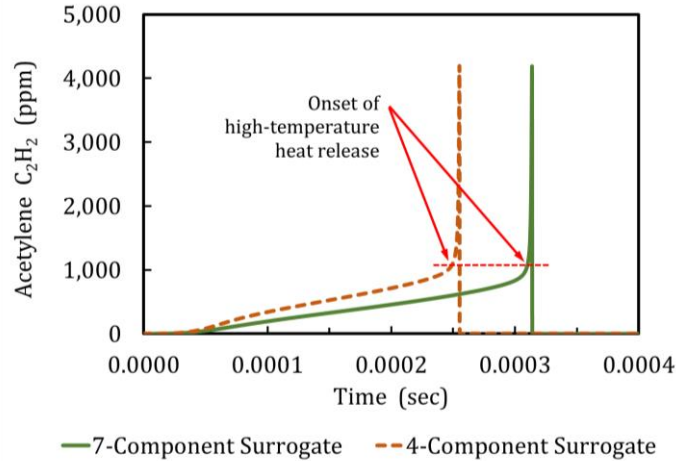


Figure 6-35: Acetylene formed during the ignition delay period for a seven-component and a four-component surrogate both with 50 cetane number and 31 TSI. Temperature = 1000 °C, Pressure = 50 bar, and Equivalence Ratio=1.0.

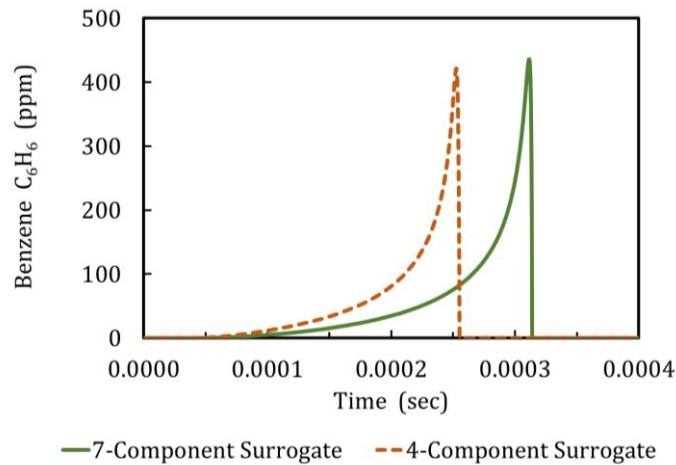


Figure 6-36: Benzene formed during the ignition delay period for a seven-component and a four-component surrogate both with 50 cetane number and 31 TSI. Temperature = 1000 °C, Pressure = 50 bar, and Equivalence Ratio=1.0.

The closed-homogenous reactor simulations suggest that low-temperature kinetics of fuels with the same global properties (cetane number, TSI, density, heating value) but consisting of different hydrocarbon compounds may provide the same effective pool of light, unsaturated hydrocarbons prior to ignition.

The following narrative is provided to explain the why the engine test results with the surrogate fuel closely agreed with the target Diesel fuel:

- Well-matched engine operating conditions provided effectively the same in-cylinder conditions at the time of fuel injection (pressure, temperature, density, oxygen, carbon dioxide and mixture motion).
- Well-matched fuel physical properties resulted in sprays, fuel and vapor distributions, and local equivalence ratios that were effectively the same for both fuels.
- Well-matched fuel combustion and chemical properties resulted in ignition delay times and low-temperature kinetics that decomposed the fuels and formed the same effective pool of unsaturated, light hydrocarbons such as acetylene (C_2H_2), ethylene (C_2H_4), and propene (C_3H_6). The light hydrocarbons reacted to form larger unsaturated hydrocarbons such as benzene (C_6H_6).
- Upon ignition, the target Diesel and surrogate fuels had essentially the same in-cylinder local conditions namely, temperature, pressure, oxygen, and hydrocarbon chemistry.
- During the high-temperature combustion region, the remaining fuel rapidly decomposed. The surrogate and target Diesel fuels formed the same effective pool of unsaturated, light hydrocarbons.
- With the local equivalence ratios and high-temperature hydrocarbon chemistry well-matched, the soot formation and oxidation mechanisms provided the same exhaust soot and particle distributions and the late stage CO oxidation mechanism provided the same exhaust CO for both fuels.
- With well-matched fuel cetane number, density and heating values, both fuels released the same thermal energy with the same combustion rates and phasing.

- With the in-cylinder oxygen chemistry and thermal environments well matched, the factors driving the NO_x formation mechanism were essentially the same for both fuels which resulted in the same engine NO_x emissions.

6.7. Summary

In Chapter 5 a library of surrogate Diesel fuels was developed. In particular, surrogate fuel CN50_TSI31 was formulated to closely mimic the combustion, physical and chemical properties of a full-range petroleum Diesel fuel. In this chapter, test results from a contemporary Diesel engine operating on the target Diesel and CN50_TSI31 fuels were presented. The engine was operated at a part-load condition that resulted in conventional Diesel combustion modes. The combustion process exhibited regions of low-temperature heat release, premixed, and diffusion combustion. Engine testing consisted of EGR and combustion phasing sweeps with other engine parameters such as IMEP, intake temperature, pressure, fuel injection pressure and exhaust pressure tightly controlled. The test results clearly demonstrated that the combustion, gaseous emissions, exhaust smoke and particle distributions from the target Diesel fuel were very closely matched by the four-component surrogate fuel CN50_TSI31. It was proposed that by matching key fuel physical properties (density, viscosity, surface tension, distillation curve) the surrogate fuel matched the fuel spray, vapor formation and local equivalence ratios as the target Diesel fuel. By matching key combustion and chemical properties (cetane number, TSI, density, heating value), prior to ignition the surrogate fuel decomposed to the same effective unsaturated, light hydrocarbons as the target Diesel fuel. As a result, the target Diesel and surrogate fuel provided essentially the same in-cylinder conditions at ignition. During the premixed and diffusion combustion regions, both fuels rapidly decomposed and formed the same effective light hydrocarbons. As a result, the high-temperature mechanisms that drive combustion, gaseous emissions, and exhaust smoke and particles responded to both fuels in like manner. Thus, the target Diesel and surrogate fuels resulted in essentially the same engine combustion, gaseous emissions, exhaust smoke and particles.

6.8. References

- [6.1] Benajes, J., López, J., Novella, R. and García, A., "Advanced Methodology for Improving Testing Efficiency in a Single-Cylinder Research Diesel Engine", *Experimental Techniques* 32(6):41-47, 2008, doi:10.1111/j.1747-1567.2007.00296.x.
- [6.2] Bardi, M., Payri, R., Malbec, L., Bruneaux, G., Pickett, L., Manin, J., Bazyn, T. and Genzale, C., "Engine Combustion Network: Comparison of Spray Development, Vaporization, and Combustion in Different Combustion Vessels", *Atomization and Sprays* 22(10):807-842, 2012, doi:10.1615/atomizspr.2013005837.
- [6.3] Desantes, J., Payri, R., Salvador, F. and De la Morena, J., "Influence of Cavitation Phenomenon on Primary Break-Up and Spray Behavior at Stationary Conditions", *Fuel* 89(10):3033-3041, 2010, doi:10.1016/j.fuel.2010.06.004.
- [6.4] Payri, R., Viera, J., Gopalakrishnan, V. and Szymkowicz, P., "The Effect of Nozzle Geometry over the Evaporative Spray Formation for Three Different Fuels", *Fuel* 188:645-660, 2017, doi:10.1016/j.fuel.2016.10.064.
- [6.5] Payri, R., Viera, J., Gopalakrishnan, V. and Szymkowicz, P., "The Effect of Nozzle Geometry over Internal Flow and Spray Formation for Three Different Fuels", *Fuel* 183:20-33, 2016, doi:10.1016/j.fuel.2016.06.041.
- [6.6] Desantes, J., Lopez, J., Garcia, J. and Pastor, J., "Evaporative Diesel Spray Modeling", *Atomization and Sprays* 17(3):193-231, 2007, doi:10.1615/atomizspr.v17.i3.10.
- [6.7] Payri, F., Payri, R., Salvador, F. and Gimeno, J., "Influence of Nozzle Geometry on Spray Characteristics in Non-evaporative and Evaporative Conditions", *SAE Technical Paper Series*, 2007, doi:10.4271/2007-24-0023.
- [6.8] Heywood, J., "Internal combustion engine fundamentals", 1st ed., McGraw-Hill, New York, 2000.

- [6.9] Warnatz, J., Maas, U. and Dibble, R., "Combustion", 1st ed., Springer, Berlin, 2006.
- [6.10] Stiesch, G., "Modeling Engine Spray and Combustion Processes", Springer, Berlin, 2016.
- [6.11] Kamimoto, T. and Bae, M., "High Combustion Temperature for the Reduction of Particulate in Diesel Engines", *SAE Technical Paper Series*, 1988, doi:10.4271/880423.
- [6.12] Akihama, K., Takatori, Y., Inagaki, K., Sasaki, S. and Dean, A., "Mechanism of the Smokeless Rich Diesel Combustion by Reducing Temperature", *SAE Technical Paper Series*, 2001, doi:10.4271/2001-01-0655.
- [6.13] Kitamura, T., Ito, T., Senda, J. and Fujimoto, H., "Mechanism of Smokeless Diesel Combustion with Oxygenated Fuels based on the Dependence of the Equivalence Ratio and Temperature on Soot Particle Formation", *International Journal of Engine Research* 3(4):223-248, 2002, doi:10.1243/146808702762230923.
- [6.14] Merkisz, J. and Pielecha, J., "Nanoparticle Emissions from Combustion Engines", 1st ed., Springer, New York, 2015.
- [6.15] Eastwood, P., "Particulate Emissions from Motor Vehicles", Wiley, Chichester, 2008.
- [6.16] Szymkowicz, P., French, D. and Crellin, C., "Effects of Advanced Fuels on the Particulate and NO_x Emissions from an Optimized Light-Duty CIDI Engine", *SAE Technical Paper Series*, 2001, doi:10.4271/2001-01-0148.
- [6.17] Payri, F., Benajes, J., Arrègle, J. and Riesco, J., "Combustion and Exhaust Emissions in a Heavy-Duty Diesel Engine with Increased Premixed Combustion Phase by Means of Injection Retarding", *Oil & Gas Science and Technology* 61(2):247-258, 2006, doi:10.2516/ogst:2006018x.

- [6.18] Payri, F., Benajes, J., Molina, S. and Riesco, J., "Reduction of Pollutant Emissions in a HD Diesel Engine by Adjustment of Injection Parameters, Boost Pressure and EGR", *SAE Technical Paper Series*, 2003, doi:10.4271/2003-01-0343.
- [6.19] Desantes, J., Luján, J., Pla, B. and Soler, J., "On the combination of high-pressure and low-pressure exhaust gas recirculation loops for improved fuel economy and reduced emissions in high-speed direct-injection engines", *International Journal of Engine Research* 14(1):3-11, 2013, doi:10.1177/1468087412437623.
- [6.20] Henein, N. and Patterson, D., "Emissions from Combustion Engines and Their Control", 1st ed., Ann Arbor Science Publishers, 1972.
- [6.21] Miles, P., "Sources and Mitigation of CO and UHC Emissions in Low-Temperature Diesel Combustion Regimes: Insights Obtained via Homogeneous Reactor Modeling", *13th Diesel Engine-Efficiency and Emissions Research (DEER) Conference*, US DOE, 2007. http://www1.eere.energy.gov/vehiclesandfuels/pdfs/deer_2007/session8/deer07_miles.pdf
- [6.22] Harkins, J. and Goodwine, J., "Oxides of Nitrogen in Diesel Exhaust", *Journal of the Air Pollution Control Association* 14(1):34-38, 1964, doi:10.1080/00022470.1964.10468238.
- [6.23] Pipho, M., Kittelson, D. and Zarling, D., "NO₂ Formation in a Diesel Engine", *SAE Technical Paper Series*, 1991, doi:10.4271/910231.
- [6.24] Morin, J., Bion, A. and Dionnet, F., "Diesel exhaust oxidant potential assessed by the NO₂/NO concentration ratio, may be a major trigger of Diesel engine emission biological impact to rat lung tissue", Air Resource Board of California - Diesel Nitrogen Dioxide Working Group, 2004.
- [6.25] Alkidas, A., "On the Premixed Combustion in a Direct-Injection Diesel Engine", *ASME Energy-Sources and Technology Conference and Exhibition*, ASME Paper 86-ICF-4, 1986.

- [6.26] Dec, J., "A Conceptual Model of DI Diesel Combustion Based on Laser-Sheet Imaging*", *SAE Technical Paper Series*, 1997, doi:10.4271/970873.
- [6.27] Kee, S., Mohammadi, A., Kidoguchi, Y. and Miwa, K., "Effects of Aromatic Hydrocarbons on Fuel Decomposition and Oxidation Processes in Diesel Combustion", *SAE Technical Paper Series*, 2005, doi:10.4271/2005-01-2086.
- [6.28] Hidaka, Y., Nishimori, T., Sato, K., Henmi, Y., Okuda, R., Inami, K. and Higashihara, T., "Shock-Tube and Modeling Study of Ethylene Pyrolysis and Oxidation", *Combustion and Flame* 117(4):755-776, 1999, doi:10.1016/s0010-2180(98)00128-x.
- [6.29] Hidaka, Y., Sato, K., Hoshikawa, H., Nishimori, T., Takahashi, R., Tanaka, H., Inami, K. and Ito, N., "Shock-Tube and Modeling Study of Ethane Pyrolysis and Oxidation", *Combustion and Flame* 120(3):245-264, 2000, doi:10.1016/s0010-2180(99)00102-9.
- [6.30] McEnally, C., Ciuparu, D. and Pfefferle, L., "Experimental Study of Fuel Decomposition and Hydrocarbon Growth Processes for Practical Fuel Components: Heptanes", *Combustion and Flame* 134(4):339-353, 2003, doi:10.1016/s0010-2180(03)00113-5.
- [6.31] McEnally, C. and Pfefferle, L., "Experimental Study of Fuel Decomposition and Hydrocarbon Growth Processes for Cyclohexane and Related Compounds in Nonpremixed Flames", *Combustion and Flame* 136(1-2):155-167, 2004, doi:10.1016/j.combustflame.2003.09.012.
- [6.32] Tosaka, S., "The Characteristics of Chemical Reaction of Diesel Fuel", *JSAE Review* 21(4):463-468, 2000, doi:10.1016/s0389-4304(00)00065-5.

- [6.33] Lea-Langton, A., Andrews, G., Bartle, K., Jones, J. and Williams, A., "Combustion and Pyrolysis Reactions of Alkylated Polycyclic Aromatic Compounds: The Decomposition of ¹³C Methylarenes in Relation to Diesel Engine Emissions", *Fuel* 158:719-724, 2015, doi:10.1016/j.fuel.2015.05.043.

7. PCCI and LTC Combustion

Contents

7.	PCCI and LTC Combustion	189
7.1.	Introduction.....	191
7.2.	Engine Operating Conditions.....	193
7.3.	Combustion Analysis.....	195
7.4.	Gaseous Emissions.....	214
7.5.	Smoke and Particle Emissions	219
7.6.	Summary	226
7.7.	References	227

7.1. Introduction

Chapter 6 demonstrated that under conventional Diesel combustion conditions the surrogate fuel CN50_TSI31 closely matched the combustion and emissions from engine test results with the petroleum Diesel fuel. The goal of this chapter was to experimentally investigate the surrogate and petroleum fuels under Premixed Charge Compression Ignition (PCCI) and Low Temperature Combustion (LTC) conditions. Figure 7-1 illustrates these combustion concepts on a plot of local equivalence ratio versus local combustion temperature [7.1].

PCCI combustion avoids the soot formation region by achieving fuel-air mixtures with local equivalence ratios that are generally less than 2. This is also known as smoke-free combustion. Figure 7-2 shows a typical PCCI heat-release rate illustrating fuel evaporation, LTHR, and the premixed combustion region. The diffusion combustion region is essentially absent under PCCI conditions thereby eliminating the primary source of soot formation. Depending on the engine operating conditions, PCCI combustion can occur at temperatures that extend into the NO_x formation region.

LTC avoids the soot and NO_x formation regions by achieving local combustion at low temperatures. This is generally accomplished through charge dilution with high EGR levels. In general, LTC also has longer ignition delays with sufficient fuel-air mixing that results in PCCI combustion. Therefore, the diffusion combustion region is also avoided with LTC.

Researchers have demonstrated the low NO_x and low soot advantages of several LTC strategies. However, investigators also recognized the penalties associated with LTC including significantly increased CO and HC emissions due to incomplete combustion [7.2] [7.3] [7.4] [7.5] [7.6]. More recently, researchers have shown that LTC also effects the nucleation particle emissions [7.7] [7.8] [7.9] [7.10] [7.11] [7.12]. Indeed, the combustion and emissions differences between conventional Diesel combustion and LTC are significant. Therefore, this thesis utilized the substantially different aspects of PCCI and LTC to evaluate the surrogate fuel.

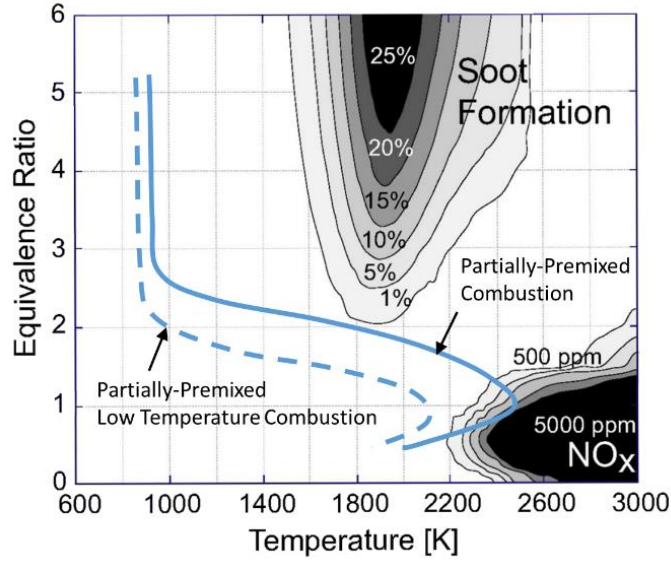


Figure 7-1: PCCI and Low Temperature Combustion strategies conceptually displayed on a chart of local fuel-equivalence ratio versus local combustion temperature. Figure adapted from Figure 7-1.

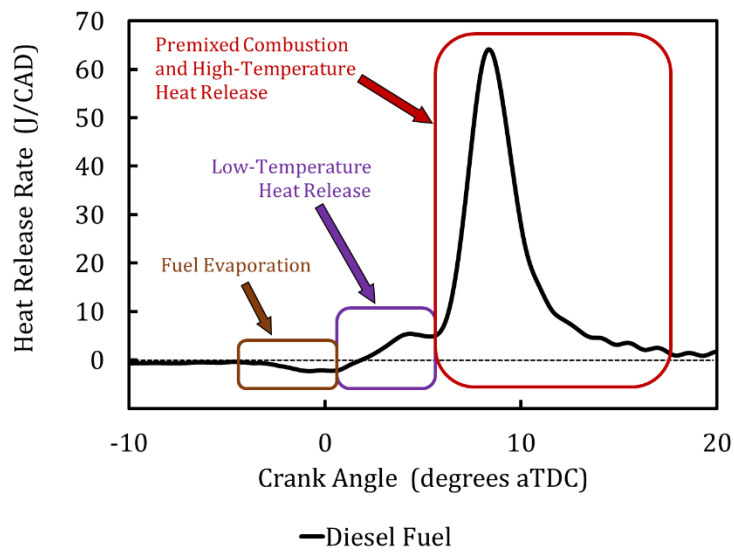


Figure 7-2: Heat release characteristics for PCCI combustion.

7.2. Engine Operating Conditions

A moderate engine speed and light engine load was used to evaluate the fuels under PCCI and LTC combustion conditions. The engine speed was held at 1500 r/min and the engine load was maintained at 3 bar IMEP by adjusting the fuel injection quantity at each test point. This operating condition was known as 1500x3. The combination of moderate engine speed and relatively small quantities of injected fuel contributed to fuel-air mixing prior to ignition. Two engine calibration parameters that have significant effects on combustion and emissions from PCCI and LTC are EGR dilution and combustion phasing. Therefore, a test matrix was developed for 1500x3 that independently varied EGR and combustion phasing while holding other operating conditions constant. The EGR sweep started at 0% which achieved PCCI combustion but did not obtain LTC due to high combustion temperatures. The EGR sweep ended at 60% EGR which simultaneously achieved both PCCI and LTC combustion. At each EGR level, the combustion phasing sweep was conducted at CA50 values of 6, 9, 12 and 15 degrees aTDC by adjusting the injection start of energizing (SOE) at each test point. All tests were run with a single injection strategy, 50 °C intake temperature, and the swirl ratio maintained at 2.9. The 1500x3 operating conditions are summarized in Table 7-1. The resulting matrix contained 24 test points for each fuel.

As mentioned above, data were acquired at EGR levels of 0, 20, 40, 50, 55 and 60%. At 1500x3, EGR levels greater than 50% transitioned combustion into the LTC regime. Therefore, EGR levels greater than 50% were more closely spaced in order to better characterize combustion, emissions and particles in the LTC region. Great care was taken to ensure the engine operating conditions were precisely repeated for both the target Diesel and the surrogate fuel.

Table 7-1: Engine operating conditions to evaluate the petroleum and surrogate fuels with PCCI and LTC combustion strategies.

Operating Condition	Units	1500x3
Engine Speed	r/min	1500
Engine IMEP	bar	3
Fuel Injection Pressure	bar	550
Intake Pressure	kPaA	102
Exhaust Pressure	kPaA	106
Fuel Injection Strategy		Single
Intake Temperature	°C	50
Swirl Ratio		2.9
EGR Level	%	0, 20, 40, 50, 55, 60
CA50	degrees aTDC	6, 9, 12, 15

7.3. Combustion Analysis

At each test condition, instantaneous cylinder-pressure data and several other high-speed data channels were acquired and analyzed. In this section the following the combustion parameters were employed to characterize the PCCI and LTC combustion:

- Cylinder pressure
- Apparent heat release rate
- Low-Temperature Heat Release (LTHR)
- Fuel Injector Start of Energizing (SOE)
- Ignition delay
- Mixing advance time
- Peak heat release rate
- Peak bulk gas temperature
- 10-90% burn duration

PCCI smokeless combustion was achieved at all of the 1500x3 test conditions. The low engine speed coupled with a small fuel injected quantity and relatively low in-cylinder pressure and temperature provided sufficient mixing time for combustion to occur at local equivalence ratios that avoided the soot formation region shown in Figure 7-1. Exhaust soot could not be detected with the AVL Smoke Meter or the AVL Opacimeter. Exhaust particles were detected and characterized with the DMS500 particle sizer.

Low Temperature Combustion was achieved at EGR levels equal to or greater than 50%. At these high EGR levels, the NO_x emissions were very low which indicated that the local combustion temperatures avoided the NO_x formation region shown in Figure 7-1.

The combustion analysis began by studying the cylinder pressure measurements and the resulting heat release profiles at 1500x3 with 0% EGR and a maximum of 60% EGR. For both tests the combustion phasing was set at CA₅₀=9 degrees aTDC which was the optimal combustion phasing for efficiency. Cylinder pressure is shown in Figure 7-3 and apparent heat release rate is given in Figure 7-4. (For brevity, the apparent heat release rate is referred to as heat release rate in this thesis.) The solid colored lines were data from the engine operating with the target Diesel fuel. The overlaid dashed lines were data from the surrogate fuel.

The cylinder pressure data shows significant differences between 0% EGR and 60% EGR. Early during the compression stroke, cylinder pressures were very similar for both EGR levels. Closer to TDC, the compression pressure from 60% EGR was less than 0% EGR. This discrepancy in cylinder pressure occurred between -10 degrees to 0 degrees aTDC and was believed to be the result of fuel vaporization. For 60% EGR, the injection SOE was near -15 degrees aTDC whereas the SOE was -5 degrees aTDC for 0% EGR. Compared to 0% EGR, the 60% EGR condition resulted in lower cylinder pressure rise rates and lower peak cylinder pressures during combustion. Very good agreement was observed between the target Diesel and surrogate fuels. As a result of maintaining the CA50 at 9 degrees aTDC, the crank-angle of the peak cylinder pressures for 0% and 60% EGR were in close agreement for all tests (10.2 ± 0.1 degrees aTDC). For 0% EGR, the target Diesel fuel had a peak pressure of 5,409 kPa while the surrogate peak pressure was 5,387 kPa (a difference of less than 0.5%).

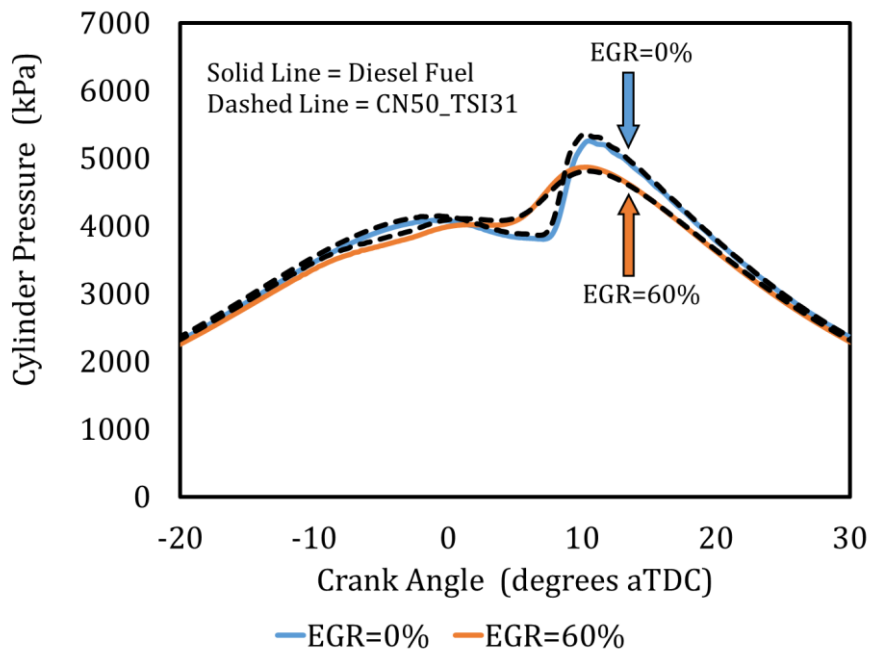


Figure 7-3: Cylinder pressure for 1500x3 with 0% EGR and with 60% EGR. Injection SOE adjusted to maintain CA50=9 degrees aTDC for all tests.

The combustion analysis continued with comparing the heat release rates, for both fuels, at 0% EGR and at 60% EGR. Again the combustion phasing was held constant with $CA_{50}=9$ degrees aTDC. The results are given in Figure 7-4.

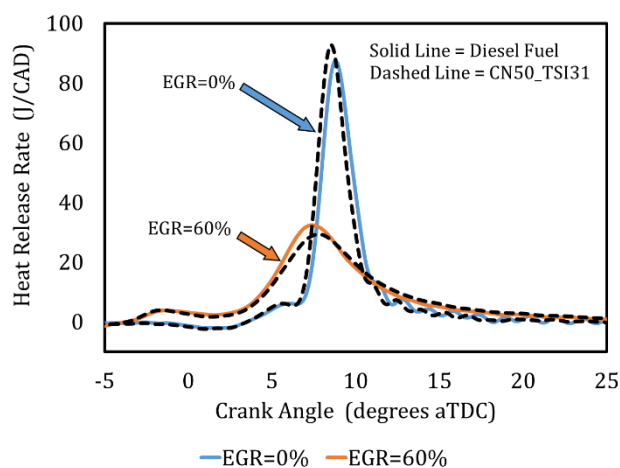


Figure 7-4: Heat release rates for 1500x3 with 0% EGR and with 60% EGR. Injection SOE adjusted to maintain $CA_{50}=9$ degrees aTDC for all tests.

First, the 0% EGR condition had a clearly defined but relatively short duration LTHR followed by very rapid premixed combustion that reached a peak heat release rate around 95 J/CAD. The overall combustion duration was also relatively short. The heat release rates from the target Diesel fuel were well-matched by the surrogate fuel. For example, at 0% EGR the peak heat release rate for the target Diesel fuel was 101.4 J/CAD while the surrogate fuel peak heat release rate was 92.7 J/CAD. Second, at 60% EGR, the LTHR was greatly extended followed by a slower, longer duration premixed combustion. The peak heat release rate for the target Diesel fuel was 32.2 J/CAD while the surrogate fuel peak heat release rate was 29.2 J/CAD. And finally, the heat release rates from the target Diesel fuel were reasonably well-matched by the surrogate fuel. The test results demonstrated that the LTHR and HTHR premixed combustion characteristics were greatly affected by the high EGR level and the advanced fuel injection SOE required to maintain CA_{50} at 9 degrees aTDC. Most importantly, the heat release rates from the surrogate fuel closely followed the target Diesel fuel.

The effects of combustion phasing on the cylinder pressure were investigated at the 1500x3 condition with 40% EGR. Figure 7-5 shows the results from both fuels as CA50 was varied from 6 degrees aTDC (advanced phasing) to 15 degrees aTDC (retarded phasing). As CA50 was retarded the ignition and peak cylinder pressure moved later into the expansion stroke which significantly reduced the peak cylinder pressure and cylinder pressure rise rate. The data shows that during the combustion phasing sweep the cylinder pressure histories for the surrogate and target Diesel fuels were in very close agreement. For the advanced combustion phasing condition where CA50=6, the target Diesel fuel had a peak pressure of 5,703 kPa compared to 5,690 kPa for the surrogate fuel; a difference of less than 0.3%. For the most retarded condition of CA50=15, the target Diesel fuel had a peak pressure of 4,046 kPa compared to 4,100 kPa for the surrogate fuel; a difference of around 1.3%.

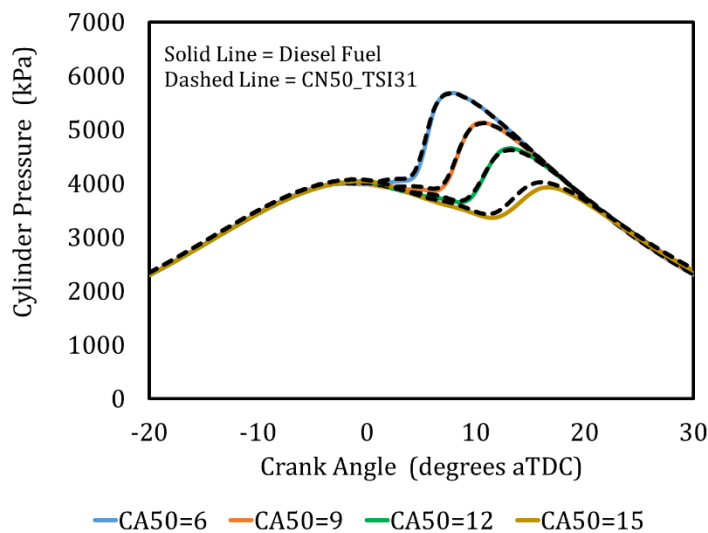


Figure 7-5: Cylinder pressure for CA50 sweeps at 1500x3 with 40% EGR.

The heat release rate data for the combustion phasing sweep are given in Figure 7-6. The results illustrate that as the CA50 was retarded from 6 to 15 degrees aTDC, the duration of the LTHR was extended, ignition moved further into the expansion stroke, the peak heat release rate was reduced and moved further into the expansion stroke and the overall combustion duration was increased. In particular, the peak heat release rates were reduced by more than 50%. Throughout the combustion phasing sweep, the target Diesel fuel tended to have slightly higher peak heat release rates. In

general, the surrogate fuel replicated the heat release rates from the target Diesel fuel.

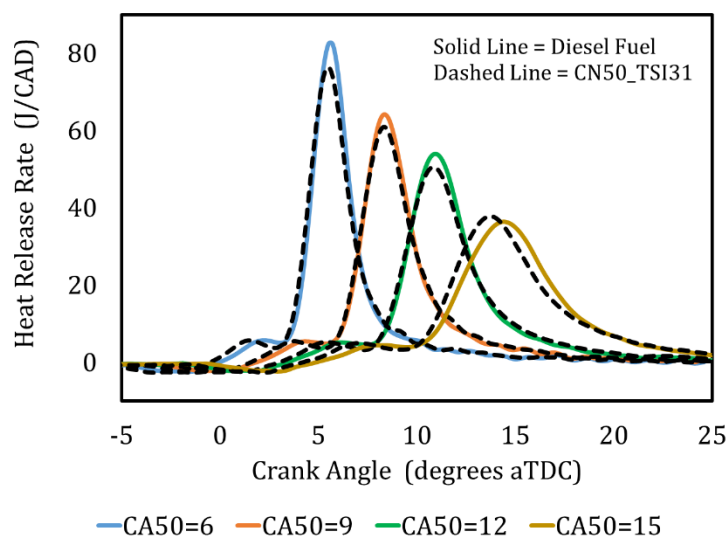


Figure 7-6: Heat release rates for CA50 sweeps at 1500x3 with 40% EGR.

The above investigation examined the cylinder pressure and heat release rates as the EGR and combustion phasing were varied. The respective impact on the heat release was clearly shown and good agreement between the surrogate and target Diesel fuels was obtained. In the following sections, the combustion analysis was expanded by examining the impact of EGR on the LTHR. This was followed by examining the EGR and CA50 effects on the injection SOE, ignition delay, mixing advance time, peak heat release rate, peak bulk gas temperature and the 10-90% burn duration.

During the investigation it was determined that the body of engine test data from the 1500x3 operating condition was well described by comparing data from EGR sweeps with CA50=9 degrees aTDC. Therefore, as the EGR level was increased the injection SOE was advanced to maintain CA50. Using this methodology, the EGR sweeps show the combined effects of EGR level and injection SOE. To provide an independent evaluation of the combustion phasing effects, test results were also shown from CA50 sweeps with 40% EGR. This approach provided clear figures that compared the response of the target Diesel and surrogate fuels.

Low Temperature Heat Release (LTHR)

Heat release rates from the 1500x3 operating condition at 0% EGR and 60% EGR with CA50=9 degrees aTDC are shown in Figure 7-7. Data from the target Diesel fuel are shown with solid lines and the surrogate fuel data are shown with dashed lines. The y-axis and x-axis scales are expanded to focus on the LTHR region.

For both EGR levels, the surrogate fuel followed the evaporation characteristics of the target Diesel fuel. For the 60% EGR condition, the advanced SOE placed the fuel evaporation period between -10 and -6 degrees aTDC. Whereas, less SOE advance was required for 0% EGR which positioned the evaporation period between -2 to 2 degrees aTDC.

The data in Figure 7-7 shows the duration of the LTHR was significantly less for 0% EGR than for to 60% EGR and the characteristic profiles were also considerably different. For both EGR levels, the surrogate fuel closely followed the heat-release attributes of the target Diesel fuel.

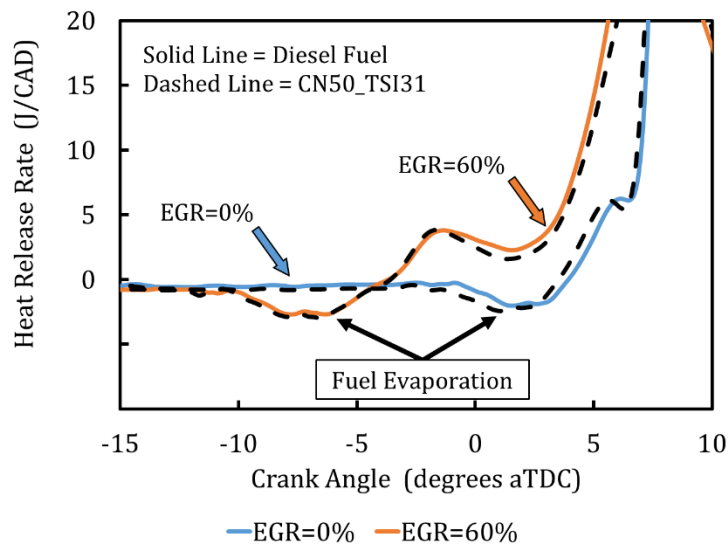


Figure 7-7: Heat release rates at 1500x3 with 0% EGR and 60% EGR. Injection SOE adjusted to maintain CA50=9 degrees aTDC. Y-axis and x-axis scaled to focus on low temperature heat release.

Two metrics were computed from the heat-release rate data to comprehend the effects of EGR and compare the surrogate and target and Diesel fuels. The first metric was the duration of the LTHR. The second metric was the total amount of heat released over the duration of the LTHR. The method used to determine the start and end of the low temperature heat release (LTHR) is illustrated in Figure 7-8 and described herein. The start of the LTHR was defined as the local minimum of the region where the fuel evaporation transitioned to LTHR. The crank-angle location for the start of LTHR was detected by measuring the slope of the heat release rate profile. LTHR started when the slope transitioned from negative, or zero, to positive values. The end of the LTHR was defined as the local minimum of the region where LTHR transitioned to the HTHR. The crank-angle location for the end of LTHR was detected by measuring the slope of the heat release rate profile. LTHR ended when the slope transitioned from negative, or zero, to positive values. The total amount of heat released during the LTHR period was calculated by summing the heat released from the start to the end of the LTHR period. Error bands for the LTHR calculations were determined by computing the difference in the LTHR with the start and end location varied by 0.2 CAD. The results were averaged and the error bands were set at 0.4 CAD for the duration and 0.5 J for the total amount of heat released.

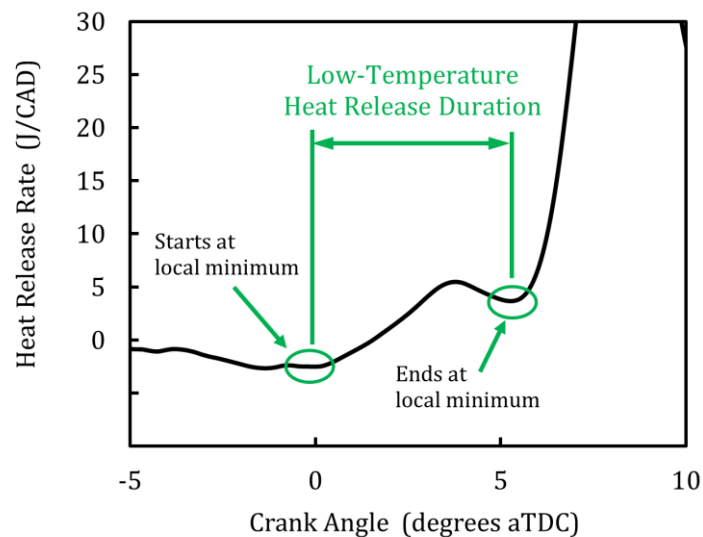


Figure 7-8: Heat release rate plot showing the method to determine the start, end and duration of the low temperature heat release.

The results in Figure 7-9 show the effects of EGR on the total amount of heat release over the LTHR period and duration of the LTHR period. As EGR was increased from 0% to 50%, the duration of the LTHR increased from about 4 CAD to 6 CAD and the total amount of heat released rose from about 9 J to around 12 J. An interesting observation is the apparent transition that occurred around 50% EGR. As EGR was increased from 50% to 60%, the total amount of heat release dropped from about 12 J to about 9 J and the duration of the LTHR increased from 6 CAD to 8 CAD. At the 1500x3 condition, EGR levels above 50% appeared to stress the LTHR. It is not clear if the observations are the result of over-mixing that stems from the increased LTHR duration, the reduction in oxygen concentration, or a combination of factors. Comparing the fuels, the data shows the surrogate fuel essentially matched the duration of LTHR from the target Diesel fuel. Good agreement between the two fuels was also obtained for the total amount of heat release over the LTHR period with the error bars overlapping at all conditions except for 60% EGR. Both fuels exhibited the apparent transition in LTHR around 50% EGR.

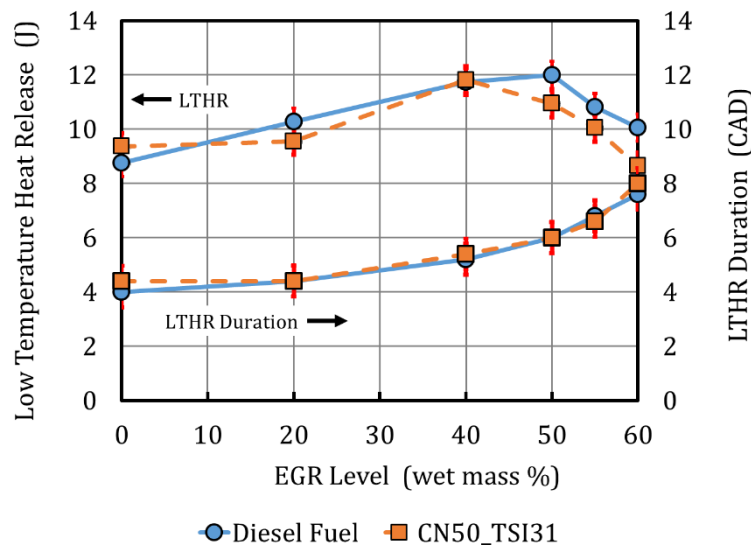


Figure 7-9: EGR effects on total amount of heat released over the LTHR period and the duration of the LTHR at 1500x3 with the injection SOE adjusted to maintain CA50=9 degrees aTDC.

Injection Start of Energizing (SOE)

Test results from the EGR and CA50 sweeps are shown in Figure 7-10 and Figure 7-11, respectively. At the start of the EGR sweep, the injection SOE advance was about -5 degrees aTDC. As EGR was increased, the SOE required more advance to maintain CA50=9 degrees aTDC. From 0% to 40% EGR the SOE required 2.5 degrees of additional advance to maintain combustion phasing. However, from 40% to 60% EGR the SOE required more than 7 degrees of additional advance to maintain CA50. Overall, the injection SOE advance for the target Diesel and surrogate fuel were in good agreement. The average difference was only 0.3 CAD and the maximum difference was 0.7 CAD.

The combustion phasing sweep was conducted at 40% EGR. Figure 7-11 shows the injection SOE advance from the target Diesel and surrogate fuel were in close agreement. Over the CA50 sweep the average difference in SOE advance was 0.4 CAD and the maximum difference was 0.5 CAD.

Throughout the EGR and CA50 sweeps, the target Diesel and surrogate fuels essentially required the same injection SOE advance to control the combustion phasing. With the SOE advance closely replicated, it was concluded that the target Diesel and surrogate fuels were injected into essentially the same in-cylinder conditions namely, temperature, pressure, density, mixture motion, and piston position. This was an important finding that would tend to eliminate the in-cylinder conditions at the time of injection as a cause for combustion or emission differences observed between the target Diesel and surrogate fuels.

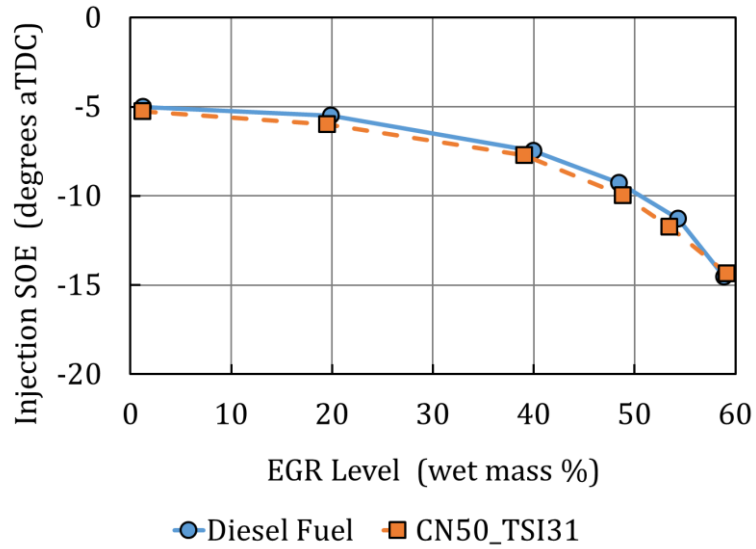


Figure 7-10: The required injection SOE to achieve $CA_{50}=9$ degrees aTDC as EGR level was increased from 0% to 60% at the 1500x3 operating condition.

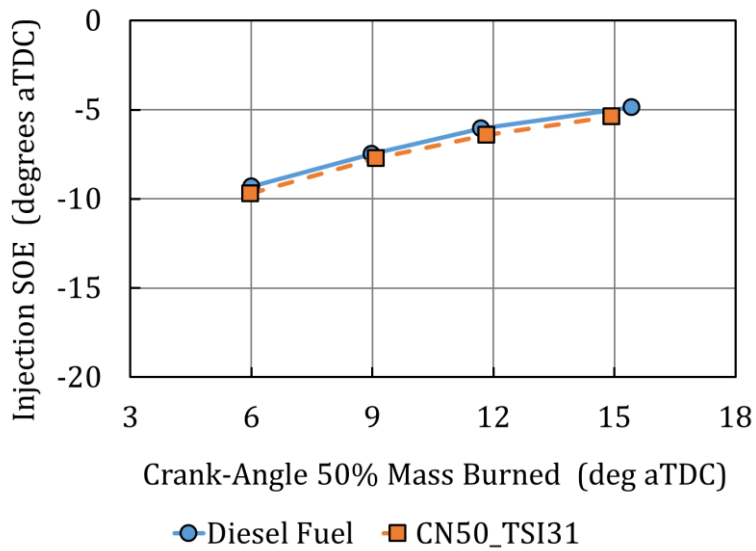


Figure 7-11: The required injection SOE to achieve $CA_{50}=6, 9, 12$ and 15 degrees aTDC at the 1500x3 operating condition with 40% EGR.

Ignition Delay

The impact of EGR on the ignition delay is shown in Figure 7-12. During the EGR sweep the combustion phasing was maintained at CA50=9 degrees aTDC. At 0% EGR the ignition delay was approximately 12 CAD and increased to almost 19 CAD at 60% EGR. The test results show the ignition delay times for the target Diesel and surrogate fuels were in good agreement. The average difference in ignition delay was only 0.2 CAD and the maximum observed difference was 0.6 CAD.

Figure 7-13 shows the effects of combustion phasing on ignition delay at 40% EGR. Retarding the CA50 from 6 to 15 degrees aTDC increased the ignition delay by approximately 2 CAD. The test data shows the target Diesel and surrogate fuels had nearly identical ignition delays. The average difference in ignition delay was only 0.07 CAD and the maximum observed difference was 0.17 CAD.

During the course of the EGR and CA50 sweeps, the target Diesel and surrogate fuels had nearly the same ignition delay times. The data shown in Figure 7-9 suggested that fuels also had very similar low-temperature heat release during the ignition delay. With the SOE advance, ignition delay time, and low-temperature heat release well-matched for both fuels, it was concluded that nearly the same in-cylinder conditions such as, temperature, pressure, density, mixture motion, and piston position were present at the onset of ignition. This was an important finding that would tend to eliminate the in-cylinder conditions at the time of ignition as a cause for combustion or emission differences observed between the target Diesel and surrogate fuels.

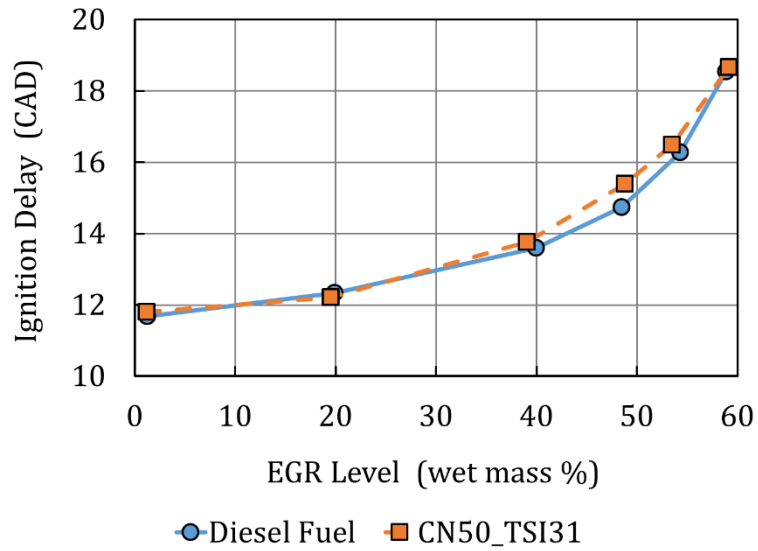


Figure 7-12: EGR effects on ignition delay at 1500x3 with the injection SOE adjusted to maintain CA50=9 degrees aTDC.

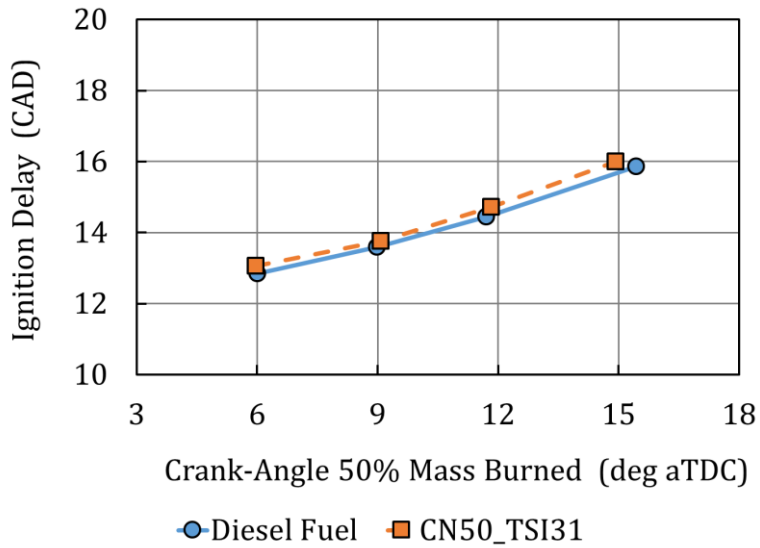


Figure 7-13: Combustion phasing effects on ignition delay at 1500x3 with 40% EGR.

Mixing Advance Time

As presented in Chapter 4, the mixing advance time was defined as the period between the end of fuel injection and the ignition or the beginning of the high-temperature heat release. The end of fuel injection was detected from the pressure measured in the high-pressure fuel line approximately 5 mm from the injector inlet. Ignition was defined as the crank angle of 5% mass fraction burned. A schematic diagram of the methodology is given in Figure 4-6.

To ensure that the target Diesel and surrogate fuels experienced the same mixture formation process, it was important to provide the same time period for spray formation, vaporization and mixing. This was accomplished by confirming the mixing advance times for both fuels were in good agreement throughout the EGR and CA50 sweeps.

The results in Figure 7-14 present the effect of EGR on the mixing advance times. At the 1500x3 condition with 0% EGR, the mixing advance time was about 3.5 crank-angle degrees (0.39 ms). As EGR increased and injection SOE was advanced to maintain CA50=9, the mixing advance time also increased. At 60% EGR the mixing advance time more than doubled to 8.4 degrees (0.93 ms). The surrogate fuel closely followed the mixing advance times from the target Diesel fuel. During the EGR sweep the average difference was 0.7 CAD and the maximum observed difference was 0.9 CAD.

The impact of combustion phasing on the mixing advance time with 40% EGR is provided in Figure 7-15. Retarding the combustion phasing increased ignition delay which correspondingly increased the mixing advance time. Retarding from CA50=6 to 15 degrees aTDC increased the mixing advance time by approximately 2 CAD. Throughout the CA50 sweep the average difference between the two fuels was 0.5 CAD and the maximum observed difference was 0.6 CAD.

The effects of EGR and combustion phasing on ignition delay corresponded to nearly identical changes in the mixing advance time. Throughout the EGR and CA50 sweeps, the injection SOE advance, ignition delay and mixing advance time data from both fuels were in good agreement. This suggests the injection, mixture preparation and low-temperature heat release processes for the surrogate fuel were nearly the same as target Diesel fuel.

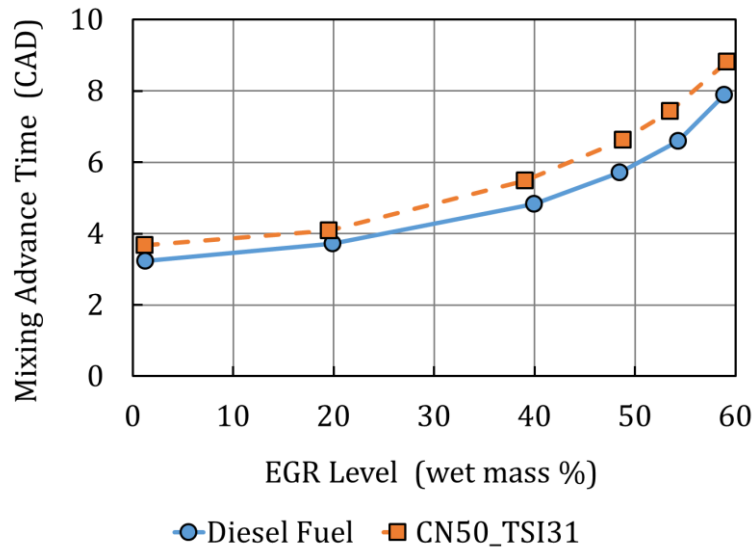


Figure 7-14: Effects of EGR on mixing advance time at 1500x3 with the injection SOE adjusted to maintain CA50=9 degrees aTDC.

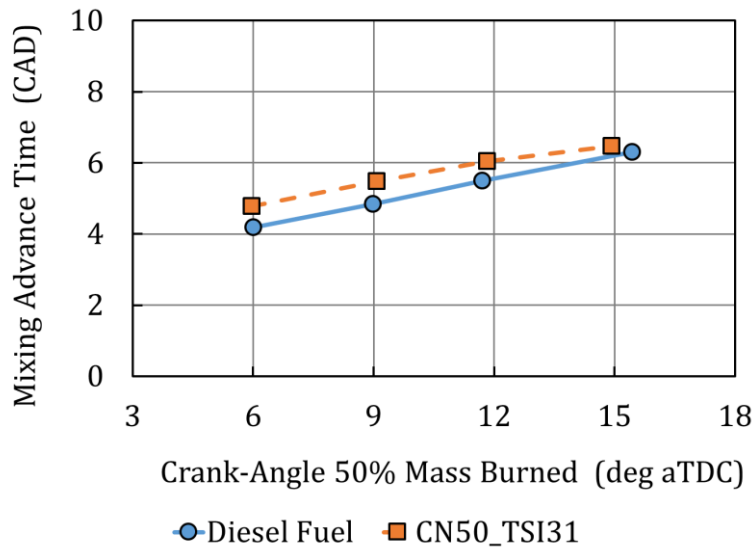


Figure 7-15: Effects of combustion phasing on mixing advance time at 1500x3 with 40% EGR.

Peak Heat Release Rate

The results in Figure 7-16 present the effect of EGR on the peak heat release rates for the target and surrogate fuels. At 0% EGR, the peak heat release rates were about 95 J/CAD. As EGR increased and injection SOE was advanced to maintain CA50=9, the peak heat release rate dropped considerably. At 60% EGR the peak heat release rate fell to about 30 J/CAD. The surrogate fuel closely followed the peak heat release rates of the target Diesel fuel. During the EGR sweep the average difference was 4 J/CAD and the maximum observed difference was 10 J/CAD.

The effects of combustion phasing on the peak heat release rate with 40% EGR is provided in Figure 7-17. Retarding from CA50=6 to 15 degrees aTDC reduced the peak heat release rate by approximately 40 J/CAD. The surrogate fuel closely followed the peak heat release rate of the target Diesel fuel. During the CA50 sweep the average difference between the two fuels was about 3 J/CAD and the maximum observed difference was about 6 J/CAD.

Peak Bulk Gas Temperature

The impact of EGR on peak bulk gas temperature is shown in Figure 7-18. During the EGR sweeps the CA50 was held constant at 9 degrees aTDC. At 0% EGR, the peak bulk gas temperature was about 1,340 K and dropped to about 1,200 K at 60% EGR. Test results from the CA50 sweep at 40% EGR are given in Figure 7-19. Retarding the combustion phasing from CA50=6 to 15 degrees aTDC lowered peak bulk gas temperatures by about 100 K. Throughout the EGR and CA50 sweeps the surrogate fuel had essentially the same peak bulk gas temperatures as the target Diesel fuel. The average difference was only 7 K and the maximum observed difference was 24 K.

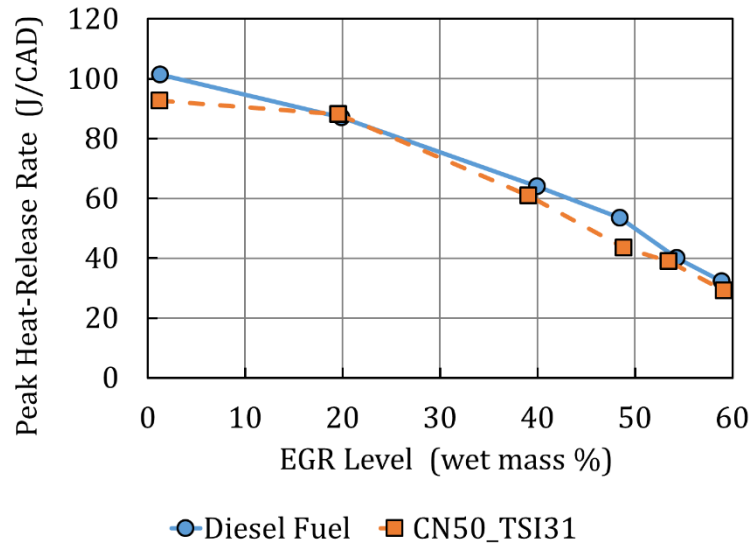


Figure 7-16: EGR effects on peak heat-release rate at 1500x3 with the injection SOE adjusted to maintain CA50=9 degrees aTDC.

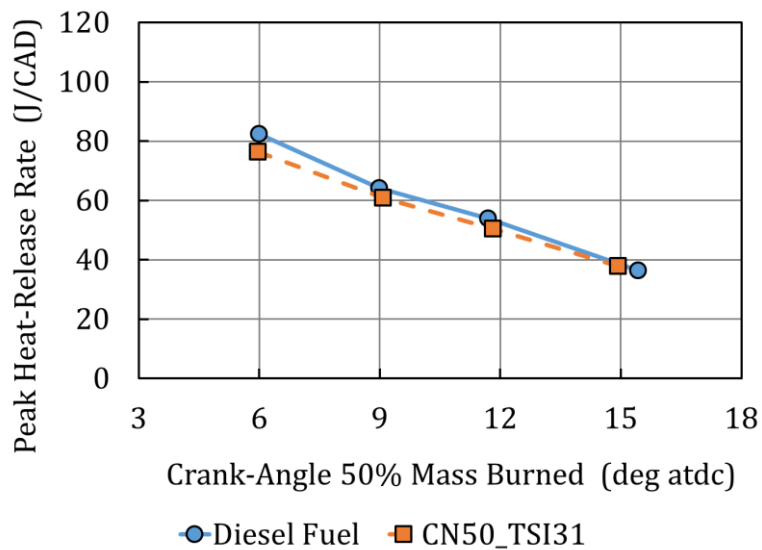


Figure 7-17: Combustion phasing effects on peak heat-release rate at 1500x3 with 40% EGR.

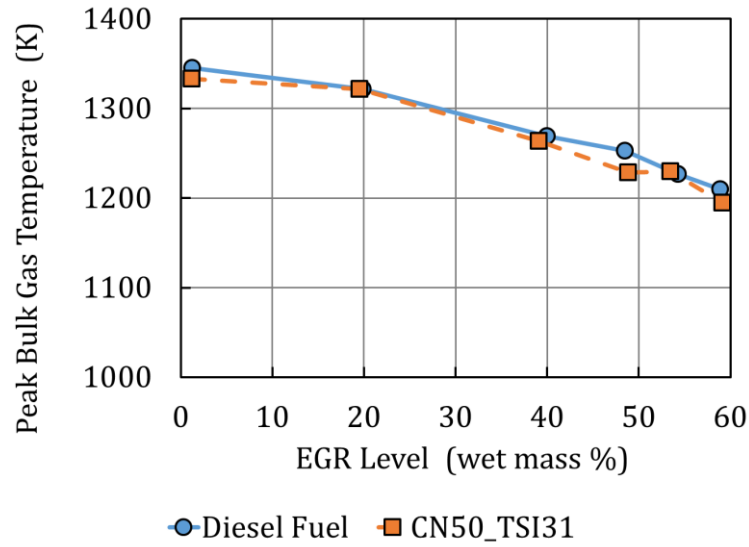


Figure 7-18: EGR effects on peak bulk gas temperature at 1500x3 with the injection SOE adjusted to maintain CA50=9 degrees aTDC.

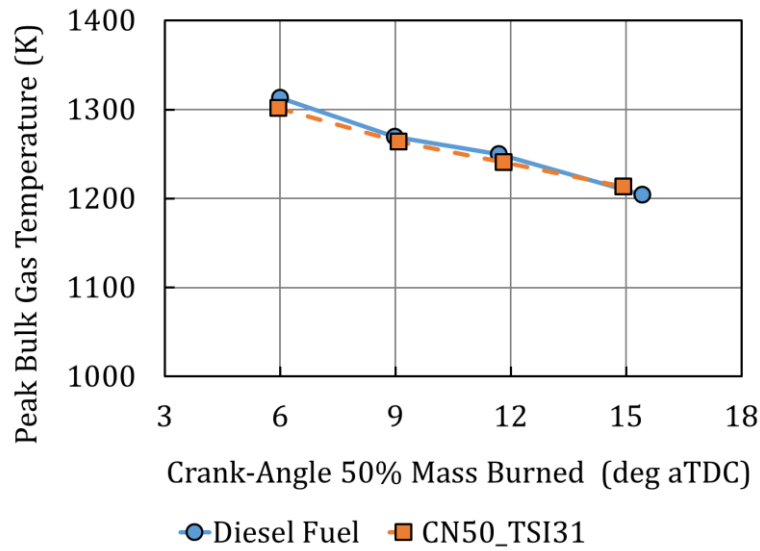


Figure 7-19: Combustion phasing effects on peak bulk gas temperature at 1500x3 with 40% EGR.

10-90% Burn Duration

Figure 7-20 presents the effects of EGR on the 10-90% burn duration. During the EGR sweep the combustion phasing was held constant at CA50=9 degrees aTDC. Increasing the EGR from 0% to 40% marginally increased the 10-90% burn duration (a total increase of about 1 CAD). As EGR was increased from 40% to 60%, the 10-90% burn duration markedly increased by about 8 CAD.

The effects of combustion phasing on the 10-90% burn duration at 40% EGR are given in Figure 7-21. As combustion phasing is retarded from CA50=6 to 15 degrees aTDC the 5 CAD.

Throughout the EGR and CA50 sweeps, the 10-90% burn durations from the target Diesel fuel were well-matched by the surrogate fuel. The average difference in the 10-90% burn duration was 0.6 CAD and the maximum observed difference was 1.6 CAD.

Combustion Analysis Summary

A combustion assessment was conducted on the target Diesel and surrogate fuel at PCCI and LTC conditions. The test conditions covered a matrix of EGR and CA50 sweeps. The injection SOE advance, ignition delay, mixing advance time and low-temperature heat release were well-matched for the two fuels. This suggested in-cylinder conditions prior to ignition, such as temperature, pressure, density, local equivalence ratio, mixture motion, and low-temperature kinetic reactions, were consistent for both fuels. Upon ignition, the peak heat release rates, peak bulk gas temperature, and 10-90% burn durations were also well-matched for both fuels. The combined results suggest that at the 1500x3 operating conditions the surrogate fuel combustion process closely replicated the target Diesel fuel combustion process.

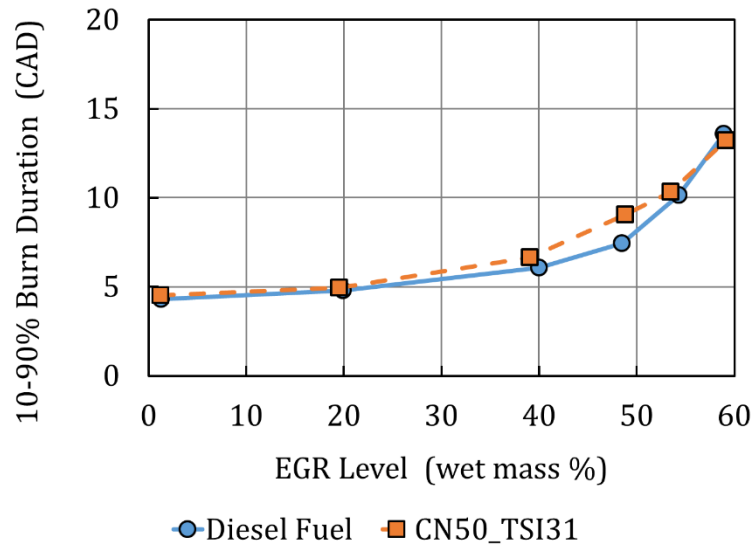


Figure 7-20: EGR effects on 10-90% burn duration at 1500x3 with the injection SOE adjusted to maintain CA50=9 degrees aTDC.

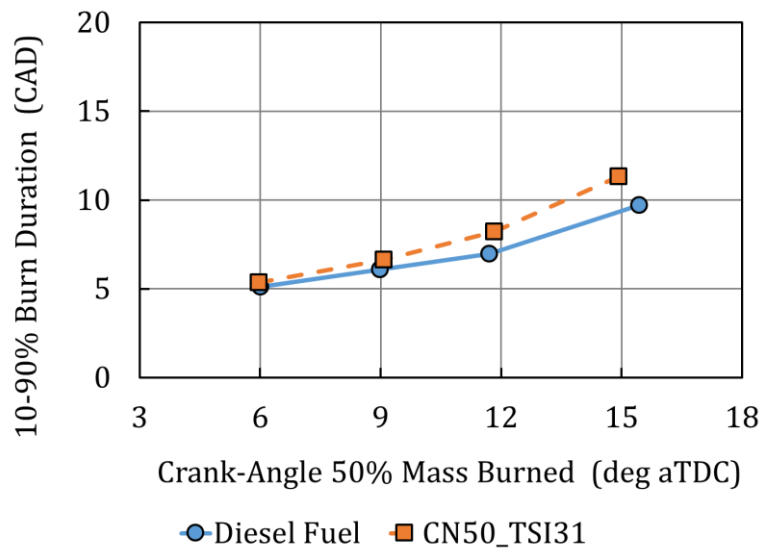


Figure 7-21: Combustion phasing effects on 10-90% burn duration at 1500x3 with 40% EGR.

7.4. Gaseous Emissions

This section provides an assessment of the gaseous emissions from the target Diesel and surrogate fuels. The assessment was conducted over a matrix of EGR and CA50 sweeps at the 1500x3 operating condition. The engine CO, HC and NO_x emissions as presented on the emission index basis, i.e., grams of emission per kg of fuel (g/kg-fuel). The EGR sweeps were conducted with the injection SOE adjusted to maintain CA50=9 degrees aTDC. The combustion phasing sweeps were performed at 40% EGR.

Carbon Monoxide

CO emissions for the EGR and CA50 sweeps are shown in Figure 7-22 and Figure 7-23, respectively. The results show that CO emissions from 1500x3 were significantly higher than the 1500x9 operating condition. For example, at 0% EGR, the EI-CO was about 2 g/kg-fuel for 1500x9 compared to about 50 g/kg-fuel at the 1500x3 condition. As expected, low combustion temperatures and more time for mixing resulted in less CO oxidation and higher engine CO emissions. As EGR increased from 0% to 60%, combustion transitioned into the LTC region and the CO emissions increased to a final value of about 150 g/kg-fuel. At the 1500x9 condition, combustion phasing had little effect on CO emissions. However, at 1500x3 with 40% EGR, Figure 7-23 shows that retarding the combustion phasing from CA50=6 to 15 essentially doubles the EI-CO to a final value of 120 g/kg-fuel. Even at these elevated CO levels the surrogate fuel replicated the emissions from the target Diesel fuel. During the EGR and CA50 sweeps the average difference in CO-EI was about 9 g/kg-fuel and the maximum observed difference was 19 g/kg-fuel. The results suggest that the overall mechanisms leading to incomplete CO oxidation to CO₂ were not significantly different between the two fuels.

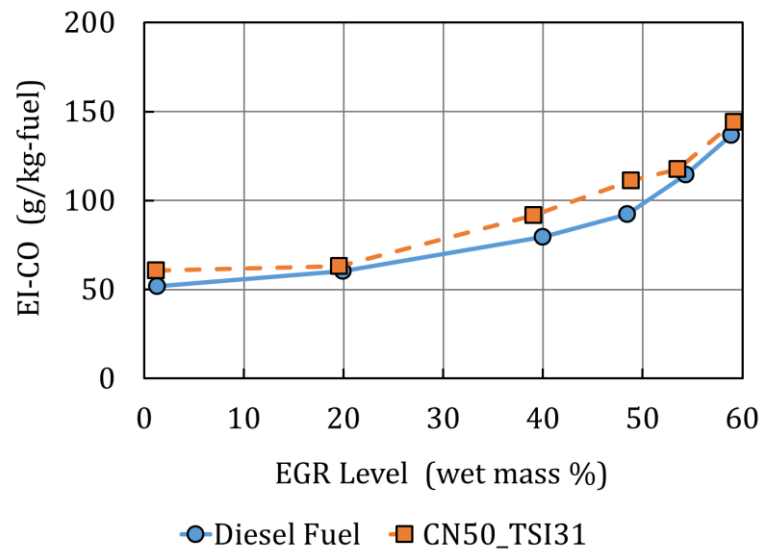


Figure 7-22: Effects of EGR on CO emissions at 1500x3 with the injection SOE adjusted to maintain CA50=9 degrees aTDC.

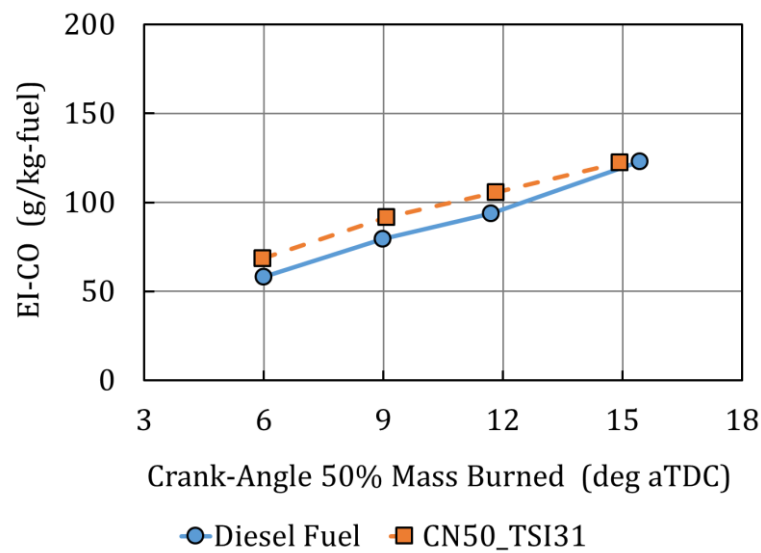


Figure 7-23: Effects of combustion phasing on CO emissions at 1500x3 with 40% EGR.

Hydrocarbons

The exhaust HC emissions for the EGR sweep are given in Figure 7-24 and the results from the combustion phasing sweep are provided in Figure 7-25. Recall that at the 1500x9 operating condition the HC emissions were very low (~ 1 g/kg-fuel). For 1500x3 at 0% EGR, the EI-HC emissions were 10 g/kg-fuel. Since there was no EGR, the HCs were elevated by over-mixing. As EGR was added, local oxygen concentrations and temperature were further reduced and EI-HC increased to about 40 g/kg-fuel at 60% EGR. For the combustion phasing sweep, retarded phasing increased the mixing time and lowered combustion temperatures which coupled to greatly increase the HC emissions. At 40% EGR with CA50=6, the EI-HC was about 10 g/kg-fuel and increased to almost 50 g/kg-fuel at CA50=15 degrees aTDC. As a result of the in-cylinder conditions, the EGR and CA50 sweeps at 1500x3 had profound effects on the HC emissions. Turning the attention to a comparison of the target Diesel and surrogate fuels, the data shows at EGR levels less than 60%, the two fuels had very good agreement. For this data, the average difference in HC-EI was only 3.6 g/kg-fuel. At 60% EGR, the surrogate fuel resulted in somewhat higher HCs than the target Diesel fuel. It's not clear if the surrogate fuel properties resulted in the higher HC emissions or if the reproducibility of operating conditions resulted in the increased HC emissions. Overall, the surrogate fuel adequately replicated the HC emission results obtained with the target Diesel fuel.

Nitrogen Oxides

Figure 7-26 shows the effects of EGR on NO_x emissions. At 0% EGR, combustion temperatures were sufficiently high to produce considerable NO_x (47 g/kg-fuel). As EGR exceeded 50% the combustion transitioned into the LTC region. At 60% EGR the NO_x emissions were extremely low and approached the detectability levels of the emission analyzer (EI-NO_x=0.5 g/kg-fuel). The results from the combustion phasing sweep are given in Figure 7-27. During the CA50 sweep, the surrogate fuel was tested with slightly less EGR. This resulted in the slightly higher NO_x emissions from the surrogate fuel. Both fuels demonstrated the same NO_x reduction as combustion phasing was retarded. The test results from the EGR and combustion phasing sweeps show the target Diesel and CN50_TSI31 fuels produced essentially the same NO_x emissions. For the EGR sweep, the average difference in EI-NO_x was only 0.3 g/kg-fuel and the maximum observed difference was 1.4 g/kg-fuel.

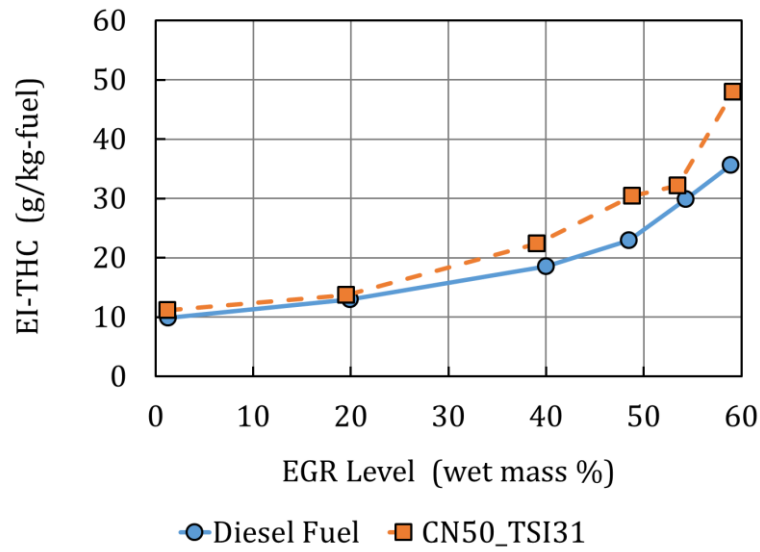


Figure 7-24: Effects of EGR on HC emissions at 1500x3 with the injection SOE adjusted to maintain CA50=9 degrees aTDC.

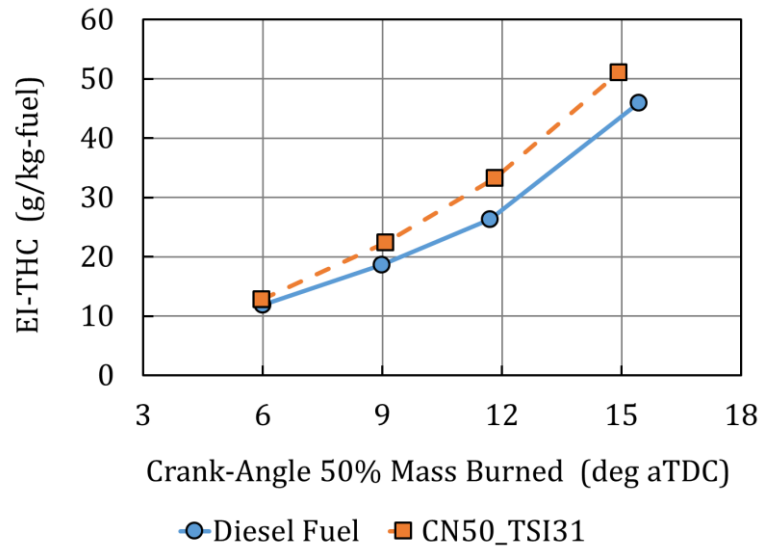


Figure 7-25: Effects of combustion phasing on HC emissions at 1500x3 with 40% EGR.

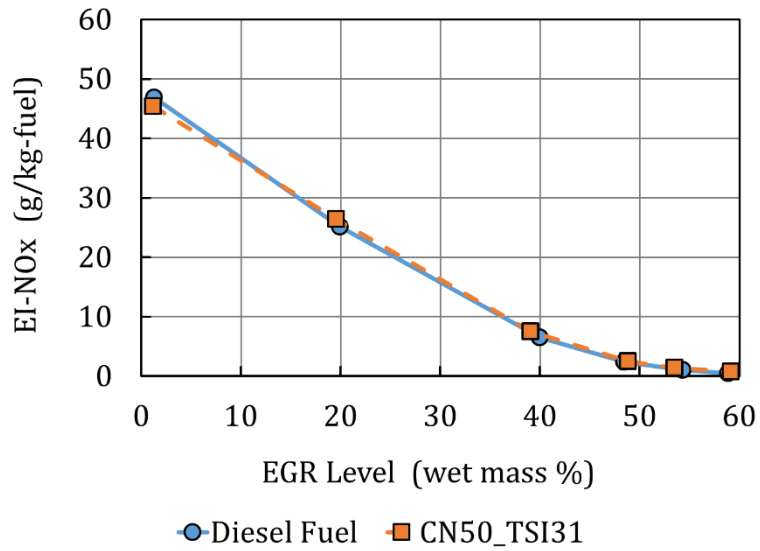


Figure 7-26: Effects of EGR on NOx emissions at 1500x3 with the injection SOE adjusted to maintain CA50=9 degrees aTDC.

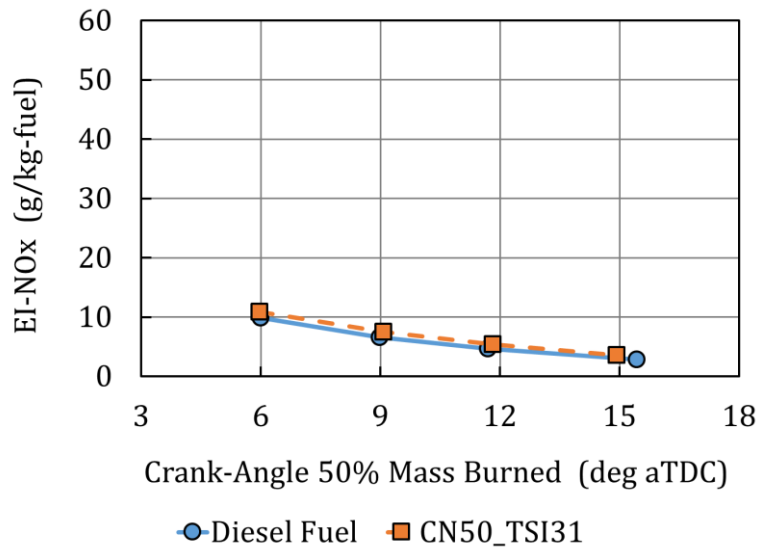


Figure 7-27: Effects of combustion phasing on NOx emissions at 1500x3 with 40% EGR.

7.5. Smoke and Particle Emissions

This section presents the exhaust smoke and particle data from the engine test matrix at the 1500x3 operating conditions.

Exhaust Smoke

The 1500x3 operating condition was developed to provide PCCI combustion that transitioned into low temperature combustion with the addition of EGR. The in-cylinder conditions provided sufficient fuel-air mixing that resulted in smoke-free combustion at all of the 1500x3 test points.

Exhaust Particles

The Cambustion DMS500 was used to measure the exhaust particles as described in Chapter 4. The particle number (N), particle diameter (D_p), and the particle expression $dN/d\log D_p$ were determined from the measurements. Plotting the particle expression $dN/d\log D_p$ as a function of D_p generates a graph known as the particle size distribution. An example particle size distribution graph was provided in Chapter 6, Figure 6-27 where conventional Diesel combustion generated nucleation and accumulation mode particles. Recall that nucleation mode particles were considered to be volatile materials while accumulation mode particles were considered to be solid agglomerates of smaller carbonaceous particles. Statistics were also calculated from the particle size distributions. The particle number concentration (N/cc) was calculated from the integrated particle size distributions for each mode. That is to say, the nucleation and accumulation mode particles were integrated separately. The particle count median diameter (CMD) was the particle diameter at the peak of each mode, as shown in Figure 6-27.

Recognizing that the 1500x3 conditions were smoke-free, the characteristics of the particle size distributions should be considerably different from the results presented in Chapter 6. Figure 7-28 shows the particle size distributions from an EGR sweep with the CA50=9 degrees aTDC and the engine operating on the target Diesel fuel. In contrast to the particle size distributions for conventional Diesel combustion, the particles from PCCI (0% EGR) and LTC (60% EGR) were primarily nucleation mode particles with trace amounts of accumulation mode particles. Comparing the conventional Diesel combustion results from Figure 6-28 with the LTC results in Figure 7-28 illustrates that the exhaust particle characteristics

changed from primarily accumulation mode for conventional combustion to principally nucleation mode for PCCI and LTC. Small amounts of EGR, for example 20%, had little impact on the particle size distribution. Greater amounts of EGR steadily increased the number of nucleation mode particles. The peak of the distribution, also known as the count median diameter (CMD) also shifted to larger diameters.

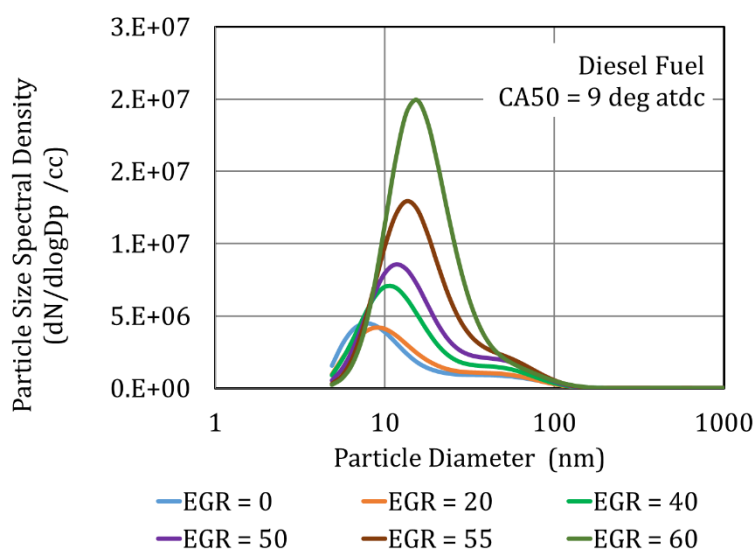


Figure 7-28: EGR effects on particle size spectral density for Diesel fuel at 1500x3 with the injection SOE adjusted to maintain CA50=9 degrees aTDC.

The effect of combustion phasing on the particle size distribution is illustrated in Figure 7-28. The CA50 sweep was conducted at 60% EGR which was considered to be low temperature combustion. The results show that retarded combustion phasing had a substantial impact on the particle size distribution. The number of nucleation mode particles increased and the distribution shifted to larger diameters.

Given the general understanding of the effects of EGR and combustion phasing on the particle size distributions for PCCI and low temperature combustion, the next step was to compare the exhaust particles from the target Diesel fuel with the particles from the surrogate fuel. Using the methodology presented in Chapter 6, this was accomplished by comparing the particle number concentrations (N/cc) and count median diameters (CMD) in lieu of generating numerous overlays of particle size distributions.

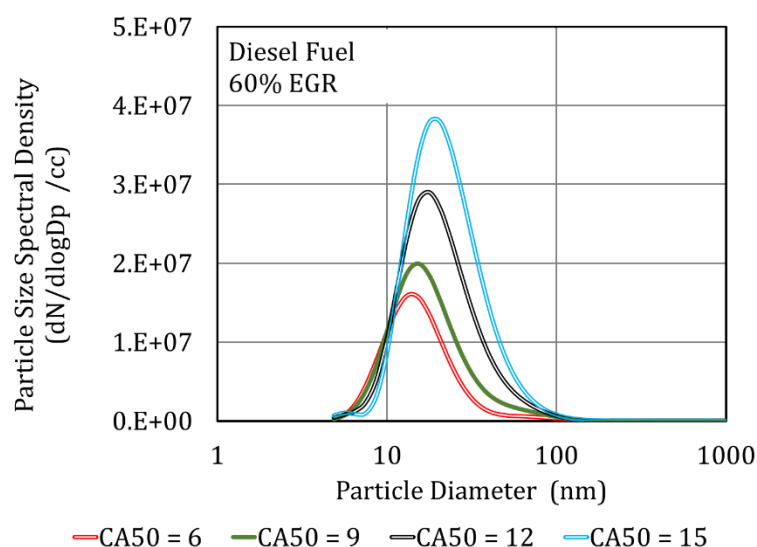


Figure 7-29: Combustion phasing effects on particle size spectral density for Diesel fuel at 1500x3 with 60% EGR.

The effects of EGR on the particle number concentration is given in Figure 7-30. The data were acquired at the 1500x3 condition with the combustion phasing set at CA50=9 degrees aTDC. The figure provides the nucleation and accumulation mode results for both fuels.

The data in Figure 7-30 shows accumulation mode number concentrations for the target Diesel and surrogate fuels were in relatively good agreement. Throughout the EGR sweep the accumulation mode particle number concentrations were very low and not significantly affected by EGR. At 0% EGR the accumulation particle number concentrations for the fuels averaged $5.5E+05$ N/cc, at 40% EGR the number concentration averaged $5.9E+05$ N/cc and at 60% EGR the average was $1.4E+06$ N/cc. The data suggests the accumulation particle number concentration increased with EGR. This interesting result that was observed for the target Diesel and the surrogate fuel.

The nucleation mode particle number concentration steadily rose as EGR was increased from 0% to 50%. Above 50% EGR, the nucleation particle number concentration increased at an increasing rate. The EGR effects were similar to the trends for CO and HC emissions (Figure 7-22 and Figure 7-24). The target Diesel and surrogate fuels followed the same trends with increasing EGR. However, the target Diesel fuel exhibited somewhat higher

nucleation particle concentration throughout the EGR sweep. At 0% EGR the nucleation particle concentration was $2.08\text{E}+06$ N/cc for the target Diesel and $1.10\text{E}+06$ N/cc for the surrogate fuel.

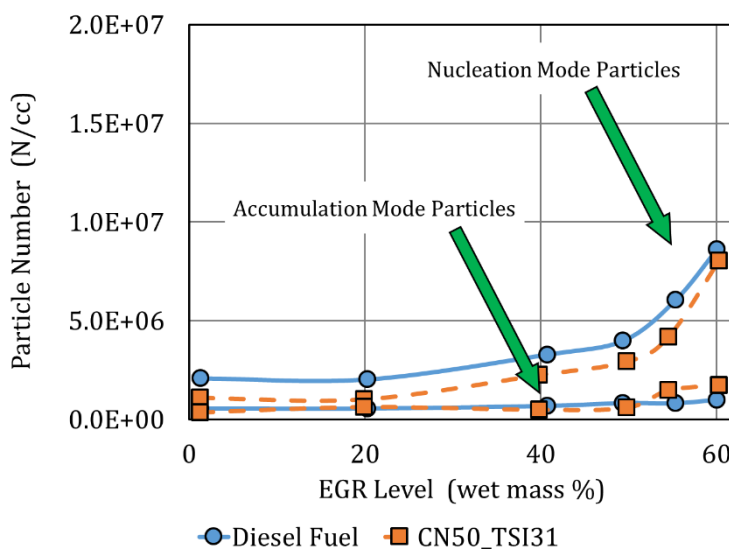


Figure 7-30: EGR effects on accumulation and nucleation mode particle number concentrations for Diesel and CN50_TSI31 at 1500x3 with the injection SOE adjusted to maintain $CA_{50}=9$ degrees aTDC.

The effects of combustion phasing on the particle number concentration is given in Figure 7-31. The data were acquired at the 1500x3 condition with 60% EGR which was considered to be a low temperature combustion condition. At 60% EGR, the nucleation particle concentration had increased to about $8.3\text{E}+06$ N/cc. A combustion phasing sweep at this condition should provide a rigorous comparison of the fuel particle concentrations.

The accumulation particle concentrations slightly increased as combustion phasing was retarded from $CA_{50}=6$ to 12 degrees aTDC then reduced to lower concentrations at the most retarded phasing of $CA_{50}=15$ degrees aTDC. The target Diesel and surrogate fuels followed the same trends. On average, the accumulation mode particle number concentration from the surrogate fuel was 54% greater than the target Diesel fuel. The nucleation particle concentrations greatly increased as combustion phasing was retarded. At $CA_{50}=6$, the average nucleation particle concentration was $7.0\text{E}+6$ N/cc and increased to $1.7\text{E}+07$ N/cc at $CA_{50}=15$ degrees aTDC. In

general, the nucleation particle concentrations from the target Diesel and surrogate fuels were in good agreement; although the surrogate fuel trend was not as smooth as the target Diesel fuel.

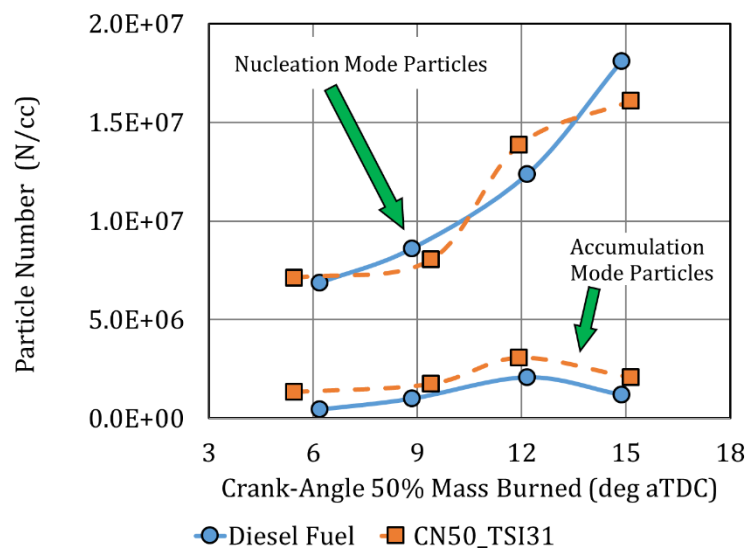


Figure 7-31: Combustion phasing effects on particle number concentration for Diesel and CN50_TSI31 fuels at 1500x3 with 60% EGR.

The particle count median diameter (CMD) results from the EGR sweeps are shown in Figure 7-32. For both fuels, the nucleation particle CMD steadily increased with increasing EGR. The surrogate fuel closely replicated the nucleation particle CMD from the target Diesel fuel. At 0% EGR, the nucleation particle CMD averaged 8.4 nm and increased to an average of 14.0 nm at 60% EGR. As EGR was increased the accumulation particle CMD also increased for both fuels. At 0% EGR, the accumulation particle CMD was about 39 nm and increased to approximately 46 nm at 50% EGR. For both fuels, an interesting trend occurred above 50% EGR namely, the accumulation particle CMD reduced to about 39 nm at 60% EGR.

Count median diameter results from the combustion phasing sweep at 60% EGR are given in Figure 7-33. As CA50 was retarded from 6 to 15 degrees aTDC, the nucleation particle CMD steadily increased. At CA50=6 degrees aTDC, the nucleation particle CMD was about 13 nm for both fuels. At CA50=15 degrees aTDC, the nucleation particle CMD for the target Diesel fuel increased to 20 nm whereas the surrogate fuel increased to 15 nm. The accumulation particle CMD were essentially unchanged averaging 40 nm as

the combustion phasing was retard from CA50=6 to 12 degrees aTDC. The data shows the accumulation particle CMD somewhat increased at the most retarded combustion phasing of CA50=15 degrees aTDC. The test results suggest that overall, the accumulation and nucleation particle CMD from the target Diesel fuel were reasonable well-matched by the surrogate fuel.

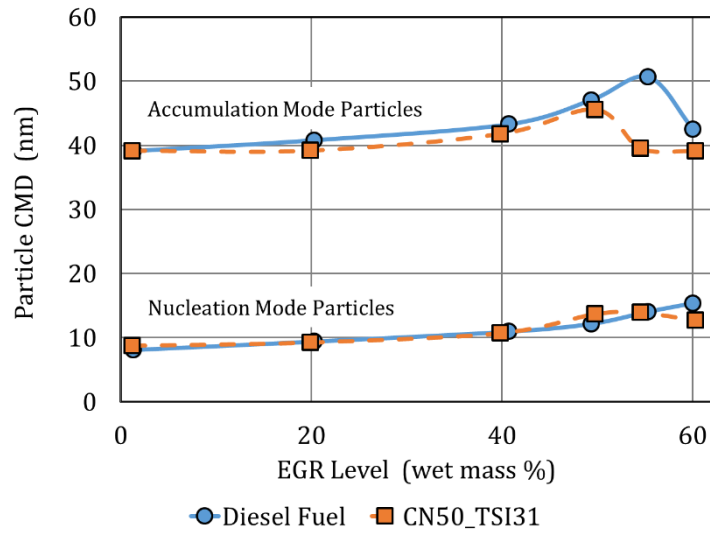


Figure 7-32: EGR effects on particle count median diameter (CMD) for Diesel and CN50_TSI31 fuels at 1500x3 with the injection SOE adjusted to maintain CA50=9 degrees aTDC.

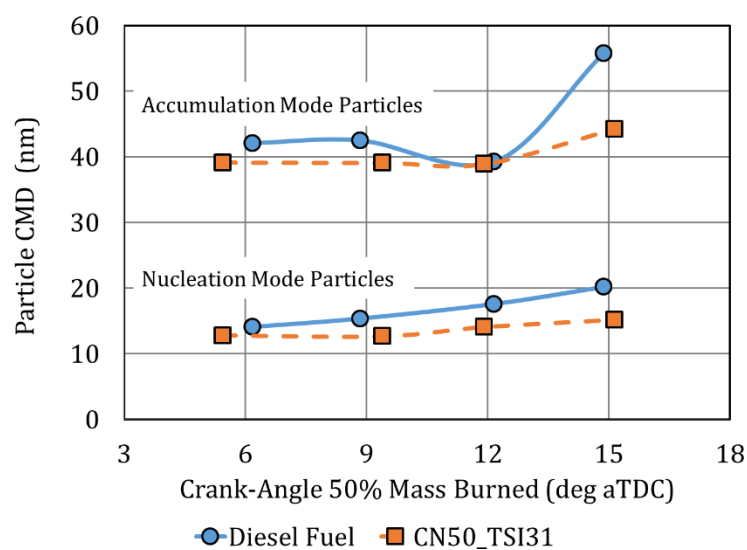


Figure 7-33: Combustion phasing effects on particle count median diameter (CMD) for Diesel and CN50_TSI31 fuels at 1500x3 with 60% EGR.

The PCCI and LTC operating conditions resulted in smoke-free combustion. Particle number and size distribution measurements showed the exhaust particles were primarily nucleation mode particles while relatively small concentrations of accumulation mode particles were detected. The effects of EGR and combustion phasing on accumulation and nucleation particle number concentrations and count median diameters were quantified for the target Diesel and surrogate fuels. Throughout the EGR and CA50 sweeps, the particle number concentration and CMD measurements showed good agreement between the target Diesel fuel and the surrogate fuel.

7.6. Summary

In this chapter, Diesel engine test results operating on the target Diesel and CN50_TSI31 fuels at PCCI and LTC conditions were presented. The engine was operated at a light-load condition with sufficient in-cylinder fuel-air mixing to obtain PCCI combustion. High EGR levels were used to obtain both PCCI and LTC combustion.

At low EGR levels, the PCCI combustion conditions were smoke-free and yielded relatively high HC and CO emissions compared to the conventional Diesel combustion results presented in Chapter 6. With low EGR levels the combustion temperatures were sufficiently high to produce significant NO_x emissions. Exhaust particles were dominated by nucleation mode particles that increased with increased EGR levels. The effects of combustion phasing were quantified with CA50 sweeps from 6 degrees to 15 degrees aTDC. The results showed that retarded phasing increased HC, CO and nucleation mode particles. Throughout the PCCI operating conditions, the engine combustion (LTHR and HTHR), gaseous emissions and particle data obtained from the surrogate fuel closely matched the data from the engine operating on the target Diesel fuel.

At EGR levels greater than 50%, the combustion transition into the LTC regime and the engine produced very low NO_x emissions. Peak heat release rates and bulk gas temperatures were significantly reduced by the high EGR levels. In addition, the duration of the LTHR and the ignition delay times were significantly increased. The HC, CO and nucleation mode particles were also greatly increased by the high EGR levels. Throughout the LTC operating conditions, the engine test results demonstrated that the combustion, gaseous emissions, and exhaust particle distributions from the target Diesel fuel were well-matched by the four-component surrogate fuel CN50_TSI31.

7.7. References

- [7.1] Kitamura, T., Ito, T., Senda, J. and Fujimoto, H., "Mechanism of Smokeless Diesel Combustion with Oxygenated Fuels based on the Dependence of the Equivalence Ratio and Temperature on Soot Particle Formation", *International Journal of Engine Research* 3(4):223-248, 2002, doi:10.1243/146808702762230923.
- [7.2] Amorim, R., Novella, R., Garcia, A. and Molina, S., "Study on LTC for light duty engines – Part 2 – Spray enhancements", *Fuel* 193:206-219, 2017, doi:10.1016/j.fuel.2016.12.050.
- [7.3] Benajes, J., Molina, S., De Rudder, K. and Amorim, R., "Optimization Towards Low-temperature Combustion in a HSDI Diesel Engine, Using Consecutive Screenings", *SAE Technical Paper Series*, 2007, doi:10.4271/2007-01-0911.
- [7.4] Benajes, J., Molina, S., Novella, R. and Amorim, R., "Study on Low Temperature Combustion for Light-Duty Diesel Engines", *Energy & Fuels* 24(1):355-364, 2010, doi:10.1021/ef900832c.
- [7.5] Desantes, J., Lopez, J., Redon, P. and Arregle, J., "Evaluation of the Thermal NO formation mechanism under low-temperature diesel combustion conditions", *International Journal of Engine Research* 13(6):531-539, 2012, doi:10.1177/1468087411429638.
- [7.6] Jacobs, T., Bohac, S., Assanis, D. and Szymkowicz, P., "Lean and Rich Premixed Compression Ignition Combustion in a Light-Duty Diesel Engine", *SAE Technical Paper Series*, 2005, doi:10.4271/2005-01-0166.
- [7.7] Kolodziej, C., "Particulate Matter Emissions from Premixed Diesel Low Temperature Combustion", PhD, Universitat Politècnica de València, 2012.
- [7.8] Payri, F., Benajes, J., Novella, R. and Kolodziej, C., "Effect of Intake Oxygen Concentration on Particle Size Distribution Measurements from Diesel Low Temperature Combustion", *SAE International Journal of Engines* 4(1):1888-1902, 2011, doi:10.4271/2011-01-1355.

- [7.9] Benajes, J., García-Oliver, J., Novella, R. and Kolodziej, C., "Increased particle emissions from early fuel injection timing Diesel low temperature combustion", *Fuel* 94:184-190, 2012, doi:10.1016/j.fuel.2011.09.014.
- [7.10] Benajes, J., Novella, R., Arthozoul, S. and Kolodziej, C., "Particle Size Distribution Measurements from Early to Late Injection Timing Low Temperature Combustion in a Heavy Duty Diesel Engine", *SAE International Journal of Fuels and Lubricants* 3(1):567-581, 2010, doi:10.4271/2010-01-1121.
- [7.11] Desantes, J., Benajes, J., Garcia-Oliver, J. and Kolodziej, C., "Effects of intake pressure on particle size and number emissions from premixed diesel low-temperature combustion", *International Journal of Engine Research* 15(2):222-235, 2013, doi:10.1177/1468087412469514.
- [7.12] Desantes, J., Bermúdez, V., García, J. and Fuentes, E., "Effects of current engine strategies on the exhaust aerosol particle size distribution from a Heavy-Duty Diesel Engine", *Journal of Aerosol Science* 36(10):1251-1276, 2005, doi:10.1016/j.jaerosci.2005.01.002.

8. Conclusions and Future Research

Contents

8.	Conclusions and Future Research	229
8.1.	Introduction.....	231
8.2.	Summary	231
8.3.	Conclusions	244
8.4.	Furture Research	245

8.1. Introduction

The objective of this chapter is to provide a thorough summary of the highlights and major results from this research. With the essence of the investigation summarized, the conclusions drawn from the work are presented. This study provides useful results and insight but much more research is warranted to understand and utilize multi-component surrogate fuels. Therefore, this thesis proposes some ideas for further research.

8.2. Summary

Objective

From a high-level perspective, the objective of this research was to design and prove fully representative multi-component surrogate Diesel fuels that, along with their chemical kinetic mechanisms, could be routinely used by researchers and the Diesel engine development community. To accomplish this, the surrogate fuels must be fully representative of full-range petroleum Diesel fuels. To account for regional and seasonal variability in fuel properties, the surrogate fuels must cover a broad range of cetane number and TSI. Providing a variety of surrogates provides the opportunity to select the optimum surrogate fuel for the investigation.

Surrogate Fuel Development Process

This thesis developed and employed a systematic methodology to formulate surrogate fuel blends. The computational methods, which included closed-homogeneous reactor simulations, surrogate blend optimization and fuel property predictions, are provided in *Chapter 3 Computational Methods*. A simple schematic diagram of the methodology is shown in Figure 8-1 and more details are found in *Chapter 5.2 Surrogate Fuel Formulation*. The methodology may be applied to create surrogates for a variety of hydrocarbon fuels including, Diesel, gasoline, jet fuel, and alternative fuels such as naphtha, oxygenated fuels and fuel mixtures.

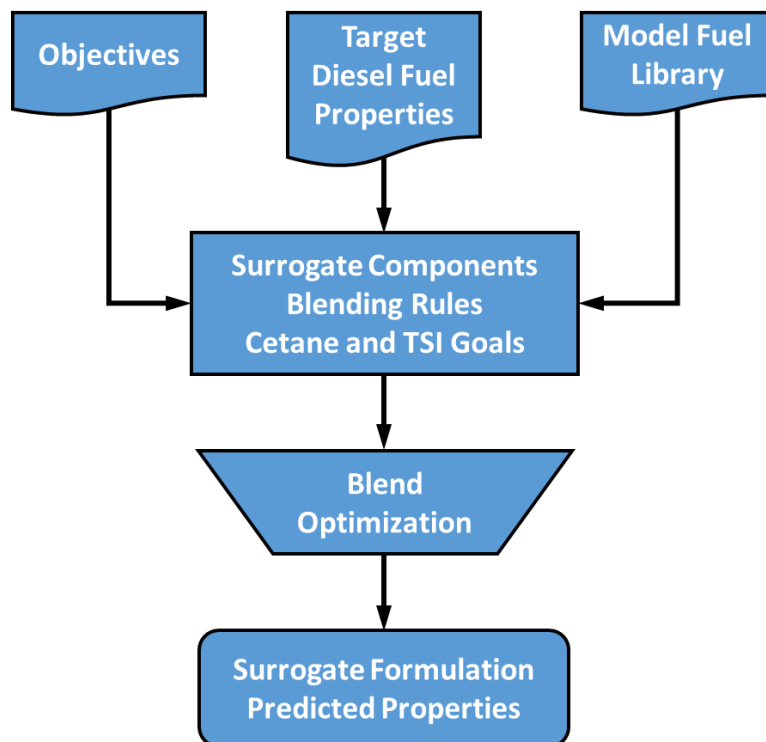


Figure 8-1: Surrogate fuel development methodology.

An initial investigation of the Model Fuel Library identified the best 13 hydrocarbon components for potential use in Diesel surrogate fuels. Several surrogate formulations were developed and evaluated using the Surrogate Blend Optimizer and closed-homogeneous reactor simulations. The investigation resulted in a seven-component surrogate and a four-component surrogate both of which closely matched the properties of the full-range target Diesel fuel. To minimize complexity, the four-component surrogate was selected. The fuel components consisted of a normal-alkane, an iso-alkane, a cyclo-alkane and an aromatic. The hydrocarbon species were n-hexadecane, heptamethylnonane, decahydronaphthalene and 1-methylnaphthalene, respectively. Further exploration with the four components lead to a set of blending rules that guided the blend formulations for 18 separate surrogate Diesel fuels which were called the Surrogate Fuel Library.

Surrogate Fuel Library

Since Diesel fuel properties such as cetane number and TSI can vary regionally and seasonally, an objective of this thesis was to develop surrogate fuels that spanned a broad range of cetane number and TSI while retaining acceptable values for other properties such as density, viscosity, heating value and distillation temperatures. In all, 18 surrogate fuels were formulated to span a cetane number range from 35 to 60 and a TSI range from 17 to 48. Table 8-1 shows the surrogate fuel names, cetane number and TSI values. Surrogate fuel CN50_TSI31 was tailored to closely match the combustion, physical and chemical properties of the full-range target Diesel fuel. Table 8-2 shows the four fuel components and blend formulation for the surrogate fuel CN50_TSI31.

Table 8-1: The Surrogate Fuel Library.

	Low Soot Fuels TSI=17	Mid Soot Fuels TSI = 31	High Soot Fuels TSI = 48
CN=35	CN35_TSI17	CN35_TSI31	CN35_TSI48
CN=40	CN40_TSI17	CN40_TSI31	CN40_TSI48
CN=45	CN45_TSI17	CN45_TSI31	CN45_TSI48
CN=50	CN50_TSI17	CN50_TSI31 <i>Target Diesel Fuel</i>	CN50_TSI48
CN=55	CN55_TSI17	CN55_TSI31	CN55_TSI48
CN=60	CN60_TSI17	CN60_TSI31	CN60_TSI48

Table 8-2. Surrogate fuel components and blend formulation for the surrogate fuel CN50_TSI31 which was developed to match the properties of the target Diesel fuel.

Hydrocarbon Class	Surrogate Fuel Specie	Volume Fraction
n-Alkanes	n-Hexadecane	0.37
iso-Alkanes	Heptamethylnonane	0.33
cyclo-Alkanes	Decahydronaphthalene	0.18
Aromatics	1-Methylnaphthalene	0.12

The blend formulations and predicted properties for each surrogate fuel were determined and are provided in *Appendix 10.1 Surrogate Fuel Library*. Predicted fuel properties included cetane number, TSI, density, kinematic viscosity, lower heating value, molar H/C and the distillation curve from T₁₀ to T₉₀.

Surrogate Fuel Property Validation

A set of 5 surrogate fuels were selected, blended and characterized with a set of comprehensive ASTM fuel property tests. Surrogate fuels CN40_TSI31, CN50_TSI31, CN60_TSI31 were selected to cover a broad cetane number range while surrogates CN50_TSI17 and CN50_TSI48 were chosen to bracket the TSI range. Detailed property comparisons are given in *Chapter 5.3 Predicted and Measured Property Comparisons* and the complete test results are provided in *Appendix 10.3 Surrogate Fuel Property Validation*. As an example of the results, shows a comparison between the measured and predicted cetane number for the 5 surrogate fuels. Table 8-3 summarizes the maximum differences observed between the predicted and measured fuel properties. Overall, very good agreement between the predicted and measured fuel properties were obtained. This part of the investigation validated the component blending methodology and predicted fuel property results for the Surrogate Fuel Library.

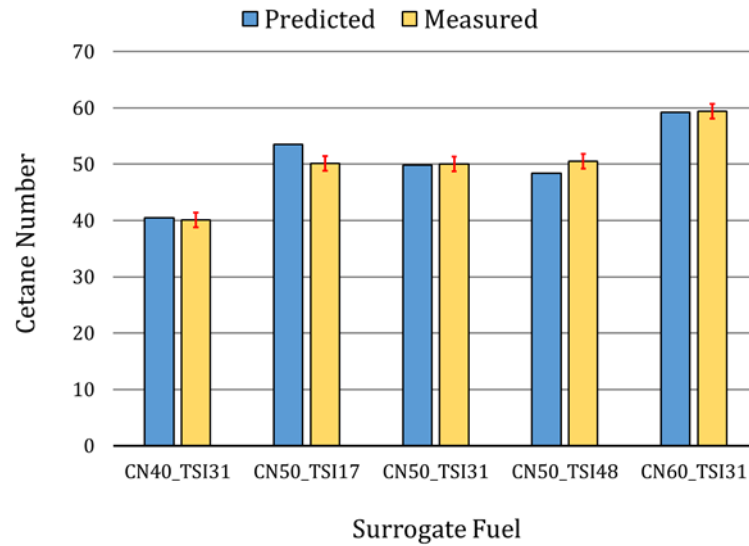


Figure 8-2: Predicted and measured cetane numbers. Error bands reflect the reproducibility specified within the ASTM procedure.

Table 8-3: Maximum observed differences between predicted and measured fuel properties.

Fuel Property	Maximum Observed Difference between Predicted and Measured Fuel Properties
Cetane	Within measurement error
TSI	Within measurement error
Density	2%
Lower Heating Value	4%
Kinematic Viscosity	15%
Distillation Temperature T ₁₀	10 °C
Distillation Temperature T ₉₀	6 °C

Surrogate CN50_TSI31 Validation with Target Diesel Fuel

For the final fuel property validation, the surrogate CN50_TSI31 was compared to the target Diesel fuel. Detailed ASTM fuel property measurements were conducted on both fuels. Complete results are given in *Chapter 5.4 Surrogate and Petroleum Fuel Comparison*. The cetane number, TSI and lower heating value matched within the reproducibility of the test procedures. Good agreement was achieved for density, viscosity, surface tension and the low end of the distillation curve. For the mid to upper range of the curve the distillation temperatures of surrogate fuel CN50_TSI31 were about 35 °C lower than the target Diesel fuel. As a result of this work, it was determined that a minimum of four hydrocarbon species were required to achieve the objectives of this thesis which included a fully-representative surrogate fuel that closely mimicked the combustion, physical and chemical properties of full-range petroleum Diesel fuel.

Single-Cylinder Engine Investigation - Conventional Diesel Combustion

A fully-instrumented single-cylinder research engine was equipped with a contemporary Diesel engine combustion and injection system; details are given in *Chapter 4 Experimental Methods*. A part-load operating condition was established at 1500 r/min and 9 bar IMEP (1500x9) that exhibited conventional Diesel combustion which included premixed and diffusion combustion regions. The target Diesel and surrogate CN50_TSI fuels were tested through a matrix of EGR and CA50 sweeps. Engine combustion, gaseous emissions, smoke and exhaust particle size distributions were recorded and analyzed. The complete engine test results are given in *Chapter 6 Conventional Diesel Combustion*. Since the surrogate was tailored to have the same cetane number and TSI as the target Diesel fuel, particular attention was paid to the heat release, smoke and particle results. Overall, the engine test results from the surrogate CN50_TSI31 showed very close agreement with the results from the target Diesel fuel. The combustion, gaseous emissions, smoke, and exhaust particles from the target Diesel fuel were closely replicated by CN50_TSI31. For example, Figure 8-3 shows the heat-release rates for both fuels as CA50 was swept from advanced to retarded combustion phasing. In this example, retarding the combustion phasing increased the fraction of fuel consumed in the premixed combustion region and increased the peak heat release rates. The surrogate fuel closely followed the heat release characteristics of the target Diesel fuel. In another example, the smoke-NO_x tradeoff for an EGR sweep is given in Figure 8-4. The results from the surrogate fuel and essentially indistinguishable from the target Diesel fuel. A rigorous test of the surrogate fuel was the comparison of the exhaust particle number and size distributions. Throughout the EGR and CA50 sweeps, the characteristics of exhaust particles from both fuels were well-matched. Results from an EGR are given in Figure 8-5 which shows the particle number concentration and Figure 8-6 which provides the particle count median diameter. Good agreement was obtained for the accumulation and nucleation mode particles. The engine test results at the 1500x9 conditions with conventional Diesel combustion demonstrated that the surrogate fuel essentially matched the combustion, gaseous emissions, smoke and exhaust particles obtained from the full-range target Diesel fuel.

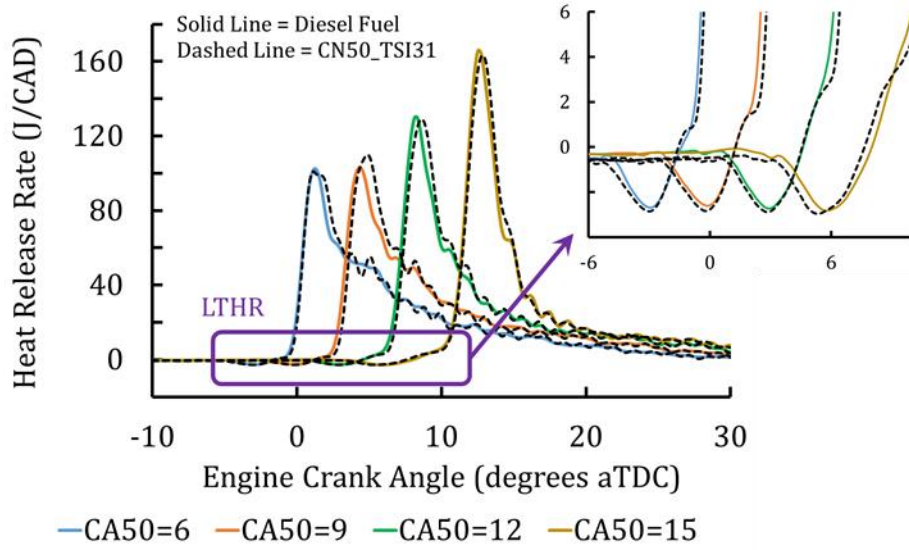


Figure 8-3: Heat release rates for CA50 sweeps at 1500x9 with 15% EGR.

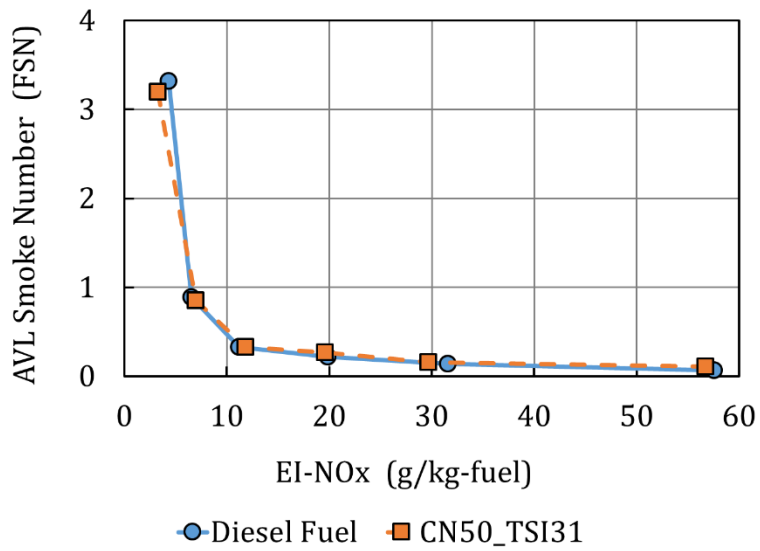


Figure 8-4: Smoke-NOx tradeoff for the target Diesel and CN50_TSI31 fuels.

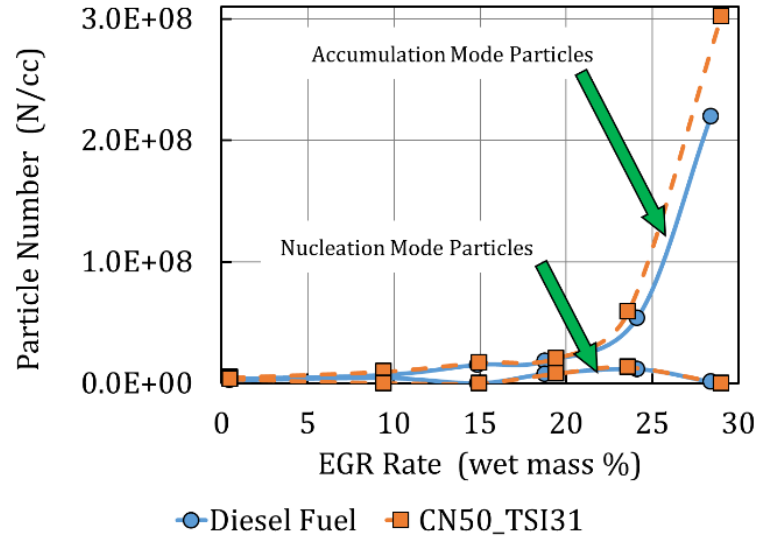


Figure 8-5: Effects of EGR on exhaust particle number concentration at 1500x9 with the injection SOE adjusted to maintain CA50=9 degrees aTDC.

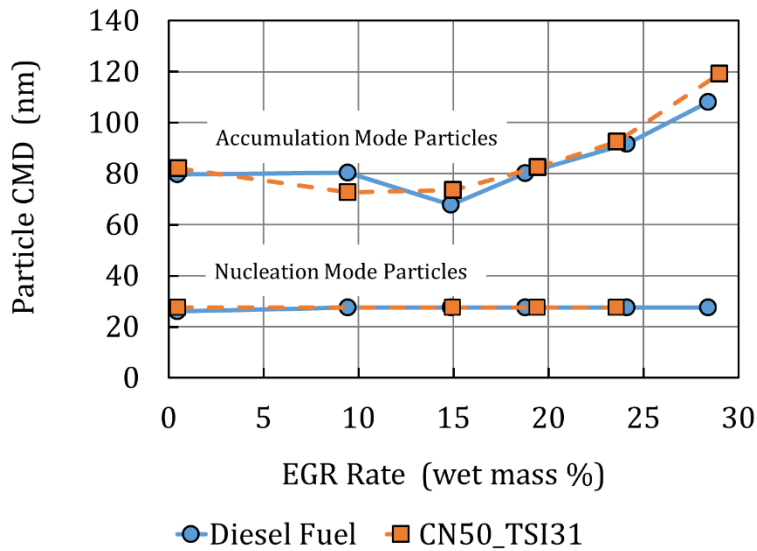


Figure 8-6: Effects of EGR on exhaust particle count mean diameter at 1500x9 with the injection SOE adjusted to maintain CA50=9 degrees aTDC.

Single-Cylinder Engine Investigation – PCCI and LTC Combustion

The single-cylinder engine investigation was expanded with a study of the target Diesel and CN50_TSI31 fuels under Premixed Charge Compression Ignition (PCCI) and Low Temperature Combustion (LTC) conditions. A light-load operating condition was established at 1500 r/min and 3 bar IMEP (1500x3). This operating condition exhibited PCCI combustion at all of the test conditions. The in-cylinder conditions, small fuel injection quantity, and extended mixing advance time combined to provide sufficient fuel-air mixing to result in smoke-free combustion. The LTC condition was achieved at high EGR levels where the NO_x emissions dropped to very low levels (~10 ppm). The target Diesel and surrogate CN50_TSI fuels were tested using a matrix of EGR and CA50 sweeps. Engine combustion, gaseous emissions, and exhaust particle size distributions were recorded and analyzed. The complete engine test results are given in *Chapter 7 PCCI and LTC Combustion*. Since the 1500x3 conditions provided extensive fuel-air mixing, special attention was paid to the low-temperature heat release and the exhaust particle results. Overall, the test results from the PCCI and LTC conditions showed good agreement between the target Diesel fuel and surrogate CN50_TSI31. For example, Figure 8-7 shows the heat-release rates for both fuels with 0% and 60% EGR. The 0% EGR condition exhibited a relatively short low-temperature heat release period followed by rapid combustion and a high peak heat release rate. With 60% EGR, the low-temperature heat release times were greatly extended, combustion rates were much slower and the peak heat release rates were significantly reduced. For both 0% and 60% EGR, the heat-release rates from the surrogate fuel and the target Diesel fuel were in good agreement. In another example, the gaseous emissions for an EGR sweep are given in Figure 8-8. The CO, HC and NO_x emissions were well-matched for both fuels. The exhaust particle characteristics were also investigated. Results from an EGR sweep are given in Figure 8-9 which shows the particle number concentration and Figure 8-10 which provides the particle count median diameter. As a result of PCCI combustion, the particle number concentration and count median diameter for the accumulation mode particles were greatly reduced and demonstrated little response to EGR. The nucleation mode particle number concentration and count median diameter both increased with EGR. Overall, very good agreement was obtained for the accumulation and nucleation mode particles. The engine test results at the 1500x3 conditions with PCCI and LTC Diesel combustion demonstrated that the surrogate fuel closely

followed the combustion, gaseous emissions, and exhaust particles obtained from the full-range target Diesel fuel.

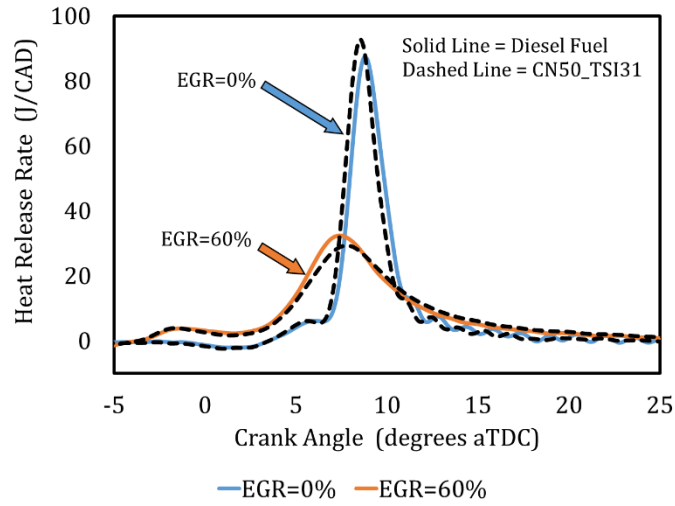


Figure 8-7: Heat release rates from the target Diesel and CN50_TSI31 fuels at 1500x3 with 0% and 60% EGR with the injection SOE adjusted to maintain CA50=9 degrees aTDC.

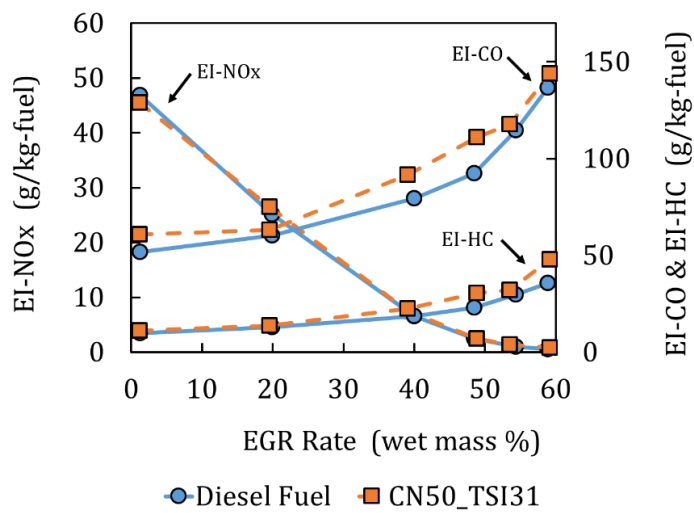


Figure 8-8: Gaseous emission results from an EGR sweep at 1500x3 with the injection SOE adjusted to maintain CA50=9 degrees aTDC.

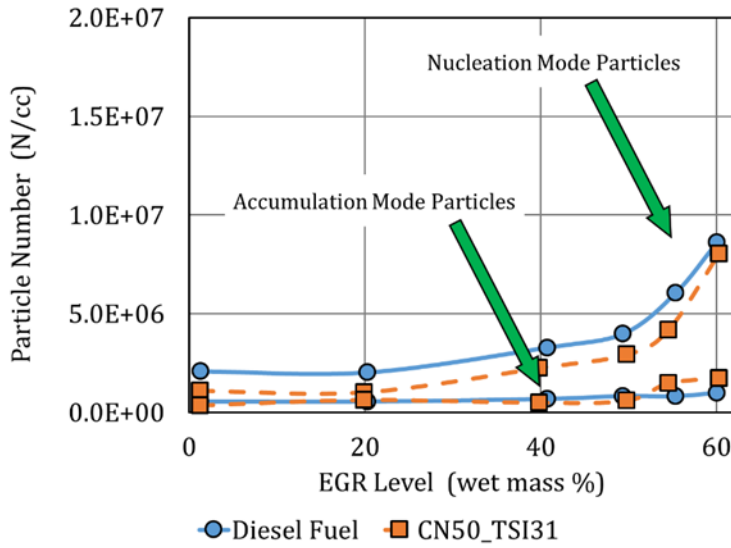


Figure 8-9: EGR effects on accumulation and nucleation mode particle number concentrations for Diesel and CN50_TSI31 at 1500x3 with the injection SOE adjusted to maintain CA50=9 degrees aTDC.

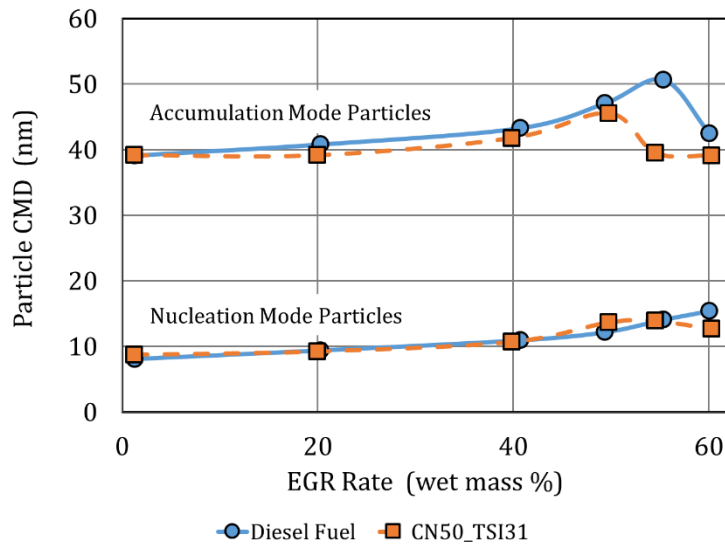


Figure 8-10: EGR effects on particle count median diameter (CMD) for Diesel and CN50_TSI31 fuels at 1500x3 with the injection SOE adjusted to maintain CA50=9 degrees aTDC.

For the engine conditions examined within this thesis, the test results from the surrogate fuel closely matched the results from the target Diesel fuel. Even the smoke, particle size and number distributions were in close agreement for conventional, PCCI and LTC combustion. This was considered a desired and successful outcome but raised a question. Why? It was true that the two fuels had nearly the same fuel properties but the target Diesel fuel did not contain any of the hydrocarbon species contained in the surrogate fuel. To probe the “Why?” question, closed-homogeneous reactor simulations were run using two surrogates with the essentially same properties but containing different hydrocarbons (seven-component and four-component surrogates). This work can be found in *Chapter 6.6 Discussion*. The seven-component surrogate contained aromatics with 1 benzene ring and 2 benzene rings whereas the four-component surrogate only contained a 2-ring aromatic. For both surrogates, the reactor simulations suggest that all of the fuel components completely decomposed into unsaturated, light hydrocarbons prior to ignition. At the time of ignition, both surrogates formed nearly the same concentrations of acetylene (C_2H_2) and benzene (C_6H_6). Although certainly not an exhaustive study, the simulation results combined with the engine results lead to a hypothesis that may provide a starting point to answer the question “Why?”

Hypothesis: Hydrocarbon mixtures, similar to Diesel fuel, with key combustion, physical and chemical properties closely matched may decompose and undergo low-temperature kinetic reactions that form the same effective pool of light, unsaturated hydrocarbons prior to ignition.

Assuming the in-cylinder conditions and the mechanisms governing combustion and emissions are consistent, Diesel fuels that provide the same effective pool of unsaturated hydrocarbons at the onset of ignition will yield the same combustion, gaseous emissions, smoke and exhaust particles.

8.3. Conclusions

The following conclusions are drawn from this research:

1. A methodology to develop multi-component surrogate Diesel fuels with independent control of cetane number and TSI was validated. The methodology was used to develop the Surrogate Fuel Library.
2. The least complicated surrogate fuel that achieved the objectives of this thesis, including independent control of cetane number and TSI, consisted of the following 4 hydrocarbon species: n-hexadecane, 2,2,4,4,6,8,8-heptamethylnonane, decahydronaphthalene and 1-methylnaphthalene.
3. With minor exceptions, the 4-component surrogate fuel formulated to match the full-range target Diesel fuel achieved the fuel property requirements of ASTM D975 and EN590. (Discrepancies are documented within this thesis.)
4. The Surrogate Blend Optimizer predicted properties for cetane number, TSI, density, kinematic viscosity, lower heating value, molar H/C and the T_{10} - T_{90} distillation curve were validated for the 4 hydrocarbon components and surrogate fuels developed within this thesis.
5. The formulations and predicted properties for the Surrogate Fuel Library were computationally and experimentally validated.
6. Diesel engine combustion and emissions from a multi-component surrogate fuel are expected to match the results from a full-range petroleum Diesel fuel when the combustion, physical and chemical properties of both fuels are closely matched. (For steady-state, fully warmed-up conditions.)
7. The Surrogate Fuel Library may be used to represent full-range Diesel fuels covering a broad range of cetane number and TSI.
8. The fuel formulations and properties within the Surrogate Fuel Library can be combined with chemical kinetic mechanisms and used for Diesel combustion simulation.

8.4. Future Research

This thesis provided an in-depth investigation into the development and validation of multi-component surrogate Diesel fuels. Although comprehensive, this first work is not nearly complete. This research effort resulted in a Surrogate Fuel Library containing fuels that vary cetane number from 35 to 60. The surrogates also vary in sooting tendency. In fact, the lowest sooting tendency fuel does not contain any aromatic compounds. Much more research is required to better understand and apply these new multi-component surrogate fuels. The following is a list of ideas for further study.

Study of Chemical Kinetic Mechanisms

Kinetic mechanisms are needed to use the surrogate fuels for combustion simulation. This study would create and investigate a set of kinetic mechanisms that would be focused on the Surrogate Fuel Library. First a Master Mechanism needs to be assembled based on the 4 surrogate fuel components: n-hexadecane, heptamethylnonane and 1-methylnaphthalene. Then a systematic methodology for mechanism reduction would be proposed and investigated. The study would examine the tradeoff between mechanism complexity and the accuracy obtained from combustion simulation. The study would identify the point at which mechanism reduction significantly impacts combustion simulation results. The initial effort would focus on reactor simulations such as closed-homogeneous and opposed flow reactors. The end result would be a library of kinetic mechanisms tailored for specific applications. For example, high-fidelity skeletal mechanisms for reactor simulations, moderate fidelity mechanisms for full 3-dimensional Diesel combustion simulation targeted at quantitative prediction of HC and CO emissions, and highly reduced mechanisms that still capture cetane number effects for ignition delay and heat-release prediction.

Experimental Investigation of the Influence of Surrogate Fuel Characteristics on Spray Atomization, Mixing Process and Combustion

This objective of this research would be to experimentally investigate the ignition and sooting characteristics of select surrogate fuels to shed new light on the chemistry and physics of Diesel fuel ignition and soot production.

This new work would employ several macroscopic and microscopic combustion diagnostic techniques to examine the non-reacting and reacting Diesel spray. Surrogate fuels with varying cetane number would be used to study ignition while surrogates with varying TSI would be used to study the sooting characteristics. Data would be collected from a high-pressure, high-temperature chamber. The experiments would characterize the spray primary break-up, liquid and vapor penetration. Reacting spray measurements would include Schlieren to obtain temperature gradients and determine ignition delay, OH measurements to measure lift off length, and Soot-DBI, for evaluating the soot distribution in the diffusive flame. Surrogate fuels would include single-component fuels such as n-heptane, dodecane, and decahydronaphthalene. Multi-component surrogates would be used to investigate cetane number and TSI effects. A full-range petroleum Diesel fuel would be tested to serve as a basis for comparison. This study would provide a wealth of experimental data that would also be useful for validating combustion CFD simulations for the reacting sprays.

9. Bibliography

- 5 Oaks Commodities, "Petroleum Products", *5 Oaks Commodities*, <http://www.5oakscommodities.com/petroleum-products.html>, 2017.
- A&D Technology, "CAS 4.0 Reference Manual", *A&D Technology, Inc.*, First Edition, 2009.
- A&D Technology, "ADAPT Test Automation System", A&D Technology, Inc., 2014. <http://www.aanddtech.com/ADAPT.html>, 2014.
- A&D Technology, "Phoenix AM/RT Combustion Analysis Systems" *A&D Technology, Inc.*, 2014. <http://www.aanddtech.com/Phoenix.html>, 2017.
- Abianeh, O., Oehlschlaeger, M. and Sung, C., "A surrogate mixture and kinetic mechanism for emulating the evaporation and autoignition characteristics of gasoline fuel", *Combustion and Flame* 162(10):3773-3784, 2015, doi:10.1016/j.combustflame.2015.07.015.
- Abu-Jrai, A., Rodríguez-Fernández, J., Tsolakis, A., Megaritis, A., Theinnoi, K., Cracknell, R. and Clark, R., "Performance, Combustion and Emissions of a Diesel Engine Operated with Reformed EGR. Comparison of Diesel and GTL Fuelling", *Fuel* 88(6):1031-1041, 2009, doi:10.1016/j.fuel.2008.12.001.
- ACEA, "Worldwide Fuel Charter 2013", *European Automobile Manufacturers' Association*, <http://www.acea.be/publications/article/worldwide-fuel-charter>, 2017.
- Ahmedi, A., Ahmed, S. and Kalghatgi, G., "Simulating Combustion in a PCI (Premixed Compression Ignition) Engine using DI-SRM and 3 Components Surrogate Model", *Combustion and Flame* 162(10):3728-3739, 2015, doi:10.1016/j.combustflame.2015.07.011.

- Akihama, K., Takatori, Y., Inagaki, K., Sasaki, S. and Dean, A., "Mechanism of the Smokeless Rich Diesel Combustion by Reducing Temperature", *SAE Technical Paper Series*, 2001, doi:10.4271/2001-01-0655.
- Alkidas, A., "On the Premixed Combustion in a Direct-Injection Diesel Engine", *ASME Energy-Sources and Technology Conference and Exhibition*, ASME Paper 86-ICF-4, 1986.
- Amorim, R., Novella, R., Garcia, A. and Molina, S., "Study on LTC for light duty engines – Part 2 – Spray enhancements", *Fuel* 193:206-219, 2017, doi:10.1016/j.fuel.2016.12.050.
- Anand, K., Ra, Y., Reitz, R. and Bunting, B., "Surrogate Model Development for Fuels for Advanced Combustion Engines", *Energy & Fuels* 25(4):1474-1484, 2011, doi:10.1021/ef101719a.
- ANSYS, "ANSYS Chemkin-Pro Input Manual", *ANSYS, Inc.*, 2017.
- ANSYS, "ANSYS Chemkin-Pro Theory Manual", *ANSYS, Inc.*, 2017.
- ANSYS, "ANSYS Chemkin Reaction Workbench Manual", *ANSYS, Inc.*, 2017.
- ANSYS, "ANSYS Model Fuel Library", *ANSYS, Inc.*, 2015.
- ANSYS, "ANSYS Model Fuel Library", *ANSYS, Inc.*, 2016.
- ANSYS, "The Model Fuels Library: Accurate Combustion Chemistry for the Real World", *ANSYS, Inc.*, 2016. <http://www.ansys.com/-/media/Ansys/corporate/resourcelibrary/brochure/ansys-model-fuel-library-brochure.pdf>, 2017.
- ANSYS, "Surrogate Blend Optimizer", *ANSYS, Inc.*, 2016.
- ASTM International, "Test Method for Cetane Number of Diesel Fuel Oil", *ASTM International*, ASTM D 613-13, May 2017, doi:10.1520/d0613-13.
- ASTM International, "Test Method for Determination of Ignition Delay and Derived Cetane Number (DCN) of Diesel Fuel Oils by Combustion in a Constant Volume Chamber", *ASTM International*, ASTM D 6890, May 2017, doi:10.1520/d6890-13b.

- ASTM International, "Test Method for Smoke Point of Kerosine and Aviation Turbine Fuel", *ASTM International*, ASTM D 1322-12, May 2017, doi:10.1520/d1322-12.
- ASTM International, "Standard Test Method for Heat of Combustion of Liquid Hydrocarbon Fuels by Bomb Calorimeter", *ASTM International*, ASTM D 240-09, 2009.
- ASTM International, "Test Method for Dynamic Surface Tension by the Fast-Bubble Technique", *ASTM International*, ASTM D 3825-09, 2009, doi:10.1520/d3825-09.
- ASTM International, "Test Method for Density, Relative Density, and API Gravity of Liquids by Digital Density Meter", *ASTM International*, ASTM D 4052-11, 2011, doi:10.1520/d4052-11.
- ASTM International, "Test Method for Kinematic Viscosity of Transparent and Opaque Liquids (and Calculation of Dynamic Viscosity)", *ASTM International*, ASTM D 445-12, 2012, doi:10.1520/d0445-12.
- ASTM International, "Test Method for Distillation of Petroleum Products at Atmospheric Pressure", *ASTM International*, ASTM D 86-12, May 2017, doi:10.1520/d0086-12.
- ASTM International, "Test Method for Hydrocarbon Types in Liquid Petroleum Products by Fluorescent Indicator Adsorption", *ASTM International*, ASTM D 1319-13, May 2017, doi:10.1520/d1319-13.
- ASTM International, "Standard Test Method for Determination of the Aromatic Content and Polynuclear Aromatic Content of Diesel Fuels and Aviation Turbine Fuels By Supercritical Fluid Chromatography", *ASTM International*, ASTM D 5186, May 2017.
- ASTM International, "Test Methods for Flash Point by Pensky-Martens Closed Cup Tester", *ASTM International*, ASTM D 93-13, May 2017, doi:10.1520/d0093-13.
- ASTM International, "Specification for Diesel Fuel Oils", *ASTM International*, ASTM D 975-16a, 2016, doi:10.1520/d0975-16a.

- AVL, "AVL Product Description, Emission Test Instruments - AVL 439 Opacimeter", AVL List GmbH, Graz, Austria, 2008.
- AVL, "Smoke Value Measurement with the Filter-Paper-Method, AT1007E, Rev. 02", *AVL List GmbH*, Graz, Austria, 2nd ed., 2005.
- Banerjee, S., Tangko, R., Sheen, D., Wang, H. and Bowman, C., "An Experimental and Kinetic Modeling Study of n -Dodecane Pyrolysis and Oxidation", *Combustion and Flame* 163:12-30, 2016, doi:10.1016/j.combustflame.2015.08.005.
- Bardi, M., Payri, R., Malbec, L., Bruneaux, G., Pickett, L., Manin, J., Bazyn, T. and Genzale, C., "Engine Combustion Network: Comparison of Spray Development, Vaporization, and Combustion in Different Combustion Vessels", *Atomization and Sprays* 22(10):807-842, 2012, doi:10.1615/atomizspr.2013005837.
- Beatrice, C., Avolio, G., Del Giacomo, N. and Guido, C., "Compression Ratio Influence on the Performance of an Advanced Single-Cylinder Diesel Engine Operating in Conventional and Low Temperature Combustion Mode", *SAE Technical Paper Series*, 2008, doi:10.4271/2008-01-1678.
- Benajes, J., García, A., Monsalve-Serrano, J. and Boronat, V., "Achieving Clean and Efficient Engine Operation up to Full Load by Combining Optimized RCCI and Dual-Duel Diesel-Gasoline Combustion Strategies", *Energy Conversion and Management* 136:142-151, 2017, doi:10.1016/j.enconman.2017.01.010.
- Benajes, J., García-Oliver, J., Novella, R. and Kolodziej, C., "Increased particle emissions from early fuel injection timing Diesel low temperature combustion", *Fuel* 94:184-190, 2012, doi:10.1016/j.fuel.2011.09.014.
- Benajes, J., López, J., Novella, R. and García, A., "Advanced Methodology for Improving Testing Efficiency in a Single-Cylinder Research Diesel Engine", *Experimental Techniques* 32(6):41-47, 2008, doi:10.1111/j.1747-1567.2007.00296.x.

- Benajes, J., Molina, S., De Rudder, K. and Amorim, R., "Optimization Towards Low-temperature Combustion in a HSDI Diesel Engine, Using Consecutive Screenings", *SAE Technical Paper Series*, 2007, doi:10.4271/2007-01-0911.
- Benajes, J., Molina, S., Novella, R. and Amorim, R., "Study on Low Temperature Combustion for Light-Duty Diesel Engines", *Energy & Fuels* 24(1):355-364, 2010, doi:10.1021/ef900832c.
- Benajes, J., Novella, R., Arthozoul, S. and Kolodziej, C., "Particle Size Distribution Measurements from Early to Late Injection Timing Low Temperature Combustion in a Heavy Duty Diesel Engine", *SAE International Journal of Fuels and Lubricants* 3(1):567-581, 2010, doi:10.4271/2010-01-1121.
- Bolla, M., Chishty, M., Hawkes, E. and Kook, S., "Modeling Combustion under Engine Combustion Network Spray A Conditions with Multiple Injections using the Transported Probability Density Function Method", *International Journal of Engine Research* 18(1-2):6-14, 2017, doi:10.1177/1468087416689174.
- Calcote, H. and Manos, D., "Effect of Molecular Structure on Incipient Soot Formation", *Combustion and Flame* 49(1-3):289-304, 1983, doi:10.1016/0010-2180(83)90172-4.
- California Environmental Protection Agency - Air Resources Board, "California Diesel Fuel Program", *California Environmental Protection Agency*, <https://www.arb.ca.gov/fuels/diesel/diesel.htm>, 2017.
- Cambustion, "DMS500 User Manual Version 3.1", *Cambustion Limited*, Cambridge, UK, 2010, <http://www.cambustion.com>, 2017..
- Cambustion, "DMS500 Fast Particle Analyzer", *Cambustion Limited*, Cambridge, UK, 2014, <http://www.cambustion.com/products/dms500>, 2017.

- Chang, J., Kalghatgi, G., Amer, A., Adomeit, P., Rohs, H. and Heuser, B., "Vehicle Demonstration of Naphtha Fuel Achieving Both High Efficiency and Drivability with EURO6 Engine-Out NO_x Emission", *SAE International Journal of Engines* 6(1):101-119, 2013, doi:10.4271/2013-01-0267.
- Chevron, "Diesel Fuels Technical Review", *Chevron Products Company* <http://www.chevron.com/products/prodserv/fuels/bulletin/diesel>, 2007.
- Chu, S. and Majumdar, A., "Opportunities and Challenges for a Sustainable Energy Future", *Nature* 488(7411):294-303, 2012, doi:10.1038/nature11475.
- Ciajolo, A., D'Anna, A., Barbella, R. and Bertoli, C., "Combustion of Tetradecane and Tetradecane/ α -Methylnaphthalene in a Diesel Engine with Regard to Soot and PAH Formation", *Combustion Science and Technology* 87(1-6):127-137, 1993, doi:10.1080/00102209208947211.
- Curran, H., Gaffuri, P., Pitz, W. and Westbrook, C., "A Comprehensive Modeling Study of n-Heptane Oxidation", *Combustion and Flame* 114(1-2):149-177, 1998, doi:10.1016/s0010-2180(97)00282-4.
- DC Scientific, "SP10–Automated Smoke Point", *DC Scientific - Petroleum Testing Equipment*, 2017.
- Dec, J., "A Conceptual Model of DI Diesel Combustion Based on Laser-Sheet Imaging*", *SAE Technical Paper Series*, 1997, doi:10.4271/970873.
- Desantes, J., Benajes, J., Garcia-Oliver, J. and Kolodziej, C., "Effects of intake pressure on particle size and number emissions from premixed diesel low-temperature combustion", *International Journal of Engine Research* 15(2):222-235, 2013, doi:10.1177/1468087412469514.
- Desantes, J., Bermúdez, V., García, J. and Fuentes, E., "Effects of current engine strategies on the exhaust aerosol particle size distribution from a Heavy-Duty Diesel Engine", *Journal of Aerosol Science* 36(10):1251-1276, 2005, doi:10.1016/j.jaerosci.2005.01.002.

- Desantes, J., Luján, J., Pla, B. and Soler, J., "On the combination of high-pressure and low-pressure exhaust gas recirculation loops for improved fuel economy and reduced emissions in high-speed direct-injection engines", *International Journal of Engine Research* 14(1):3-11, 2013, doi:10.1177/1468087412437623.
- Desantes, J., Lopez, J., Garcia, J. and Pastor, J., "Evaporative Diesel Spray Modeling", *Atomization and Sprays* 17(3):193-231, 2007, doi:10.1615/atomizspr.v17.i3.10.
- Desantes, J., Lopez, J., Redon, P. and Arregle, J., "Evaluation of the Thermal NO formation mechanism under low-temperature diesel combustion conditions", *International Journal of Engine Research* 13(6):531-539, 2012, doi:10.1177/1468087411429638.
- Desantes, J., Payri, R., Salvador, F. and De la Morena, J., "Influence of Cavitation Phenomenon on Primary Break-Up and Spray Behavior at Stationary Conditions", *Fuel* 89(10):3033-3041, 2010, doi:10.1016/j.fuel.2010.06.004.
- Design Institute for Physical Properties, "AIChE DIPPR Project 801 - Full Version", *KNovel Corporation*, (2005; 2008-2012; 2015; 2016)", [Http://App.Knovel.Com/Hotlink/Toc/Id:Kpdipprpf7/Dippr-Project-801-Full/Dippr-Project-801-Full](http://App.Knovel.Com/Hotlink/Toc/Id:Kpdipprpf7/Dippr-Project-801-Full/Dippr-Project-801-Full), 2016.
- Di Blasio, G., Beatrice, C. and Molina, S., "Effect of Port Injected Ethanol on Combustion Characteristics in a Dual-Fuel Light Duty Diesel Engine", *SAE Technical Paper Series*, 2013, doi:10.4271/2013-01-1692.
- DieselNet, "Diesel Fuels", *DieselNet Internet Resources*, <https://www.dieselnet.com/links/fuel.html>, 2017.
- DieselNet, "What is Diesel Fuel", *DieselNet Internet Resources*, https://www.dieselnet.com/tech/fuel_diesel.php, 2017.
- Diez, A., Crookes, R. and Lovas, T., "Experimental studies of autoignition and soot formation of diesel surrogate fuels", *Proceedings of The Institution of Mechanical Engineers, Part D: Journal of Automobile Engineering* 227(5):656-664, 2012, doi:10.1177/0954407012458402.

- Dong-Ryul, R. and Farrel, P., "Air Flow Characteristics Surrounding Evaporating Transient Diesel Sprays", *SAE Technical Paper Series* 2002-01-0499, 2002.
- Dooley, S., Won, S., Chaos, M., Heyne, J., Ju, Y., Dryer, F., Kumar, K., Sung, C., Wang, H., Oehlschlaeger, M., Santoro, R. and Litzinger, T., "A jet fuel surrogate formulated by real fuel properties", *Combustion and Flame* 157(12):2333-2339, 2010, doi:10.1016/j.combustflame.2010.07.001.
- Eastwood, P., "Particulate Emissions from Motor Vehicles", Wiley, Chichester, 2008.
- European Committee for Standardization (CEN), "Automotive fuels - Diesel - Requirements and test methods", *European Committee for Standardization*, EN 590:2009: E, 2009.
- European Committee for Standardization (CEN), "Fuel", *European Committee for Standardization*, <https://www.cen.eu/work/areas/energy/fuel/Pages/default.aspx>, 2017.
- Farrell, J., Cernansky, N., Dryer, F., Law, C., Friend, D., Hergart, C., McDavid, R., Patel, A., Mueller, C. and Pitsch, H., "Development of an Experimental Database and Kinetic Models for Surrogate Diesel Fuels", *SAE Technical Paper Series* 2007-01-0201, 2007.
- Flores, V., "Reaction Design's Automotive Fuels Consortium Revs Up with Five New Members," *Reaction Design*, April 16, 2007.
<http://www.modelfuelsconsortium.com/news/39/95/Reaction-Design-s-Automotive-Fuels-Consortium-Revs-Up-with-Five-New-Members/>, 2017.
- Flores, V., "Reaction Design Introduces Industry's Most Well Validated Model Fuel Library", *Reaction Design*, November 7, 2012.
<http://www.reactiondesign.com/news/2/95/Reaction-Design-Introduces-Industry-s-Most-Well-Validated-Model-Fuel-Library/>, 2017.
- Fisher, B. and Mueller, C., "Effects of Injection Pressure, Injection-Rate Shape, and Heat Release on Liquid Length", *SAE International Journal of Engines* 5(2):415-429, 2012, doi:10.4271/2012-01-0463.

- Fisher, B. and Mueller, C., "Liquid penetration length of heptamethylnonane and trimethylpentane under unsteady in-cylinder conditions", *Fuel* 89(10):2673-2696, 2010, doi:10.1016/j.fuel.2010.04.024.
- Gatowski, J., Balles, E., Chun, K., Nelson, F., Ekchian, J. and Heywood, J., "Heat Release Analysis of Engine Pressure Data", *SAE Technical Paper Series*, 1984, doi:10.4271/841359.
- Green Car Congress, "Reaction Design introduces model fuel library resulting from work of Model Fuels Consortium", *Green Car Congress*, November 14, 2010.
<http://www.greencarcongress.com/2012/11/reaction-design-introduces-model-fuel-library-resulting-from-work-of-model-fuels-consortium.html>, 2017.
- Hakka, M., Glaude, P., Herbinet, O. and Battin-Leclerc, F., "Experimental Study of the Oxidation of Large Surrogates for Diesel and Biodiesel Fuels", *Combustion and Flame* 156(11):2129-2144, 2009, doi:10.1016/j.combustflame.2009.06.003.
- Harkins, J. and Goodwine, J., "Oxides of Nitrogen in Diesel Exhaust", *Journal of the Air Pollution Control Association* 14(1):34-38, 1964, doi:10.1080/00022470.1964.10468238.
- Henein, N. and Patterson, D., "Emissions from Combustion Engines and Their Control", 1st ed., Ann Arbor Science Publishers, 1972.
- Hernandez, J., Sanz-Argent, J., Benajes, J. and Molina, S., "Selection of a diesel fuel surrogate for the prediction of auto-ignition under HCCI engine conditions", *Fuel* 87(6):655-665, 2008, doi:10.1016/j.fuel.2007.05.019.
- Heywood, J., "Internal combustion engine fundamentals", 1st ed., McGraw-Hill, New York, 1988.
- Hidaka, Y., Nishimori, T., Sato, K., Henmi, Y., Okuda, R., Inami, K. and Higashihara, T., "Shock-Tube and Modeling Study of Ethylene Pyrolysis and Oxidation", *Combustion and Flame* 117(4):755-776, 1999, doi:10.1016/s0010-2180(98)00128-x.

- Hidaka, Y., Sato, K., Hoshikawa, H., Nishimori, T., Takahashi, R., Tanaka, H., Inami, K. and Ito, N., "Shock-Tube and Modeling Study of Ethane Pyrolysis and Oxidation", *Combustion and Flame* 120(3):245-264, 2000, doi:10.1016/s0010-2180(99)00102-9.
- Infineum International, Limited, "Worldwide Winter Diesel Fuel Quality Survey 2014", Infineum International Limited, 2014.
- Jacobs, T., Bohac, S., Assanis, D. and Szymkowicz, P., "Lean and Rich Premixed Compression Ignition Combustion in a Light-Duty Diesel Engine", *SAE Technical Paper Series*, 2005, doi:10.4271/2005-01-0166.
- Jacobs, T., Knafl, A., Bohac, S., Assanis, D. and Szymkowicz, P., "The Development of Throttled and Unthrottled PCI Combustion in a Light-Duty Diesel Engine", *SAE Technical Paper Series*, 2006, doi:10.4271/2006-01-0202.
- Kalghatgi, G., Hildingsson, L., Harrison, A. and Johansson, B., "Surrogate Fuels for Premixed Combustion in Compression Ignition Engines", *International Journal of Engine Research* 12(5):452-465, 2011, doi:10.1177/1468087411409307.
- Kamimoto, T. and Bae, M., "High Combustion Temperature for the Reduction of Particulate in Diesel Engines", *SAE Technical Paper Series*, 1988, doi:10.4271/880423.
- Kee, S., Mohammadi, A., Kidoguchi, Y. and Miwa, K., "Effects of Aromatic Hydrocarbons on Fuel Decomposition and Oxidation Processes in Diesel Combustion", *SAE Technical Paper Series*, 2005, doi:10.4271/2005-01-2086.
- Kim, D., Martz, J. and Violi, A., "A surrogate for emulating the physical and chemical properties of conventional jet fuel", *Combustion and Flame* 161(6):1489-1498, 2014, doi:10.1016/j.combustflame.2013.12.015.
- Kirchen, P., Boulouchos, K., Obrecht, P. and Bertola, A., "Exhaust-Stream and In-Cylinder Measurements and Analysis of the Soot Emissions from a Common Rail Diesel Engine using Two Fuels", *ASME 2009 Internal Combustion Engine Division Fall Technical Conference*, ASME Internal Combustion Engine Division, Lucerne, Switzerland, 2009.

- Kitamura, T., Ito, T., Senda, J. and Fujimoto, H., "Mechanism of Smokeless Diesel Combustion with Oxygenated Fuels based on the Dependence of the Equivalence Ratio and Temperature on Soot Particle Formation", *International Journal of Engine Research* 3(4):223-248, 2002, doi:10.1243/146808702762230923.
- Kokjohn, S., Hanson, R., Splitter, D. and Reitz, R., "Fuel Reactivity Controlled Compression Ignition (RCCI): A Pathway to Controlled High-Efficiency Clean Combustion", *International Journal of Engine Research* 12(3):209-226, 2011, doi:10.1177/1468087411401548.]
- Kolodziej, C., "Particulate Matter Emissions from Premixed Diesel Low Temperature Combustion", PhD, Universitat Politècnica de València, 2012.
- Krieger, R., Siewert, R., Pinson, J., Gallopoulos, N., Hilden, D., Monroe, D., Rask, R., Solomon, A. and Zima, P., "Diesel Engines: One Option to Power Future Personal Transportation Vehicles", *SAE Technical Paper Series*, 1997, doi:10.4271/972683.
- Labeckas, G. and Slavinskas, S., "Performance and Emission Characteristics of a Direct Injection Diesel Engine Operating on KDV Synthetic Diesel Fuel", *Energy Conversion and Management* 66:173-188, 2013, doi:10.1016/j.enconman.2012.10.004.
- Lapuerta, M., Armas, O. and Hernández, J., "Diagnosis of DI Diesel combustion from in-cylinder pressure signal by estimation of mean thermodynamic properties of the gas", *Applied Thermal Engineering* 19(5):513-529, 1999, doi:10.1016/s1359-4311(98)00075-1.
- Lea-Langton, A., Andrews, G., Bartle, K., Jones, J. and Williams, A., "Combustion and Pyrolysis Reactions of Alkylated Polycyclic Aromatic Compounds: The Decomposition of 13C Methylarenes in Relation to Diesel Engine Emissions", *Fuel* 158:719-724, 2015, doi:10.1016/j.fuel.2015.05.043.
- Liang, L., Naik, C., Puduppakkam, K., Wang, C., Modak, A., Meeks, E., Ge, H., Reitz, R. and Rutland, C., "Efficient Simulation of Diesel Engine Combustion Using Realistic Chemical Kinetics in CFD", *SAE Technical Paper Series*, 2010, doi:10.4271/2010-01-0178.

- Lindstedt, R. and Maurice, L., "Detailed Kinetic Modelling of n-Heptane Combustion", *Combustion Science and Technology* 107(4-6):317-353, 1995, doi:10.1080/00102209508907810.
- Luo, J., Yao, M., Liu, H. and Yang, B., "Experimental and Numerical Study on Suitable Diesel Fuel Surrogates in Low Temperature Combustion Conditions", *Fuel* 97:621-629, 2012, doi:10.1016/j.fuel.2012.02.057.
- Marsh, G., Hill, N. and Sully, J., "Consultation on the Need to Reduce the Sulphur Content of Petrol and Diesel Fuels Below 50 PPM: A Policy Makers Summary", AEA Technology Environment, 2000.
- McEnally, C., Ciuparu, D. and Pfefferle, L., "Experimental Study of Fuel Decomposition and Hydrocarbon Growth Processes for Practical Fuel Components: Heptanes", *Combustion and Flame* 134(4):339-353, 2003, doi:10.1016/s0010-2180(03)00113-5.
- McEnally, C. and Pfefferle, L., "Experimental Study of Fuel Decomposition and Hydrocarbon Growth Processes for Cyclohexane and Related Compounds in Nonpremixed Flames", *Combustion and Flame* 136(1-2):155-167, 2004, doi:10.1016/j.combustflame.2003.09.012.
- Meeks, E., "Consortium Advances Combustion Simulation for Engine Design", *Automotive Industries*, Issue: Feb 2009, 2009. http://www.ai-online.com/Adv/Previous/show_issue.php?id=2449#sthash.FazewLfs.dpbs, 2017.
- Merkisz, J. and Pielecha, J., "Nanoparticle Emissions from Combustion Engines", 1st ed., Springer, New York, 2015.
- Miles, P., "Sources and Mitigation of CO and UHC Emissions in Low-Temperature Diesel Combustion Regimes: Insights Obtained via Homogeneous Reactor Modeling", *13th Diesel Engine-Efficiency and Emissions Research (DEER) Conference*, US DOE, 2007. http://www1.eere.energy.gov/vehiclesandfuels/pdfs/deer_2007/session_8/deer07_miles.pdf

- Morin, J., Bion, A. and Dionnet, F., "Diesel exhaust oxidant potential assessed by the NO₂/NO concentration ratio, may be a major trigger of Diesel engine emission biological impact to rat lung tissue", Air Resource Board of California - Diesel Nitrogen Dioxide Working Group, 2004.
- Mueller, C., Cannella, W., Bruno, T., Bunting, B., Dettman, H., Franz, J., Huber, M., Natarajan, M., Pitz, W., Ratcliff, M. and Wright, K., "Methodology for Formulating Diesel Surrogate Fuels with Accurate Compositional, Ignition-Quality, and Volatility Characteristics", *Energy & Fuels* 26(6):3284-3303, 2012, doi:10.1021/ef300303e.
- Naik, C., Puduppakkam, K., Wang, C., Kottalam, J., Liang, L., Hodgson, D. and Meeks, E., "Applying Detailed Kinetics to Realistic Engine Simulation: the Surrogate Blend Optimizer and Mechanism Reduction Strategies", *SAE International Journal of Engines* 3(1):241-259, 2010, doi:10.4271/2010-01-0541.
- National Instruments, "Powertrain Controls - National Instruments", *National Instruments*, 2015. <http://www.ni.com/powertrain-controls/>, formerly <http://www.drivven.com>, 2016.
- Northrop, W., Bohac, S., Chin, J. and Assanis, D., "Comparison of Filter Smoke Number and Elemental Carbon Mass From Partially Premixed Low Temperature Combustion in a Direct-Injection Diesel Engine", *Journal Of Engineering For Gas Turbines And Power* 133(10):102804, 2011, doi:10.1115/1.4002918.
- Patel, A., Kong, S. and Reitz, R., "Development and Validation of a Reduced Reaction Mechanism for HCCI Engine Simulations", *SAE Technical Paper Series*, 2004, doi:10.4271/2004-01-0558.
- Payri, F., Benajes, J., Novella, R. and Kolodziej, C., "Effect of Intake Oxygen Concentration on Particle Size Distribution Measurements from Diesel Low Temperature Combustion", *SAE International Journal of Engines* 4(1):1888-1902, 2011, doi:10.4271/2011-01-1355.
- Payri, F., Lopez, J., Pla, B. and Graciano Bustamante, D., "Assessing the Limits of Downsizing in Diesel Engines", *SAE Technical Paper Series*, 2014, doi:10.4271/2014-32-0128.

- Payri, F., Luján, J., Guardiola, C. and Pla, B., "A Challenging Future for the IC Engine: New Technologies and the Control Role", *Oil & Gas Science and Technology - Revue D'IFP Energies Nouvelles* 70(1):15-30, 2014, doi:10.2516/ogst/2014002.
- Payri, F., Molina, S., Martín, J. and Armas, O., "Influence of measurement errors and estimated parameters on combustion diagnosis", *Applied Thermal Engineering* 26(2-3):226-236, 2006, doi:10.1016/j.applthermaleng.2005.05.006.
- Payri, F., Benajes, J., Arrègle, J. and Riesco, J., "Combustion and Exhaust Emissions in a Heavy-Duty Diesel Engine with Increased Premixed Combustion Phase by Means of Injection Retarding", *Oil & Gas Science and Technology* 61(2):247-258, 2006, doi:10.2516/ogst:2006018x.
- Payri, F., Benajes, J., Molina, S. and Riesco, J., "Reduction of Pollutant Emissions in a HD Diesel Engine by Adjustment of Injection Parameters, Boost Pressure and EGR", *SAE Technical Paper Series*, 2003, doi:10.4271/2003-01-0343.
- Payri, F., Payri, R., Salvador, F. and Gimeno, J., "Influence of Nozzle Geometry on Spray Characteristics in Non-evaporative and Evaporative Conditions", *SAE Technical Paper Series*, 2007, doi:10.4271/2007-24-0023.
- Payri, R., Viera, J., Pei, Y. and Som, S., "Experimental and numerical study of lift-off length and ignition delay of a two-component diesel surrogate", *Fuel* 158:957-967, 2015, doi:10.1016/j.fuel.2014.11.072.
- Payri, R., Viera, J., Gopalakrishnan, V. and Szymkowicz, P., "The Effect of Nozzle Geometry over the Evaporative Spray Formation for Three Different Fuels", *Fuel* 188:645-660, 2017, doi:10.1016/j.fuel.2016.10.064.
- Payri, R., Viera, J., Gopalakrishnan, V. and Szymkowicz, P., "The Effect of Nozzle Geometry over Internal Flow and Spray Formation for Three Different Fuels", *Fuel* 183:20-33, 2016, doi:10.1016/j.fuel.2016.06.041.
- Pipho, M., Kittelson, D. and Zarling, D., "NO₂ Formation in a Diesel Engine", *SAE Technical Paper Series*, 1991, doi:10.4271/910231.

- Pitz, W. and Mueller, C., "Recent Progress in the Development of Diesel Surrogate Fuels", *Progress in Energy and Combustion Science* 37(3):330-350, 2011, doi:10.1016/j.pecs.2010.06.004.
- Pitz, W., Westbrook, C., Herbinet, O. and Silke, E., "Progress in Chemical Kinetic Modeling for Surrogate Fuels", *7th International Conference on Modeling and Diagnostics for Advanced Engine Systems, COMODIA 2008*, Sapporo, Japan: Pages 9-15, 2008.
- Ra, Y., Reitz, R., McFarlane, J. and Daw, C., "Effects of Fuel Physical Properties on Diesel Engine Combustion using Diesel and Bio-diesel Fuels", *SAE International Journal of Fuels and Lubricants* 1(1):703-718, 2008, doi:10.4271/2008-01-1379.
- Sáez-Martínez, F., Lefebvre, G., Hernández, J. and Clark, J., "Drivers of Sustainable Cleaner Production and Sustainable Energy Options", *Journal of Cleaner Production* 138:1-7, 2016, doi:10.1016/j.jclepro.2016.08.094.
- Siebers, D., "Scaling Liquid-Phase Fuel Penetration in Diesel Sprays Based on Mixing-Limited Vaporization", *SAE Technical Paper Series* 1999-01-0528, 1999.
- Stiesch, G., "Modeling Engine Spray and Combustion Processes", Springer, Berlin, 2016.
- Sutton, M., "GM Joins Advanced Fuel-Modeling and Simulation Group", *Wards Auto*, September 20, 2007. <http://wardsauto.com/news-analysis/gm-joins-advanced-fuel-modeling-and-simulation-group>, 2017.
- Szymkowicz, P., French, D. and Crellin, C., "Effects of Advanced Fuels on the Particulate and NO_x Emissions from an Optimized Light-Duty CIDI Engine", *SAE Technical Paper Series*, 2001, doi:10.4271/2001-01-0148.
- Szymkowicz, P., Personal Communication with Fuels Group, General Motors Global Research and Development, 2017.

- Tao, F., Reitz, R. and Foster, D., "Revisit of Diesel Reference Fuel (n-Heptane) Mechanism Applied to Multidimensional Diesel Ignition and Combustion Simulations", Seventeenth International Multidimensional Engine Modeling User's Group Meeting, 2007.
- Tosaka, S., "The Characteristics of Chemical Reaction of Diesel Fuel", *JSAE Review* 21(4):463-468, 2000, doi:10.1016/s0389-4304(00)00065-5.
- Totten, G., Westbrook, S. and Shah, R., "Fuels and lubricants handbook", 1st ed., ASTM International, West Conshohocken, Pa, 2003.
- US EPA, "Diesel Fuel Standards", *US EPA*, <https://www.epa.gov/diesel-fuel-standards>, 2017.
- Vendeuvre, C., Ruiz-Guerrero, R., Bertoncini, F., Duval, L., Thiébaud, D. and Hennion, M., "Characterisation of Middle-Distillates by Comprehensive Two-Dimensional Gas Chromatography (GC×GC): A Powerful Alternative for Performing Various Standard Analysis of Middle-Distillates", *Journal Of Chromatography A* 1086(1-2):21-28, 2005, doi:10.1016/j.chroma.2005.05.106.
- Wade, L., "Organic chemistry", Prentice Hall, Upper Saddle River, N.J., 2003.
- Wang, F., Wu, J. and Liu, Z., "Surface Tensions of Mixtures of Diesel Oil or Gasoline and Dimethoxymethane, Dimethyl Carbonate, or Ethanol", *Energy & Fuels* 20(6):2471-2474, 2006, doi:10.1021/ef060231c.
- Warnatz, J., Maas, U. and Dibble, R., "Combustion", 1st ed., Springer, Berlin, 2006.
- Westbrook, C., Pitz, W., Herbinet, O., Curran, H. and Silke, E., "A comprehensive detailed chemical kinetic reaction mechanism for combustion of n-alkane hydrocarbons from n-octane to n-hexadecane", *Combustion and Flame* 156(1):181-199, 2009, doi:10.1016/j.combustflame.2008.07.014.

-
- Yang, H., Shuai, S., Wang, Z., Wang, J. and Xu, H., "New Premixed Compression Ignition Concept for Direct Injection IC Engines Fueled with Straight-Run Naphtha", *Energy Conversion and Management* 68:161-168, 2013, doi:10.1016/j.enconman.2013.01.006.

10. Appendix

Contents

10.	Appendices	265
10.1.	Surrogate Fuel Library	267
10.2.	Target and Surrogate Fuel Properties	271
10.3.	Surrogate Fuel Property Validation	276

10.1. Surrogate Fuel Library

This section provides tables showing the fuel component blend fractions (volume, mass and molar) along with the predicted properties for all of the fuels contained in the Surrogate Fuel Library. Table 10-1 shows Surrogate Fuel Library in a matrix format. Surrogate CN50_TSI31 was developed to match the target Diesel fuel. Table 10-2 shows the formulations and properties for the six surrogate fuels with TSI=17. Table 10-3 provides the formulations and properties for the six surrogate fuels with TSI=31 and Table 10-4 contains the formulations and properties for the six surrogate fuels with TSI=48.

Table 10-1: Surrogate Fuel Library matrix.

	Low Soot Fuels TSI=17	Mid Soot Fuels TSI = 31	High Soot Fuels TSI = 48
CN=35	CN35_TSI17	CN35_TSI31	CN35_TSI48
CN=40	CN40_TSI17	CN40_TSI31	CN40_TSI48
CN=45	CN45_TSI17	CN45_TSI31	CN45_TSI48
CN=50	CN50_TSI17	CN50_TSI31 <i>Target Diesel Fuel</i>	CN50_TSI48
CN=55	CN55_TSI17	CN55_TSI31	CN55_TSI48
CN=60	CN60_TSI17	CN60_TSI31	CN60_TSI48

Table 10-2: Volume, mass and molar blending fractions and predicted properties for the low sooting tendency surrogate fuels (TSI=17).

Fuel Property	Units	CN35_TSI17	CN40_TSI17	CN45_TSI17	CN50_TSI17	CN55_TSI17	CN60_TSI17
n-Hexadecane	v/v	0.13	0.20	0.25	0.34	0.37	0.43
Heptamethylnonane	v/v	0.57	0.50	0.45	0.33	0.33	0.27
Decahydronaphthalene	v/v	0.30	0.30	0.30	0.33	0.30	0.30
1-Methylnaphthalene	v/v	0.00	0.00	0.00	0.00	0.00	0.00
n-Hexadecane	m/m	0.122	0.189	0.236	0.320	0.350	0.408
Heptamethylnonane	m/m	0.550	0.484	0.436	0.319	0.321	0.263
Decahydronaphthalene	m/m	0.327	0.328	0.328	0.361	0.329	0.330
1-Methylnaphthalene	m/m	0.000	0.000	0.000	0.000	0.000	0.000
n-Hexadecane	M/M	0.101	0.156	0.195	0.261	0.290	0.337
Heptamethylnonane	M/M	0.455	0.400	0.360	0.259	0.265	0.217
Decahydronaphthalene	M/M	0.443	0.444	0.445	0.480	0.446	0.446
1-Methylnaphthalene	M/M	0.000	0.000	0.000	0.000	0.000	0.000
Cetane Number		34.8	40.7	45.0	53.5	55.2	60.3
Threshold Soot Index		19.0	18.2	17.6	16.6	16.2	15.5
Saturated Hydrocarbons	%v/v	100.0	100.0	100.0	100.0	100.0	100.0
Olefinic Hydrocarbons	%v/v	0.0	0.0	0.0	0.0	0.0	0.0
Aromatic Hydrocarbons	%v/v	0.0	0.0	0.0	0.0	0.0	0.0
Density at 25 °C	g/cm3	0.806	0.805	0.804	0.806	0.803	0.802
Lower Heating Value	MJ/kg	44.040	44.090	44.130	44.160	44.230	44.280
Molar H/C		2.017	2.017	2.017	2.016	2.016	2.016
Kinematic Viscosity at 25 °C	cSt	3.6401	3.6179	3.6020	3.5122	3.5638	3.5447
Distillation Temperature - T₁₀	°C	215.3	216.5	217.0	216.5	219.2	220.7
Distillation Temperature - T₂₀	°C	218.9	220.3	221.5	221.2	224.3	226.4
Distillation Temperature - T₃₀	°C	222.9	224.9	226.6	226.8	231.3	233.6
Distillation Temperature - T₄₀	°C	228.0	231.1	233.2	234.5	239.3	242.3
Distillation Temperature - T₅₀	°C	234.1	237.8	241.0	244.3	248.9	252.8
Distillation Temperature - T₆₀	°C	240.8	245.7	249.4	254.6	258.7	263.1
Distillation Temperature - T₇₀	°C	247.4	253.6	257.4	264.6	267.1	271.6
Distillation Temperature - T₈₀	°C	254.4	260.9	264.9	272.2	274.0	277.2
Distillation Temperature - T₉₀	°C	261.7	268.9	272.6	278.5	279.6	281.4

Table 10-3: Volume, mass and molar blending fractions and predicted properties for the mid sooting tendency surrogate fuels (TSI=31).

Fuel Property	Units	CN35_TSI31	CN40_TSI31	CN45_TSI31	CN50_TSI31	CN55_TSI31	CN60_TSI31
n-Hexadecane	v/v	0.19	0.26	0.31	0.37	0.43	0.48
Heptamethylnonane	v/v	0.51	0.44	0.39	0.33	0.27	0.22
Decahydronaphthalene	v/v	0.20	0.18	0.19	0.18	0.18	0.18
1-Methylnaphthalene	v/v	0.10	0.12	0.11	0.12	0.12	0.12
n-Hexadecane	m/m	0.177	0.242	0.289	0.345	0.401	0.449
Heptamethylnonane	m/m	0.487	0.420	0.373	0.316	0.259	0.211
Decahydronaphthalene	m/m	0.216	0.194	0.205	0.195	0.195	0.195
1-Methylnaphthalene	m/m	0.121	0.145	0.133	0.145	0.145	0.145
n-Hexadecane	M/M	0.146	0.200	0.239	0.285	0.332	0.371
Heptamethylnonane	M/M	0.403	0.347	0.308	0.261	0.214	0.174
Decahydronaphthalene	M/M	0.292	0.263	0.278	0.263	0.264	0.264
1-Methylnaphthalene	M/M	0.159	0.190	0.175	0.191	0.191	0.191
Cetane Number		35.5	40.5	45.2	49.9	55.0	59.2
Threshold Soot Index		31.1	32.8	30.9	31.5	30.8	30.3
Saturated Hydrocarbons	%v/v	90.0	88.0	89.0	88.0	88.0	88.0
Olefinic Hydrocarbons	%v/v	0.0	0.0	0.0	0.0	0.0	0.0
Aromatic Hydrocarbons	%v/v	10.0	12.0	11.0	12.0	12.0	12.0
Density at 25 °C	g/cm ³	0.820	0.822	0.820	0.821	0.820	0.819
Lower Heating Value	MJ/kg	43.740	43.730	43.800	43.810	43.860	43.900
Molar H/C		1.897	1.873	1.884	1.872	1.872	1.871
Kinematic Viscosity at 25 °C	cSt	3.6817	3.6716	3.6497	3.6367	3.6176	3.6017
Distillation Temperature - T₁₀	°C	224.1	226.8	227.0	229.2	230.9	231.8
Distillation Temperature - T₂₀	°C	227.1	230.8	231.5	234.0	235.5	236.9
Distillation Temperature - T₃₀	°C	231.4	234.5	236.0	238.9	241.2	243.1
Distillation Temperature - T₄₀	°C	235.4	239.3	241.2	244.3	247.0	249.5
Distillation Temperature - T₅₀	°C	239.9	244.3	246.9	250.1	254.0	256.9
Distillation Temperature - T₆₀	°C	245.0	249.4	252.7	256.9	260.4	263.9
Distillation Temperature - T₇₀	°C	250.7	255.4	259.5	263.4	267.2	270.2
Distillation Temperature - T₈₀	°C	257.0	262.2	266.8	270.2	274.2	276.7
Distillation Temperature - T₉₀	°C	265.7	271.7	274.8	277.7	279.9	281.8

Table 10-4: Volume, mass and molar blending fractions and predicted properties for the high sooting tendency surrogate fuels (TSI=48).

Fuel Property	Units	CN35_TSI48	CN40_TSI48	CN45_TSI48	CN50_TSI48	CN55_TSI48	CN60_TSI48
n-Hexadecane	v/v	0.26	0.32	0.38	0.42	0.50	0.56
Heptamethylnonane	v/v	0.44	0.38	0.32	0.25	0.20	0.14
Decahydronaphthalene	v/v	0.05	0.05	0.05	0.06	0.05	0.04
1-Methylnaphthalene	v/v	0.25	0.25	0.25	0.27	0.25	0.26
n-Hexadecane	m/m	0.238	0.293	0.349	0.384	0.460	0.515
Heptamethylnonane	m/m	0.413	0.357	0.301	0.234	0.189	0.132
Decahydronaphthalene	m/m	0.053	0.053	0.053	0.063	0.053	0.043
1-Methylnaphthalene	m/m	0.296	0.297	0.297	0.319	0.298	0.310
n-Hexadecane	M/M	0.197	0.242	0.288	0.312	0.380	0.426
Heptamethylnonane	M/M	0.341	0.295	0.249	0.190	0.156	0.109
Decahydronaphthalene	M/M	0.072	0.072	0.072	0.084	0.072	0.058
1-Methylnaphthalene	M/M	0.390	0.391	0.391	0.413	0.392	0.407
Cetane Number		34.8	39.9	45.0	48.4	55.2	59.9
Threshold Soot Index		48.8	48.1	47.5	48.9	46.2	46.8
Saturated Hydrocarbons	%v/v	75.0	75.0	75.0	73.0	75.0	74.0
Olefinic Hydrocarbons	%v/v	0.0	0.0	0.0	0.0	0.0	0.0
Aromatic Hydrocarbons	%v/v	25.0	25.0	25.0	27.0	25.0	26.0
Density at 25 °C	g/cm3	0.842	0.841	0.840	0.845	0.839	0.839
Lower Heating Value	MJ/kg	43.290	43.340	43.380	43.310	43.470	43.490
Molar H/C		1.725	1.724	1.724	1.693	1.723	1.711
Kinematic Viscosity at 25 °C	cSt	3.7505	3.7315	3.7124	3.6507	3.6743	3.6613
Distillation Temperature - T₁₀	°C	239.1	240.4	241.8	241.8	245.0	248.0
Distillation Temperature - T₂₀	°C	240.6	242.1	244.3	244.2	247.7	250.6
Distillation Temperature - T₃₀	°C	242.1	244.3	246.6	246.8	250.7	253.5
Distillation Temperature - T₄₀	°C	244.3	246.7	249.1	249.4	254.0	256.7
Distillation Temperature - T₅₀	°C	246.7	249.3	251.9	252.5	257.1	259.8
Distillation Temperature - T₆₀	°C	249.3	252.0	255.1	256.8	261.8	264.5
Distillation Temperature - T₇₀	°C	252.4	256.6	259.8	261.9	267.1	269.6
Distillation Temperature - T₈₀	°C	258.0	262.3	266.9	268.9	273.6	275.8
Distillation Temperature - T₉₀	°C	267.8	272.4	276.2	277.6	280.4	282.1

10.2. Target and Surrogate Fuel Properties

A subset of five fuels from the Surrogate Fuel Library, highlighted in Table 10-5, were chosen for detailed fuel property analyses. This section provides the ASTM test results for the combustion properties (Table 10-6), physical properties (Table 10-7), hydrocarbon classes (Table 10-8), distillation temperatures (Table 10-9), chemical properties (Table 10-10), and fuel contamination tests (Table 10-11) conducted on the target Diesel and five surrogate fuels.

Table 10-5: Five surrogates from the library (highlighted in green) that were blended and comprehensively analyzed with ASTM test procedures.

	Low Soot Fuels TSI=17	Mid Soot Fuels TSI = 31	High Soot Fuels TSI = 48
CN=35	CN35_TSI17	CN35_TSI31	CN35_TSI48
CN=40	CN40_TSI17	CN40_TSI31	CN40_TSI48
CN=45	CN45_TSI17	CN45_TSI31	CN45_TSI48
CN=50	CN50_TSI17	CN50_TSI31 <i>Target Diesel Fuel</i>	CN50_TSI48
CN=55	CN55_TSI17	CN55_TSI31	CN55_TSI48
CN=60	CN60_TSI17	CN60_TSI31	CN60_TSI48

Table 10-6: Fuel combustion properties for the target Diesel fuel and the (5) surrogate fuels.

Combustion Properties	Units	ASTM Method	Target Diesel	CN40_TSI31	CN50_TSI31	CN60_TSI31	CN50_TSI17	CN50_TSI48
Cetane Number of Diesel Fuel Oils by Combustion in a Constant Volume Chamber		D6890	50.85	40.12	50.08	59.43	50.11	50.48
Ignition Delay of Diesel Fuel Oils by Combustion in a Constant Volume Chamber	msec	D6890	4.023	5.233	4.091	3.395	4.087	4.033
Smoke Point	mm	D1322	19	18.2	18.8	19.2	18.8	13.2
Threshold Soot Index			31	34.9	33.7	33	18.3	47.7
Net Heat of Combustion	MJ/kg	D240N	43.004	43.008	42.857	42.882	42.51	42.336

Table 10-7: Fuel physical properties for the target Diesel fuel and the (5) surrogate fuels.

Physical Properties	Units	ASTM Method	Target Diesel	CN40_TSI31	CN50_TSI31	CN60_TSI31	CN50_TSI17	CN50_TSI48
Density at 15 °C	g/ml	D4052	0.8489	0.8313	0.8305	0.8295	0.8167	0.8538
Density at 40 °C	g/ml	D4052	0.8316	0.8144	0.8131	0.8122	0.7996	0.8356
Density at 60 °C	g/ml	D4052	0.8178	0.8004	0.7991	0.7982	0.7857	0.8215
Density at 90 °C	g/ml	D4052	0.7969	0.7794	0.7781	0.777	0.7647	0.8003
Kinematic Viscosity at 40 °C	cSt	D445	3.063	2.411	2.41	2.402	2.484	2.326
Kinematic Viscosity at 80 °C	cSt	D445	1.58	1.36	1.4	1.35	1.39	1.3
Kinematic Viscosity at 100 °C	cSt	D445	1.259	1.074	1.075	1.079	1.108	1.04
Kinematic Viscosity at 120 °C	cSt	D445	0.99	0.89	0.89	0.89	0.91	1.92
Major Axis - Lubricity of Diesel Fuels (HFRR)	µm	D6079	516	455	473	456	508	427
Minor Axis - Lubricity of Diesel Fuels (HFRR)	µm	D6079	462	369	407	380	423	356
Wear Scar Diameter - Lubricity of Diesel Fuels	µm	D6079	489	412	440	418	466	392
Fuel Temperature - Lubricity of Diesel Fuels	°C	D6079	60	60	60	60	60	60
Cloud Point	°C	D2500	-17.4		1.7			
Flash Point - Pensky - Martens	°C	D93	83	81	80	80	71	94

Table 10-8: Fuel hydrocarbon classes for the target Diesel fuel and the (5) surrogate fuels.

Hydrocarbon Classes	Units	ASTM Method	Target Diesel	CN40_ TSI31	CN50_ TSI31	CN60_ TSI31	CN50_ TSI17	CN50_ TSI48
Aromatic Hydrocarbons by Fluorescent Indicator Adsorption	%v/v	D1319	16.5	12.5	12.4	17.0	1.8	32.0
Olefinic Hydrocarbons by Fluorescent Indicator Adsorption	%v/v	D1319	7.5	5.1	4.9	3.3	3.5	2.0
Saturated Hydrocarbons by Fluorescent Indicator Adsorption	%v/v	D1319	76.0	82.4	82.7	79.7	94.7	66.0
Total aromatic hydrocarbons by Supercritical Fluid Chromatography	%m/m	D5186	16.4	16.1	16.4	16.3	1.0	34.6
Mono aromatic hydrocarbons by Supercritical Fluid Chromatography	%m/m	D5186	16.2	0.4	0.4	0.3	0.4	0.3
Polynuclear aromatic hydrocarbons by Supercritical Fluid Chromatography	%m/m	D5186	0.2	15.7	16.0	16.0	0.6	34.4

Table 10-9: Fuel distillation temperatures for the target Diesel fuel and the (5) surrogate fuels.

Distillation Temperatures	Units	ASTM Method	Target Diesel	CN40_ TSI31	CN50_ TSI31	CN60_ TSI31	CN50_ TSI17	CN50_ TSI48
Distillation Temperature - Initial Boiling Point	°C	D86	187.4	204.2	208.1	204.7	194.9	222.4
Distillation Temperature - 5% v/v evaporation	°C	D86	214.1	217.1	217.5	218.4	204.3	232.9
Distillation Temperature - 10% v/v evaporation	°C	D86	226.8	218.9	220.6	221.8	207.1	234.7
Distillation Temperature - 15% v/v evaporation	°C	D86	237.1	220.9	223.4	225.0	208.9	236.8
Distillation Temperature - 20% v/v evaporation	°C	D86	248.4	223.3	225.9	228.3	211.3	238.6
Distillation Temperature - 30% v/v evaporation	°C	D86	264.8	228.5	231.9	235.8	217.4	241.7
Distillation Temperature - 40% v/v evaporation	°C	D86	274.5	234.5	238.7	244.3	225.6	245.2
Distillation Temperature - 50% v/v evaporation	°C	D86	280.7	240.3	245.2	251.9	237.2	248.2
Distillation Temperature - 60% v/v evaporation	°C	D86	286.4	245.4	251.5	258.9	249.8	252.0
Distillation Temperature - 70% v/v evaporation	°C	D86	292.2	250.3	257.4	265.1	259.3	256.9
Distillation Temperature - 80% v/v evaporation	°C	D86	299.5	256.8	264.5	271.2	266.4	264.2
Distillation Temperature - 90% v/v evaporation	°C	D86	311.7	267.6	272.4	276.1	272.9	273.6
Distillation Temperature - 95% v/v evaporation	°C	D86	324.8	274.0	275.9	277.6	276.0	276.6
Distillation Temperature - Final Boiling Point	°C	D86	330.1	276.4	278.6	279.5	277.6	278.3

Table 10-11: Target Diesel and CN50_TSI31 contamination results.

Fuel Contamination	Units	ASTM Method	Target Diesel	CN50_TSI31
Particulate Contamination	mg/l	D6217	1	0.9
Ash Contamination	%m/m	D482	<0.001	<0.001
Sulfated Ash Content	%m/m	D874	<0.001	<0.001
Water & Sediment	%v/v	D2709	< 0.005	< 0.005
Water (H ₂ O) Content by Coulometric Karl Fischer Titration	ppm	D6304	35	7
Total Chloride by ICP using Aqueous Sample Injection	ppm	D7328	1	0
Existent Inorganic Sulfate by ICP using Aqueous Sample Injection	ppm	D7328	0.4	0
Potential Sulfate by ICP using Aqueous Sample Injection	ppm	D7328	0.3	0
Aluminum (Al) - Elemental Analysis by ICP	ppm	D5185	<1	<1
Barium (Ba) - Elemental Analysis by ICP	ppm	D5185	<1	<1
Boron (B) - Elemental Analysis by ICP	ppm	D5185	<1	1
Cadmium (Cd) - Elemental Analysis by ICP	ppm	D5185	<1	<1
Calcium (Ca) - Elemental Analysis by ICP	ppm	D5185	<1	<1
Chromium (Cr) - Elemental Analysis by ICP	ppm	D5185	<1	<1
Copper (Cu) - Elemental Analysis by ICP	ppm	D5185	<1	<1
Iron (Fe) - Elemental Analysis by ICP	ppm	D5185	<1	<1
Lead (Pb) - Elemental Analysis by ICP	ppm	D5185	<1	<1
Magnesium (Mg) - Elemental Analysis by ICP	ppm	D5185	<1	<1
Manganese (Mn) - Elemental Analysis by ICP	ppm	D5185	<1	<1
Molybdenum (Mo) - Elemental Analysis by ICP	ppm	D5185	<1	<1
Nickel (Ni) - Elemental Analysis by ICP	ppm	D5185	<1	<1
Phosphorus (P) - Elemental Analysis by ICP	ppm	D5185	<1	<1
Potassium (K) - Elemental Analysis by ICP	ppm	D5185	<5	<5
Silicon (Si) - Elemental Analysis by ICP	ppm	D5185	<1	<1
Silver (Ag) - Elemental Analysis by ICP	ppm	D5185	<1	<1
Sodium (Na) - Elemental Analysis by ICP	ppm	D5185	<5	<5
Strontium (Sr) - Elemental Analysis by ICP	ppm	D5185	<1	<1
Tin (Sn) - Elemental Analysis by ICP	ppm	D5185	<1	<1
Titanium (Ti) - Elemental Analysis by ICP	ppm	D5185	<1	<1
Vanadium (V) - Elemental Analysis by ICP	ppm	D5185	<1	<1
Zinc (Zn) - Elemental Analysis by ICP	ppm	D5185	<1	1

10.3. Surrogate Fuel Property Validation

This section provides tabulated results comparing the predicted fuel properties with the measured properties for five surrogate fuels. Table 10-12 shows the predicted-measured property comparison for three fuels with 40, 50 and 60 cetane number that have a constant TSI=31. Table 10-13 compares the predicted and measured fuel properties for three fuels with the cetane number of 50 and TSI values of 17, 31 and 48.

Table 10-12: Comparison of predicted and measured fuel properties for surrogate fuels with increasing cetane number (40, 50, 60) and a constant TSI=31.

Fuel Property	Units	CN40_TSI31		CN50_TSI31		CN60_TSI31	
		Predicted	Measured	Predicted	Measured	Predicted	Measured
Cetane Number		40.5	40.1	49.9	50.1	59.2	59.4
Threshold Soot Index		32.8	34.9	31.5	33.7	30.3	33.0
Saturated Hydrocarbons	%v/v	88.0	82.4	88.0	82.7	88.0	79.7
Olefinic Hydrocarbons	%v/v	0.0	5.1	0.0	4.9	0.0	3.3
Aromatic Hydrocarbons	%v/v	12.0	12.5	12.0	12.4	12.0	17.0
Density at 25 °C	g/cm ³	0.822	0.824	0.821	0.824	0.819	0.823
Lower Heating Value	MJ/kg	43.730	43.008	43.810	42.857	43.900	42.882
Molar H/C		1.873	1.874	1.872	1.870	1.871	1.868
Kinematic Viscosity at 40 °C	cSt	2.749	2.411	2.728	2.410	2.707	2.402
Distillation Temperature - T ₁₀	°C	226.8	218.9	229.2	220.6	231.8	221.8
Distillation Temperature - T ₂₀	°C	230.8	223.3	234.0	225.9	236.9	228.3
Distillation Temperature - T ₃₀	°C	234.5	228.5	238.9	231.9	243.1	235.8
Distillation Temperature - T ₄₀	°C	239.3	234.5	244.3	238.7	249.5	244.3
Distillation Temperature - T ₅₀	°C	244.3	240.3	250.1	245.2	256.9	251.9
Distillation Temperature - T ₆₀	°C	249.4	245.4	256.9	251.5	263.9	258.9
Distillation Temperature - T ₇₀	°C	255.4	250.3	263.4	257.4	270.2	265.1
Distillation Temperature - T ₈₀	°C	262.2	256.8	270.2	264.5	276.7	271.2
Distillation Temperature - T ₉₀	°C	271.7	267.6	277.7	272.4	281.8	276.1

Table 10-13: Comparison of predicted and measured fuel properties for surrogate fuels with increasing TSI (17, 31, 48) and a constant cetane number=50.

Fuel Property	Units	CN50_TSI17		CN50_TSI31		CN50_TSI48	
		Predicted	Measured	Predicted	Measured	Predicted	Measured
Cetane Number		53.5	50.1	49.9	50.1	48.4	50.5
Threshold Soot Index		16.6	18.3	31.5	33.7	48.9	47.7
Saturated Hydrocarbons	%v/v	100.0	94.7	88.0	82.7	73.0	66.0
Olefinic Hydrocarbons	%v/v	0.0	3.5	0.0	4.9	0.0	2.0
Aromatic Hydrocarbons	%v/v	0.0	1.8	12.0	12.4	27.0	32.0
Density at 25 °C	g/cm3	0.806	0.810	0.821	0.824	0.845	0.847
Lower Heating Value	MJ/kg	44.160	42.510	43.810	42.857	43.310	42.336
Molar H/C		2.016	2.017	1.872	1.870	1.693	1.684
Kinematic Viscosity at 40 °C	cSt	2.654	2.484	2.728	2.410	2.720	2.326
Distillation Temperature - T ₁₀	°C	216.5	207.1	229.2	220.6	241.8	234.7
Distillation Temperature - T ₂₀	°C	221.2	211.3	234.0	225.9	244.2	238.6
Distillation Temperature - T ₃₀	°C	226.8	217.4	238.9	231.9	246.8	241.7
Distillation Temperature - T ₄₀	°C	234.5	225.6	244.3	238.7	249.4	245.2
Distillation Temperature - T ₅₀	°C	244.3	237.2	250.1	245.2	252.5	248.2
Distillation Temperature - T ₆₀	°C	254.6	249.8	256.9	251.5	256.8	252.0
Distillation Temperature - T ₇₀	°C	264.6	259.3	263.4	257.4	261.9	256.9
Distillation Temperature - T ₈₀	°C	272.2	266.4	270.2	264.5	268.9	264.2
Distillation Temperature - T ₉₀	°C	278.5	272.9	277.7	272.4	277.6	273.6

